UAB
Universitat Autònoma de Barcelona

Proteomics analysis for the identification of biomarkers and potential therapeutic targets for HIV-1 control and HIV-related neurological dysfunction

Clara Duran Castells

Departament de Biologia Cel·lular, Fisiologia i d'Immunologia

Facultat de Medicina

Universitat Autònoma de Barcelona

Proteomics analysis for the identification of biomarkers and potential therapeutic targets for HIV-1 control and HIV-related neurological dysfunction

Clara Duran Castells

Institut de Recerca de la Sida (IrsiCaixa), Hospital Germans Trias i Pujol i Institut d'Investigació en Ciències de la Salut Germans Trias i Pujol (IGTP)

Directors de tesi:

Dra. Marta Ruiz Riol i Dr. Christian Brander

IrsiCaixa
Institut de Recerca de la Sida

El Dr. Christian Brander (Director i tutor) i la Dra. Marta Ruiz Riol (Directora), investigadors de l'Institut de Recerca de la Sida (IrsiCaixa) de l'Hospital Germans Trias i Pujol,

Fan constar:

Que el treball experimental i la redacció de la memòria de la Tesi Doctoral titulada "Proteomics analysis for the identification of biomarkers and potential therapeutic targets for HIV-1 control and HIV-related neurological dysfunction" ha estat realitzada per Clara Duran Castells sota la tutoria i direcció i consideren que és apta per ser presentada per optar al grau de Doctora en Immunologia per la Universitat Autònoma de Barcelona.

I perquè en quedi constància, signen el present document:

Badalona, 14 de març del 2023

Dr. Christian Brander   Dra. Marta Ruiz Riol

A tothom qui m'ha acompanyat en aquest camí,

especialment la familia, l'Arnau i les amigues

ABREVIATIONS

ADAM15: ADAM metallopeptidase domain 15

ADMA: asymmetric dimethylarginine

AIDS: acquired immune deficiency syndrome

ANI: asymptomatic neurocognitive disorders

ANOVA: analysis of variance

APOBEC3: apolipoprotein B

ART: antiretroviral therapy

AZT: azidothymidine

Aβ: amyloid beta

BBB: blood brain barrier

BDNF: brain-derived neutrophic factor

BnAbs: broadly neutralizing antibodies

CAR-T: chimeric antigen receptor T cell

cART: combined antiretroviral therapy

CASP-8: caspase-8

CCR5, CCR6: C-C chemokine receptor type 5, 6

CD33/SIGLEC3: sialic acid binding Ig like lectin 3

CDC: center of diseases control

CNS: central nervous system

CRTAM: cytotoxic and regulatory T cell molecule

CSF: cerebrospinal fluid

CXCR4, CXCR3: C-X-C chemokine receptor 4, 3

DMPs: differentially methylated positions

DMSO: dimetilsulfoxid

DNA: deoxyribonucleic acid

dsRNA: double strand ribonucleic acid

EC: elite controllers

EI: entry inhibitor

ELISA: enzyme-linked immunosorbent assay

env: envelope gene

FDR: false discovery rate

FI: fusion inhibitor

fMRI: functional magnetic resonance imaging

GAG: group-specific antigen

GDNF: glial cell derived neurotrophic factor

GEO: gene expression omnibus

GFAP: glial fibrillary acidic protein

GFP: green fluorescence protein

GGT5: gamma-glutamyltransferase 5

GM-CSF: granulocyte macrophage colony stimulating factor

GO: gene ontology

Gp140, Gp160, Gp41: envelope glycoproteins

GPNMB: glycoprotein nonmetastatic melanoma protein B

GZMA/B: granzyme A/B

HAD: HIV-associated dementia

HAND: HIV-associated neurocognitive disorders

HBV: hepatitis virus B

HDAC: histone deacetylase inhibitor

HIV: human immunodeficiency virus

HLA: human leucocyte antigen

IFN: interferon

IgG/IgM: immunoglobulin G/M

IL-10, IL-2, IL-7: interleukine-10, -2, -7

INI: integrase inhibitor

INSTI: integrase strand transfer inhibitors

ISGs: interferon stimulated genes

KIR: killer immunoglobulin-like receptor

LAG-3: lymphocyte activating 3 protein

LRA: latency reversal agent

LTNP: long term non-progressors

LTR: long terminal repeat

mAb: monocloncal antibody

MANF: mesencephalic astrocyte derived neurotrophic factor

MAP: monitored antiretroviral pause

MAPT: microtubule associated protein tau

MCP-1: monocyte chemoattractant protein 1

M-CSF: macrophage colony-stimulating factor

MDMs: monocyte-derived macrophages

MND: mild neurocognitive disorders

MOI: multiplicity of infection

MRI: magnetic resonance imaging

MSM: men who have sex with men

NAD: nicotinamide adenine dinucleotide

nef: negative regulatory factor

NFL: neurofilament light chain

NK: natural killer cell

NNRTI: non-nucleoside reverse transcriptase inhibitor

NPX: normalized protein expression

NPZ12/6: neuropsychological test score

NRTI: nucleoside reverse transcriptase inhibitor

PAMPs: pathogen associated molecular patterns

PBMCs: peripheral blood mononuclear cells

PCA: principal component analysis

PD-1: programmed cell death 1

PDGF: platelet-derived growth factor

PEA: proximity extension assay

PHA: phytohaemagglutinin

PI: protease inhibitor

PMA: phorbol myristate acetate

pol: polymerase gene

PRRs: pattern recognition receptors

pTfh: peripheral T follicular helper cell

pVL: plasma viral load

PWH: people with HIV.

rev: regulator of gene expression

RMD: romidepsin

RNA: ribonucleic acid

RPP30: ribonuclease P/MRP subunit p30

RT-PCR: reverse transcription polymerase chain reaction

SAMHD1: SAM/HD domain containing deoxynucleoside triphosphate triphosphohydrolase 1

SERINC5: serine incorporator 5

SIGLEC1: sialic acid binding Ig like lectin 1

SIRT2: sirtuin-2

SIV: simian immunodeficiency virus

SLFN11: schlafen 11 protein

SN: seronegative

SNCA: alpha-synuclein

SNPs: single nucleotide polymorphisms

tat: trans-activating regulatory gene

Tau: tau protein

TBP: TATA-box binding protein

TCR: T cell receptor

Tfh: T follicular helper cell

TGF-β: transforming growth factor beta

TIGIT: T cell immunoreceptor with Ig and ITIM domains

TIM-3: T cell immunoglobulin and mucin domain-containing protein 3

TLR: toll-like receptor

TNF: tumor necrosis factor

TRIM5α: tripartite motif containing 5 alpha

Trm: resting memory T cell

Tscm: stem cell-like memory T cell

UCHL1: ubiquitin carboxyl-terminal hydrolase L1

UNAIDS: united nations programme on HIV/AIDS

VC: viremic controller

vif: virion infectivity factor

VNP: viremic non-progressor

Vpr: viral protein R

Vpu: viral protein U

ABSTRACT

Combined antiretroviral therapy (cART) is the current treatment for people with HIV (PWH) that allows to turn this otherwise deadly disease into a chronic infection. Although these drugs maintain undetectable viral load and stop the progression of AIDS disease, access to cART is not ensured worldwide, requires life-long medication and can cause secondary effect associated with drug toxicity. Additionally, if the medication is stopped, a rapid viral rebound occurs due to the virus ability to establish a latent viral reservoir.

One of the strategies to develop potential HIV-1 cure strategies, is to analyze a small subset of HIV-1 infected individuals that present the natural capacity to control the virus, known as elite controllers or long term non-progressors. Although some aspects such as neutralizing antibodies, NK cells and CD8 T-cell response or soluble factors differ between individuals that can control the infection versus those that cannot, the mechanisms associated with this natural control are not fully understood. In the present thesis, we have used different proteomics approaches to identify plasma factors associated with HIV-1 control or non-control and to define biomarkers linked to neurological dysfunction in HIV-1 infection. In parallel, this proteomics analysis was applied to the BCN02 clinical trial, a "kick and kill" HIV-1 therapeutic strategy, to identify plasma factors that can predict viral rebound before initiating an antiretroviral treatment pause.

In Chapter I, we identified different plasma factors associated with HIV-1 control in the absence of treatment compared to HIV-1 uninfected individuals. In brief, the plasma as well as cerebrospinal fluids were analyzed in individuals with different levels of control of HIV-1 infection and compared to HIV-1 uninfected individuals. Then, we selected those plasma markers that differed between individuals that control the virus and HIV-1 non-controllers. These markers were strongly associated with additional viral parameters and other well-known biomarker related to neuroinflammation. Interestingly, cART treatment restored the plasma levels of these proteins, suggesting that cART treatment may reduce HIV-related neurological dysfunction.

In chapter II, we studied neuro-tailored plasma proteomes of PWH with different capabilities to control HIV-1 infection. Interestingly, a NAD (nicotinamide adenine dinucleotide)-dependent deacetylase, Sirtuin-2, was differentially detected and associated with viral control. Also, Sirtuin-2 was related to biomarkers described in other neurological diseases. The plasma levels of Sirtuin-2 were dependent on the time when cART was initiated and were associated with the involution of a specific brain region, in particular the orbitofrontal cortex. Moreover, *in vitro* targeting of SIRT2 reduced viral reactivation from latency and viral replication in peripheral blood cells and primary microglial cells. These results suggest that SIRT2 can serve as a biomarker of HIV-1 control and neurological dysfunction and could be a potential therapeutic target for a HIV-1 cure strategy.

In Chapter III, we analyzed the plasma proteome during the BCN02 clinical trial, which was based on a "kick and kill" HIV-1 cure strategy. Participants in the clinical trial were treated with romidepsin to reactivate HIV-1 in latently infected cells and vaccinated with HIVconsv vaccines to generate robust T-cell responses. Then, participants interrupted their cART treatment during a monitored antiretroviral pause (MAP) to evaluate the efficacy of this "kick and kill" strategy. In this context, we identified possible candidate plasma markers that predicted the viral rebound during the monitored antiretroviral pause. This exploratory study revealed how this intervention modified the levels of plasma proteins, especially after romidepsin infusions. Moreover, proteomics analysis identified the levels of the plasma CD33 protein to be associated with viral parameters, establishing it as a possible plasma biomarker indicative of monitored antiretroviral virus control, at least during short-term treatment interruption.

Overall, proteomics analyses allowed us to identify possible biomarkers that reflect pathogenic processes or the responses to therapeutic interventions. These candidate proteins may provide new potential therapeutic targets for novel HIV-1 cure strategies.

RESUM

La teràpia antirretroviral combinada és el tractament actual per a persones amb VIH que permet convertir aquesta malaltia mortal a una infecció crònica. Tot i que aquests fàrmacs mantenen la càrrega viral indetectable i frenen la progressió de la malaltia de la Sida, l'accés als antirretrovirals no està garantit a tot el món, requereix medicació de per vida i també pot causar efectes secundaris associats a la toxicitat d'aquests fàrmacs. A més a més, si s'atura la medicació, es produeix un ràpid rebot viral causat per la capacitat que té el virus d'establir reservori latent viral.

Una de les estratègies per desenvolupar potencials teràpies per la cura del VIH-1 és analitzar un petit subconjunt d'individus infectats pel VIH-1 que presenten la capacitat natural de controlar el virus, aquests individus es coneixen com a controladors d'èlit. Tot i que alguns elements com els anticossos neutralitzants, les cèl·lules NK i la resposta de les cèl·lules T CD8 o els factors solubles difereixen entre aquests individus que poden controlar la infecció del VIH-1 i els que no, els mecanismes associats a aquest control natural encara no estan ben descrits. En aquesta tesi, hem utilitzat diferents eines proteòmiques per identificar factors plasmàtics associats al control o no control del VIH-1, per tal de definir biomarcadors relacionats amb la disfunció neurològica causada per la infecció del VIH-1. Paral·lelament, aquesta anàlisi proteòmica es va aplicar a l'assaig clínic BCN02, una intervenció terapèutica per la cura del VIH-1 basada en la estratègia "kick and kill", per identificar altres factors plasmàtics que poden predir el rebot viral abans d'iniciar una pausa del tractament amb antirretrovirals.

En el capítol I, vam identificar diferents factors plasmàtics associats al control del VIH-1 en absència de tractament en comparació amb individus no infectats pel VIH-1. En resum, es van analitzar el plasma i el líquid cefaloraquidi d'individus amb diferents nivells de control de la infecció pel VIH-1 en comparació amb els individus no infectats pel VIH-1. A continuació, vam seleccionar aquells marcadors plasmàtics que diferien entre individus que controlen el virus i no controladors del VIH-1. A més a més, alguns dels marcadors selccionats vam veure que estaven fortament associats amb paràmetres virals i altres biomarcadors coneguts relacionats amb neuroinflamació.

Curiosament, el tractament amb antirretrovirals va restaurar els nivells plasmàtics d'aquests candidats, cosa que indica que el tractament amb antirretrovirals pot reduir la disfunció neurològica causada pel VIH-1.

En el capítol II, hem estudiat proteomes plasmàtics, amb en enfoc neurològica, en persones amb VIH-1 amb diferents capacitats per controlar la infecció amb el VIH-1. Curiosament, vam detectar de manera significativament diferent una desacetilasa dependent de NAD (dinucleòtid de nicotinamida i adenina), Sirtuin-2, que també es va veure associada amb el control viral. A més a més, aquest marcador estava relacionat amb alguns biomarcadors descrits en altres malalties neurològiques. Els nivells plasmàtics de SIRT2 vam observar que depenien del moment en què es va iniciar el tractament combinat amb antirretrovirals i estaven associats amb la involució d'una regió específica del cervell, l'escorça orbitofrontal. A més a més, els experiments *in vitro* d'inhibició de SIRT2 van reduir la reactivació viral de la latència i la replicació viral en cèl·lules de la sang perifèrica i en cèl·lules glials primàries. Aquests resultats suggereixen que SIRT2 pot servir com a biomarcador del control del VIH-1 i de la disfunció neurològica i podria ser una potencial diana terapèutica per a una estratègia per la cura del VIH-1.

En el capítol III, es va analitzar el proteoma plasmàtic de participants de l'assaig clínic BCN02, basat en una estratègia "kick and kill". Els participants de l'assaig clínic van ser tractats amb romidepsina per reactivar les cèl·lules latents infectades pel VIH-1 i vacunats amb l'immunogen HIVconsv per generar resposta de cèl·lules T. Per avaluar l'eficàcia d'aquesta estratègia els participants van interrompre el tractament d'antirretrovirals durant una pausa antirretroviral controlada. En aquest estudi, vam identificar possibles marcadors plasmàtics que es poden utilitzar per predir el rebot viral durant una pausa antirretroviral controlada després de la intervenció. Aquest estudi exploratori ens va permetre revelar com la intervenció va modificar els nivells de proteïnes plasmàtiques, especialment després de les infusions de romidepsina. A més a més, l'anàlisi proteòmica va identificar l'associació entre els nivells plasmàtics de CD33 amb paràmetres virals, establint-lo com a un possible biomarcador plasmàtic indicatiu del control viral durant la monitorització de la interrupció del tractament, almenys durant la interrupció del tractament a curt termini.

En conjunt, aquestes anàlisis proteòmiques ens van permetre identificar possibles biomarcadors que reflecteixen processos patogènic o la resposta a intervencions terapèutiques. Aquestes proteïnes candidates poden proporcionar noves dianes terapèutics per a noves estratègies per la cura del VIH-1.

RESUMEN

La terapia antirretroviral combinada es el tratamiento actual para las personas con VIH que les permite convertir esta enfermedad mortal en una infección crónica. Aunque estos fármacos mantienen la carga viral indetectable y frenan la progresión de la enfermedad del Sida, el acceso a los antirretrovirales no está garantizado en todo el mundo, requiere medicación de por vida y también puede causar efectos secundarios asociados a la toxicidad de estos fármacos. Además, si se interrumpe la medicación, se produce un rápido rebote viral causado por la capacidad que tiene el virus en establecer un reservorio latente viral.

Una de las estrategias para desarrollar potenciales terapias para la cura del VIH-1 es analizar un pequeño subconjunto de individuos infectados por VIH-1 que presentan la capacidad natural de controlar el virus, estos individuos se conocen como controladores de élite. Aunque algunos elementos como los anticuerpos neutralizantes, las células NK y la respuesta de las células T CD8 o los factores solubles difieren entre los individuos que pueden controlar la infección y los que no, los mecanismos asociados a este control natural todavía no están bien descritos. En esta tesis, hemos utilizado diferentes herramientas proteómicas para identificar factores plasmáticos asociados al control o no control del VIH-1 para definir biomarcadores relacionados con la disfunción neurológica causada por la infección por VIH-1. Paralelamente, este análisis proteómico se aplicó en el ensayo clínico BCN02, una estrategia terapéutica "kick and kill" contra el VIH-1, para identificar otros factores plasmáticos que puedan predecir el rebote viral antes de iniciar la interrupción del tratamiento con antirretrovirales.

En el capítulo I, hemos identificado distintos factores plasmáticos asociados al control del VIH-1 en ausencia de tratamiento en comparación con individuos no infectados por el VIH-1. En resumen, se analizaron el plasma y el líquido cefalorraquídeo de individuos con distintos niveles de control de la infección por el VIH-1 en comparación con los individuos no infectados por el VIH-1. A continuación, seleccionamos aquellos marcadores plasmáticos que diferían entre individuos que controlan el virus y no controladores del VIH-1. Además, estos marcadores estaban fuertemente asociados a

parámetros virales y otros biomarcadores conocidos relacionados con neuroinflamación. Curiosamente, el tratamiento con antirretrovirales restauró los niveles plasmáticos de estos candidatos, indicando que el tratamiento con antirretrovirales puede reducir la disfunción neurológica relacionada con el virus.

En el capítulo II, hemos estudiado proteomas plasmáticos, con un enfoque neurológico, en personas con VIH-1 con diferentes capacidades para controlar la infección por el VIH-1. Curiosamente, detectamos de forma significativamente diferente una desacetilasa dependiente de NAD (dinucleótido de nicotinamida y adenina), Sirtuin-2, que también se vio asociada con el control viral. Este marcador, además, estaba relacionado con algunos biomarcadores descritos en otras enfermedades neurológicas. Curiosamente, observamos que los niveles plasmáticos de SIRT2 eran dependientes del momento del inicio del tratamiento con antirretrovirales, y estos niveles estaban asociados con la involución de una región específica del cerebro, la corteza orbitofrontal. Además, los experimentos *in vitro* de inhibición de SIRT2 redujeron la reactivación viral de la latencia y la replicación viral en células de la sangre periférica y en células gliales primarias. Estos resultados sugieren que SIRT2 puede servir como biomarcador del control del VIH-1 y la disfunción neurológica y podría ser una potencial diana terapéutica para una estrategia de cura del VIH-1.

En el capítulo III, se analizó el proteoma plasmático de participantes del ensayo clínico BCN02, basado en una estrategia "kick and kill". Los participantes del ensayo clínico fueron tratados con romidepsina para reactivar las células latentes infectadas por el VIH-1 y vacunados con el inmunogeno HIVconsv para generar respuesta de células T. Para evaluar la eficacia de esta estrategia los participantes interrumpieron el tratamiento con antirretrovirales durante una pausa antirretroviral controlada. En este estudio, identificamos posibles marcadores plasmáticos que se pueden utilizar para predecir el rebote viral durante una pausa antirretroviral controlada después de la intervención. Este estudio exploratorio nos permitió revelar cómo la intervención modificó los niveles de proteínas plasmáticas, especialmente después de las infusiones de romidepsina. Además, el análisis proteómico identificó la asociación entre los niveles plasmáticos de CD33 con parámetros virales, estableciéndolo como un posible biomarcador plasmático indicativo del control viral durante la monitorización de la

interrupción del tratamiento, al menos durante la interrupción del tratamiento a corto plazo.

En conjunto, estos análisis proteómicos nos permitieron identificar posibles biomarcadores que reflejan procesos patogénicos o la respuesta a intervenciones terapéuticas. Estas proteínas candidatas pueden proporcionar nuevas dianas terapéuticos para nuevas estrategias para la cura del VIH-1.

INTRODUCTION

1.1. Introduction to HIV-1 and AIDS

1.1.1. Epidemiology of HIV

In 1981, the Center of Diseases Control (CDC) in USA reported five cases of *Pneumocystis carinii* in healthy young men, that had no previous record of disease (1), but presented with the same clinical manifestations, most markedly with a profound depletion of CD4 T-lymphocytes. This unknown disease was called Acquired Immune Deficiency Syndrome (AIDS) (2). In 1983, researchers of the Institute Pasteur discovered a new retrovirus that was proposed to be the causative microorganism of AIDS (3). Between 1984-1985, two independent groups confirmed the relationship between AIDS and the new virus. In parallel, a T-cell tropic virus was discovered in monkeys that was closely related to the new retrovirus (4)(5). In 1986, the retrovirus, known as human T-cell leukemia virus type III or AIDS-associated retrovirus was renamed to Human Immunodeficiency Virus (HIV) by the International Committee on the Taxonomy of Viruses (6). Thereafter, many groups have investigated the commonalities between simian immunodeficiency virus (SIV) and HIV, concluding that the origin of the HIV was a zoonotic infection, transferred from chimpanzees to humans (7)(8).

Forty years after the first AIDS cases, HIV infection remains a devastating pandemic that poses a major global health issue. According to the Joint United Nations Programme on HIV/AIDS (UNAIDS), since the pandemic started, 76.1 million people have been infected by HIV and 35 million people have died due to AIDS or related disease. Approximately 38.4 million of people are currently infected with HIV. Despite being a worldwide pandemic, prevalence of this infection is very different between continents. Africa is the most affected continent with 43% of all new worldwide infections. Importantly, at the end of 2021, 28.7 million people with HIV were receiving antiretroviral therapy (ART), still leaving 9.7 million people that cannot access treatment (9). The access to effective ART has significantly reduced the infection rate and the number of HIV-related deaths. ART has thus effectively helped to transform HIV infection from an infection with highl mortality into a chronic and manageable disease (10). With early diagnosis and treatment, patients in developed countries can

expect a close to normal life expectancy, although this varies depending on the mode of HIV transmission, race and CD4 T cell count (11).

1.1.2. HIV-1 structure and genome

HIV virus is a retro transcribing virus that belongs to the *Retroviridae* family *and Lentivirus* genus (12). There are two different types of HIV: HIV-1 and HIV-2, which differ in their pathogenesis and replicative capacity and in the prevalence in the world. HIV-1 virus are spherical particles of 80-150nm wrapped by an envelope (13). This envelope

outer coat of HIV-1, made up of two layers of lipids that contain trimers of the envelope glycoproteins Gp160. The Gp160 protein consist of a Gp120 protein anchored to the membrane by the Gp41 transmembrane protein (14). Attached to the envelope there is the matrix, that provides the structure and mechanical support of the virus. The matrix contains the capsid core and the nucleocapsid. Within the capsid, there is a double single-stranded positive-sense RNA protected by the nucleocapsid proteins along with protease, reverse transcriptase and integrase enzymes (Figure 1) (15).
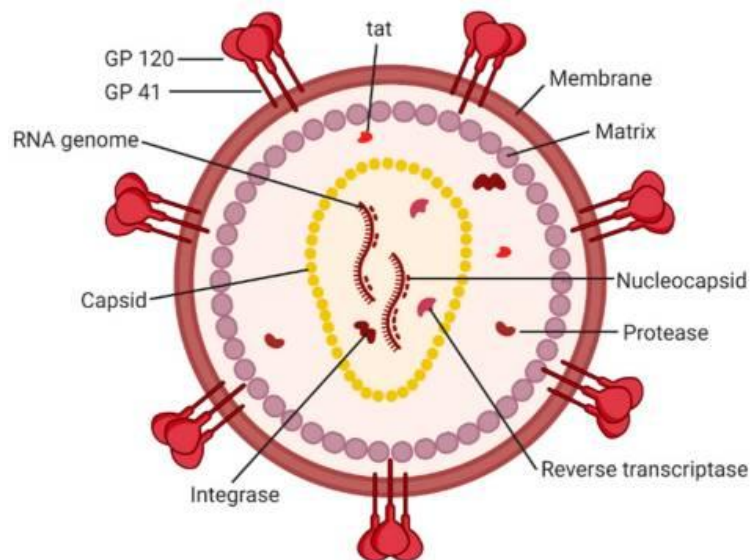
Figure 1. Structure of HIV-1 virion. Schematic representation of the structure of the mature infectious HIV-1 viral particle. Image adapted from (16).

The HIV-1 genome has a length of approximately 10 kb, flanked by a repeat sequence known as the long terminal repeats (LTR) (17)(18). The HIV-1 genome contains nine genes that encode for sixteen proteins.

- Group-specific antigen (gag) gene sequence that codifies for the Gag polyprotein, which is expressed to generate the viral structure and which contains the matrix (or p17), capsid (or p24) and nucleocapsid (or p7) and late assembly (or p6) proteins.

- Polymerase gene (pol) that codes for viral enzymes including reverse transcriptase to transcribe RNA to DNA, integrase responsible to integrate the viral DNA into the host genome and protease, which cleaves the immature Gag polyprotein into its subunits.

- Envelope gene (env) codifies for the gp160 protein which consists of gp120 and gp41 proteins, localized in the viral enveloped and responsible for viral fusion with infected cells.

- Regulatory genes include the trans-activating regulatory gene (tat) that codifies Tat protein required for the elongation of viral transcripts and regulator of gene expression (rev) that promotes nuclear export of spliced viral RNAs.

- Accessory genes such as virion infectivity factor (vif), viral protein R (vpr), viral protein U (vpu) and negative factor (nef), which are necessary proteins to regulate viral replication and can mediate evasion from host defense mechanisms (Figure 2) (17)(18)(19).
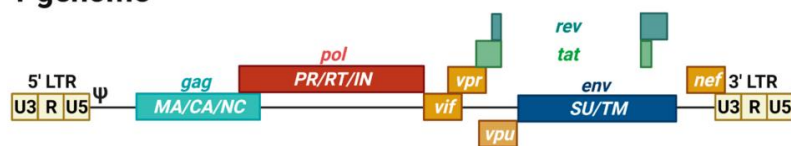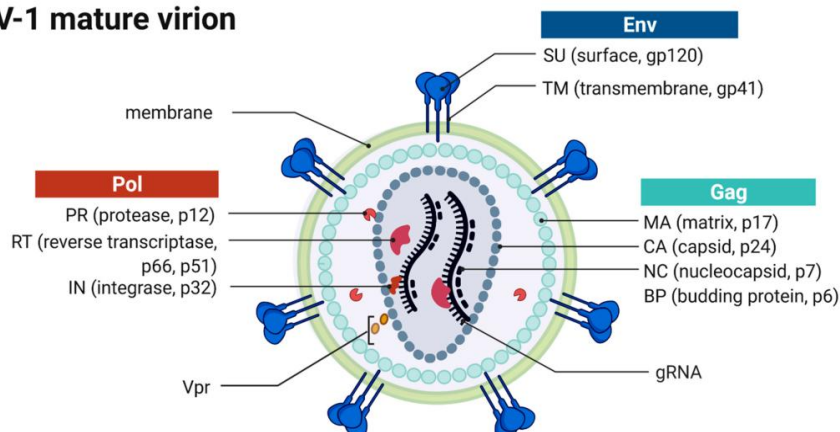
Figure 2. HIV-1 genome and virion structure. (Top) Schematic representation of the HIV-1 genome encompassing the open reading frames coding for the different structural, regulatory, and accessory proteins. (Bottom) Schematic representation of the structure of the mature infectious HIV-1 virion. Image adapted from (18)

1.1.3. HIV-1 life cycle

The HIV-1 life cycle has seven steps. The first step is the binding or attachment which starts when the envelope protein Gp120 of the virus binds to the host receptor of the CD4 expressing target cell together with the co-receptors C-C chemokine receptor type 5, CCR5 (viral co-receptor on macrophages) or C-X-C chemokine receptor type 4, CXCR4 (viral co-receptor on T-cell) (20)(21). After the binding occurs, the conformation of the envelope protein changes, exposing Gp41 coiled coils which leads to the fusion of HIV-1 with the host cell membrane (22). Then, viral RNA and viral proteins are released into the cytoplasm of the host cell while the capsid is disintegrated (23). One of the released proteins, reverse transcriptase then retro-transcribes single-stranded RNA into double-stranded DNA (24). Due to the poor fidelity of the reverse retro-transcriptase enzyme, the retro-transcription generates some DNA mutations that contribute to virus genome variability and evolution (25). After generating the dsRNA, integrase enzymes remove two nucleotides of the 3' end of the viral DNA, and with the involvement of host and viral proteins, the pre-integration complex is formed. This is then transported into the nucleus where the integrase enzyme ligate the processed DNA into the host chromosome (26). Then, a portion of intagrated DNA can be transcribed by polymerase enzyme generating HIV-1 RNA transcripts or can remain latent forming the viral reservoir. HIV-1 RNA transcripts are translated in the cytoplasm producing the early proteins Tat, Rev and Nef. Then, Tat and Rev are translocated into the nucleus where Tat increases the rate of transcription and Rev leads to the transcription of single and unspliced mRNAs of gag, pol, env, vif, vpr and vpu (27)(28). All these transcripts are translocated to the cytoplasm to be translated into viral proteins. Immature HIV-1 particles are generated with all the newly translated proteins, locate to the host cell membrane where the viral protease enzyme cleaves

Gag and Gag-Pol polyproteins to form new mature viral particles containing viral RNA and HIV-1 accessory proteins (Figure 3) (29).
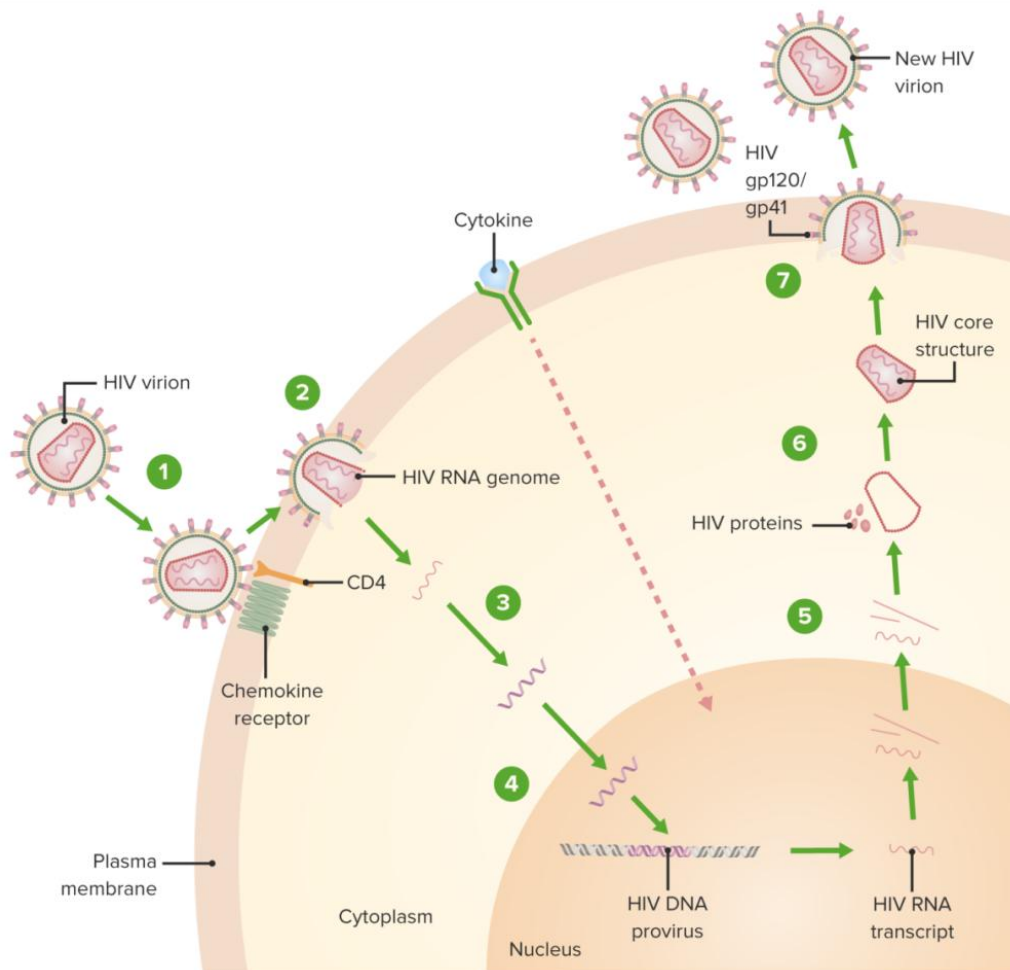
Figure 3. HIV-1 life cycle. Schematic overview of the HIV-1 replication cycle. The figure illustrates the main steps in the HIV-1 life cycle. (1) Attachment or binding of the HIV-1 virus receptors with the host receptor cells. (2) Fusion of both membranes. (3) Viral RNA is retro-transcribed by the viral retro-transcriptase. (4) Viral DNA is transported into the nucleus and integrated in the host genome by the viral integrase. (5) HIV-1 DNA can be transformed in a latent state (HIV-1 DNA provirus) or can be transcribed into new viral RNA molecules. (6) Viral RNA is transported to the cytoplasm where it is translated into viral proteins to form new HIV-1 virions. (7) New HIV-1 virions are released into the extracellular compartment to infect new cells. Image adapted from www.lecturio.com

1.2. Clinical course of HIV-1 infection and host immune response

1.2.1. Clinical course of HIV-1 infection

The HIV-1 transmission can occur by body fluids of infected people including semen, vaginal secretion, blood or breast milk. It can also be transmitted from mother to child in utero or during delivery by vertical transmission. The route that represents the highest proportion of new infections is the sexual transmission via the lower genital tract and rectal mucosa (30). HIV-1 infection has been thought to be established by the propagation of a single transmitted virus, but this view has been questioned and depends on the route of transmission. For example, in the case of sexual transmission, virus can penetrate the epithelium reaching dendritic cells, Langerhans cells and intraepithelial CD4 T-cells, from where the virus reaches the lymph nodes and is disseminated into the blood to establish infection in CD4 T-cells (31)(32). The natural course of HIV-1 infection evolves from acute to established chronic infection which, in the absence of treatment, progresses in the vast majority of individuals to AIDS. The clinical course of HIV-1 infection is characterized by an increase of the HIV-1 viral load, a reduction in the CD4 T-cell counts and a chronic immune activation, which leads to exhaustion of the immune system (33)(34).

The first days of HIV-1 infection are referred to as the eclipse phase, when the virus starts to replicate and the infection spreads to different tissues, while the plasma HIV-1 viral load is still undetectable (35). Then, during the acute HIV-1 infection phase, HIV-1 plasma viral load increase exponentially with the consequence of a notable decrease of CD4 T-cells, which is thought to be at least partly driven by viral cytopathic effects for the host immune response. During this phase, individuals develop an acute retroviral syndrome that is characterized by fever, lymphadenopathy and rash. Usually, the viral load increases drastically to a peak and then drops rapidly to a stable steady state, this is often referred to the viral set point. Also, seroconversion occurs when immune system starts to generate antibodies against HIV-1 antigens (36)(37).

Thereafter, the infection enters into a chronic phase that can last from 8 to 10 years and is characterized by stable levels of HIV-1 viral load and slowly decreasing CD4 T-cell counts. In that phase, the virus is disseminating and replicating, for that reason, the

immune system is continuously activated and generates cytokines in response to the virus, viral antigens and the virus-specific immune response (31).

Finally, in the absence of treatment, the patient starts manifesting AIDS defining symptoms with CD4 T-cells counts dropping to below 200 cells/mm^3 and HIV-1 viral load increasing. At this point, opportunistic infections and AIDS-related diseases occur, including cancers, kidney failure and opportunistic infections that can cause death of the infected individual (Figure 4) (38).
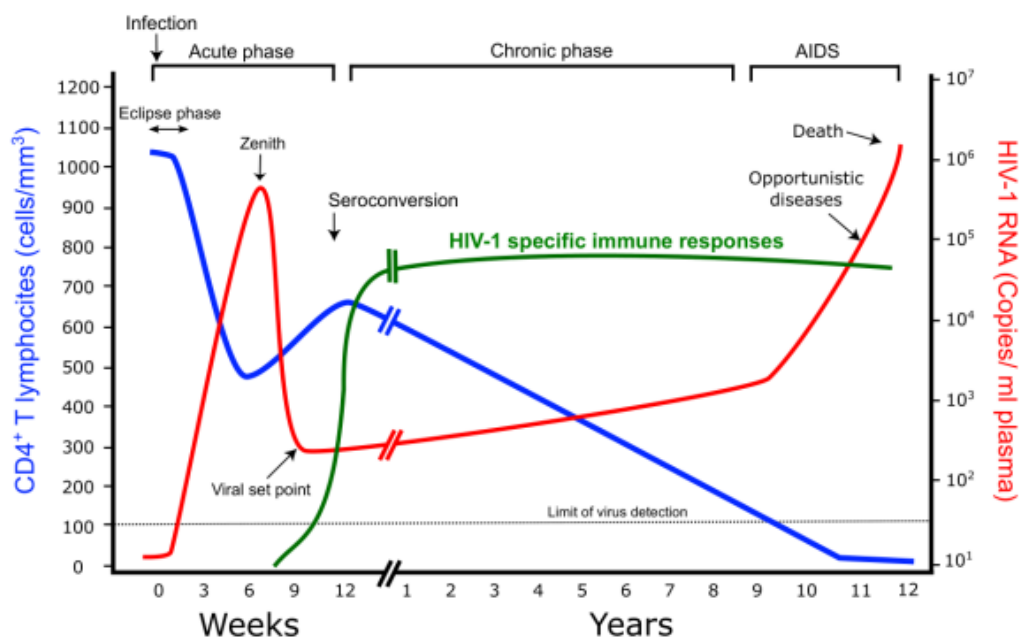
Figure 4. Clinical course of HIV-1 infection. Schematic representation of the natural HIV-1 course of infection in the absence of antiretroviral therapy. Represented in blue CD4 T-lymphocytes count, in red HIV-1 RNA copies/ml and in green HIV-1 specific immune responses. Image adapted from www.scistyle.com.

1.2.2. HIV-1 associated comorbidities

With the introduction of cART, HIV-1 infection and viral disease has been transformed from a progressive deadly infection to a stable chronic and treated disease. This fact means that PWH live longer but may suffer the effects of long-term cART toxicity and an increase in the prevalence of comorbidities. The appearance of such comorbidities occurs at an earlier age compared to non-HIV-1 infected people, suggesting a

premature aging in PWH (39)(40), The most frequent comorbidities in this individuals are: cardiovascular diseases, chronic renal disease, manifestations of hepatitis B and C infections, malnutrition that can cause anemia and nutritional deficiencies, mental/psychiatric disorders and malignant neoplasms especially affecting connective and soft tissue, digestive organs and lymphoid and hematopoietic tissues (40).

Of note, also mental and psychiatric disorders referred to globally as HIV-associated neurocognitive disorders (HAND) can occur when HIV-1 penetrates the brain and causes, neuronal damage and neurocognitive dysfunction (40). The mechanisms that causes HAND comorbidities are not clearly understood and it is unclear whether infection of the CNS is an absolute prerequisite for HAND. Different types of mechanisms have been suggested for CNS infection. For instance, infection with HIV-1 causes a systemic activation of immune cells that can stimulate transmigration of lymphocytes and monocytes across the blood brain barrier (BBB) (41). Within the CNS, immune cells release pro-inflammatory signals that stimulate immune cell influx and can disrupt the BBB (42). Some of the attracted cells can also be infected with HIV-1, promoting the local production of virions that infect CNS cells, including perivascular macrophages, microglial cells and astrocytes. This facilitates the generation of the CNS HIV-1 compartmentalization and can facilitate the formation of a HIV-1 reservoir in the brain (41)(43)(44). Finally, activated microglia and perivascular macrophages release neurotoxic immune products and neurotoxic HIV-1 proteins, such as Tat, which can further drive neuronal dysfunction and damage, producing neopterin, platelet-derived growth factor (PDGF) and monocyte chemoattractant protein 1 (MCP-1) (45). Thus, HIV-1 can affect directly and indirectly normal neuronal activity by a combination of neurotoxic proteins and inflammatory cytokines altering neuronal pathways and promoting neuroinflammation (Figure 5) (46).

HAND can be classified in different stages depending on the severity of the neurocognitive disorder, ranging from asymptomatic neurocognitive impairment (ANI), mild neurocognitive disorder (MND), to HIV-associated dementia (HAD). With the introduction of cART, the incidence of the severe conditions has reduced and the majority of neurologically affected PWH suffer a mild or asymptomatic disease (47)(48). Interstingly, these neurocognitive disorders present commonalities with some

other neurodegenerative disorders, not driven by HIV-1 infection and can share different dysregulated genes and biological process (49). For example, it has been reported that an increase of beta-amyloid plaques, a common biomarker of Alzheimer disease, can be detected in post-mortem brain tissues of PWH. Moreover, some studies reported an association between Parkinson´s Disease and viral infections, but these Parkinson´s-like syndrome can be reverted by ART (50). Furthermore, HIV-1 infection decreased dopamine levels which could be associated with the decrease of dopamine transporters, as dopamine can activate and produce inflammatory molecules. This could change the immune system of the central nervous system (CNS), contributing to similar pathological changes that occur in multiple sclerosis (51).
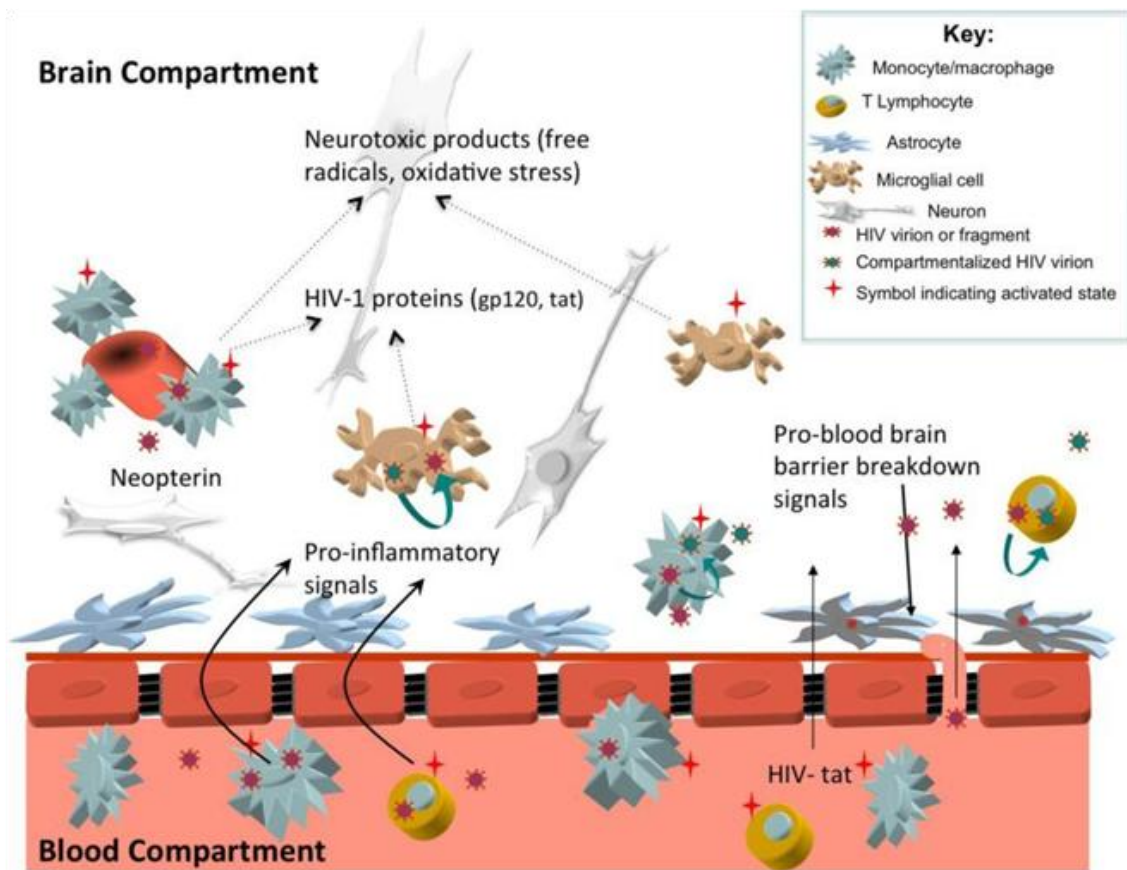
Figure 5. Mechanisms of HIV-1 viral entry and establishment producing inflammation and injury in the CNS. Image adapted from (46).

1.2.3. Host immune response and host restriction factors

The innate immune response represents the first barrier of defense against a pathogen and it is initiated by the recognition of conserved molecular structures of the pathogen, known as pathogen associated molecular patterns (PAMPs). Such PAMPs can be recognized by pattern recognition receptors (PRRs) of the host cells, many of which are expressed on innate immune cells as well. There are different PRRs receptors depending on the biological compound that they recognize. For example, toll-like receptors (TLRs) recognize intracelular and exrtacellular lipids, lipoproteins and proteins originating from virus, bacterial, parasite and fungus, RIG-I receptors that recognize viral RNA molecules and cGAS-STING that recognize cytosolic DNA. Once the PAMP is recognized by PRR, a cascade of innate signaling pathways is initiated, leading to the activation of the host´s anti-viral response (52)(53). The anti-viral response is characterized by the activation of NF-kB transcription factor that leads to the production and secretion of inflammatory interferon type I cytokines. These in turn are potent inhibitors of viral pathogens and stimulate expression of some interferon stimulated genes (ISGs) that excert antiviral activities. For example, there are different restriction factors induced by interferon that have the ability to restrict viral replication at different stages in the virus life cycle, including APOBEC3, SAMHD1, TRIM5alpha, Tetherin and SERINC5, has been described (54)(53).

Macrophages and dendritic cells are the major producer of interferon (IFN), generating a pro-inflammatory environment that enhances the migration of natural killers and more macrophages and dendritic cells into the site of infection. These cells are professional antigen presenting cells (pAPC), that serve to recruit and stimulate adaptive immune cells such as CD4 T-helpers cells, B-cells and CD8 T-cells. Natural killers (NKs) are the intermediary cells between innate and adaptive immune response. NK immunoglobulin-like receptors (KIR) interact with human leukocyte antigen (HLA) class I molecules, triggering a quick activation and expansion of NK cell to eliminate virally infected cells. Another way to eliminate HIV-1 infected cells is via CD8 T-cells that recognize HIV-1 infected cells presenting HIV-1 derived epitopes on their HLA class I molecules. Interaction with the T-cell receptor (TCR) of these CD8 T-cells leads to a

cytotoxic program in the CD8 T-cells, effectively eliminating the HIV-1 infected cells (55). Although CD4 T-cells are the target cells of HIV-1, the vast majority of CD4 T-cells remain uninfected and these can be activated upon recognition of HIV-1 presented peptides by antigen-presenting cells through HLA class II molecules enhancing the CD4 and CD8 T-cell response (56).

Furthermore, B-cells are also activated and mature into plasma cells and generate antibodies. Among the different types of antibodies that can be generated, IgM are the first type to be produced and then IgG antibodies are produced in collaboration with CD4 T-cell help. Nevertheless, these antibodies are generally inefficient and lack the capacity to neutralize the autologous virus and to block or eliminate the infection (57).

The immune system is not capable to resolve HIV-1 infection due to the virus capacity to escape the adaptive immune responses by evolving rapidly variants that are not detected by HIV-1 specific T-cells or antibodies. Thus, during the chronic phase of the infection, innate immune response is continuously active but the adaptive immune response is disrupted by viral escape or exhaustion. Toghether with the establishment of viral reservoir, this leads to the chronic state of the infection with ongoing viral replication (58).

1.2.4. Cellular and anatomical establishment of HIV-1 reservoir

Several studies have shown that the latent HIV-1 reservoir is established in very early stages of the infection (59). While the administration of cART does not prevent the establishment of the viral reservoir, the early administration of cART reduces the viral reservoir size and its diversity, as viral replication is limited (60)(61)(62)(63).

A large number of studies have investigated which cells and cell types are the main components of the viral reservoir. While it has been well established that the HIV-1 infected resting memory CD4 T-cells (Trm) contribute importantly to viral reservoir, over the last years additional cell populations have been shown to harbor latent virus as well, including stem cell-like memory T-cells (Tscm), T-follicular helper cells in the germinal center (Tfh) and peripheral T-follicular helper cells (pTfh). In addition,

different myeloid cell types have been shown to contribute to the latent viral reservoirs, complicating viral eradication strategies (64).

There are several models that aim to explain the establishment of HIV-1 latency in the T-cell compartment, yet the precise mechanisms still remain elusive. One possible model suggests that latency is established by activated HIV-1 infected CD4 T-cells that revert to a resting state in which there is no viral gene expression. Another model suggests that direct infection of CD4 T-cells reverting to a G0 resting memory state contain latent virus (65). Alternatively, latency may be established through direct infection of tissue resident memory T-cells or the infection of activated CD4 T-cell that return to a resting state as Trm cells (66)(67)(68)(69). All these mechanisms are not mutually exclusive and all mechanisms may contribute to the overall reservoir pool. Tscm is another cell population that contributes to the latent viral reservoir, especially also because these cells express the HIV-1 correceptors (CCR5 and CXCR4) (70)(71). Furthermore, the long half-life and capacity for self-renewal, suggest that Tscm could be involved in maintenance of the latent HIV-1 reservoir through homeostatic proliferation (72). In addition, the formation of HIV-1 reservoirs in Tfh and pTfh is thought to depend on the infection of Tfh precursor cells, rather than Tfh themselves, as Tfh cells have low CCR5 expression (Figure 6) (73)(74).

Moreover, a recent study that analyzed the transcriptomic differences between HIV-1 DNA$^+$ and HIV-1 DNA$^-$ in memory CD4 T-cells reported that a set of four genes *EHMT1*, *RBBP4* and *MTA1* are linked to negative regulation of HIV-1 transcription and are higher expressed in HIV-1 DNA$^+$ cells. Oppositely, four different genes; *GTF2I*, *MAPKAPK3*, *NCOA1* and *SNW1* are linked to positive regulation of HIV-1 transcriptional process and were lower expressed in HIV-1 DNA$^+$ cells (75).
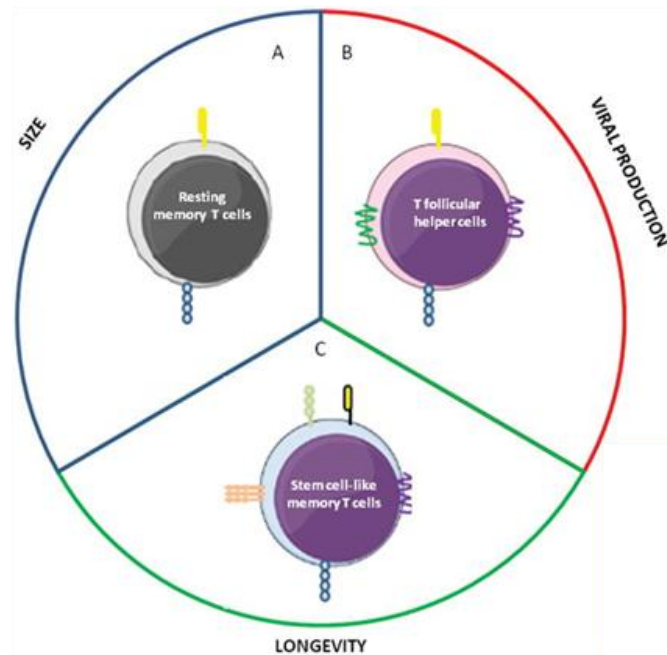
Figure 6. Main cellular compartments of HIV-1 reservoir. A) Resting memory CD4 T-cells (Trm) could contribute to the size of viral reservoir. B) Follicular helper CD4 T-cells may contribute to viral production of the viral reservoir. (C) Stem cell-like memory T-cells (Tscm) could be involved in maintenance/longevity of the latent HIV-1 reservoir. Image adapted from (64).

Finally, some studies have focused their attention on soluble or cell surface markers in latently infected cells to identify potentially targetable molecules that could be leveraged for the elimination of such latently infected cells. Soluble factors such as immunomodulatory cytokines have an important role in the establishment of the viral reservoir. For example, IL-10 and TGF-beta, are involved in the immunosuppressive phase of the immune response contributing to the generation of a viral reservoir with latently infected cells by reducing T-cell activation (76). Other cytokines, such as IL-2 and IL-7 induce SAMHD1 phosphorylation in primary CD4 T-lymphocytes, removing the antiviral activity of SAMHD1 and thereby facilitating the infection of memory T-cells and possibly allowing for the establishment of a viral reservoir in these cells (77).

Alternatively, molecules referred to as immune checkpoint inhibitors, regulate the immune responses and activation levels of T-cells. Thus, immune checkpoint regulators

can control T-cell activation and promote quiescence and HIV-1 latency (78). It has been reported that a combination of three immune checkpoints, PD-1, TIGIT and LAG-3, correlates with the presence of integrated HIV-1 DNA. Indeed, CD4 T-cells expressing the three markers simultaneously contain ten times more HIV-1 DNA than total CD4 T-cells (79)(80). Another CD4 T-cell surface marker for transcriptionally active HIV-1 reservoirs is CD30. Targeting CD30 was shown to decrease HIV-1 outgrowth activity, indicating that cells expressing CD30 carry replication-competent proviruses (81). Similarly, analyzing the transcriptome of unstimulated latently infected primary CD4 T-cells, CD32a was detected as a marker of the CD4 T-cell HIV-1 reservoir harboring replication-competent proviruses. Indeed, sorted CD32a$^+$ CD4 T-cells from ART-treated individuals showed a 30 times higher HIV-1 DNA content and elevated replication competent viruses than cells in the CD32a negative fraction (80)(82). Additionally, it has been reported that cell markers such as CD2, CXCR3 and CCR6 are enriched in latently infected cells (82)(83)(84).

HIV-1 research has focused predominantly on the main cellular target of HIV-1, CD4 T-cell, while other cell types such as monocytes and macrophages and their role in reservoir persistence is less well understood. These cells may be particularly suited to maintain a latent reservoir over time, due to their ability to resist cytopathic effect of HIV-1 infection and the immune response. Also, it has been suggested that macrophages could be a source of low-level plasma viremia in patients on ART, because they present a longer viral decay than T-cells (85). Macrophages can be divided into multiple subsets, all of them are susceptible to HIV-1 infection, including Langerhans cells, alveolar macrophages, mucosal macrophages and microglial cells. Viral dynamics in each of these specific tissue macrophages is different because these cells can be found in every organ with different microenvironments where HIV-1 can establish latent infection (86).

In addition to cell type differences, tissue specific compartmentalization of the HIV-1 reservoir has also been studied. Two different cell types are thought to be the main responsible for disseminating the virus throughout the body. On one hand, after exposure of HIV-1 virus in the mucosal surface, viruses are carried to the local lymph node by dendritic cells, where these infected cells get in close contact with CD4 T-cells,

resulting in infection of CD4 T-cells and the consequently burst in viral replication. Infected CD4 T-cells are released into the peripheral blood stream, disseminating the virus into different organs generating anatomical reservoirs. On the other hand, macrophages play a key role in cell-to-cell HIV-1 transmission. These cells can be infected by different mechanisms; one possibility is forming intercellular bridges by attachment receptors between HIV-1 infected cells and macrophages and the other mechanism is the fusion between macrophages and actively infected CD4^{+} T-cells and capture and phagocytosis of the viral particles (87). Infected macrophages can also differentiate in different cell types, such as Langerhans cells, alveolar macrophages, mucosal macrophages and microglial cells, which allows the virus to reach different organs including genital tract, spleen, thymus and bone marrow, gastrointestinal tract, respiratory tract, liver and the CNS (88). Neuroinvasion may dysregulate the blood brain barrier, altering its permeability and driving chronic inflammation of the CNS (Figure 7) (89).

From the above, it is clear that an effective cure of HIV-1 will need to target not only CD4 T-cells reservoir, but also all other types of cells that contribute to the viral reservoir but which are located in sanctuaries that in some cases present low drug penetrance, slow cellular turn-over or long half-live and immune privileged sites. An example of this are microglial cells in the central nervous system that contribute to a life-long reservoirs and may be critical for the development of HIV-associated neurocognitive diseases (HAND) (89).
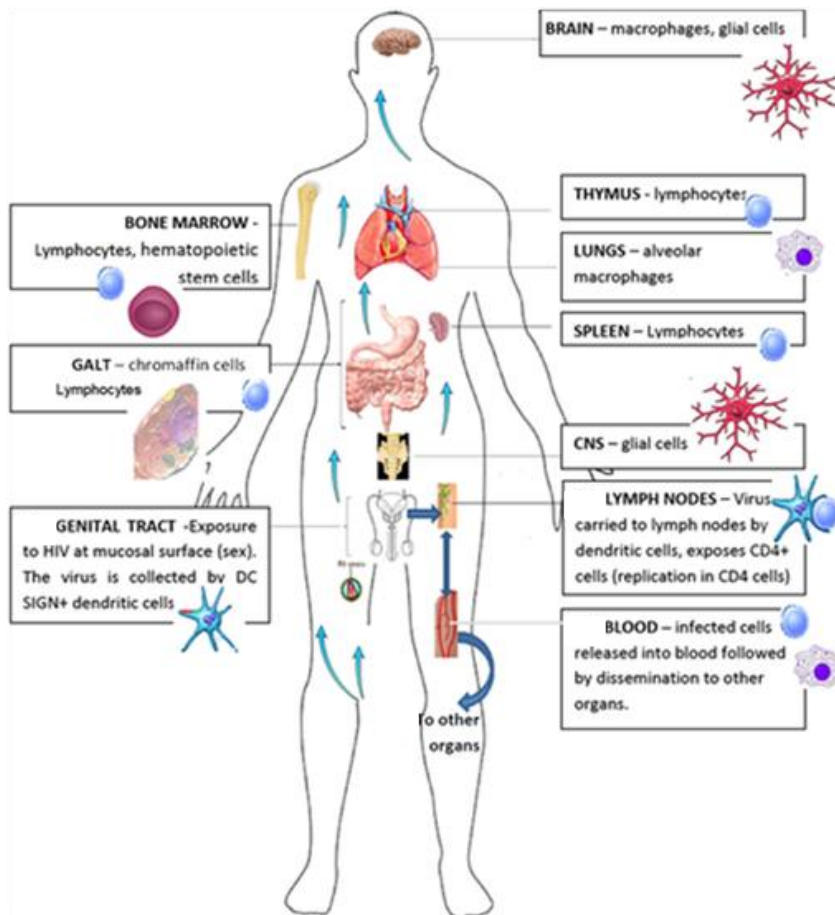
Figure 7. HIV-1 body compartments. Different HIV-1 infected body compartments such as brain and CNS, thymus, lungs, spleen, lymph nodes, genital tract, GALT and bone marrow. Image adapted from (88).

1.3. Treatments and strategies for HIV-1 cure

1.3.1. Natural control of HIV-1 infection

Although most HIV-1 infected individuals will show, in the absence of treatment, a progressive disease course leading eventually to AIDS, between 5 and 15% of individuals infected with HIV-1 are able to remain clinically stable and without fast disease progression in the absence of antiretroviral treatment. This group of HIV-1 infected individuals has being referred to as long term non-progressors (LTNP) (90). This group of PWH can further be classified in two types of individuals depending on

their virological control; elite controllers (EC) (<1%) who, in absence of treatment, have the ability to suppress viral load levels to undetectable levels (<50 HIV-1 RNA copies/ml) and maintaining elevated CD4 T-cell counts (200-1000cells/mm^3) and viremic controllers (VC) who present a lower degree of virus control (200-2000 HIV-1 RNA copies/ml) but still maintain elevated CD4 T-cells counts (200-1000cells/mm^3) (90)(91)(92). In contrast, there is a small group of HIV-1 infected individuals that are referred to as rapid progressors, individuals who present a rapid decline in their CD4 T-cell counts and high levels of plasma viremia, with a rapid progression to AIDS, often within 2-3 years after infection (Figure 8) (93).
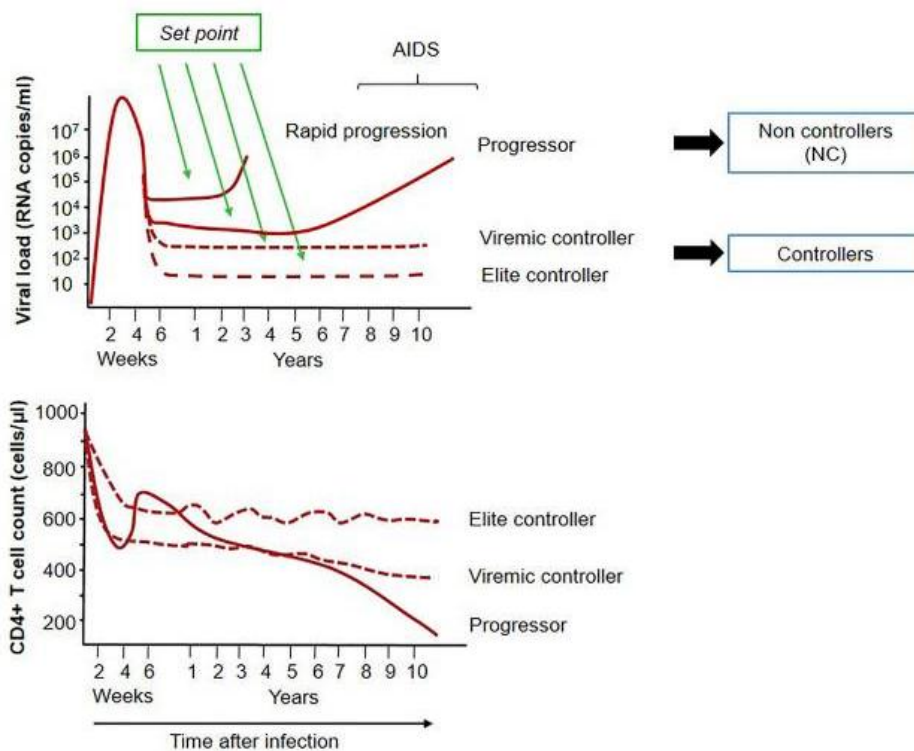
Figure 8. Progression of the HIV-1 disease after the infection in HIV-1 progressors, elite controllers and viremic controllers. Image adapted from (94).

1.3.2. Early combined antiretroviral treatment

One of the greatest success in the HIV-1 field is the development of antiretroviral treatment (ART). ART are grouped in different classes, depending on their mode of

action and the steps in the viral life cycle they inhibit and, when used in combination, can confer generally stable suppression of viremia to undetectable levels, with stable CD4 T-cells counts (95). Thus, the availability of ART has allowed to transform HIV-1 infection into a more or less stable disease with treated individuals having a close to normal life expectancy.

The first drug discovered to treat HIV-1 infection was azidothymidine (AZT), a nucleoside reverse transcriptase inhibitor (NRTI) that inhibits the viral reverse transcriptase. During several years, NRTI drugs were administrated as monotherapy and/or in combination with non-nucleoside reverse transcriptase inhibitor (NNRTI) drugs, oftentimes leading to treatment failure, incomplete suppression of viremia and resistance development. Additional classes of drugs were gradually developed and included in such combined antiretroviral therapy (cART), which normally consists of a combination of three different drugs and achieves suppression of viral load to undetectable levels (95). These drugs include, aside from nucleoside reverse transcriptase inhibitors (NRTIs), also non-nucleoside reverse transcriptase inhibitors (NNRTIs), integrase inhibitors (INIs), protease inhibitors (PIs), fusion inhibitors (FIs) and entry inhibitors (EIs) (96). Of note, these treatments do not only suppress active viral replication, but can also limit the size of the latent reservoir when treatment is initiate dearly after HIV-1 infection (97)(98).

1.3.3. Gene therapy and stem cell transplantation

Although cART is highly effective in suppressing replication, cART alone cannot eradicate the infection. Aside from "kick and kill" and other strategies that are further discussed below, other innovative strategies are being developed to try to eliminate the latent virus. Some of these strategies employ hematopoietic stem cell transplantation from donors with natural resistance to HIV-1, or genome editing of HIV-1 infected cells from the infected individual. The latter group of strategies includes diverse approaches that are focused on inhibiting viral and cellular gene transcripts required for viral replication genes (99):

- Ribozyme: enzymatic degradation of target RNAs.

- Silencing RNA/: enzymatic degradation of target mRNAs (100).

- Antisense RNA: complementary binding to viral mRNAs preventing mRNA translation (101).

- Dominant negative Tat/Rev: inhibition of Tat/Rev gene products binding to TAR/PRE region (102).

- TAR/PRE RNA decoys: binding and blocking Tat or Rev proteins (103).

- Suicide genes: enhancing expression of suicide genes causing cell death (104).

- Intracellular antibodies: binding to target proteins and initiating their degradation (105).

- Intracellular chemokines: retention or blocking of co-receptors in the endoplasmic reticulum to prevent surface expression (106).

These strategies can target CD4+ T-cells, macrophages and their progenitors and their delivery can be accomplished by various vectors, including lentiviral, retroviral or adenoviral vectors (107)(108).

On the other hand, allogeneic hematopoietic stem-cell transplantation is the only strategy that has succeeded in curing three HIV-1 infected individuals from their infection, including the "Berlin" patient who was the first individual in whom this strategy was tested. Stem cell transplantation was indicated in these individuals as cancer treatment and was refined by identifying a stem cell donor with a homozygous mutation in the HIV-1 co-receptors CCR5 (CCR5Δ32/Δ32). The individuals stopped cART at the time of the transplant and remained undetectable for HIV-1. Also, no HIV-1 RNA or HIV-1 DNA were detectable in GALT, bone marrow or peripheral blood (109)(110).

1.3.4. "Kick and kill" cure strategy

One of the most developed HIV-1 cure strategy is the "kick and kill" strategy. This approach consists in a "kick" part when a latency reversal agent (LRA) is administered to reactivate the latent virus, so that the infected cells start producing HIV-1 particles and thus render the cell visible for the immune system. These cells should then be eliminated by an effective host immune responses that provides the "kill" (111). There are several latency reversal agents that increase viral gene expression from latency proviruses, including: epigenetic modifiers such as histone deacetylase inhibitors (HDACs), histone methyltransferase inhibitors, DNA methyltransferase inhibitors and bromodomain inhibitors, protein kinase C agonists and PI3K/Akt pathway inhibitors that affect cell survival, and agonist for the innate immune receptors TLR7 and TLR9 (Figure 9) (112).

A growing number of latency reversal agents have been tested in clinical trials including HDACs inhibitors such as vorinostat, panobinostat, romidepsin and chidamide. A clear example of the effect of the latency reversal agent romidepsin (RMD) is the phase A of the clinical trial REDUC, which has demonstrated increased HIV-1 RNA transcription after infusions of RMD, however, without causing a clinically relevant reduction of the size of the latent reservoir (113). Similarly, the latency reversal agent chidamide showed comparable results, with an increase of HIV-1 gene transcription and cyclic viremia peaks, but a modest reduction of the cell-associated HIV-1 DNA (114). Given the minimal effects on reservoir size with a LRA treatment only, it is thought that combinations of a potent latency reversal agent along with a boost of the immune system could be an effective strategy to purge the viral reservoir (112). As a proof of concept, the phase B of the REDUC clinical trial combined RMD infusions with vaccination with Vacc-4x together with the adjuvant rhuGM-CSF. The results of the REDUC clinical trial show however only a slight reduction in the total HIV-1 DNA copy number, possibly due to the weak immunogenicity of the vaccine regimen (115). Similarly, the clinical trial RIVER, which compared a "Kick and kill" strategy (LRA vorinostat and T-cell vaccine) with ART regimen alone, showed no significant difference in terms of measurements of HIV-1 reservoir neither; even though in this

case, the vaccine intervention was more potent than in REDUC (116). Finally, the BCN02 clinical trial, on which several of the analyses presented in this thesis are based, analyzed the "kick and kill" strategy based on infusions of RMD and the same T-cell vaccine as in RIVER clinical trial. The efficacy and safety results indicate that infusions of romidepsin was well tolerated and resulted in higher expression of apoptosis markers and a decrease of CD4 T-cell counts, without a notable increase in viral transcriptional activity or reduction of the reservoir size (117)(118).
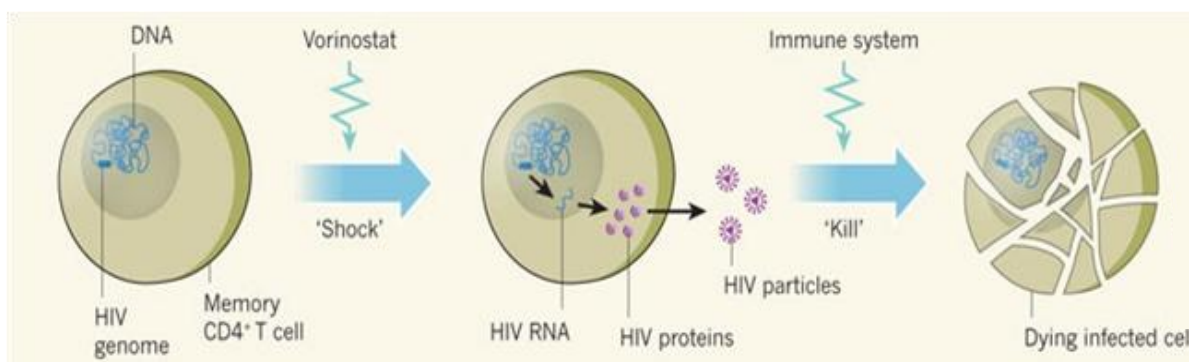
Figure 9. "Kick and kill" or "shock and kill" strategy. In the representation vorinostat appears as a latency reversing agent and then reactivation of the immune system is generated to eliminate HIV-1 infected cells . Image adapted from (119).

1.3.5. "Block and lock" cure strategy

A different and quite opposite approach to modulate the HIV-1 viral reservoir is the "block and lock" approach. This consist in transcriptional gene silencing in the HIV-1 promoter to suppress virus replication (120). This strategy mimics natural virus latency but maintains the virus in a "deep latency". The block part consists first in blocking the viral transcription and the lock stage aims to maintain the virus in a latent state. To silence the latent reservoir in a permanently dormant state, different groups have used various latency promoting agents (LPAs). The silencing can be induced by different RNA techniques; short hairpin RNA, short interfering RNA and long non-coding RNA targeting mTOR and NF-kB pathway or Tat and integrase proteins (121). For examples, the first therapy to induce silencing via silencing of the DNA, emlpoyed a siRNA that

suppreses transcription and induces CpG methylation, targeting the NK-KB sites in the HIV-1 promoter to cause transcriptional gene silencing (Figure 10) (122).
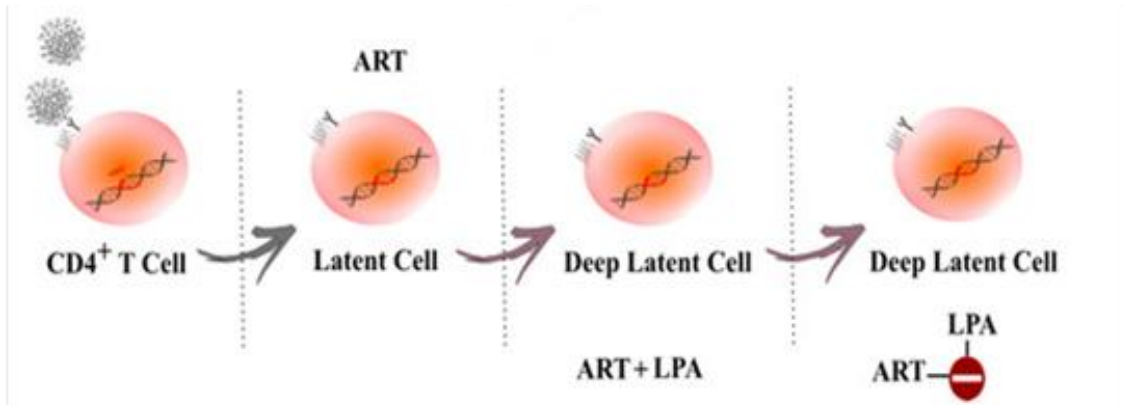
Figure 10. "Block and lock" strategy. In the figure, administration of latency promoter agent and antiretroviral treatment induced a deep latent state cell. Image adapted from (123).

1.3.6. HIV-1 specific immune enhancement

The HIV-1 specific enhancement strategies used for therapeutic vaccination alone or in combination with LRA as in "kick and kill" approaches, consists in enhancing the virus-specific host immune response to eliminate or reduce the number of virally infected cells and to neutralize and eliminate viral particles. Different tools have been tested *in vitro* and in pre-clinical and clinical studies:

- Therapeutic T-cell vaccination aims to increase the cellular immune responses in an immunocompromised host and to provide additional capacity to cover some of the T-cell epitopes that have not been targeted upon natural infection or which have not been present in the ever evolving autologous virus. So far, the vaccines that are developed for human use, are generated with various vaccine vectors. More recently developed vaccines are based on viral or bacterial vectors and RNA or DNA vectors. Designed immunogens for therapeutic vaccination can be directed to structural genes, regulatory genes or viral enzymes (124). All these different vaccines try to boost the magnitude, breath and antigen-specificities of HIV-1 T-cell responses to clean the

organism of HIV-1 infected cells (125). Some past clinical trials have shown an improvement of the HIV-1 specific T-cell responses but with weak or poor viral control during subsequent analytical treatment interruption (ATI) (126). A very recent study that combined a vaccination regimen using the HTI immunogen in DNA with ChAd and MVA vectors in early ART-treated HIV-1 infected individuals show strong immunogenicity and an improved viral control after ART interruption in a subset of individuals (127).

- HIV-1 specific broadly neutralizing antibodies (bnAbs) and binding antibodies have also gained interest for the therapeutic use of this infection. To date, most encouraging experiences have been made with passive immunization using single or multiple bnAbs. When administrated to individuals undergoing ATI, these antibodies are capable to suppress viral rebound in the absence of ART, at least as long as the Ab titers remain sufficiently high and no (pre-existing) viral resistance variants dominate the viral population (128). Through a mechanism referred to as "vaccinal effect" bnAbs can form immune complexes with the bound virus, which then are presented by professional APC and can enhance CD8 T-cell immunity able to control viral rebound long after the antibody has vanished (129). Indeed, in non-human primate studies, bnAbs administration produced a reduction of plasma viral load and reduced proviral DNA in some body compartments (130), and the early administration of bnAbs resulted in a elimination of the viral foci of SIV infection and limited the establishmet of the viral reservoir (131). In human clinical trials, administration of the combination of 3BNC177 and 10-1074 resulted in a suppression of viral rebound for a median of 21 weeks (132). These observations highlight the potential of bnAbs based treatments and have spurred the development of long-acting antibodies that could allow HIV-1 infected individuals to effectively suppress viral replication for prolonged periods of time.

- Chimeric antigen receptors T-cells (CAR-T) are another treatment modality that have been tested clinically. These CAR-T cells are T-cells genetically engineered to expressed an extracellular domain corresponding to an anti-HIV-1 antibody linked with an intracellular domain that contains the CD3/TCR-signaling complex leading to a

cytotoxic response after the cells bind its specific antigen (133). *In vitro* experiments have shown clearing of HIV-1 infected cells by anti-HIV-1 CAR-T cells. Moreover, CAR-T cells targeting different antigens have demonstrated in a humanized mice model the elimination of HIV-1 infected cells (134). Although the FDA recentlly approved a CAR T-cell therapy for B-cell leukemia, and despite numerous studies in progress for cancer immunotherapies, only few clinical trials have been initiated for anti-HIV-1 CAR T-cells. A published clinical trial using CD4 and CD8 T-cells engineered with CD4ζ CAR including a CD28 costimulatory domain, showed a slight decrease for at least 14 days in rectal tissue-associated HIV-1 RNA (135). Also, a recently study clinical trial has reported that all participants that recived a bNAb-derived CAR T-cells showed a viral rebound kinetics but a slight reduction of the viral reservoir (136). Some others clinical trials are ongoing, evaluating different types of CAR T-cells engineered (137).

Overall, these HIV-1 cure strategies target HIV-1 infection from different sides, but despite some encouraging results, none of them has proven clinically sufficiently effective. This may at least partly be due to the fact that functional immune correlates of controlled HIV-1 infection remain incompletely defined, which complicates further refinement of these strategies. It is therefore important to elucidate the potential mechanisms of protection in clinical trials with an at least partly clinical efficacy signals. In this thesis, we provide some insights into biomarkers associated with the observed efficacy signals and have explored for some of them their mechanisms of antiviral activity.

1.5. <u>Biomarkers in HIV-1 infection to guide future cure interventions</u>

Many studies have analyzed HIV-1 infected individuals that naturally control the virus, with the aim to identify host immune cells, molecules or genes believed to act on viral replication by various mechanisms, including virus-specific CD8 T-cells, neutralizing antibodies, NK cells, genetic markers and soluble factors. For example, it has been reported that IL-18 and IP10, in combination with the frequency of $CD8^+CD38^+HLA\text{-}DR^+$ T cells can be a useful biomarker to identify effective functional cure for HIV-1

(138). Indeed, functional analyses showed that elite controllers expressed lower levels of these CD38/HLA-DR activation markers and maintained instead CD57+ cytolytic CD4 T-cells with lower PD-1 and TIM-3 expression compared to non-controller HIV-1 infected individuals. In addition, virus-specific T-cells in elite controllers were also found to secrete effector cytokines like IFNγ and TNF and cytolytic proteins GZMA/B and FasL (139). In addition to such functional characteristics, host genetics can also play an important role in HIV-1 control, especially specific class I HLA molecules (such as HLA-B5701, B2705 and others) which may have a direct bearing on the functional and phenotypic characteristics of virus-specific T-cells (140). Host genetics and epigenetics may also impact the effectiveness of host restriction factors, which can control viral replication, for instance the expression of schlafen 11, which is elevated in CD4 T-cells from elite controllers compared to HIV-1 non-controllers (141). However, in many of these analyses, it is inherently difficult to solve the cause-effect conundrum. For instance, the SPARTAC trial aimed to define biomarkers that predict post-treatment control in individuals who stop their ART, and identified three markers of T-cell exhaustion PD-1, TIM-3 and Lag-3 that strongly predicted the time to viral rebound in ATI (142). However, what exactly drives the expression of such exhaustion markers and whether exhausted cells are the cause or consequence of loss of viral control awaits clarification.

1.4.1. Soluble proteomics in HIV-1 viral control and reservoir

Proteomics analyses consist in the application of technologies for the identification and quantification of a diverse set of proteins present in a cell, tissue or body fluids. Technologies based on proteomics are used in different research areas such as detection of disease-specific diagnostics markers, identifying candidates for vaccines refinement and for the understanding of pathogological mechanisms. Proteomics technologies have advanced a lot from conventional techniques such as chromatography, ELISA or Western blotting with more advanced techniques including gel-based approaches, mass spectrometry, edman sequencing, X-ray crystallography, NMR-spectroscopy and large multiplexed protein arrays to more advanced techniques

like throughput protein sequencing and ultrasensitive arrays (143). Specifically in this thesis, we used different techniques for exploratory and large screening analysis as well as ultrasensitive proteins arrays to identify protein biomarkers of HIV-1 disease and virus control, post-treatment control, and potentially novel therapeutic targets in HIV-1 infection to monitor or guide future HIV-1 cure interventions.

Proteomics studies can be performed with different types of samples; blood plasma, cerebrospinal fluid (CSF), cells, tissues, saliva, among others. In this thesis we focus our proteomics analysis on peripheral blood plasma samples and CSF. The benefits of working with plasma is that it can be obtained with a non-invasive blood draw, compared to more complicated procedures like CSF puncture or lymph node biopsies. Plasma contains a complex mixture of water, inorganic salts, organic compounds, and more than 1000 proteins, and can be a reflection of different physiological and pathological processes at distant sites in the body compartments. Moreover, measuring protein levels in plasma as indicator of cell-to-cell communication, mediated by ligand/receptor interactions, hormones, content of extracellular vesicles and other soluble factors have helped to understand the mechanisms of a HIV-1 pathologenesis and may inform future HIV-1 cure interventions (144).

In our own laboratory, we have reported that the IL-27 cytokine is crucial for the antiviral immune response and strongly correlates with viral load and total proviral reservoir size in PBMCs, suggesting that it could serve as a plasma biomarker of HIV-1 control (145). Similarly, it has been reported that TL1A is associated with the presence of a T-cell regulator subsets and DR3 expressing CD8 T-cells, which could be leveraged by immune-based interventions to enhance the antiviral T-cell responses to achieve better virus control (146). Importantly though, biomarkers can not only be employed to refine antiviral strategies but, even when assessed in peripheral blood, may inform about existing and developing comorbidities due to HIV-1 infection, chronic immune activation and inflammation or, long-term antiviral treatment toxicity. Some of these comorbidities also extend to the CNS and the work presented here and reported by other groups, have shown plasma proteomics to deliver relatively easy to capture and highly informative data for diagnostic and treatment purposes, including CNS pathologies. However, the correlations between peripheral blood plasma and for

instance CSF have not been assessed for large number of proteins and for different disease settings.

1.4.2. Biomarkers of neurological manifestations of HIV-1 infection

While cART has certainly reduced the mortality of HIV-1 infection and increased the average life expectancy of treated PWH, it does not revert the accelerated aging observed in this patient population. As a consequence, comorbidities of HIV-1 infection with neurological manifestation may have been reduced in severity, but not in prevalence. Indeed, cART has reduced the incidence of HIV-associated dementia (HAD) in persons living with HIV-1 but still 18-50% of HIV-1 infected individuals with chronic HIV-1 on cART manifest HIV-associated neurocognitive disorders (HAND) (147), in different severities ranging from asymptomatic neurocognitive impairment to fully manifest HAD (148). In an effort to better understand how HIV-1 affects the CNS, currently available diagnostic tools lack the sensitivity and specificity needed for an accurate monitoring and diagnosis for HAND. Therefore, there is an urgent need for biomarkers to diagnose and/or predict the manifestations and progression of HAND.

Different neurological biomarkers have been proposed in different neurological diseases, among them neurofilament light chain (NFL). NFL concentrations in plasma and CSF fluids have been shown to strongly correlate in HIV-1 infected individuals and also, it is modulated by initiation of cART (149)(150)(151). Another marker of neurological dysfunction, amyloid beta (Aβ) is also altered in HIV-1 infection, possibly through the actions of viral Tat protein, which inhibits its degradation. As Tat-Aβ complexes can influence the phosphorylation of MAPT, these complexes could contribute importantly to increased neurotoxicity (152). However, these reported markers are very common in other neurological diseases.

Recently, other markers have been found to be altered in individuals with asymptomatic HIV-1 infection, such as ADMA, a molecule of endothelial dysfunction and which could be associated with disruption of the blood brain barrier and development of HAND (153). Moreover, neopterin produced by

monocyte/macrophage under the stimulus of interferons, has been found at increased levels in untreated HIV-1 infected individuals in both, plasma and CSF (154). Finally, platelet-derived growth factor (PDGF) is up-regulated by the viral Tat protein, inducing the expression of monocyte chemoattractabt protein-1 (MCP-1) production by astrocytes and thereby increasing monocyte migration across the BBB and possibly leading to further neuroinflammation (45).

HYPOTHESIS AND AIMS

2. HYPOTHESIS AND AIMS

Despite the fact that current combined antiretroviral therapy (cART) is highly effective in reducing HIV-1 viral replication to low or undetectable levels, HIV-1 remains an incurable viral infection due to the viral reservoir that is established during the initial stages of the infection. As a consequence, cART interruption results in a fast viral rebound due to the unhindered viral replication from the reactivated latently infected cells in the viral reservoir. Therefore, different strategies are being developed to avoid, limit or slow this viral rebound to achieve an improved control of viral replication in the absence of cART (functional cure). Hopefully leading one day to strategies capable to mediate complete elimination of the HIV-1 virus (sterilizing cure).

-The **main hypothesis** of the present thesis is that plasma proteomes of HIV-1 infected individuals can reveal biomarkers that reflect the pathologic processes at peripheral blood as well as in the central nervous system and are associated with virus control in natural infection and post-treatment intervention and neurological dysfunction. These biomarkers may also reveal novel targets that can be leveraged by novel therapeutic interventions for HIV-1 cure.

The specific aims of the thesis in each of the chapters are:

CHAPTER I. Identification of plasma biomarkers in natural control of HIV-1 infection in the absence of cART.

> 1.1. To detect soluble factors in the peripheral blood of HIV-1 infected individual that are also reflected in the CSF.
>
> 1.2. To identify specific molecules that are associated with viral control and potential neurological impact in HIV-1 infected individuals.
>
> 1.3. To understand the modulation of these markers in response to cART initiation.

CHAPTER II. Plasma HDAC class II factor (Sirtuin-2) as biomarker and potential therapeutic target for HIV-1 infection and neurological dysfunction.

> 2.1. To identify plasma factors indicative of natural control of HIV-1 infection.

2.2. Evaluate the role of plasma markers, including HDAC class II factor (Sirtuin-2) in neurological dysfunction.

2.3. *In vitro* targeting of HDAC class II factor (Sirtuin-2) for its evaluation as future therapeutic target in HIV infection.

CHAPTER III. Plasma proteomics analysis in the BCN02 clinical trial, based on a "kick and kill" strategy for HIV-1 cure.

3.1. To explore the effect of therapeutic vaccination and the latency-reversing agent romidepsin on plasma proteomes in samples from BCN02 participants.

3.2. Identification of plasma biomarkers predictive of virus rebound kinetics during the monitored cART-interruption pause in BCN02.

3.3. In vitro targeting of CD33/SIGLEC3 protein and its effect on virus replication and reservoir formation.

MATERIALS AND METHODS

3.1. Participants and samples

CHAPTER I:

- **Main cohort of study; chronic untreated HIV-1 infected individuals** (n=20) and seronegative individuals (n=5) enrolled at the University of Gothenburg (Sweden) and University of California San Francisco (USA) were classified according to their degree of control of viral replication. HIV-1 low-viremia individuals (HIV-Low; n=10) were defined as individuals with plasma viral loads (pVL) of <10,000 HIV-1 RNA copies/ml (range: 36 to 8,981; median 3,897 HIV-1 RNA copies/ml) in the absence of antiretroviral treatment; HIV-1 high-viremia individuals (HIV-High; n=10*)* were untreated individuals with >100,000 HIV-1 RNA copies/ml (range: 113,000 to 1,150,000; median 287,000 HIV-1 RNA copies/ml) and a group of HIV-1 seronegative individuals (n=5). Plasma and CSF paired samples were taken of each one of the individuals and stored until use (Table 1).

Patients	Age	Gender	Plasma HIV-1 viral load	CSF HIV-1 viral load	Measurement (sample)
HIV-high1	37	M	146000	11600	PEA (CSF and plasma)
HIV-high2	34	M	425000	295	PEA (CSF and plasma)
HIV-high3	55	F	113000	73400	PEA (CSF and plasma)
HIV-high4	37	M	134000	53600	PEA (CSF and plasma)
HIV-high5	34	F	1150000	96400	PEA (CSF and plasma)
HIV-high6	43	M	149000	6440	PEA (CSF and plasma)
HIV-high7	50	M	905000	672	PEA (CSF and plasma)
HIV-high8	32	F	879000	56000	PEA (CSF and plasma)
HIV-high9	36	M	429000	168000	PEA (CSF and plasma)
HIV-high10	43	M	139000	3520	PEA (CSF and plasma)
HIV-low1	45	M	4234	307	PEA (CSF and plasma)
HIV-low2	44	F	6090	1160	PEA (CSF and plasma)
HIV-low3	40	M	36	22	PEA (CSF and plasma)
HIV-low4	39	M	1313	276	PEA (CSF and plasma)
HIV-low5	29	M	8981	5447	PEA (CSF and plasma)
HIV-low6	27	F	5680	102	PEA (CSF and plasma)
HIV-low7	47	F	3560	1970	PEA (CSF and plasma)
HIV-low8	30	M	4580	60	PEA (CSF and plasma)
HIV-low9	41	M	1730	148	PEA (CSF and plasma)
HIV-low10	54	M	231	39	PEA (CSF and plasma)
Seronegative1	33	M	NA	NA	PEA (CSF and plasma)
Seronegative2	19	M	NA	NA	PEA (CSF and plasma)
Seronegative3	28	M	NA	NA	PEA (CSF and plasma)
Seronegative4	29	M	NA	NA	PEA (CSF and plasma)
Seronegative5	34	M	NA	NA	PEA (CSF and plasma)

Table 1. Viral and clinical data of chronic untreated HIV-1 infected individuals. NA: not available, M: male; F: female, Plasma/CSF HIV-1 viral load: HIV-1 RNA copies/ml, PEA: Proximity Extension Assay, CSF: cerebrospinal fluid.

- **Validation cohort; longitudinally evaluated treated HIV-1 infected individuals** (n=18), who were recruited at Fundació Lluita per la Sida, Hospital Universitari Germans Trias i Pujol, Badalona (Spain) and who were followed longitudinally before and after cART initiation (Table 2).

Patients	Age	Untreated				Treated 1Y	
		Plasma HIV-1 viral load	CD4 cell counts	CD8 cell counts	CD4/CD8 ratio	Plasma HIV-1 viral load	Measurement (sample)
HIV-1 positive1	22	543549	743	844	0,879	<40	PEA (plasma)
HIV-1 positive2	43	339798	165	981	0,17	<40	PEA (plasma)
HIV-1 positive3	60	4598720	385	391	0,98	<40	PEA (plasma)
HIV-1 positive4	33	3721	854	528	1,62	<40	PEA (plasma)
HIV-1 positive5	33	16789	365	484	0,75	<40	PEA (plasma)
HIV-1 positive6	34	119128	630	1136	0,55	<40	PEA (plasma)
HIV-1 positive7	23	209602	342	780	0,4399	<40	PEA (plasma)
HIV-1 positive8	39	4361	713	1190	0,6	<40	PEA (plasma)
HIV-1 positive9	24	794200	742	1534	0,48	<40	PEA (plasma)
HIV-1 positive10	29	90083	238	907	0,2599	<40	PEA (plasma)
HIV-1 positive11	32	93977	641	3662	0,18	<40	PEA (plasma)
HIV-1 positive12	32	11179	238	612	0,46	<40	PEA (plasma)
HIV-1 positive13	31	56932	382	539	0,709	<40	PEA (plasma)
HIV-1 positive14	47	45301	696	910	0,7699	<40	PEA (plasma)
HIV-1 positive15	31	4995	554	964	0,569	<40	PEA (plasma)
HIV-1 positive16	48	15744	402	473	0,85	<40	PEA (plasma)
HIV-1 positive17	20	2801	936	2109	0,439	<40	PEA (plasma)
HIV-1 positive18	22	105	580	800	0,72	<40	PEA (plasma)

Table 2. Viral and clinical data of longitudinally evaluated, treated HIV-1 infected individuals. Plasma HIV-1 viral load: HIV-1 RNA copies/ml, CD4 counts: cells/mm^3, CD8 counts: cells/mm^3, PEA: Proximity Extension Assay.

CHAPTER II:

- **Main cohort of study; untreated chronically HIV-1 infected individuals** (n=40) enrolled at the IMPACTA clinics (Lima, Peru) and at Hospital Germans Trias i Pujol

(Badalona, Spain) were classified according to their degree of control of viral replication. Individuals with relative control were classed as "HIV-low" (n=20) and had a plasma viral load (pVL) <10,000 HIV-1 RNA copies/ml (range: 49 to 10,000; median: 435 HIV-1 RNA copies/ml) and a median of 665 CD4 cells/mm^3 (range: 438 to 1,083 cells/mm^3). Individuals with uncontrolled disease were classed as "HIV-high" (n=20) and had a pVL >15,000 HIV-1 RNA copies/ml (range: 15,000 to 1,200,000; median: 108,000 HIV-1 RNA copies/ml) and a median of 384 CD4 cells/mm^3 (range <50 to 726 cells/mm^3). Additionally, a cohort of HIV-1 elite controllers (n=12; undetectable viral loads: <50 HIV-1 copies/ml) and more HIV-low individuals (n=10) was used to validate downstream gene expression (Table 3).

Patients	Age	Gender	Plasma HIV-1 RNA copies/ml	CD4 counts	Measurement (sample)
HIV-high1	24	M	220000	726	Proteomic array and RT-PCR (plasma and PBMCs dry pellet)
HIV-high2	35	M	79000	384	Proteomic array and RT-PCR (plasma and PBMCs dry pellet)
HIV-high3	27	M	250000	704	Proteomic array and RT-PCR (plasma and PBMCs dry pellet)
HIV-high4	32	M	55000	17	Proteomic array and RT-PCR (plasma and PBMCs dry pellet)
HIV-high5	45	F	68000	98	Proteomic array and RT-PCR (plasma and PBMCs dry pellet)
HIV-high6	NA	NA	14000	NA	Proteomic array and RT-PCR (plasma and PBMCs dry pellet)
HIV-high7	33	F	1200000	75	Proteomic array and RT-PCR (plasma and PBMCs dry pellet)
HIV-high8	47	F	510000	33	Proteomic array and RT-PCR (plasma and PBMCs dry pellet)
HIV-high9	50	F	54000	67	Proteomic array and RT-PCR (plasma and PBMCs dry pellet)
HIV-high10	23	M	610000	505	Proteomic array and RT-PCR (plasma and PBMCs dry pellet)
HIV-high11	28	M	200000	544	Proteomic array and RT-PCR (plasma and PBMCs dry pellet)
HIV-high12	NA	NA	52000	NA	Proteomic array and RT-PCR (plasma and PBMCs dry pellet)
HIV-high13	30	M	55000	380	Proteomic array and RT-PCR (plasma and PBMCs dry pellet)
HIV-high14	33	M	53000	451	Proteomic array and RT-PCR (plasma and PBMCs dry pellet)
HIV-high15	21	M	320000	437	Proteomic array and RT-PCR (plasma and PBMCs dry pellet)
HIV-high16	NA	NA	96000	NA	Proteomic array and RT-PCR (plasma and PBMCs dry pellet)
HIV-high17	44	F	510000	12	Proteomic array and RT-PCR (plasma and PBMCs dry pellet)
HIV-high18	31	M	39000	365	Proteomic array and RT-PCR (plasma and PBMCs dry pellet)
HIV-high19	25	M	170000	634	Proteomic array and RT-PCR (plasma and PBMCs dry pellet)
HIV-high20	32	M	120000	480	Proteomic array and RT-PCR (plasma and PBMCs dry pellet)
HIV-low1	NA	NA	66	NA	Proteomic array and RT-PCR (plasma and PBMCs dry pellet)
HIV-low2	46	M	1100	485	Proteomic array and RT-PCR (plasma and PBMCs dry pellet)
HIV-low3	46	F	49	1083	Proteomic array and RT-PCR (plasma and PBMCs dry pellet)
HIV-low4	48	F	210	913	Proteomic array and RT-PCR (plasma and PBMCs dry pellet)
HIV-low5	40	M	8900	786	Proteomic array and RT-PCR (plasma and PBMCs dry pellet)
HIV-low6	28	M	1000	889	Proteomic array and RT-PCR (plasma and PBMCs dry pellet)
HIV-low7	37	F	1800	511	Proteomic array and RT-PCR (plasma and PBMCs dry pellet)
HIV-low8	50	F	49	487	Proteomic array and RT-PCR (plasma and PBMCs dry pellet)

HIV-low9	40	F	340	832	Proteomic array and RT-PCR (plasma and PBMCs dry pellet)
HIV-low10	37	F	49	665	Proteomic array and RT-PCR (plasma and PBMCs dry pellet)
HIV-low11	33	M	530	948	Proteomic array and RT-PCR (plasma and PBMCs dry pellet)
HIV-low12	38	M	160	512	Proteomic array and RT-PCR (plasma and PBMCs dry pellet)
HIV-low13	34	M	4300	587	Proteomic array and RT-PCR (plasma and PBMCs dry pellet)
HIV-low14	NA	NA	88	NA	Proteomic array and RT-PCR (plasma and PBMCs dry pellet)
HIV-low15	27	M	7700	733	Proteomic array and RT-PCR (plasma and PBMCs dry pellet)
HIV-low16	NA	NA	950	NA	Proteomic array and RT-PCR (plasma and PBMCs dry pellet)
HIV-low17	56	F	49	873	Proteomic array and RT-PCR (plasma and PBMCs dry pellet)
HIV-low18	41	M	49	616	Proteomic array and RT-PCR (plasma and PBMCs dry pellet)
HIV-low19	35	M	10000	438	Proteomic array and RT-PCR (plasma and PBMCs dry pellet)
HIV-low20	37	M	810	665	Proteomic array and RT-PCR (plasma and PBMCs dry pellet)
HIV-low21	29	M	49	892	RT-PCR (PBMCs dry pellet)
HIV-low22	45	F	2900	582	RT-PCR (PBMCs dry pellet)
HIV-low23	46	F	2800	434	RT-PCR (PBMCs dry pellet)
HIV-low24	38	M	49	583	RT-PCR (PBMCs dry pellet)
HIV-low25	26	M	2300	642	RT-PCR (PBMCs dry pellet)
HIV-low26	44	M	50	872	RT-PCR (PBMCs dry pellet)
HIV-low27	41	F	25	672	RT-PCR (PBMCs dry pellet)
HIV-low28	50	F	50	1228	RT-PCR (PBMCs dry pellet)
HIV-low29	51	M	25	450	RT-PCR (PBMCs dry pellet)
HIV-low30	48	F	230	516	RT-PCR (PBMCs dry pellet)
EC_01	31	F	25	922	RT-PCR (PBMCs dry pellet)
EC_02	31	F	40	752	RT-PCR (PBMCs dry pellet)
EC_03	40	F	25	1557	RT-PCR (PBMCs dry pellet)
EC_04	46	F	25	372	RT-PCR (PBMCs dry pellet)
EC_05	43	F	25	411	RT-PCR (PBMCs dry pellet)
EC_06	59	M	25	245	RT-PCR (PBMCs dry pellet)
EC_07	40	F	56	898	RT-PCR (PBMCs dry pellet)
EC_08	48	M	25	450	RT-PCR (PBMCs dry pellet)
EC_09	40	F	25	940	RT-PCR (PBMCs dry pellet)
EC_10	50	M	25	667	RT-PCR (PBMCs dry pellet)
EC_11	51	F	25	959	RT-PCR (PBMCs dry pellet)
EC_12	46	M	50	838	RT-PCR (PBMCs dry pellet)

Table 3. Viral and clinical data of untreated HIV-1 infected individuals. Viral load: plasma HIV-1 RNA copies/ml, CD4 counts: cells/mm^3, NA: not available, RT-PCR: reverse transcription polymerase chain reaction, PBMCs: peripheral blood mononuclear cells.

- **Validation cohorts of the study; chronic untreated HIV-1 infected individuals** used and described in chapter 1 and **HIV-1 infected participants from the ARBRE study** (NCT03835546), who were recruited at Fundació Lluita per la Sida, Hospital Universitari Germans Trias i Pujol, Badalona (Spain) and who underwent longitudinal neurological

evaluations, including neurocognitive tests and brain image assessments (155). These participants were divided into two groups according to the time from estimated date of HIV-1 acquisition to initiation of cART. The first group ("early-cART" group, n=9) met the following criteria: acute infection confirmed by 1) positive plasma viral load and/or presence of p24 antigen with a negative enzyme-linked immunosorbent assay (ELISA) or 2) positive ELISA result and undefined Western blot, or 3) positive ELISA result and absence of antigen band p31 in a positive Western blot test, or 4) seroconversion according to ELISA in less than three months; and who started cART within less than 90 days from the estimated date of HIV-1 acquisition. The second group ("later-cART group", n=10) comprised participants who did not meet the criteria for the early-cART group and whose estimated time since HIV-1 acquisition was longer than six months, as confirmed by viral load set-point criteria after two consecutive viral loads determinations, and who started cART six months after the estimated date of HIV-1 acquisition (Table 4).

	Early-cART (n=9)	Later-cART (n=10)
Age, years	33 (22-60)	33 (20-48)
Male, n (%)	9 (100)	10 (100)
Route of transmission, MSM, n (%)	9 (100)	10 (100)
Estimated days since infection to cART	70 (12-81)	360 (180-660)
INSTI, n (%)		
Raltegravir	2 (22.2)	1 (10)
Elvitegravir	4 (44.4)	3 (30)
Dolutegravir	3 (33.3)	6 (60)
Plasma viral load Log_{10}*	5.3 (3.6-6.7)	4.2 (2-5)
CD4 cell count	630 (165-854)	554 (238-936)
CD8 cell count	844 (391-1534)	907 (473-3662)
CD4 / CD8 ratio	0.6 (0.2-1.6)	0.6 (0.2-0.9)
SIRT2 ELISA (n)	9	10
Cognitive Test Evaluation (n)	9	9
Brain Neuro-image Assessment (n)	9	8

Table 4. Clinical information of neurologically evaluated HIV-1 infected participants from the ARBRE study. Values expressed as median with range, MSM: men who have sex with men, cART: combined antiretroviral treatment, INSTI: integrase strand transfer inhibitors, *Plasma viral load determined on

the day of cART initiation, CD4 and CD8 counts: cells/mm^3, (n) Indicates the number of individuals tested by ELISA, neurocognitive evaluations and Neurological image assessments.

CHAPTER III:

- Main cohort of study; the BCN02 clinical trial (NCT02616874) was a phase I, open-label, single-arm, multicenter study conducted in Spain (156). Fifteen participants were immunized with MVA.HIVconsv followed by three weekly-doses of romidepsin (RMD 1−2−3, 5 mg/m2) and a second MVA.HIVconsv vaccination before undergoing a monitored antiretroviral pause (MAP) for a maximum of 32 weeks. During MAP, the participants restarted cART treatment once they reached the threshold of >2000 HIV-1 RNA copies/mL or complete the 32 weeks with controlled virus rebound. Available plasma samples from 11 participants were used for the proteomics profiling analysis, including participants that did not control virus rebound during MAP (MAP-NC, n=8) and those that completed the 32 weeks of monitored antiretroviral pause (MAP-C, n=3). The corresponding timepoints of these 11 samples are baseline (BSL) which is the roll-over timepoint from the previous BCN01 trial, after romidepsin infusions (post-RMD) which is after one week of the 3 romidepsin infusions and during the monitored antiretroviral pause (MAP), at viral rebound timepoint or at week 32 for those that control the virus (Table 5).

	MAP-NC (n=8)	MAP-C (n=3)
Age, years	41 (37-48)	32 (30-40)
Male, n (%)	8 (100)	3 (100)
Route of transmission, MSM, n (%)	8 (100)	3 (100)
INSTI, n (%)		
TVD+RAL	4 (50)	3 (100)
KVX+RAL	2 (25)	0
TRI	2 (25)	6 (60)
Time on cART (years)	3.30 (3.07-3.77)	3.47 (3.08-3.53)
Early treatment timepoint initiation		
HIV plasma viral load	2.2 (1.11-22.56)	1.1 (1.11)
CD4 counts	686.5 (416-1408)	657 (648-971)
CD4/CD8 ratio	1.31 (1-1.72)	1.33 (0.97-1.74)
cART Resumption Timepoint		

HIV plasma viral load	1.79 (1.00-16.14)	1.25 (1.25)
CD4 counts	647.5 (468-1230)	854 (496-950)
CD4 / CD8 ratio	1.34 (0.87-1.75)	1.52 (0.76-1.61)

Table 5. Clinical information of neurologically evaluated HIV-infected participants from the ARBRE study. Median (IQR) are shown, MSM: men who had sex with men, INSTI: integrase strand transfers inhibitors; TVD: Truvada, RAL: raltegravir, KVX: Kivexa, TRI: Triumeq, cART: combination antiretroviral therapy, HIV plasma viral load: plasma HIV RNA copies/ml, CD4 counts: cells/mm^3.

- **Validation cohort of the study; chronic untreated HIV-1 infected individuals** (n=96), enrolled at the IMPACTA clinics (Peru) and Hospital Germans Trias i Pujol (Spain), were classed according to their degree of control of viral replication; HIV-high (n=47) and had a pVL >50,000 HIV-1 RNA copies/ml (range: 53,000-1,200,000 HIV-1 RNA copies/ml) and CD4 counts range 11-729 cells/mm^3 and HIV-low (n=49) and had pVL <10,000 HIV-1 RNA copies /ml (range: 25-9,999 HIV-1 RNA copies/ml) and CD4 counts range 289-1,343 cells/mm^3) (Table 6).

Patients	Age	Gender	HIV-1 plasma viral load	HIV-1 proviral	CD4 count	CD33 plasma level	CD33 gene expression
HIV-low 1	34	M	950	163.59	608	2649.80	1.956
HIV-low 2	56	F	49	16.02	873	1152.80	NA
HIV-low 3	41	M	49	NA	616	1948.60	NA
HIV-low 4	35	M	9999	317.73	438	1925.40	1.616
HIV-low 5	46	M	1100	76.67	485	12.20	1.474
HIV-low 6	46	F	49	6.70	1083	17.40	1.280
HIV-low 7	40	M	210	NA	786	1798.00	NA
HIV-low 8	48	F	8900	412.47	913	1437.40	1.689
HIV-low 9	28	M	1000	NA	889	3298.60	NA
HIV-low 10	37	M	810	NA	665	2246.40	NA
HIV-low 11	37	F	1800	180.82	511	1415.00	4.015
HIV-low 12	50	F	49	9.15	487	842.80	3.942
HIV-low 13	40	F	340	294.31	832	867.00	0.586
HIV-low 14	37	F	49	25.67	665	1362.60	NA
HIV-low 15	38	M	160	NA	512	2783.20	NA
HIV-low 16	33	M	530	25.81	948	1256.80	0.435
HIV-low 17	34	M	4300	NA	587	1.00	NA
HIV-low 18	29	M	49	0.00	892	1125.20	1.089
HIV-low 19	27	M	7700	NA	733	9105.60	NA
HIV-low 20	45	F	2900	278.48	582	1859.60	1.559
HIV-low 21	30	F	49	NA	1114	1.00	NA
HIV-low 22	46	F	2800	32.47	434	862.20	2.276
HIV-low 23	38	M	49	90.41	583	1235.00	1.993

HIV-low 24	26	M	2300	49.10	642	1320.40	0.690
HIV-low 25	42	M	5600	NA	531	1029.20	NA
HIV-low 26	44	M	50	6.20	872	1492.20	1.347
HIV-low 27	48	M	50	NA	657	2833.00	NA
HIV-low 28	41	F	25	20.90	672	2424.00	1.727
HIV-low 29	50	F	50	0.00	1228	1960.00	1.717
HIV-low 30	46	M	66	28.60	755	3483.40	1.221
HIV-low 31	51	M	25	41.50	450	664.00	3.149
HIV-low 32	48	F	230	15.90	516	539.40	NA
HIV-low 33	43	M	330	31.30	1237	3883.40	0.491
HIV-low 34	40	F	1500	NA	1084	1408.60	NA
HIV-low 35	48	M	50	18.40	601	1.00	NA
HIV-low 36	35	F	25	11.50	930	1.00	0.572
HIV-low 37	36	F	880	12.10	1343	978.20	1.344
HIV-low 38	40	F	4800	153.50	569	675.00	NA
HIV-low 39	57	F	50	NA	485	2569.60	NA
HIV-low 40	45,8	M	1700	NA	742	1904.60	NA
HIV-low 41	48	M	25	NA	593	971.20	NA
HIV-low 42	31	M	9756	620.70	404	1003.20	NA
HIV-low 43	29	M	5624	1662.40	823	1693.20	0.641
HIV-low 44	41	M	6127	50.20	531	1035.80	NA
HIV-low 45	34	M	400	220.10	1035	1.00	1.339
HIV-low 46	33	F	7923	366.50	524	37.20	0.267
HIV-low 47	30	F	8858	NA	289	1320.40	NA
HIV-low 48	39	F	4424	NA	419	968.00	NA
HIV-low 49	30	M	4482	0.00	1151	1775.40	0.427
HIV-high 1	21	F	269431	4.20	212	1627.20	NA
HIV-high 2	28	F	74922	NA	571	1874.00	NA
HIV-high 3	27	F	108103	NA	369	710.80	NA
HIV-high 4	37	F	140000	231.90	11	532.00	NA
HIV-high 5	40	F	64000	922.60	282	43.40	16.460
HIV-high 6	45	F	86000	NA	90	3813.80	NA
HIV-high 7	24	F	610000	1722.40	128	3758.40	11.725
HIV-high 8	47	F	510000	NA	33	1536.80	NA
HIV-high 9	33	F	1200000	80.10	75	10612.80	23.898
HIV-high 10	50	F	54000	363.60	67	2429.00	39.370
HIV-high 11	42	F	1100000	NA	283	1633.80	NA
HIV-high 12	45	F	68000	NA	98	1296.00	NA
HIV-high 13	44	F	510000	NA	12	1745.20	NA
HIV-high 14	21	M	80328	NA	437	316.20	NA
HIV-high 15	22	M	152554	3143.40	293	471.60	NA
HIV-high 16	22	M	53299	NA	356	606.40	NA
HIV-high 17	23	M	70393	223.70	208	2836.20	NA
HIV-high 18	23	M	55733	NA	340	2022.40	NA
HIV-high 19	23	M	50295	1176.50	505	9080.40	3.194
HIV-high 20	23	M	240039	1144.60	388	1555.60	NA

HIV-high 21	24	M	93928	3246.60	256	724.60	NA
HIV-high 22	24	M	365977	1204.60	726	2080.80	3.419
HIV-high 23	24	M	150176	NA	407	4084.60	NA
HIV-high 24	25	M	60467	NA	634	2354.80	NA
HIV-high 25	26	M	750000	941.40	239	2480.00	NA
HIV-high 26	27	M	54304	NA	704	4058.80	NA
HIV-high 27	28	M	216105	3021.10	313	5342.20	NA
HIV-high 28	28	M	327087	2127.20	544	1662.20	3.612
HIV-high 29	29	M	418022	NA	253	1316.60	NA
HIV-high 30	29	M	125701	NA	404	1890.00	NA
HIV-high 31	30	M	750000	NA	244	2148.60	NA
HIV-high 32	30	M	61078	558.40	380	1821.20	5.245
HIV-high 33	31	M	194091	1962.50	271	2669.60	NA
HIV-high 34	31	M	85102	NA	365	4121.60	NA
HIV-high 35	32	M	57021	NA	480	2885.40	NA
HIV-high 36	32	M	170000	507.00	17	4911.80	36.511
HIV-high 37	33	M	320000	NA	192	6535.60	NA
HIV-high 38	33	M	97483	NA	451	4079.80	NA
HIV-high 39	35	M	71739	1562.50	227	4400.20	NA
HIV-high 40	35	M	95365	3149.20	240	3135.00	0.537
HIV-high 41	35	M	102936	1346.30	283	82.40	2.167
HIV-high 42	35	M	63381	1128.70	384	17790.20	6.273
HIV-high 43	36	M	126557	NA	364	1067.60	NA
HIV-high 44	37	M	61000	NA	80	4010.60	NA
HIV-high 45	37	M	61011	NA	641	2227.80	NA
HIV-high 46	37	M	140000	NA	20	725.20	NA
HIV-high 47	38	M	544275	NA	402	628.40	NA

Table 6. Viral, clinical and CD33 protein and gene expression data of untreated HIV-1 infected cohorts. Age: years, gender: (M) male and (F) female, plasma HIV-1 viral load: HIV-1 RNA copies/ml, HIV-1 proviral: HIV-1 DNA copies/10^6 PBMCs, CD4 count: cells/mm^3, NA: not available.

Ethical approval: All studies were approved by the Comité Ètic d'Investigació Clínica of Hospital Germans Trias i Pujol (CEIC: EO-12-042 and PI-18-183) and all participants provided their written informed consent. All the research involving human research participants was performed in accordance with the Declaration of Helsinki.

3.2. Proteomics approaches

3.2.1. Cell-to-cell communicome array (185 proteins)

A custom-designed protein array previously used in a study of Alzheimer's disease (157) was used to detect and quantify 185 proteins in plasma samples of chronically HIV-1 infected, untreated individuals with different capacity of viral control. Briefly, for each plasma sample, two nitrocellulose membranes with each containing different antibodies in duplicate, were blocked, incubated with plasma, washed, and then incubated with a cocktail of biotin-conjugated antibodies specific for the different proteins. Membranes were developed with streptavidin-conjugated peroxidase and enhanced chemiluminescense reagent and exposed to autoradiographic film. After normalization and clustering analyses, differences between groups of patients were analyzed using the t test and molecules with a significance level (p-value<0.05 and q-value<0.1) were included in further analyses.

3.2.2. Extended cell-to-cell communicome array (612 proteins)

Communicome analyses were carried out using a custom-designed protein array that allowed for the detection and quantification of 612 individual proteins in plasma samples of chronic untreated HIV-1 infected individuals with different capacity of viral control. Multiple specific monoclonal or polyclonal antibodies for each protein were printed in triplicate on SuperEpoxy glass slides using a custom-built robotic microarray printer. The slides were dried overnight, vacuum sealed, and stored at −20°C until use. Plasma samples were platelet and lipid reduced by centrifugation and dialyzed (96-well DispoDialyzer with a 5-kDa molecular size cutoff) at 4°C to yield a maximally pure plasma protein fraction. Plasma proteins were subsequently N-terminally biotinylated, and the individual samples were incubated overnight with blocked antibody arrays at 4°C. Finally, the arrays were washed extensively and the captured proteins detected with Streptavidin-Alexa 555 on an InnoScan 700 scanner. For data analysis, raw data

were background subtracted and normalized using Cluster analysis, and the normalized values were Z-scored. Differences in the set of samples were analyzed by applying t test, Mann Whitney test, with a significance level above 95% (P value of <0.05) (145).

3.2.3. Proximity Extension Assay (PEA)

CSF and plasma samples of chronic untreated HIV-1 infected individuals with different capacity of viral control, ARBRE study and BCN02 participants were used for evaluation of inflammation, neurology and neuro-exploratory panels applying proximity extension assays with Olink® (https://www.olink.com). This technology requires low amounts of sample and consists in the hybridization of the sample with oligonucleotide pairs containing unique DNA sequences linked to specific antibodies. The binding of the oligonucleotides in close proximity, achieved by two antibodies targeting the same protein, allows the labels to create unique DNA sequences that are amplified by real-time polymerase chain reaction (PCR) and then sequenced (Figure 11). The protein quantification is expressed as relative expression levels that are indicated as normalized protein expression (NPX), an arbitrary unit expressed as Log2 scale. High NPX value equals a high protein concentration.
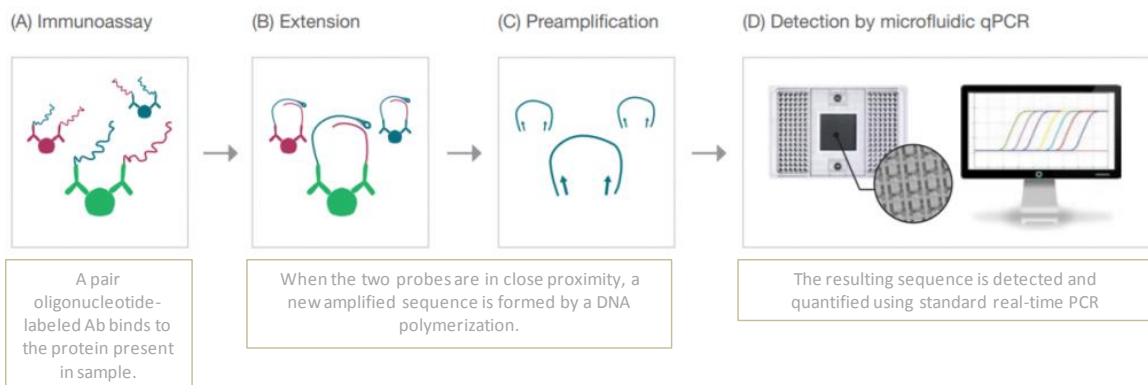
Figure 11. Proximity extension assay technology (PEA) by Olink Proteomics. Image adapted from https://www.olink.com/.

3.2.4. Ultrasensitive single-molecule array (SIMOA)

Plasma samples of ARBRE study participants were used for SIMOA detection and quantification of select proteins on a SR-X instrument, Quanterix (https://www.quanterix.com/) using the commercially available Neuro4-plex B kit for absolute quantification of Tau protein, neurofilament light protein (NFL), glial fibrillary acidic protein (GFAP) and ubiquitin carboxyl-terminal hydrolase L1 (UCHL1). In brief, samples were thawed and centrifuged and then plated in duplicates and diluted x4 with to start the establish protocol for SIMOA. First, magnetic beads coupled to target specific antibodies are incubated with sample. Then, biotinylated secondary detection antibodies and streptavidin enzyme conjugates are added to form immune complexes. Finally, beads are mixed with an enzyme substrate to generate a fluorescent signal and loaded into sample loading discs containing femtoliter measurement wells that allow for single beads to be isolated within a single well. The SR-X instrument reads the signal fluorescent of each well and transformes it into absolute protein quantification (Figure 12).
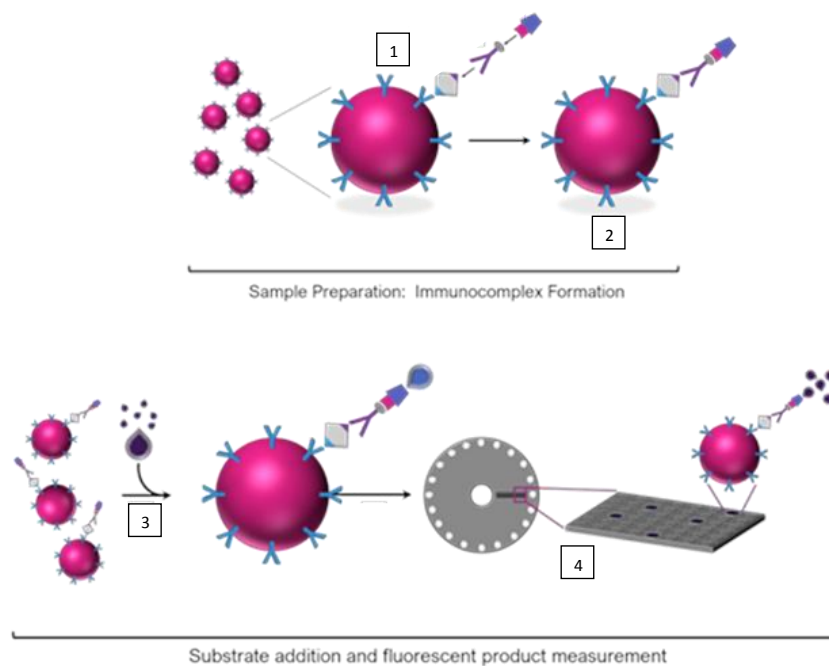
Figure 12. SIngle MOlecule Array (Simoa™) is a highly sensitive immunoassay platform by Quanterix. 1) Magnetic beads coupled to target specific antibodies are incubated with sample, (2) biotinylated secondary detection antibodies and streptavidin enzyme conjugates are added, (3) beads are mixed with an enzyme substrate and (4) loaded into sample loading discs. Image adapted from https://mitogendx.com/technologies/.

3.3. Enzyme-linked immunosorbent assay (ELISA)

All samples of each cohort were run in duplicates.

SIRT2 ELISA: Human SIRT2 ELISA Kit (Aviva Systems Biology) was used to measure the SIRT2 levels in ARBRE study plasma samples.

Neopterin ELISA: Human neopterin ELISA kit (Biorbyt) was used to measure neopterin levels in longitudinally evaluated treated HIV-infected individuals.

The absorbance reading was done at 450nm, subtracting the 550nm reading in the EnSight Multimode plate reader from PerkinElmer. The absolute levels were quantified by applying a 4 parameter logaritmic curve analysis.

3.4. Neurological assessments

3.4.1. Evaluation of CNS functioning

ARBRE study and BCN02 clinical trial participants underwent to neuropsychological evaluation covering 6 or 12 cognitive domains to provide a global composite score (NPZ-6 and NPZ-12). This included: Digit Test of the Wechsler Adult Intelligence Scale (WAIS-IV); the Trail Making Test (TMT-A) and the Symbol Digit Modalities Test (SDMT); Grooved Pegboard Test (GPT); California Verbal Learning Test (CVLT-II); the Initial Letter "p" and the Animals Test; and the Trail Making Test (TMT-B) and the Tower of London Test (TOL). The Vocabulary Test of the WAIS-IV was used to estimate premorbid intelligence.

3.4.2. Brain image assessment

ARBRE study participants underwent neurological image analysis by magnetic resonance imaging (MRI, 3 Tesla Magnetic Resonance Imaging Siemens Verio scanner). A high resolution T1-weighted 3-D structural image using a 3-T scanner (Siemens Verio,

Siemens Healthcare Sector, Germany) with a 32-phased-array head coil (192 slices in the axial plane; repetition time=1900ms; echo time=2.72ms; flip angle=9º; field of view=260x260mm; matrix size=256x256pixels; in-plane resolution=0.96x0.96mm^2; slice thickness=0.9mm) was measured. After preprocessing and inspection for the presence of artifacts, all imaging timepoints were processed following a standard VBM-DARTEL pipeline to obtain MNI (Montreal Neurological Institute) normalized and modulated images. Images were spatially smoothed with an 8-mm FWHM isotropic Gaussian kernel. Differences at the whole-brain and voxel-wise level with a p<0.05 significance threshold were explored. These analyses were controlled for age and total gray matter volume. Voxel values from significant regions were extracted to perform further statistical comparisons.

3.5. Open published datasets in Gene Expression Omnibus (GEO)

3.5.1. GEO access to post-mortem brain tissues study of HIV-1 infected individuals

The microarray dataset from the NCBI Gene Expression Omnibus (GEO, http://www.ncbi.nlm.nih.gov/geo/) databank under accession number GSE28160 was used for validation of SIRT2 expression levels in post-mortem brain tissues. For this validation, we re-analyzed seronegative (n=6) and HIV-1 infected individuals diagnosed with HAND and who died with diagnosed HAND pathology with a severe symptomatology (HIV-1 associated dementia, HAD) (n=14, of which 6 were under cART treatment and 8 without treatment), as described in the original published study (Table 7) (158).

Group	Group	Age	Gender	Race	CD4	Plasma viral load	CSF viral load	Brain DNA (copies)	Brain RNA (copies)
HIV-1 Seronegative	SN1	44	M	W	NA	NA	NA	UN	UN
	SN2	30	F	H	NA	NA	NA	UN	UN
	SN3	63	M	H	NA	NA	NA	UN	UN
	SN4	58	F	H	NA	NA	NA	UN	UN
	SN5	57	F	W	NA	NA	NA	UN	UN
	SN6	21	M	H	NA	NA	NA	UN	UN
HAD cART-untreated	cART-untreated HAD 1	47	M	W	20	210000	NA	115468	689556
	cART-untreated HAD 2	45	F	B	6	NA	NA	58001	902832
	cART-untreated HAD 3	44	M	W	7	389120	>750000	234372	762888
	cART-untreated HAD 4	58	M	B	1	750000	>750000	471248	10689754
	cART-untreated HAD 5	43	M	B	10	48520	134	UN	UN
	cART-untreated HAD 6	33	M	B	1	312240	<50	l.pos	UN
	cART-untreated HAD 7	30	M	B	8	104300	<50	l.pos	62826
	cART-untreated HAD 8	44	M	H	16	162642	NA	UN	702
HAD cART-treated	cART-treated HAD 1	46	M	W	203	80000	NA	262933	2516
	cART-treated HAD 2	40	M	H	15	750000	>750000	3789	854
	cART-treated HAD 3	51	M	H	136	65	<50	UN	UN
	cART-treated HAD 4	64	F	B	72	359	<50	UN	UN
	cART-treated HAD 5	33	M	W	66	176800	NA	UN	UN
	cART-treated HAD 6	62	M	W	20	UN	501	UN	UN

Table 7. Clinical information of individuals included in GSE28160 dataset. HAD: HIV-associated dementia, SN: HIV-1 seronegative, cART: combined antiretroviral treatment, Gender: (M) male and (F) female, Race: (W) white, (H) Hispanic and (B) black, CD4: number CD4 positive T cells per mm^3, plasma viral load: HIV-1 RNA copies/ml, CSF viral load: HIV-1 RNA copies/ml, NA: not available, UN: undetectable, l.pos: low positive by standard PCR.

3.5.2. GEO access to BCN02 transcriptomics dataset

Gene expression of CD33 was obtained from Oriol-Tordera et al, (159). The dataset is available in Gene expression Omnibus (GEO) under the accession number GSE184653. The specific values for CD33 were obtained from this dataset after log2 transformation of the TMM normalized counts.

3.6. Gene expression analysis

3.6.1. Real-time PCR *SIRT2* gene

RNA samples from PBMC dry-pellets were obtained from chronically untreated HIV-1 infected individuals (n=58) with different capacity of viral control. RNA was retrotranscribed and TaqMan gene expression assays (Applied Biosystems) were used for detection of *SIRT2* (Hs01560289_m1) and *TBP* (Hs99999910_m1). Gene amplification was performed in an Applied Biosystems 7500 Fast Real-Time PCR System thermocycler, and the relative expression was calculated as $2^{-\Delta CT}$ (where C_T is the median threshold cycle from 3 replicates).

3.6.2. Real-time PCR *CD33* gene

RNA samples from available PBMC dry-pellets from chronically untreated HIV-1 infected individuals (n=96) were retrotranscribed and TaqMan gene expression assay (Applied Biosystems) was used for quantification of *CD33* (hs01076281_m1) expression. *TBP gene (*Hs99999910_m1) was used as the housekeeping gene. Gene amplification was performed in Applied Biosystems 7500 Fast Real-Time PCR System thermocycler, and the relative expression quantification was calculated as $2^{-\Delta CT}$ (where C_T is the median threshold cycle from 3 replicates).

3.7. Virus genome quantification

3.7.1. Determination of integrated HIV-1 proviral DNA

HIV-1 proviral DNA was quantified in PBMCs from chronically untreated HIV-1 infected individuals with different capacity of viral control and in lysed extracts from CD4 T-cells

extracted from PBMCs from BCN02 clinical trial participants by droplet digital PCR (ddPCR) in duplicates. Briefly, two different primer/probe sets annealing to the 5' long terminal repeat and gag regions were used to circumvent sequence mismatch in the patients´ proviruses, and the *RPP30* housekeeping gene was quantified in parallel to normalize sample input. Raw ddPCR data were analyzed using the QX100™ droplet reader and QuantaSoft v.1.6 software (Bio-Rad) (160).

3.7.2. Real time PCR-based quantification of proviral DNA

To assess HIV-1 proviral levels, total DNA was isolated using the RNA/DNA purification Micro kit (Norgen Biotek corp.) as recommended by the manufacturer from in vitro experiments of infected PHA-blast and monocytes. Quantification of proviral HIV-1 copy numbers was determined by using a quantitative PCR assay, using TaqMan Universal Master Mix II (Applied Biosystems) in a 7500 real-time PCR system (Applied Biosystems). We used the following set of primers and probe, forward primer, 5'-GACGCAGGACTCGGCTTG-3'; reverse primer, 5'-ACTGACGCTCTCGCACCC-3'; probe, 5'-fluorescein amidite (FAM)-TTTGGCGTACTCACCAGTCGCCG-6-carboxytetramethylrhodamine (TAMRA)-3'. *GAPDH* gene (Hs02786624_g1) was used as the housekeeping gene. Gene amplification was performed in Applied Biosystems 7500 Fast Real-Time PCR System thermocycler, and the relative expression quantification was calculated as $2-\Delta CT$ (where *CT* is the median threshold cycle from 2 replicates).

3.8. Cultured primary cells and cell lines

3.8.1. HIV-1 infection of PHA-activated T-cells and monocyte-derived macrophages

Blood samples from non–HIV-1 infected donors were obtained for *in vitro* studies from the Banc de Sang i Teixits in Barcelona. Isolated PBMCs from non–HIV-1 infected

donors were stimulated with PHA at 5µg/ml (Sigma-Aldrich) and IL-2 at 10U/ml (Sigma-Aldrich). After 3 days, PHA-activated T-cells were infected with the HIV-1$_{NL4-3}$ strain (Multiplicity of Infection (MOI): 0.01). For monocyte-derived macrophages (MDMs), PBMCs were depleted to obtain monocytes using the EasySep™ Human Monocyte Enrichment Kit (Stem Cell). Monocytes were then incubated with macrophage colony-stimulating factor (M-CSF) at 1µg/ (PeproTech) for 4 days before infection with the HIV-1$_{BaL}$ strain (MOI: 0.01). HIV-1 infection in PHA-activated T-cells and MDMs was evaluated under different conditions: AZT at 200µg/ml (Sigma-Aldrich), DMSO as experimental controls and corresponding drugs; AK-1 at 10µM (Sigma-Aldrich), anti-CD33 at 0.01µg/µl (Abcam). After 3 (PHA-blast) and 4 days (MDMs), Gag p24 in culture supernatants was quantified by ELISA (INNOTEST HIV p24 Antigen mAb)**.**

3.8.2. HIV-1 infection of microglial cells

Primary microglial cells (iCell Microglia, FUJIFILM Cellular Dynamics) were thawed and cultured for 3 days in a 96-well plate at 20,000 glial cells/well following the manufacturer's recommendations. After 3 days, microglial cells were infected with the HIV-1$_{NLAD8}$ strain (MOI: 0.01) and after 16 hours, cells were washed. Then, infected microglial cells were incubated in the absence or presence of AK-1 at 10µM (Sigma-Aldrich) or AZT at 200 µg/ml (Sigma-Aldrich). After 3 days, p24 in the culture supernatant was quantified by ELISA (INNOTEST HIV p24 Antigen mAb).

3.8.3. *In vitro* HIV-1 reactivation

The J-LAT A2 cells, which are transfected Jurkat cells with a green fluorescent protein (GFP)–encoding HIV-1 minigenome, were stimulated with PMA at 1ng/ml (Sigma-Aldrich) and cultured in the presence or absence of AK-1 at 10µM (Sigma-Aldrich). After 24 hours, GFP expression was evaluated on a FACS Canto Flow Cytometer (Becton Dickinson), and the data were analyzed using FlowJo version 10 software (161)(162).

3.9. Pathway and statistical analyses

3.9.1. STRING pathway

For Protein-Protein Interaction Networks, Functional Enrichment Analysis was used to analyze interaction between proteins (https://string-db.org/cgi/input?sessionId=bcCYfoHsbNV0&input_page_active_form=multiple_identifiers).

3.9.2. Statistical analysis

Principal Component Analysis (PCAs), Heatmaps, Venn diagrams and correlograms were perform with RStudio version 1.2.5042. Univariate and multiple comparisons statistical analyses were performed using GraphPad Prism, version 8. For non-parametric data, paired comparisons used the Wilcoxon signed rank tests and for non-paired comparisons Mann-Whitney test was applied. Also, for parametric data, paired or unpaired t test were applied. For multiple group comparisons, one-way ANOVA test with False Discovery Rate (FDR) calculation using Benjamini and Hochberg method were used. The Spearman rank test and Pearson test were applied for the correlation analysis for non-parametric and parametric data, respectively. For all analyses, p-values <0.05 were considered statistically significant.

RESULTS

4.1. CHAPTER I. Identification of plasma biomarkers in natural control of HIV-1 infection in the absence of cART

Summary

A small subset of people with HIV (PWH) able to control their infection in the absence of combined antiretroviral therapy (cART) over prolonged periods are known as HIV-1 controllers. The viral control in this group of PWH is reflected in the size of the viral reservoir including sanctuaries such as the central nervous system or the cerebrospinal fluid which has been found to bear extremely low or undetectable levels of HIV-1 RNA (164)(165)(166). It is believed that HIV-1 controllers restrict viral replication by various host immune system mechanisms, including soluble factors with antiviral and/or immunoregulatory function.

In this first chapter of the thesis, we studied the biomarkers in cerebrospinal fluid that can also be detected in plasma from individuals with spontaneous natural control of HIV-1 infection in the absence of cART and which are associated with possible neurological dysfunction caused by HIV-1.

4.1.1. Dysregulated levels of soluble factors in CSF reflected at peripheral blood in HIV-1 infection

To study the proteomic differences between chronic untreated HIV-1 infected individuals and seronegative individuals in the periphery and at central nervous system, the plasma and CSF proteome of a total of 20 HIV-1 infected individuals and 5 seronegative individuals were screened using proximity extension assay focused in three different panels that cover neurology, neuro-exploratory and inflammatory molecules (Methods section Table 1). Principal Component Analysis (PCA) showed that soluble factors involved in neurological and inflammatory processes at CSF and plasma fluids clearly differ between HIV-1 infected individuals compared with seronegative (Figure 13A). Data analysis identified 28 factors (SIGLEC1, FCRL2, TNFSF14, MCP2, CXCL9, ANXA10, PFDN2, BST2, CRTM, TNFB, CXCL11, CASP8 CD244, ENRAGE, FCAR, IL7, CD8A, CD5, GZMA, MCP3, LAPTGFB, SLAMF1, TNRSF9, LXN, IL12B, IFI30, PSME1 and IL12) that were differentially detected between the CSF of HIV-1 infected individuals compared with seronegative individuals (Figure 13B). In plasma samples, 15 molecules (HAGH, GZMA, IFI30, SIGLEC1, IFNgamma, FGF5, EPHA10, ANXA10, IL24, CRTAM, IL33, EDA2R, IL32, IL6 and CDCP1) were significantly detected between the HIV-1 infected and uninfected groups (Figure 13C). Molecule interaction analysis of the 28 proteins differentially detected in the CSF showed that some of these molecules are related with *CD8A protein* mainly expressed in CD8 T cells (Figure 13D). Functional analysis of the 15 proteins differentially detected at peripheral blood belong to different functional categories compared to CSF compartment, with the *cytokine pathway* (IFNG, GZMA, IL6, Il24, IL32, Il33) being the most represented one (Figure 13E).
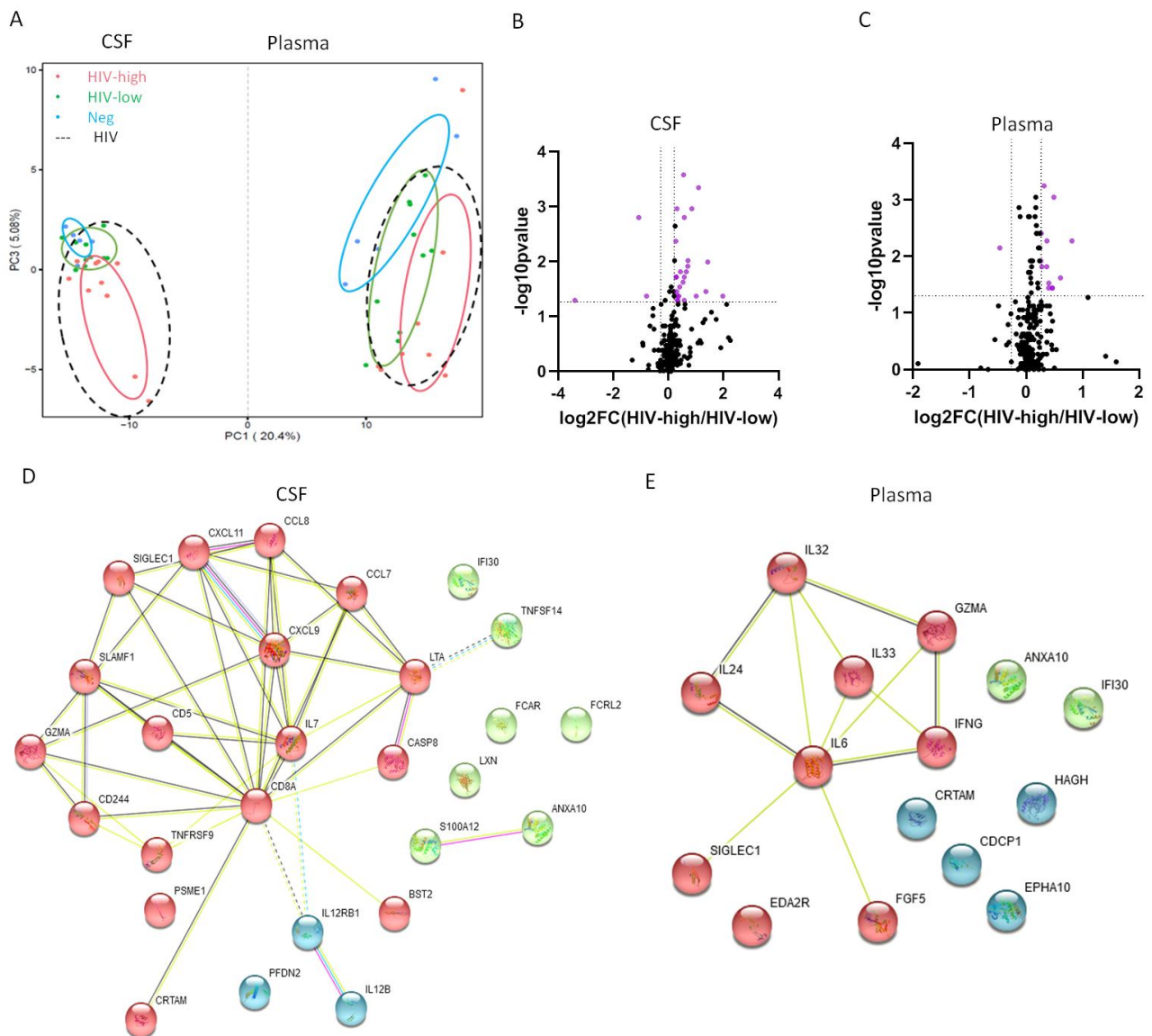
Figure 13. Differential plasma and CSF proteomes between HIV-1 infected and seronegative individuals. Soluble proteomes in CSF and plasma from 20 untreated chronic HIV-1 infected individuals and 5 seronegative were screened using proximity extension assay. A) Principal Component Analysis (PCA) shows the changes of 276 inflammation and neurological proteins of the 25 individuals at plasma and CSF level. Red points and circle indicate HIV-high individuals (>100,000 HIV-1 RNA copies/ml), green points and circle indicate HIV-low participants, blue points and circle represent seronegative and black circle indicate all the HIV-1 infected individuals (<10,000 HIV-1 RNA copies/ml). B-C) Volcano plot representing the relative expression of the 276 molecules measured using the PEA, which identified (B) 28 significantly differently detected molecules at CSF level and (C) 15 significant molecules at plasma level between HIV-1 infected individuals and seronegatives. The $\log_2$ fold-change is shown on the x-axis and the $-\log_{10}$p-value of the protein-specific comparisons on the y-axis. The significantly detected proteins are highlighted in purple dots. D-E) Protein interaction analysis considering (D) the 28 proteins differentially detected at CSF levels and (E) the 15 molecules differentially detected at plasma when comparing HIV-1 infected with seronegative individuals.

To identify CSF markers of HIV-1 infection also detectable at plasma, the levels of the 28 significantly detected CSF proteins were correlated with their respective plasma levels. Interestingly, most of the correlations were positive (Figure 14A) indicating that the differential levels of proteins were similarly detected at CSF and plasma. Also, among the 5 common proteins; SIGLEC1, CRTAM, GZMA, IFI30 and ANXA10 that discriminate between HIV-1 infected individuals and seronegative groups at both compartments, the CSF and plasma (Figure 14B), only the levels of SIGLEC1, CRTAM and GZMA in CSF correlated significantly with the levels at plasma (Figure 14C-E, SIGLEC1: rho=0.8 p=0.0001, CRTAM: rho=0.7635 p=0.0001 and GZMA: rho=0.6591 p=0.0005).

These data identify three proteins: SIGLEC1, CRTAM and GZMA that are significantly different between HIV-1 infected and seronegative individuals when measured in peripheral blood and in the CNS.
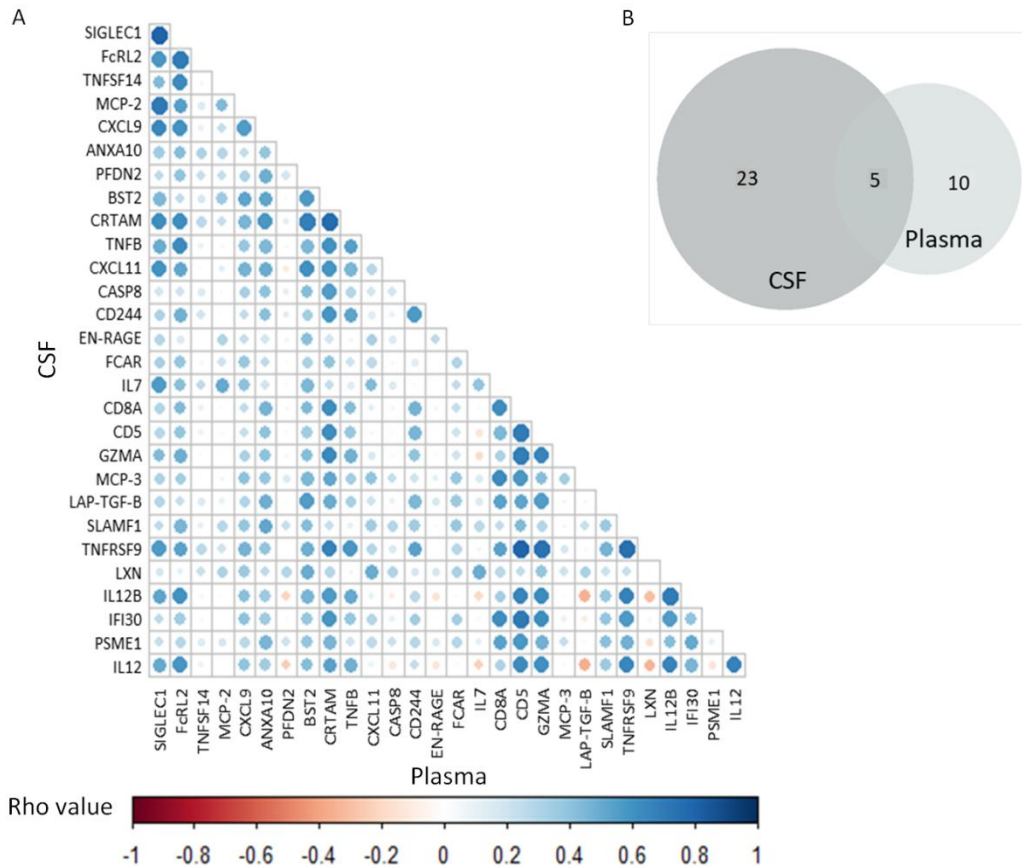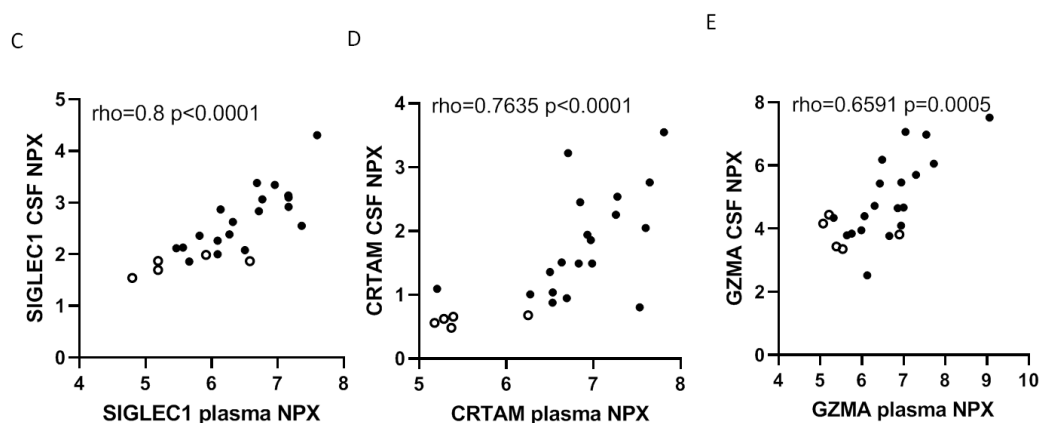
Figure 14. Correlation between plasma and CSF candidates. A) Correlogram showing the relation between CSF and plasma levels of 28 molecules found in CSF. Plotted Spearman rho values, blue means positive correlation and red negative correlation. B) Venn diagram shows significant proteins and common proteins between CSF and plasma. C-E) Correlation plots between (C) SIGLEC1, (D) CRTAM and (E) GZMA levels in both samples (CSF and plasma). Correlation analysis was based on the Spearman's rank test. Statistical significance was set at p<0.05.

4.1.2. SIGLEC1, CRTAM and GZMA protein levels are associated with natural control of HIV-1 infection in the absence of treatment

To further study whether proteome levels were also associated with control of viral replication in the absence of treatment, the HIV-1 infected individuals were classified in two groups according to their plasma viral loads (pVL) as follows: i) individuals with pVL >100,000 HIV-1 RNA copies/ml (HIV-High, n=10), and ii) individuals with pVL <10,000 HIV-1 RNA copies/ml (HIV-Low, n=10) and a group of HIV-1 seronegative individuals (n=5) (Methods section Table 1). As mentioned above, principal component analysis (Figure 13A) showed that in samples from both anatomical compartments (plasma and CSF), HIV-high individuals segregated clearly from HIV-low and seronegative groups. Moreover, given the associations of SIGLEC1, CRTAM and GZMA protein levels in CSF and plasma with HIV-1 viral load levels in both compartments (Figure 15A-B, E-F and I-J), we explored if there were differences in these markers

between HIV-1 infected individuals that can and those that cannot control viral replication in the absence of cART. SIGLEC1 is a surface adhesion molecule on human myeloid cells that acts as a receptor for sialylated molecules found on various pathogens (170). At CSF, significantly higher SIGLEC1 levels were detected in HIV-high compared to HIV-low and seronegative individuals (Figure 15C, HIV-high vs HIV-low: p=0.0052, HIV-high vs seronegative p=0.0047 HIV-low vs seronegative p=0.0047). SIGLEC1 relative plasma levels significantly differed between groups (Figure 15D, HIV-high vs HIV-low p=0.0076, HIV-high vs seronegative p=0.004). CRTAM is a cytotoxic and regulatory T-cell molecule expressed in epithelial cells along the lateral membrane and is important for cell-cell   interactions (167). Relative plasma and CSF levels of CRTAM differed significantly between HIV-high and HIV-1 seronegative individuals (Figure 15G-H, CSF: p=0.0007 and plasma: p=0.001) and between HIV-low and HIV-1 seronegative individuals (Figure 15G-H, CSF: p=0.0007 and plasma: p=0.008). Finally, GZMA is a serine protease expressed by NK and T cells that act as a pro-inflammatory mediator and could play a role in the lysis of infected cells (168)(169). Relative plasma and CSF levels were significantly elevated in HIV-high individuals compared to seronegative group in the CSF (Figure 15K, CSF: p=0.0625), while its levels in plasma were significantly higher in HIV-high compared with HIV-low or seronegative individuals (Figure 15L, HIV-high vs HIV-low: p=0.004 and HIV-high vs seronegative p=0.003). Taking together, these results show that SIGLEC1, CRTAM and GZMA allow to discriminate HIV-1 infected individuals depending on their levels of viral loads (HIV-low and HIV-high) and show these biomarkers to be present at significantly different levels between these groups using either plasma or CSF samples.
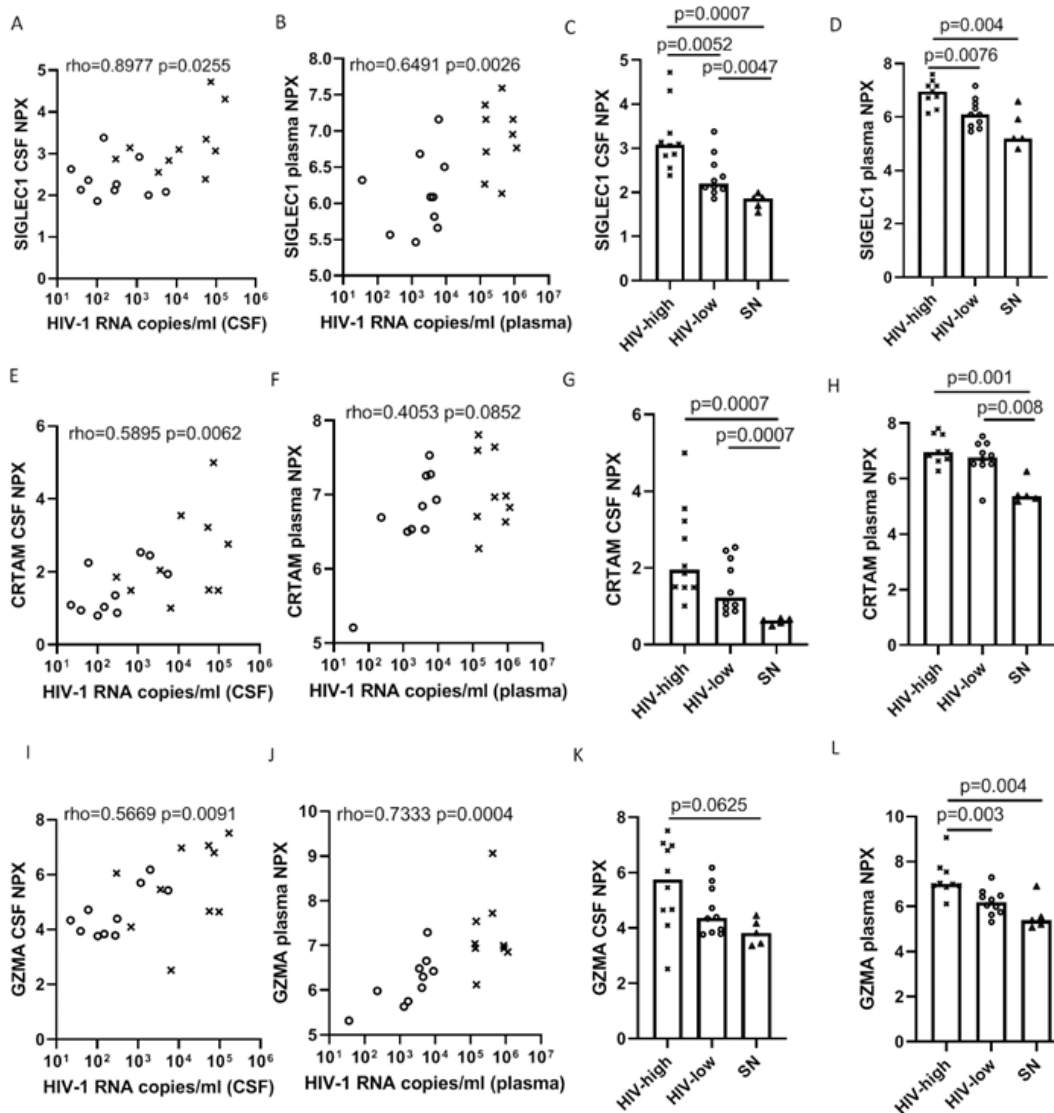
Figure 15. SIGLEC1, CRTAM and GZMA and SIGLEC1 in plasma and CSF. SIGLEC1, CRTAM and GZMA levels allow the discrimination between HIV-high (n=10) and HIV-low (n=10) and seronegative (n=5) groups and correlate with viral load in peripheral blood and CSF. A-B) Correlation between relative SIGLEC1 levels and viral load in (A) CSF and (B) plasma, respectively. C-D) relative SIGLEC1 levels between HIV-high, HIV-low and seronegative individuals represented in the x-axis and in the y-axis (C) the relative CSF levels and (D) relative plasma levels. The upper limit of the bar is the median value of SIGLEC1 levels. E-F) Correlation between relative CRTAM levels and viral load in (E) CSF and (F) plasma, respectively. G-H) relative CRTAM levels between HIV-high, HIV-low and seronegative individuals represented in the x-axis and shown in the y-axis (G) the relative CSF and (H) relative plasma levels. The upper limit of the bar is the median value of CRTAM levels. Figure I-J) Correlation between relative GZMA levels and viral load at (I) CSF and (J) plasma levels. K-L) relative GZMA levels between HIV-high, HIV-low and seronegative individuals represented in the x-axis and shown in the y-axis (K) the relative CSF and (L) relative plasma levels. The upper limit of the bar is the median value of GZMA levels. Legend: crosses represent HIV-high, circles represent HIV-low and triangles represent HIV-1 seronegative individuals. Differences between the groups were analyzed using the Mann-Whitney *U* test and the correlation analysis was based on the Spearman's rank test. Statistical significance was set at $p < 0.05$.

Apart from identifying SIGLEC1, CRTAM and GZMA proteins as markers of relative control of viral replication, we aimed to compare their plasma and CSF levels to immunological and, especially, neurological status. For that, correlation analysis was performed in a representative subset of (n=20) untreated chronically HIV-1 infected individuals and (n=5) seronegatives, comparing CD4/CD8 ratio and levels of neopterin protein, an inflammatory marker that has been associated with HIV-1 related neurocognitive disorders and immune activation in the brain (171). Figure 16 shows positive correlations between SIGLEC1, CRTAM and GZMA and neopterin in both compartments (plasma and CSF). Moreover, the CD4/CD8 ratio in PBMCs correlated with plasma protein levels of SIGLEC1, CRTAM and GZMA. These data suggest that high viremia is associated with declined immune status and high levels of neopterin and possible neuroinflammation and consequently neurological damage.
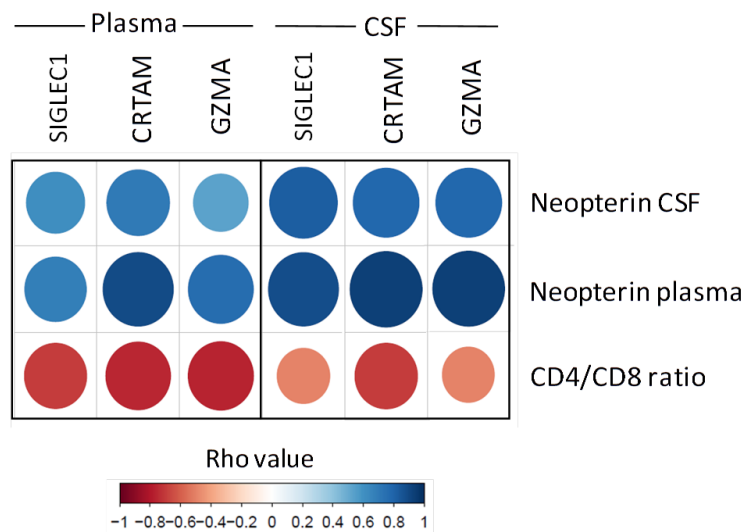
Figure 16. Correlogram between SIGLEC1, CRTAM and GZMA and the neurological biomarker neopterin and CD4/CD8 ratio. Rows show neopterin levels in plasma and CSF and CD4/CD8 T cell ratio in PBMCs; columns indicate SIGLEC1, CRTAM and GZMA levels in plasma (left) and CSF (right). Spearman rho values are indicated in colors, with blue showing positive correlations and red negative correlations. All represented Rho values were significant $p < 0.05$.

4.1.3. SIGLEC1, CRTAM and GZMA plasma levels are reduced after one year of cART in HIV-1 infected individuals.

Although access to antiretroviral treatments remains limited globally, current guidelines recommend early treatment initiation to minimize the establishment of a diverse viral reservoir, limit inflammation and slow viral evolution. To evaluate whether treatment initiation affected the levels of the above biomarkers of virus control, we determined the plasma levels of these molecules before and after initiation of treatment (Methods section Table 2). The longitudinal analysis showed that relative plasma levels of SIGLEC1, CRTAM and GZMA were significantly higher before cART treatment initiation compared to samples drawn after one year on treatment (Figure 17A-C, SIGLEC1 p=0.0003, CRTAM: p=0.0001 and GZMA: p<0.0001, Wilcoxon paired test). In addition, plasma levels of SIGLEC1, CRTAM and GZMA correlated positively with viral load when individuals were untreated (Figure 17D-F, SIGLEC1: rho=0.5196 p=0.0346, CRTAM: rho=0.2721 p=0.0289 and GZMA: rho=0.5417 p=0.0267), also the CD4/CD8 ratio correlated negatively with the plasma levels of all three molecules (Figure 17G-I, SIGLEC1: rho=-0.4902 p=0.0478, CRTAM: rho=-0.6324 p=0.0077 and GZMA: rho=-0.5123 p=0.0376).
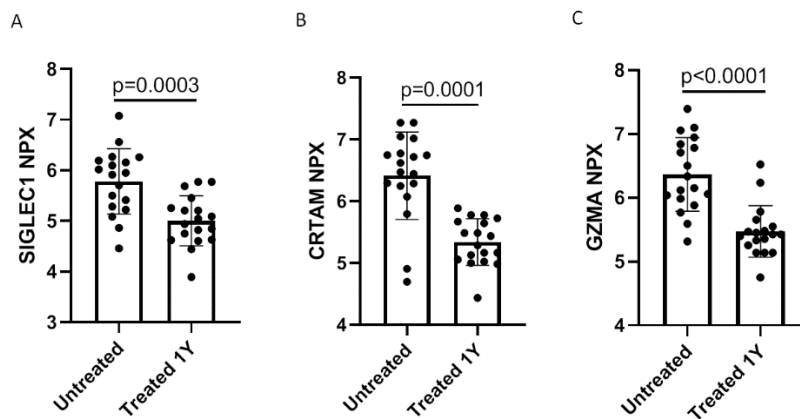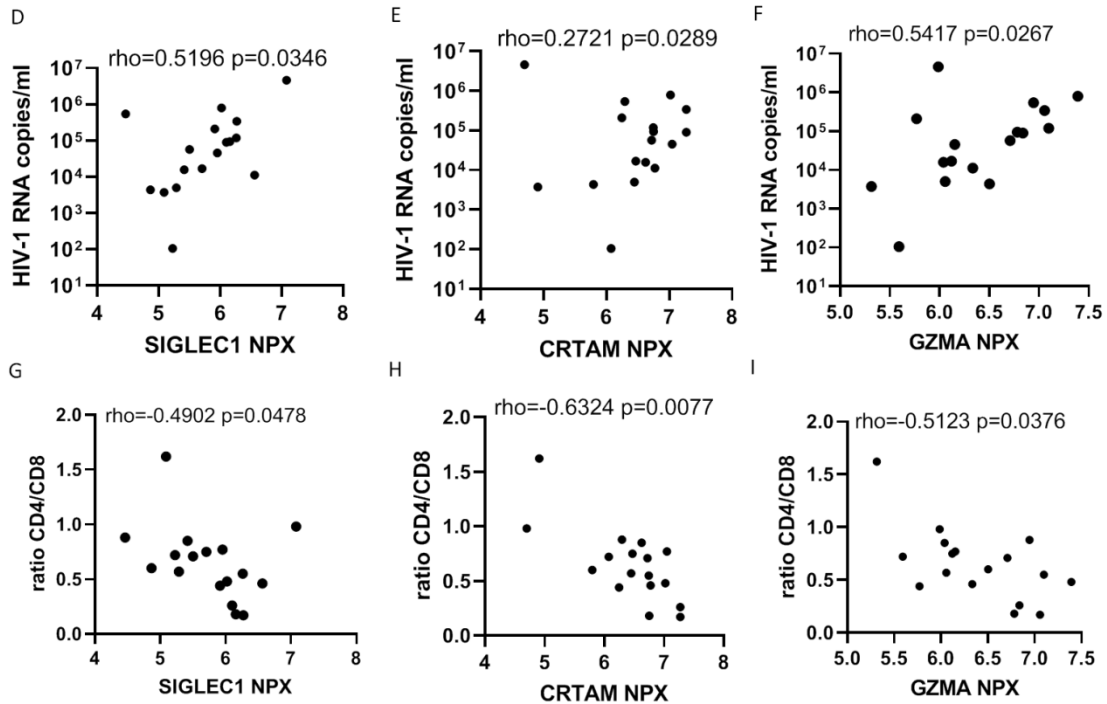
Figure 17. cART reduced the relative SIGLEC1, CRTAM and GZMA plasma levels in HIV-1 infected individuals. SIGLEC1, CRTAM and GZMA were quantified in a cohort of early treated HIV-1 infected individuals. A-C) SIGLEC1, CRTAM and GZMA relative plasma levels in early diagnosis without cART and after one year post-cART initiation. D-F) Correlation analysis between relative plasma levels of SIGLEC1, CRTAM and GZMA and plasma viral load in untreated conditions, respectively. G-I) Correlation analysis between relative plasma levels of SIGLEC1, CRTAM and GZMA and the CD4/CD8 ratio in PBMCs. Differences between the groups were analyzed using the Mann-Whitney *U* test and the correlation analysis was based on the Spearman's rank test. Statistical significance was set at p<0.05.

Furthermore, a cross-sectional analysis between i) untreated HIV-1 individuals, ii) individuals on cART for one year and iii) HIV-1 seronegative individuals showed that cART restored the plasma levels of SIGLEC1, CRTAM and GZMA similar to HIV-1 seronegative individuals (Figure 18A-C), indicating that effective suppression of viremia decreased the plasma levels of SIGLEC1, CRTAM and GZMA, latest within one year of treatment initiation.
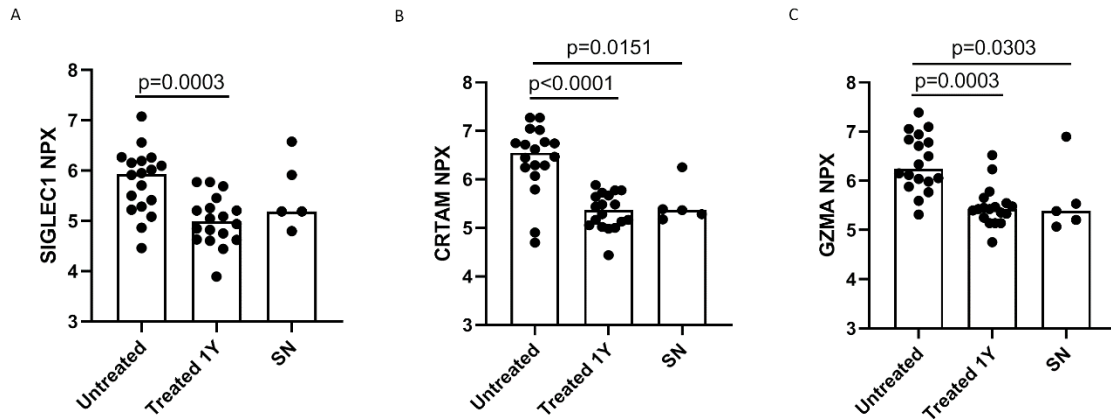
Figure 18. cART reduced SIGLEC1, CRTAM and GZMA plasma levels in HIV-1 infected individuals to levels seen in uninfected individuals. A-C) relative SIGLEC1, CRTAM and GZMA plasma levels in untreated individuals, post one year on treatment and HIV-1 seronegative individuals, respectively. Differences between the groups were analyzed using the Mann-Whitney *U*. Statistical significance was set at p<0.05.

4.2. CHAPTER II. Plasma HDAC class II factor (Sirtuin-2) as a biomarker of HIV-1 infection and neurological dysfunction

Summary

The implementation and access to combined antiretroviral treatment (cART) has dramatically improved the quality of life of people with HIV (PWH). However, some comorbidities, such as neurological disorders associated with HIV-1 infection still represent a serious clinical challenge. These neurological disorders are caused by virus replication, chronic inflammation and treatment toxicity. While a direct effect of viral replication and/or viral reservoir in the brain is likely driving these pathologies, it still remains unclear how HIV-1 enters the central nervous system and causes neuroinflammation and brain damage. Since PWH who control viral replication in the absence of cART present less inflammation and less severe impact on the central nervous system (172), we identified soluble factors in plasma that are associated with control of HIV-1 replication and neurological dysfunction. The identified markers could serve as early biomarkers of neurological consequences of HIV-1 infection and as new therapeutic targets for this comorbidity.

4.2.1. Sirtuin 2, a novel plasma biomarker associated to HIV-1 viral control

To identify peripheral blood biomarkers associated with outcome of HIV-1 infection and the development of HIV-1 related neurological disease, we employed an antibody array previously used successfully in the study of Alzheimer's disease (157). We measured levels of 185 plasma factors in samples from untreated, chronically HIV-1 infected individuals classified as "HIV-high" (n=30) with a plasma viral load (pVL) >10,000 HIV-1 RNA copies/ml (range: 15,000 to 1,200,000; median: 147,500) and a group of "HIV-low" (n=20) with plasma viral loads <10,000 HIV-1 RNA copies/ml (range: <50 to 10,000; median: 975) (Methods section Table 3). Data analyses identified 20 factors differentially detected between the two groups, of which SIRT2 emerged as the most significant marker, considering fold-change differences of plasma levels and the p-value of pairwise comparisons (Figure 19A-B)(Annexe Tables S1). Specifically, SIRT2 was elevated in the HIV-high group (Figure 19C) and the relative plasma levels of SIRT2 correlated positively with pVL and with HIV-1 proviral levels across all HIV-1 infected individuals studied (Table 8). Correspondingly, the *SIRT2* gene was also significantly higher expressed in PBMCs from the HIV-high (Figure 19D) compared to the HIV-low group. This difference was even more pronounced when comparing the HIV-high individuals to an additional cohort of HIV-elite controllers (HIV-1 infected individuals with undetectable viral load in the absence of antiretroviral treatment, Figure 19D). The same associations with viral parameters observed for SIRT2 plasma levels were also detected in PBMCs, as *SIRT2* gene expression correlated with pVL and HIV-1 proviral levels across all the groups (Figure 19E-F).
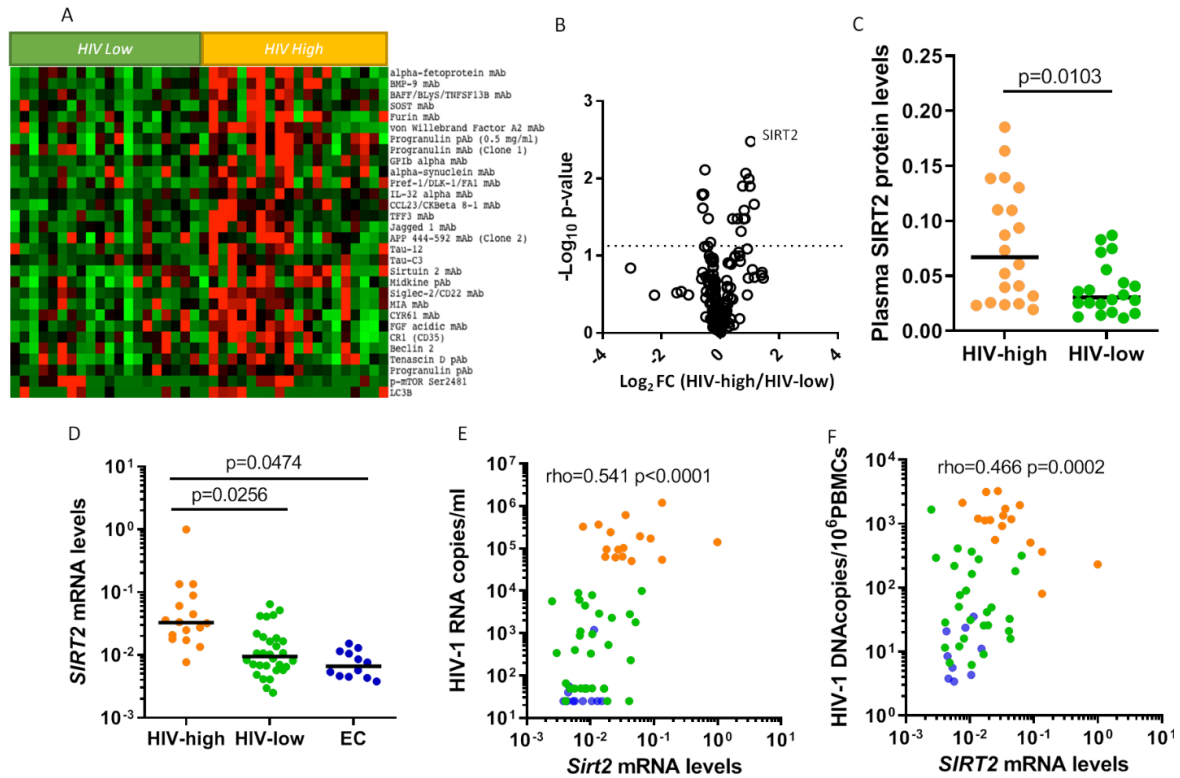
Figure 19. Plasma and gene expression levels of SIRT2 are associated with viral parameters in chronically untreated HIV-1 infection. Proteomic array (157) applied to plasma samples from chronically untreated HIV-1 infected individuals with different degrees of HIV-1 control (n=40). A) Heatmap showing the relative plasma levels of the most differentially detected soluble factors between untreated HIV-1 infected individuals with high viral loads (HIV-high, with more than 50,000 viral copies/ml, n=20) and those with low viral loads (HIV-low, viral loads < 10,000 viral copies/ml, n=20). Red indicates high protein abundance in plasma, and green indicates reduced protein levels. B). Volcano plot representing the relative expression of the 185 molecules measured, identifying SIRT2 as the most significant and differentially detected soluble factor between HIV-high and HIV-low (Log2 FC=1.039 Log10 p-value=2.478). The log2 fold-change is shown on the x-axis and the –log10 of the p-value of the comparisons on the y-axis. C) Scatter plot showing the relative plasma protein levels of SIRT2 in both study groups (HIV-high [n=20, orange dots] and HIV-low [n=20, green dots]). D) *SIRT2* gene expression in PBMCs from chronically untreated HIV-1 infected individuals grouped as HIV-high (n=16, orange dots), HIV-low (n=30 green dots, including 20 individuals tested for the plasma proteomics here and 10 additional HIV-low individuals from an unrelated cohort (see Table in Material and Methods section), and elite controllers (i.e., untreated HIV-1 infected individuals with undetectable HIV viral load in plasma n=12, blue dots). Study groups are shown on the x-axis, and relative *SIRT2* gene expression corrected for CD4 counts is shown on the y-axis. E-F) Correlation between relative *SIRT2* gene expression and (E) plasma viral load and (F) HIV-1 proviral DNA levels in PBMCs for all three groups. HIV-high patients (n=16, orange dots), HIV-low patients (n=30 green dots), and elite controllers (n=12, blue dots) are indicated in the plot. Relative *SIRT2* gene expression corrected for CD4 counts is shown on the x-axis, and viral load (HIV-1 RNA copies/ml) and proviral levels (HIV-1 DNA copies/10^6 PBMCs) are shown on the y-axis. Plasma proteome data were analyzed using the *t* test. SIRT2 plasma levels between HIV-high and HIV-low were analyzed using the Mann-Whitney test. *SIRT2* gene expression levels between HIV-high, HIV-low and EC were analyzed using ANOVA test for multiple comparisons corrected by original FDR method of Benjamini and Hochberg. The Spearman's rank test was applied for the correlation analysis. Statistical significance was set at p<0.05.

Symbol ID	Name ID	p-value	fold change	- Log$_{10}$ p-value	Log$_2$ fold change	Viral load		Proviral		CD4 counts	
						rho	p-value	rho	p-value	rho	p-value
SIRT2	Sirtuin 2	0.0033	2.0547	2.4785	1.039	0.441	0.004	0.486	0.034	-0.446	0.001
CCL23	C-C motif chemokine ligand 23	0.0086	1.8287	2.0654	0.8708	0.447	0.004	0.17	ns	-0.321	ns
TFF3	Trefoil factor 3	0.0101	1.9642	1.994	0.9739	0.526	0.001	0.339	ns	-0.204	ns
AFP	Alpha-fetoprotein	0.0125	1.6965	1.9017	0.7626	0.42	0.007	0.535	0.018	-0.096	ns
GDF2	Growth differentiation factor 2	0.0126	2.01	1.8993	1.0072	0.345	0.029	0.342	ns	-0.288	ns
GP1BA	Glycoprotein Ib platelet alpha subunit	0.0215	2.2252	1.667	1.154	0.429	0.006	0.547	0.015	-0.093	ns
CD22	Siglec-2	0.0258	1.7615	1.5889	0.8168	0.375	0.017	0.355	ns	-0.305	ns
TNFSF13B	TNF superfamily member 13b, BAFF	0.033	1.7931	1.4809	0.8425	0.392	0.012	0.214	ns	-0.355	0.033
GRN	Progranulin	0.0332	1.3422	1.4795	0.4246	0.336	0.032	0.235	ns	-0.301	ns
VWF1	Von Willebrand Factor A2	0.0334	1.7389	1.4763	0.7982	0.305	ns	0.044	ns	-0.241	ns

Table 8. Top candidates identified by plasma proteomic analysis: Log10 p-value (Unpaired t Test), Log2 Fold change (HIV high vs HIV low), VL: plasma HIV-1 RNA copies/ml, Proviral: HIV-1 DNA copies/106 PBMCs, CD4 counts: CD4 T cells/mm3, Rho= Spearman Rank test for association analysis performed HIV-1 individuals (HIV high and HIV low), ns: not significant.

In order to study the relationship between SIRT2 plasma levels and the other molecules measured in the array, we performed correlation analysis across all measured markers. Figure 20A shows the molecules in plasma that are significantly correlated with SIRT2 levels (p<0.05, Spearman's rank test). The functional relationship between these statistically related factors was further explored using the STRING application (Figure 20B). Several functions reported in open-access databases (Gene Ontology, UniProt and Reactome) were identified, including *Regulation of Cell Death* (GO: 0010941, FDR=0.00030), *Innate Immunity* (KW0399, FDR=3.57x10^7), and *Complement Cascade* (HSA-166658, FDR=3.44x10^6). Interestingly, SIRT2 was functionally connected with brain-derived neurotrophic factor (BDNF), while BDNF was at the same time connected with alpha-synuclein (SNCA) and Tau protein (MAPT) (Figure 20B), which both are substrates of SIRT2 in brain tissue (173). In addition, SNCA and MAPT are, together with BDNF, well-established biomarkers of neurological damage (174), and correlated positively with SIRT2 levels in plasma (SNCA: rho=0.3054 p=0.0553, MAPT: rho=0.4302 p=0.0056 and BDNF: rho=0.3719 p=0.0181, Figure 20C-E). Although CNS injury was not determined in the two groups of HIV-high/low, trends towards increased levels of specific markers of neurological damage (SNCA, MAPT, and BDNF) in individuals with poor virus control were observed (Figure 21A-C), with the comparison of SNCA reaching statistical significance. These data identify SIRT2 as a soluble factor in plasma that discriminates between controlled and uncontrolled HIV-1

infection and also showed a relationship with the levels of several biomarkers of neurological damage (175).
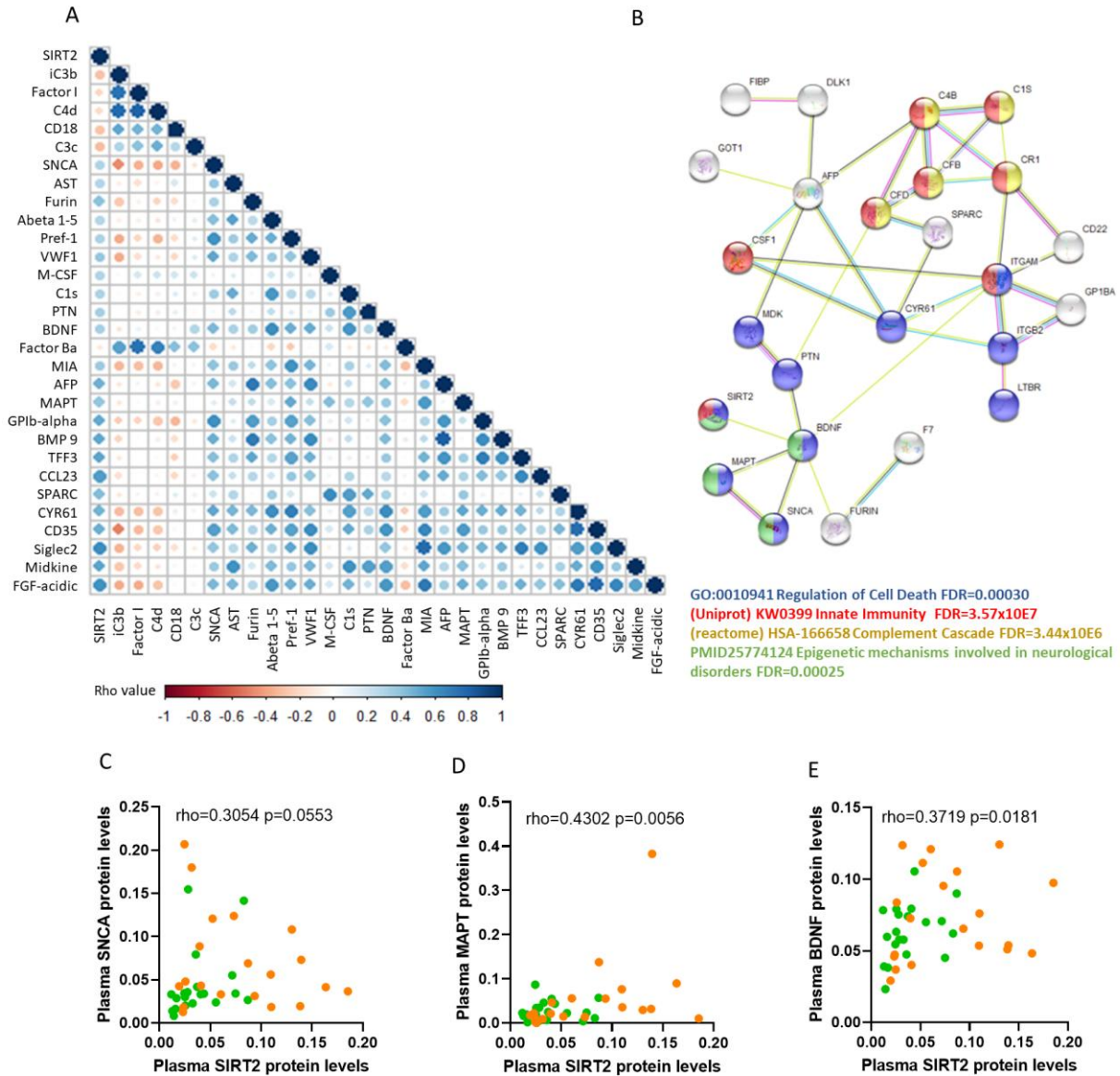
Figure 20. Plasma levels of SIRT2 are associated with neurological factors in chronic untreated HIV-1 infection. A) Correlation matrix showing the significant relationship between SIRT2 and proteins measured in the antibody array considering all HIV-1 infected groups (HIV-high and HIV-low). The color scale shows positive correlations in blue and negative correlations in red. B) The functional analysis performed using the STRING webpage represents the interaction between SIRT2 and the other correlated factors. Several functions derived from Gene Ontology, Uniprot, Reactome, and PubMed were identified: *Regulation of Cell Death* category (GO:0010941, FDR=0.0030) in blue, *Innate Immunity* (KW0399, FDR=3.57x10E7) in red, *Complement Cascade* (HSA-166658, FDR=3.44x10E6) in yellow, and epigenetic mechanisms involved in neurological disorders (PMID25774124, FDR 0,00025) in green. C-E). Correlation plots showing the associations between Sirtuin 2 and plasma levels of (C) SNCA, (D) MAPT, and (E) BDNF measured in the antibody array across all chronic untreated HIV-infected individuals. HIV-high (n=20, orange dots) and HIV-low (n=20, green dots) groups are indicated in the plot. The x-axis

shows relative plasma SIRT2 levels, and the y-axis shows the relative plasma levels for SNCA, BDNF, and MAPT, respectively. The Spearman's rank test was applied for the correlation analysis. Statistical significance was set at p<0.05.

To further explore the relationship between SIRT2 levels in plasma and CNS damage in HIV-1 infected individuals, we determined the levels of SIRT2 in matched cerebrospinal fluid (CSF) and plasma samples from chronically untreated HIV-1 infected individuals (n=10 HIV-high and n=10 HIV-low) as well as from HIV-1 seronegative individuals (n=5). While this small set of samples did not show a significant difference in SIRT2 levels in either group for CSF or plasma (Figure 21D), the CSF SIRT2 levels correlated strongly with Tau protein (MAPT: rho= 0.7569 p<0.001, Figure 21E) and neurofilament light protein (NFL: rho= 0.7131 p<0.001, Figure 21F), a well-known biomarker of neuronal damage in HIV infection (176).

These data were validated by analyzing the open access dataset GSE28160, which contains data on post-mortem brain tissue from patients who had died with diagnosed HAND pathology with a severe symptomatology (HIV associated dementia, HAD). We evaluated *SIRT2* expression levels among HIV-1 infected individuals on cART HAD (n=6) or not receiving cART (cART-untreated HAD, n=8) and seronegative individuals (n=6) (Methods section Table 7). As expected from our experimental data, brain *SIRT2* levels tended to be higher in cART-untreated individuals with HAD compared to seronegative individuals (Figure 21G), supporting our findings of increased levels of *SIRT2* in uncontrolled infection. Interestingly, *SIRT2* expression levels in brain tissue from HIV-1 infected individuals (cART-treated and cART-untreated with HAD) correlated with *MAPT* expression levels (Figure 21H), reinforcing the association in our data between SIRT2 and markers of CNS injury.

Overall, these results show that higher levels of SIRT2 are detected in the peripheral blood of individuals with uncontrolled HIV-1 infection and that these levels are directly correlated with biomarkers of neurological dysfunction.
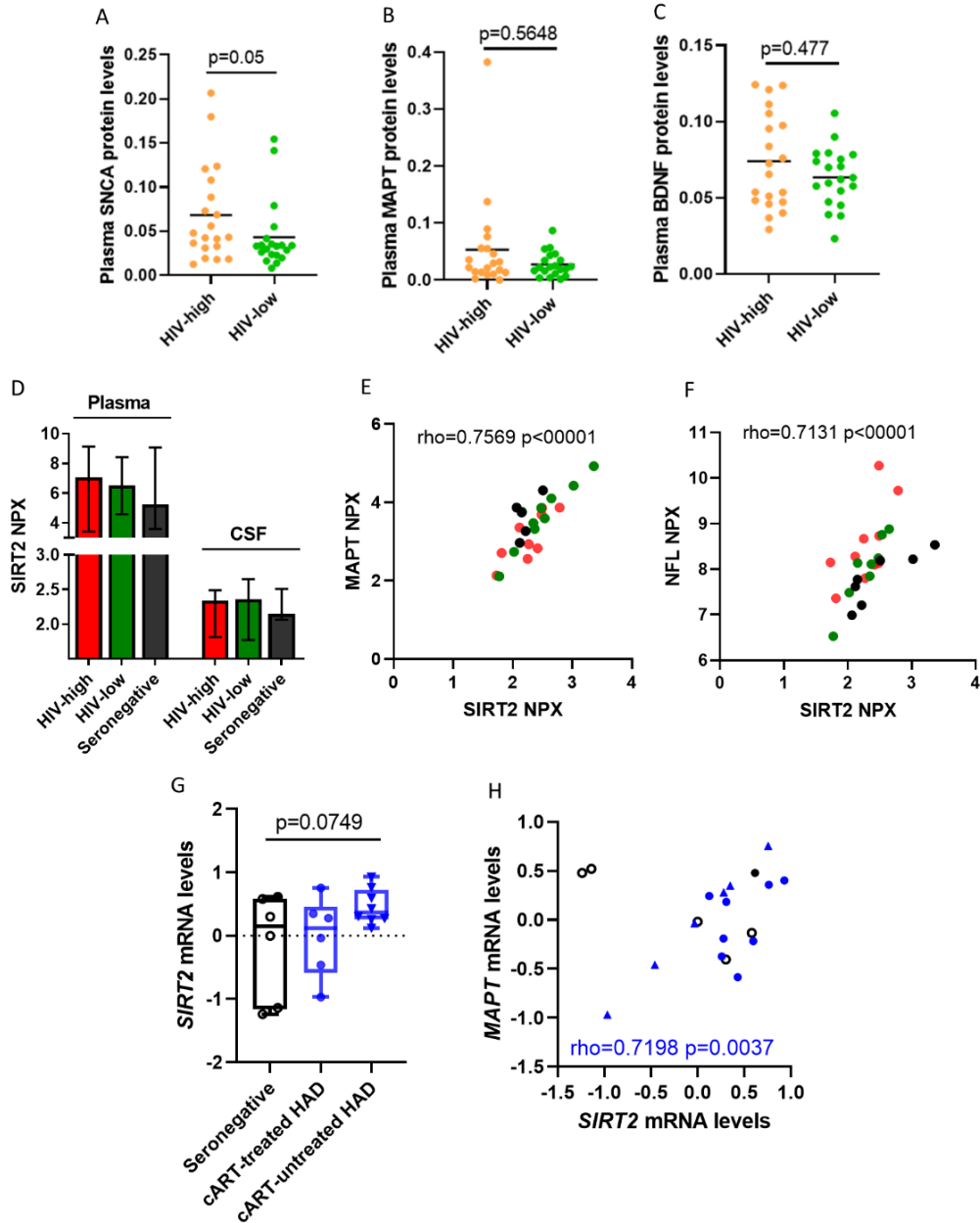
Figure 21. SIRT2 levels in the CNS of HIV-1 infected individuals. A-C) Scatter plot showing the relative plasma protein levels of (A) SNCA, (B) MAPT and (C) BDNF in both study groups (HIV-high [n=20, orange dots] and HIV-low [n=20, green dots]). D) Plot representing normalized protein expression (NPX) levels of SIRT2 in the plasma (left) and CSF (right) in HIV-high (n=10, red bar), HIV-low (n=10, green bar), and seronegative individuals (n=5, black bar). The median and range are shown. E-F) Correlation between relative SIRT2 levels and relative CSF levels of (E) MAPT and (F) NFL in HIV-high (n=10, red dots), HIV-low (n=10, green dots), and seronegative individuals (n=5, black dots). Relative MAPT and NFL levels are shown on the y-axis, and relative SIRT2 levels are shown on the x-axis. G) Plot representing *SIRT2* gene expression in post-mortem brain tissues measured by microarray in the GSE28160 study performed in HIV-1 seronegative (n=6), cART-treated HAD (HIV-associated disorders, n=6), and cART-untreated HAD individuals (n=8). Values are expressed as median and standard deviation. H) Correlation between gene expression levels of *SIRT2* (x-axis) and *MAPT* (y-axis) in post-mortem brain tissue samples in HIV-1 infected individuals (cART-treated HAD (n=6) and cART-untreated HAD individuals (n=8)). For comparisons between groups, ANOVA test for multiple comparisons corrected by original FDR method

of Benjamini and Hochberg was applied. The Spearman's rank test was applied for the correlation analysis. Statistical significance was set at p<0.05.

4.2.2. Time to cART initiation is associated with plasma SIRT2 levels and neurological dysfunction.

Several studies have suggested that HIV-related neuropathogenesis may be triggered by initial viral entry into the CNS, followed by first pathogenic processes and the establishment of the viral reservoir in the brain (177). Rapid initiation of cART is currently recommended for all newly diagnosed HIV-1 infections, with expected beneficial effects on brain reservoir and reduced longitudinal neurological dysfunction (178)(179)(180). To examine whether the time to cART initiation impacted neurologic status and whether or not SIRT2 plasma levels can be informative of this process, a cohort of HIV-1 infected individuals who underwent a prospective neurologic evaluation and started cART either (i) <3 months after ("early-cART") or (ii) >6 months after ("later-cART") the estimated date of HIV-1 acquisition was studied (Figure 22A and Methods section Table 4) (155). Both groups were longitudinally evaluated, including baseline (day of cART initiation), 4 weeks and one year on cART treatment time points (Figure 22A) (Annex section Table S2). Plasma viral loads and the estimated days since infection to cART initiation were different between groups at baseline (Methods section Table 4). While neuropsychological battery tests (NPZ12 score) and brain global gray matter volume measurements showed no differences between the two groups and over time (Figure 22B-C), an involution of the medial orbitofrontal volumetry was detected in the later-cART after one year on treatment (Figure 22D). In parallel, four markers of neurological damage (NFL, GFAP, UCHL-1 and MAPT) were measured in plasma samples (Figure 22E-H). Of these, Tau protein (MAPT) was increased in the plasma after one year on treatment in the later-cART individuals (Figure 22H-I). The degree of medial orbitofrontal volumetry and MAPT plasma levels were not significantly correlated with each other (Figure 22J).

In addition, SIRT2 plasma levels were similarly elevated after one year in the later-cART group when compared with individuals who initiated cART within less than three months from infection (Figure 22K-L). Moreover, SIRT2 plasma levels were negatively correlated with medial orbitofrontal volumetry (Spearman rho=-0.5357 p-value=0.0422, Figure 22M) indicating that early treatment is crucial for limiting the progressive neurological dysfunction in HIV-1 infection and suggesting that SIRT2 could serve as plasma biomarker for these degenerative processes.
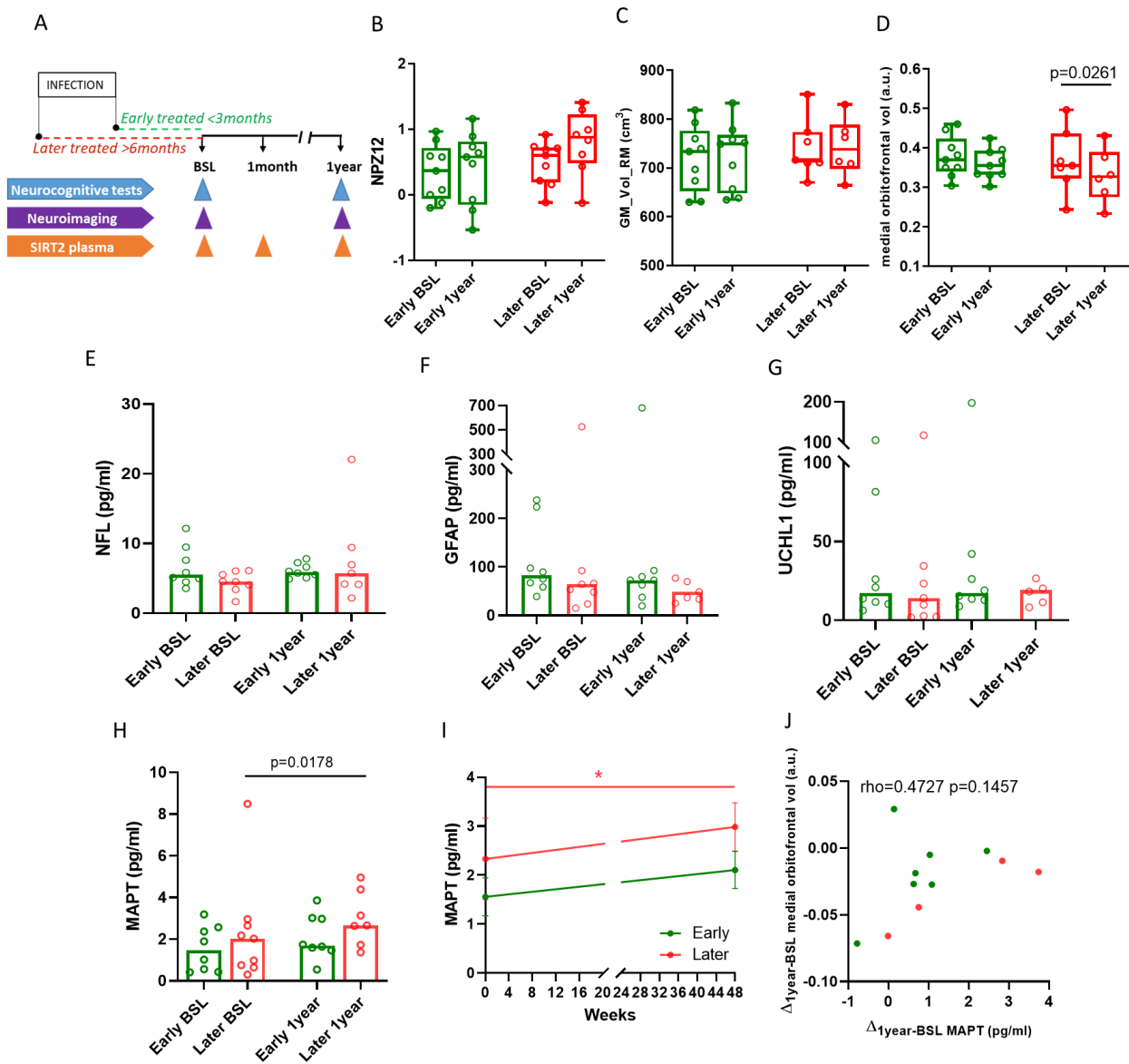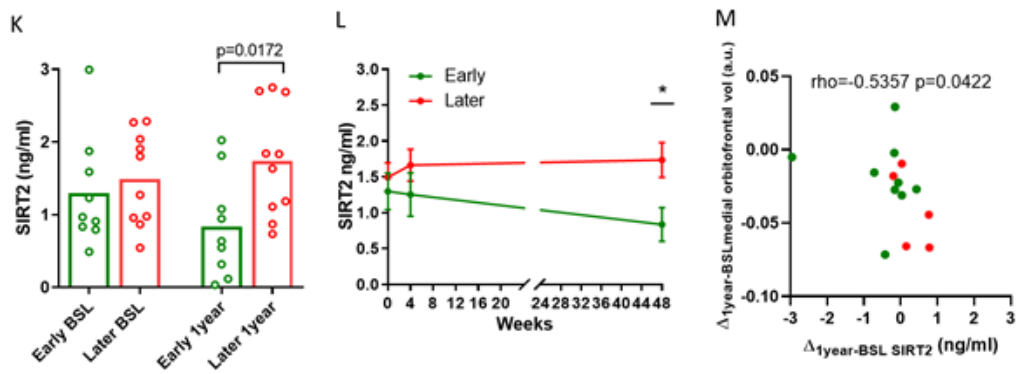
Figure 22. Plasma SIRT2 levels are associated with neurological dysfunction in treated HIV-1 infection.
A) Schematic representation of the two study arms included in the ARBRE study: early-cART (n=9) and later-cART (n=10) HIV-1 infected individuals who started cART at different timepoints after estimated HIV-1 acquisition and underwent longitudinal neurological evaluation (neuropsychological tests and neuroimaging) and quantification of SIRT2 in plasma. Early-cART individuals initiated treatment within a maximum of three months from the estimated date of infection, and later-cART patients initiated cART at least six months after the estimated date of infection. Study visits were at baseline (BSL), one month (4 weeks), and one year after initiation of cART. B-D) Plots representing results of the NPZ12 and global gray matter and medial orbitofrontal cortex volume (peak coordinate at MNI x=6, y=44, z=-29) in early and later-cART individuals at baseline and after one year on treatment (early-cART, n=9, green group; later- cART, n=9, red group). The values on the y-axis represent the NPZ12 score, global gray matter (cm^3) and medial orbitofrontal cortex volume (a.u.). The box plot shows the median and range of values for each group. E-H) Absolute plasma NFL, GFAP, UCHL1 and MAPT levels at baseline (BSL) and after one year on treatment in early-cART (n=9, green group) and later-cART (n=10, red group) individuals expressed in pg/ml. The upper limit of the bar is the median value of protein plasma levels. I) Absolute MAPT plasma levels represented longitudinally and expressed in pg/ml. J) Correlation between longitudinal plasma MAPT levels (x-axis, pg/ml) and the results for medial orbitofrontal cortex volumetry (y-axis) expressed as the difference between one year and baseline in the ARBRE study including early-cART (n=9, green dots) and later-cART individuals (n=5, red dots). K-L) Plots representing the absolute plasma SIRT2 in early- cART (n=9, green line) and later-cART (n=10, red line) individuals K) cross-sectional and L) longitudinally at BSL (baseline) and one year timepoints. Weeks of treatment are shown on the x-axis, and absolute plasma levels of SIRT2 (ng/ml) on the y-axis. M) Correlation between longitudinal plasma SIRT2 (x-axis, ng/ml) and the results for medial orbitofrontal cortex volumetry expressed as the difference between one year on cART and baseline in the ARBRE study including early-cART (n=9, green dots) and later-cART individuals (n=9, red dots). Differences between the groups were analyzed using the Mann-Whitney *U* test, changes over time were assessed using the paired *t* test, and the correlation analysis was based on the Spearman's rank test. Statistical significance was set at p<0.05.

4.2.3. *In vitro* SIRT2 targeting reduces HIV-1 replication and virus reactivation

In order to investigate more directly a potential effect of SIRT2 on HIV-1 replication and virus reactivation, we conducted *in vitro* experiments using specific SIRT2 inhibitors in models of HIV-1 replication in different target cell types. First, the specific SIRT2 inhibitor AK-1, which is actively being evaluated in neurological disease models

(181)(182), was used to test its ability to interfere with HIV-1 replication in PHA-activated T-cells and monocyte-derived macrophages (MDMs) infected *in vitro* with different HIV-1 strains. In the presence of SIRT2 inhibitor, reduced p24 levels were observed in HIV-1$_{NL4-3}$ infected PHA-activated T-cells (at day 3 and 1week post-infection, Figure 23A-B) and in HIV-1$_{BaL}$ infected MDMs (day 4 post-infection, Figure 23C). The reduction in p24 levels in both cell types was not due to cytotoxic effects, as cell viability was not affected in AK-1 treated compared to uninfected conditions and when comparing PHA-activated T-cells and MDMs (Figure 23D-F). The observed differences of AZT in different cell types is in line with previously published data (183). As SIRT2 is predominantly expressed in brain and given its association with markers of neurological damage in the participants of our study (Figure 20 and 21), we also tested its effect on viral replication in primary microglial cells, which are known target cells for HIV-1 and potential sites for brain reservoir (184). Similar to the effects observed in peripheral blood cells, the results from microglial cells showed a significant reduction of HIV-1 replication upon inhibition of SIRT2 (Figure 23G-H).
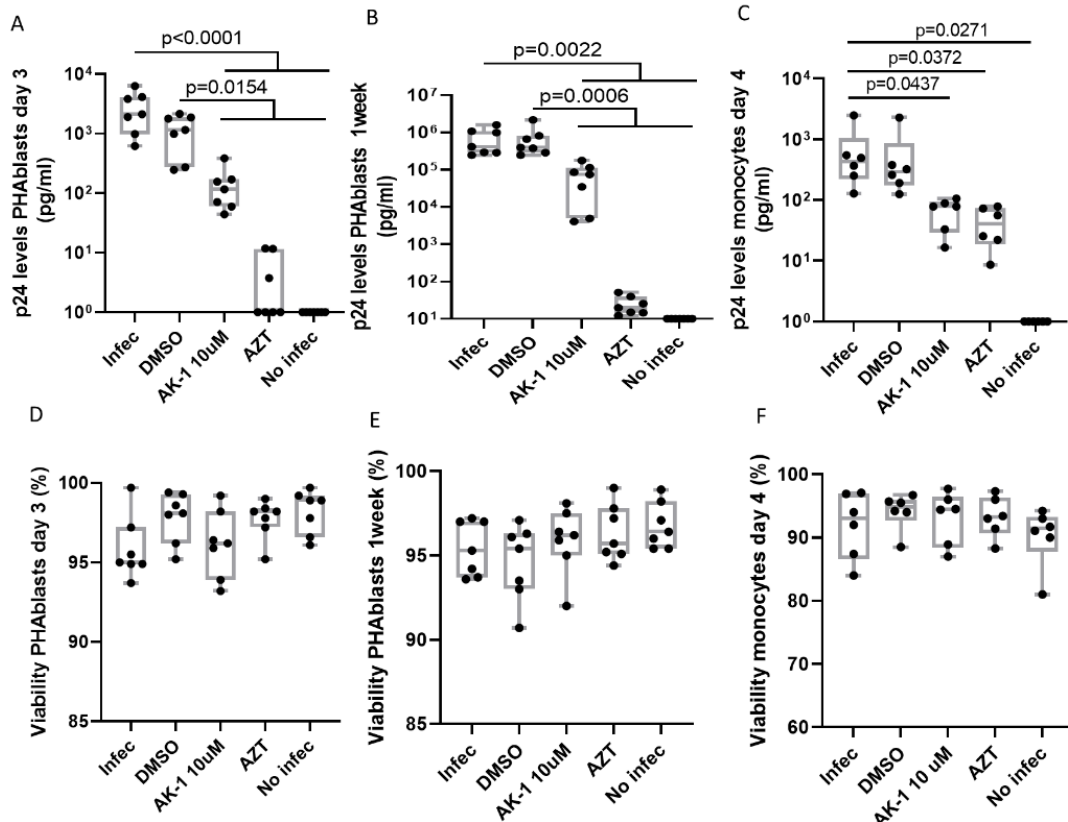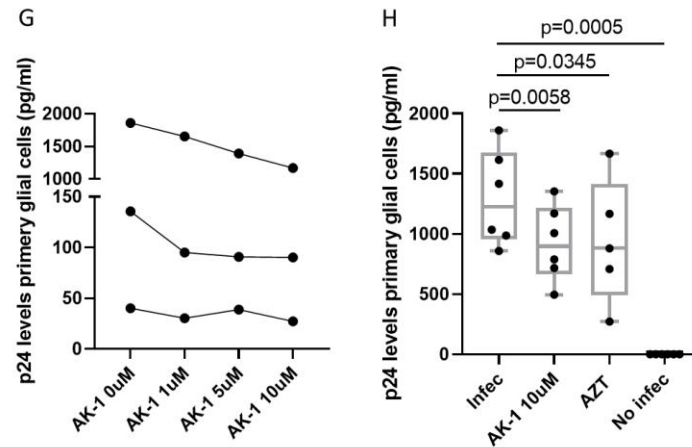
Figure 23. Effect of *in vitro* SIRT2 inhibition on HIV-1 replication. A-C) Inhibition of HIV-1 replication in the presence of SIRT2 inhibitor (AK-1), tested in A-B) HIV-infected PHA-blasts (seven independent experiments) with HIV$_{NL4-3}$ strain, at day 3 and 1week post-infection, respectively; and C) HIV-infected monocyte-derived macrophages, MDMs (six independent experiments) infected with HIV-1$_{BaL}$ strain at day 4 post-infection. D-F) Cell viability in presence of SIRT2 inhibitor (AK-1), tested in D-E) HIV-infected PHA-blasts (seven independent experiments) with HIV-1$_{NL4-3}$ strain, at day 3 and 1 week, respectively; and F) monocyte-derived macrophages, MDMs (six independent experiments) infected with HIV$_{BaL}$ strain, at day 4 post-infection. Experimental conditions are shown on the x-axis; quantification of viability (% live cells) is shown on the y-axis. G) Glial cells infected with the HIV-1$_{NLAD8}$ virus strain (MOI: 0.01) in the presence of different doses of AK-1 inhibitor. Experimental conditions are shown on the x-axis; quantification of absolute p24 supernatant (pg/ml) is shown on the y-axis. The data presented correspond to the mean of two duplicates performed in a single experiment. H) HIV-infected microglial cells (six independent experiments) with the NLAD8 virus strain in the presence of different doses of AK-1 inhibitor. Experimental conditions are shown on the x-axis; quantification of p24 levels (pg/ml) is shown on the y-axis. For results from HIV-infected PHA-blasts, MDMs and primary glial cells, ANOVA test for multiple comparisons corrected by original FDR method of Benjamini and Hochberg was used to analyze differences between conditions. For all comparisons, $p < 0.05$ was considered significant. The plots show the median of all experiments for each condition.

Since SIRT2 plasma and expression levels were also correlated with HIV-1 proviral levels (Table 8 and Figure 19F), we tested the effects of SIRT2 inhibition on HIV-1 reactivation. Inhibition of SIRT2 with AK-1 significantly reduced reactivation of HIV-1 in PMA-activated J-LAT A2 cell line (Figure 24A-C) without affecting cell viability (Figure 24D). Together, these data suggest that targeting SIRT2 reduces HIV-1 replication and virus reactivation from latency, indicating that SIRT2 is required for effective viral replication in peripheral blood cells and, given its sites of expression and associations with markers of neurological damage, likely in the CNS.
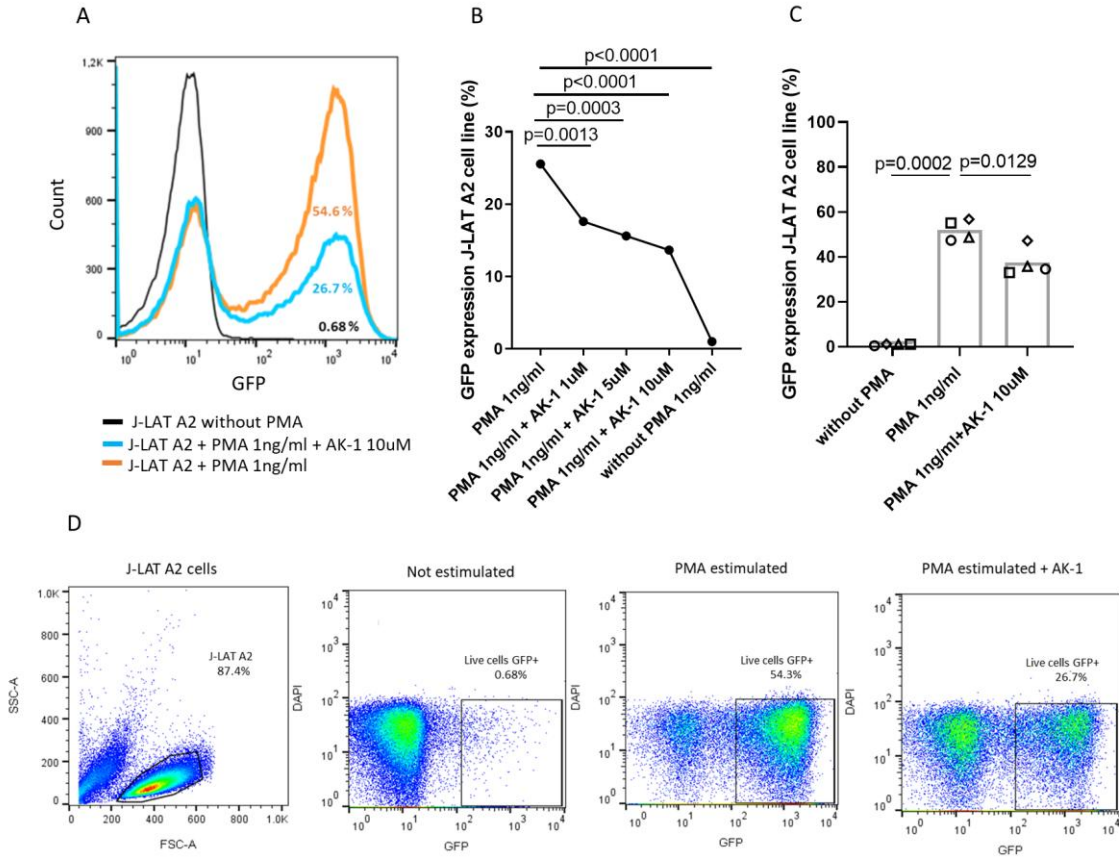
Figure 24. Effect of *in vitro* SIRT2 inhibition on HIV-1 reactivation. A) Histogram plot showing Green Fluorescent Protein (GFP) cellular counts in three different conditions of the experiment, including non-stimulated cells (black), PMA-stimulated cells (orange), and cells stimulated with PMA in the presence of AK-1 (blue) from one representative experiment. B-C) HIV-1 reactivation measured by the percentage of GFP expressing cells measured by flow cytometry in J-LAT A2 cells is shown on the y-axis; different conditions of the experiment, including non-stimulated cells, PMA-stimulated cells, and cells stimulated with PMA in the presence of AK-1, are shown on the x-axis. D) Gating strategy in the J-LAT A2 cell line experiment. For multiple comparisons ANOVA test corrected by original FDR method of Benjamini and Hochberg was used to analyze differences between conditions. For all comparisons, $p < 0.05$ was considered significant. The plots show the median of all experiments for each condition.

4.3. CHAPTER III. Plasma proteomics analysis in the BCN02 clinical trial, based on a "kick and kill" strategy for the HIV-1 cure.

Summary

A major roadblock for the development of a HIV-1 cure is the virus capacity to establish HIV-1 reservoirs in some infected cells. To overcome this hurdle towards HIV-1 cure, the BCN02 study, based on a "kick and kill" strategy, aimed to reduce the HIV-1 reservoir and to improve the antiviral immune response, combining therefore a therapeutic HIV-1 vaccine with a viral latency reversing agent, romidepsin. Moreover, to assess the efficacy of the "kick and kill" strategy, a monitored antiretroviral treatment pause (MAP) was included in study during which viral rebound kinetics after treatment stop were monitored.

In this third chapter of the thesis, we observed that the administration of an HIV-1 therapeutic vaccine together with the latency reversing agent romidepsin had an impact on the plasma proteomic profiles during the intervention. In particular, we identified the CD33 protein and expression levels to be modulated during the clinical trial. CD33 levels effectively discriminated between MAP-C and MAP-NC in samples drawn before the intervention and were positively correlated with HIV-1 proviral levels and viral loads. Subsequent validation in vitro experiments suggested an important role of CD33 in the HIV-1 cycle which may serve as a predictor of outcome after treatment interruption and/or therapeutic interventions.

4.3.1. Plasma proteomes are impacted upon RMD administration

Focused inflammatory and neurological-tailored proteomes were defined using PEA in plasmas samples from 11 BCN02 participants at baseline (BSL, week 0), 1 week after 3 infusions of RMD (post-RMD, week 6) and at MAP timepoints (Annex section Figure S1 and methods section Table 5), to identify soluble markers modulated by therapeutic vaccination and RMD. Principal Component Analysis (PCA) was based on 276 soluble factors that are involved in inflammation and neurological processes and which were assessed across the three timepoints of the clinical trial. As shown in Figure 25A, marked changes were observed after RMD treatment and, at a furher enhanced level, during MAP. When compared to BSL, the administration of RMD modulated the plasma levels of 49 proteins, while 76 molecules were significantly modulated during MAP levels (Figure 25B) (Annex section Table S3). Of these, 29 proteins were equally dysregulated in both comparisons. Proteome profiling analysis indicated that of the 20 proteins that were uniquely differentially detected between BSL and RMD administration, 17 molecules showed an increase in relative protein levels (Figure 25B Profile I. in red). Most of these proteins were related to "*cytokine release by the interaction with viral proteins*" such as CCL25, CXCL5, IL-20RA and IL-15 and "*innate and cellular adaptive immune response markers*" like CD8A and CD38. The remaining three proteins showed decreased levels after RMD administration, including CXCL10, CCL23 and GDNF (Figure 25B Profile I. in green).

When comparing baseline versus MAP timepoints, 47 proteins showed uniquely different relative protein levels between these two timepoints, with 37 being increased the relative protein levels (Figure 25B Profile III. in red) and mostly related with "*cell growth*", "*proliferation*" or "*cell structure*" such as TBCB, PFDN2, 4E-BP1, NPM1, FGF23, CD63, among others. The 10 proteins that decreased their relative levels over this period (Figure 25B Profile III. in green) were related to "*response to cytokine*" category like IL-20, IL-22RA1, LIF, GBP2, SCGB1A1 and NEP and "*regulation of epithelial cell differentiation*" such as GDNF, LIF and IL-20.

In addition, the 29 proteins that were found to be modulated between baseline versus post-RMD and between baseline versus MAP comparisons, were progressively and

significantly increased (24 molecules) or decreased (5 proteins) over-time. Most of these 24 proteins (Figure 25B Profile II. In red) were involved in "*neuronal and axonal functions*" like NFL, MANF and CLSTN1, while the other 5 molecules that decreased their plasma levels included MCP3, IL-5, TNF, CEACAM3 and TDGF1, Figure 25B Profile II. in green).

To identify potential drivers of the observed changes in protein levels from baseline to post-RMD and/or MAP timepoints, a correlation analysis was performed between relative protein levels and either virological (plasma viral load (pVL) and proviral levels) or neurological parameters (including NPZ6, Figure 25C-D). These analyses showed that after RMD infusions, 34% of all plasma proteins tested correlated positively with pVL, whereas during MAP timepoint this percentage increased up to 72% of the molecules (Figure 25C-D and p=0.0001, chi squared test). In contrast, at post-RMD timepoint, the majority of plasma proteins were positively associated with proviral level, while during MAP phase these associations decreased to 31% (Figure 25C-D and p=0.0001, chi squared test). These data suggest that proteome profiles at post-RMD are reflecting the size of the latent viral reservoir, while during MAP, the observed changes reflect likely the increased active viral replication and activation of the "*interferon signaling pathwa*y", with proteins such as IL-15, CXCL10, IFI30, TNF, IL-3, IL-12, IL-20 being more abundant.

Interestingly, correlation analysis with neurological parameters (NPZ6) showed that 71% of the molecules correlated positively with NPZ6 neurocognitive test after RMD treatment. During MAP, this proportion rose to 85% (p=0.0083, chi squared test), reflecting the higher number of proteins that was associated with neurological evaluations such as MANF, GDNF, NFL and GPNMB at the completion of the intervention and MAP (Figure 25C-D).
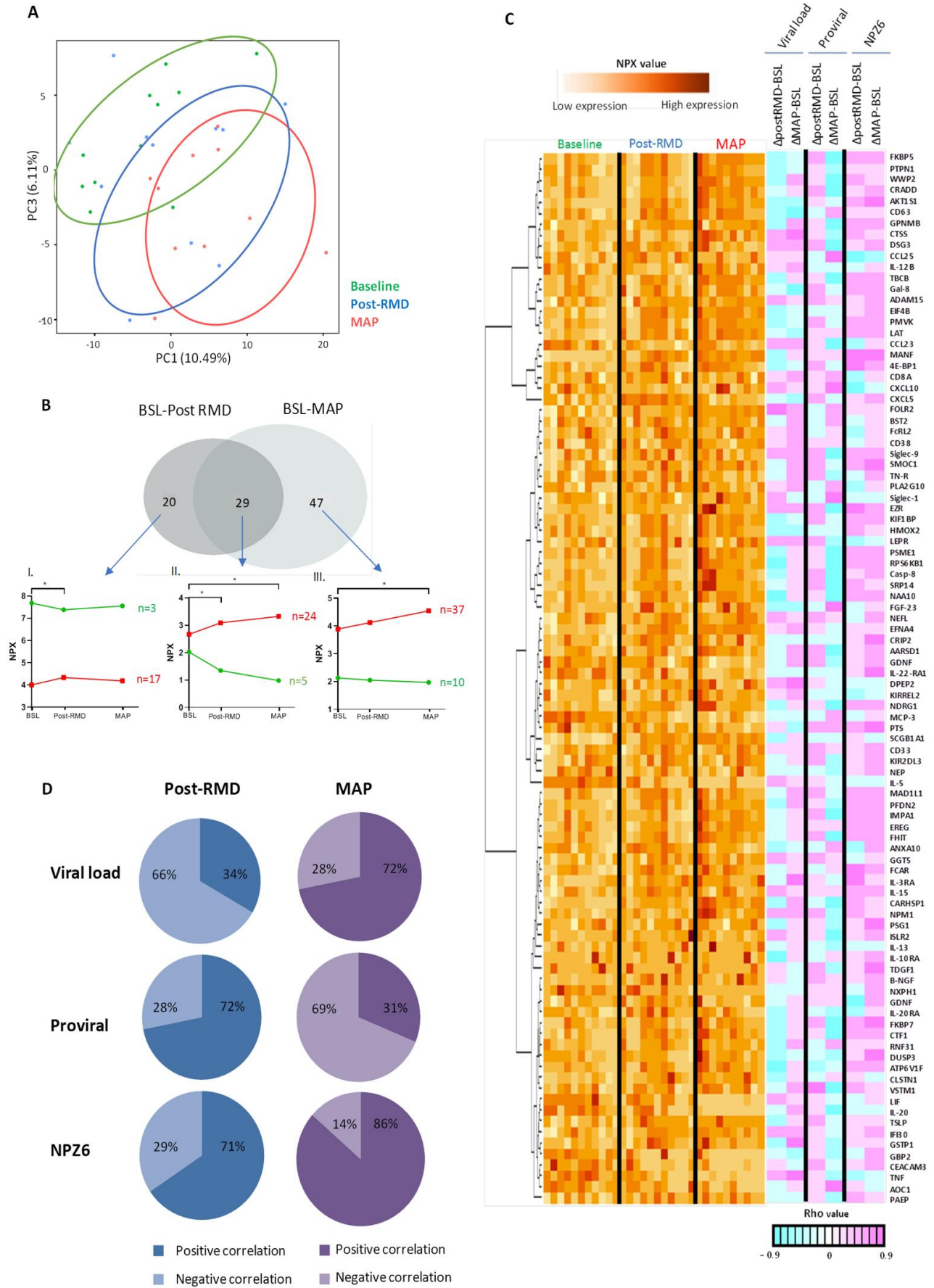
Figure 25. Changes in plasma proteomes during the BCN02 clinical trial. Soluble proteomes from 11 participants in the BCN02 trial at baseline (BSL), 1 week after 3 infusions of RMD (post-RMD) and during monitored antiretroviral pause (MAP) timepoints were determined using proximity extension assay. A) Principal Component Analysis (PCA) reflecting the changes of 276 inflammatory and neurological-related plasma proteins during the BCN02 clinical trial at each timepoint. BSL timepoint is indicated in green, post-RMD timepoint in blue and MAP timepoint in red, each point representing one participant/time point. B) Venn diagram representing differentially detected proteins (n= 96, p<0.05) when comparing BSL vs post-RMD (n=49) and BSL vs MAP phase timepoints (n=76). The different profiles indicate relative abundance of protein that were up- or down-regulated: *Profile I:* Significant protein profiles only detected when comparing BSL vs post-RMD infusions (n=20); *Profile II*: Significant protein profiles shared when comparing BSL vs post-RMD and BSL vs MAP timepoints (n=29); and *Profile III:* Significant protein profiles only detected when comparing BSL vs MAP phase (n=47). The x-axis marks the timepoints of the clinical trial and on the y-axis, the relative levels of the proteins, represented as mean of NPX values for each protein are indicated. C) Heatmap showing the relative protein levels (NPX) of all significantly modulated proteins from 1B (p<0.05, n=96) per patient and timepoint (orange-yellow scale). Each column represents a patient measured at BSL, post-RMD and MAP. Additional columns (blue-pink scale, right of the heatmap) indicate the value of correlations (Spearman's rho) between individual proteins and either plasma viral load, proviral levels or neurotest score (NPZ6). D) Pie charts representing the percentages of number of proteins that are negatively or positively correlated (Spearman's rho) with viral parameters (viral load and proviral levels) and neurological evaluation (NPZ6). Blue (post-RMD), purple (MAP), dark color indicates positive correlations and light color negative correlations. Statistical significance was set at p<0.05.

4.3.2. Plasma proteomes at baseline predict MAP-Controllers and MAP-Non-Controllers

As plasma proteomes were associated with viral loads and proviral levels, we next assessed whether baseline protein profiles or longitudinally altered proteome signatures would have the power to differentiate individuals who can or cannot control viral replication during MAP. To that end, we compared the plasma proteomes of MAP-NC individuals (>2000 HIV-1 RNA copies/ml and thus restarting ART) and MAP-C (>32weeks <2000 HIV-1 RNA copies/ml) at all the timepoints (baseline, post-RMD and MAP). PCA plots showed that proteome profiles at all timepoints, including baseline, segregated the two groups (Annex section Figure S2A-C). Specifically, the comparative analysis between MAP-C and MAP-NC by timepoints showed that differences in the proteome of both groups were observed at baseline (18 proteins, Figure 26A), post-RMD (16 molecules, Figure 26B) and, with broader profiles, during MAP (33 molecules, Figure 26C).

To gain insights into the differences at biological level between the two groups at each timepoint, Gene Ontology (GO) classification was performed (Figure 26D-F). Aside from metabolic and hormonal ontologies, the analysis at baseline indicated a differential representation between groups in "*T cell differentiation*", "*lymphocyte immunity*", "*interferon-gamma production*" and "*myeloid cell development*" ontologies (Figure 26D). After RMD administration, the major gene ontologies differentially represented between MAP-C and MAP-NC fell into several "*interferon pathways"* and in "*negative regulation of IL5 and IL13 production*" ontologies (Figure 26E). "*Innate cellular (Mast cells, Neutrophils and Monocytes)*", "*T cell immunity*" categories and the involvement of "*NF-KB and MAPK cascades*" were the major ontologies differentially represented between both groups at the MAP timepoint (Figure 26F). Although some proteins involved in neurological processes were significantly altered by the intervention, the two groups (MAP-C and MAP-NC) did not show any distinguishable features in their neurological protein profile at any of the tested time points.
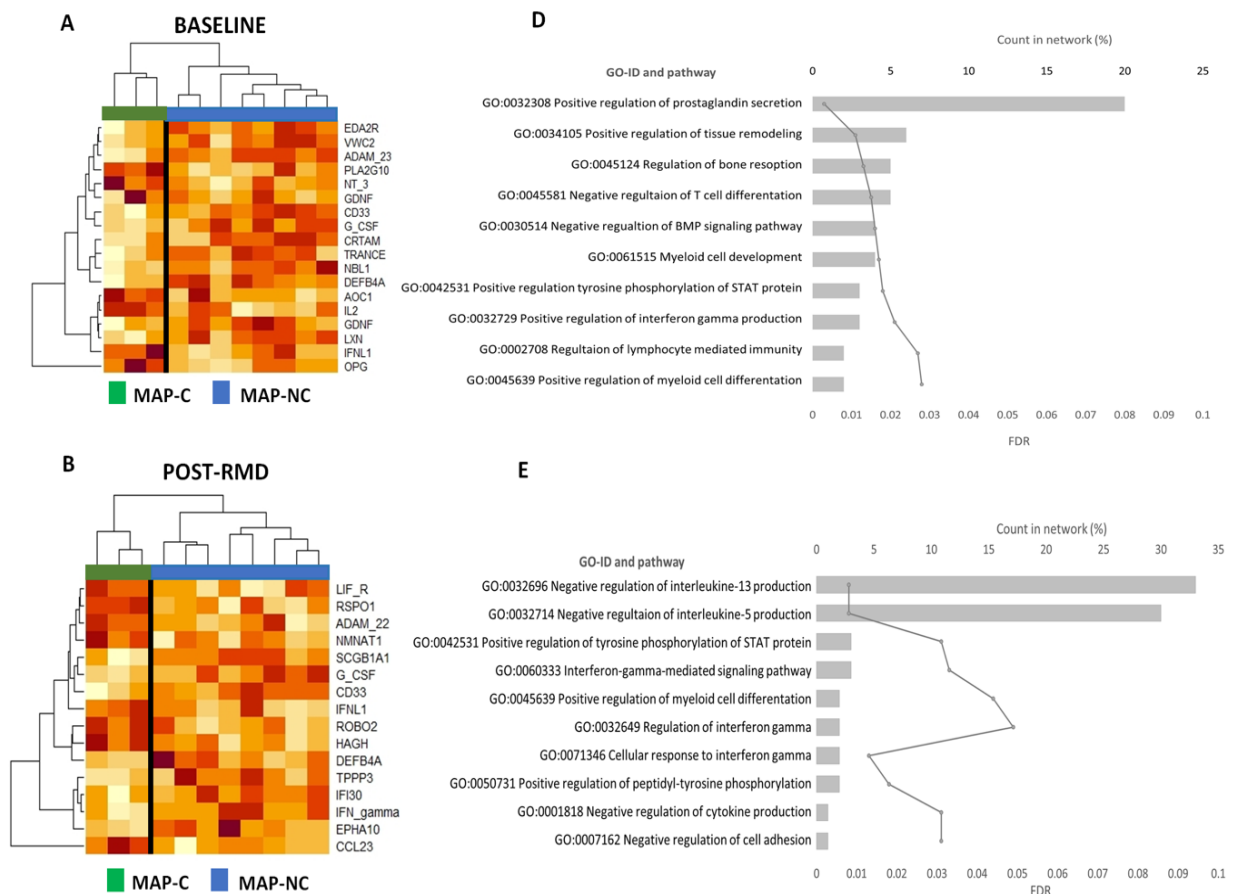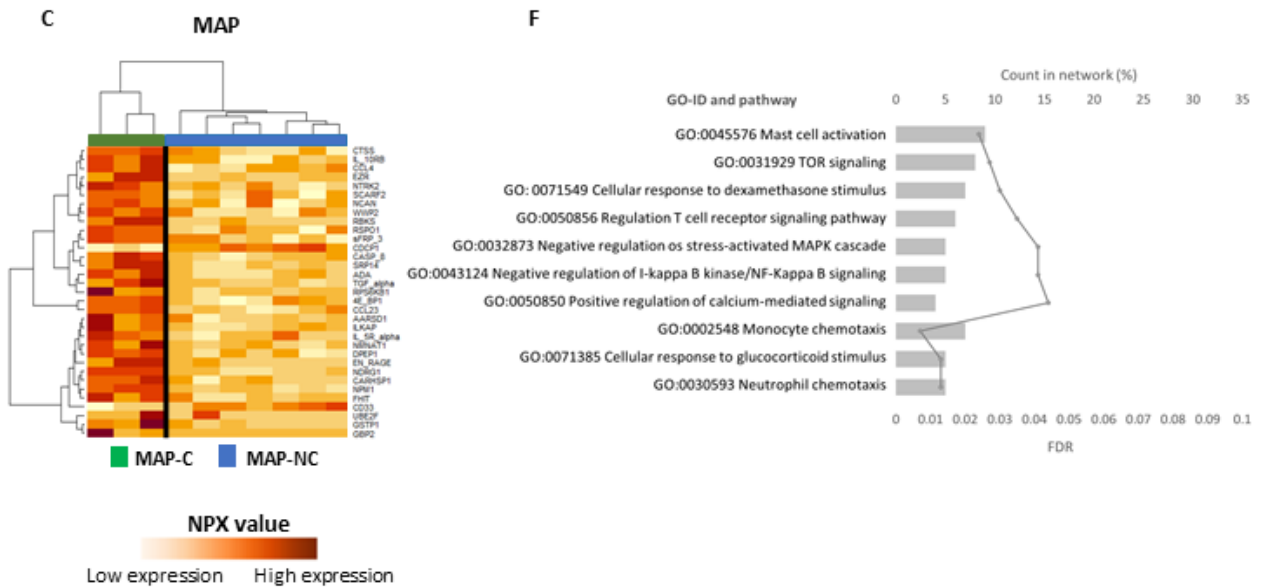
Figure 26. Differential plasma proteomes between MAP-C and MAP-NC. A-C) Heatmap of relative plasma levels (NPX) of proteins differentially detected between MAP-C and MAP-NC at (A) baseline, (B) post-RMD and (C) MAP phase of the BCN02 clinical trial. Orange-yellow scale indicates NPX values. Green represents MAP-C and blue MAP-NC participants. D-F) Gene Ontology (GO) classification of the significant proteins that differed between MAP-C and MAP-NC at each timepoint. On the y-axis, gene ontology categories are indicated, on the upper x-axis, counts in network represented as percentage in histogram (%) and on the lower x-axis, as continuous line, the false discovery rate (FDR) representation.

_____

4.3.3. CD33/SIGLEC3 is the unique discriminative plasma factor between MAP-Controllers and MAP-Non-Controllers across the BCN02 trial

When analyzing the proteome profiles discriminating MAP-C and MAP-NC, we observed that CD33/SIGLEC3 was the unique protein consistently differentially detected between the two groups across all timepoints (Figure 27A). Moreover, the plasma levels of CD33 were modulated during the intervention (Figure 27B, BSL vs post-RMD p=0.001 and BSL vs MAP p=0.002, Wilcoxon test) and, despite the small number of participants in the trial, were significantly elevated in MAP-NC compared with MAP-C in all timepoints (Figure 27C, BSL: p=0.024, post-RMD: p=0.049 and MAP: p=0.033, Mann-Whitney test). In addition, CD33 protein plasma levels positively correlated with proviral DNA copy numbers at baseline and after RMD administration (Figure 27D-E, BSL rho=0.646 p=0.037, post-RMD rho=0.647 p=0.035, Spearman rank

test). A trend towards a positive association with viral reservoir was also observed at MAP timepoint (Figure 27F, MAP rho=0.9 but with p=0.083 not reaching significance, likely due to proviral assessments missing for more than half of the participants at MAP timepoint). Still, MAP samples showed also a positive correlation between CD33 protein levels and pVL (Figure 27G, rho=0.782 p=0.011, Spearman rank test). To investigate whether cells in the peripheral blood are the major source of CD33 proteins detected in the plasma, we assessed *CD33* gene expression levels in PBMCs. The positive correlation between *CD33* expression and plasma viral load levels (Annex section Figure S3A-C), is indeed suggestive of PBMCs be a major source of the soluble CD33 protein in plasma (Figure 27G).

To gain further inside into the mechanisms by which CD33 could influence viral control, we performed a correlation analysis between CD33 and other proteins that were included in the inflammatory, neurology or neuro-exploratory cytokine panels and which significantly changed during the intervention. After RMD administration, CD33 protein levels were strongly associated with 17 proteins, most pronouncedly with ADAM15, GGT5 and NFL (Figure 27H, ADAM15 rho=0.806 p=0.0027, GGT5 rho=0.7413 p=0.009 and NFL rho=0.7064 p=0.0151, Spearman rank test). These associations were not only maintained but statistically even more pronounced at the MAP timepoint (Figure 27I, ADAM15 rho=0.9696 p<0.0001, GGT5 rho=0.9195 p=0.0002 and NFL rho=0.9223 p=0.0001, Spearman rank test). Interestingly, the NFL protein, a well-established marker for neurological damage in several diseases (185)(186), also showed increased levels upon RMD administration and more accentuated, in MAP phase, but did not reach significant difference between groups, even though at baseline, MAP-NC tend to have higher levels of this brain injury marker (Annexe section Figure S3D-E).

Overall, these data indicate that CD33 protein levels differ between MAP-C and MAP-NC, even before the BCN02 intervention and that this difference is even more pronounced after RMD treatment and showed strong positive correlations with viral parameters and markers of neurological damage.
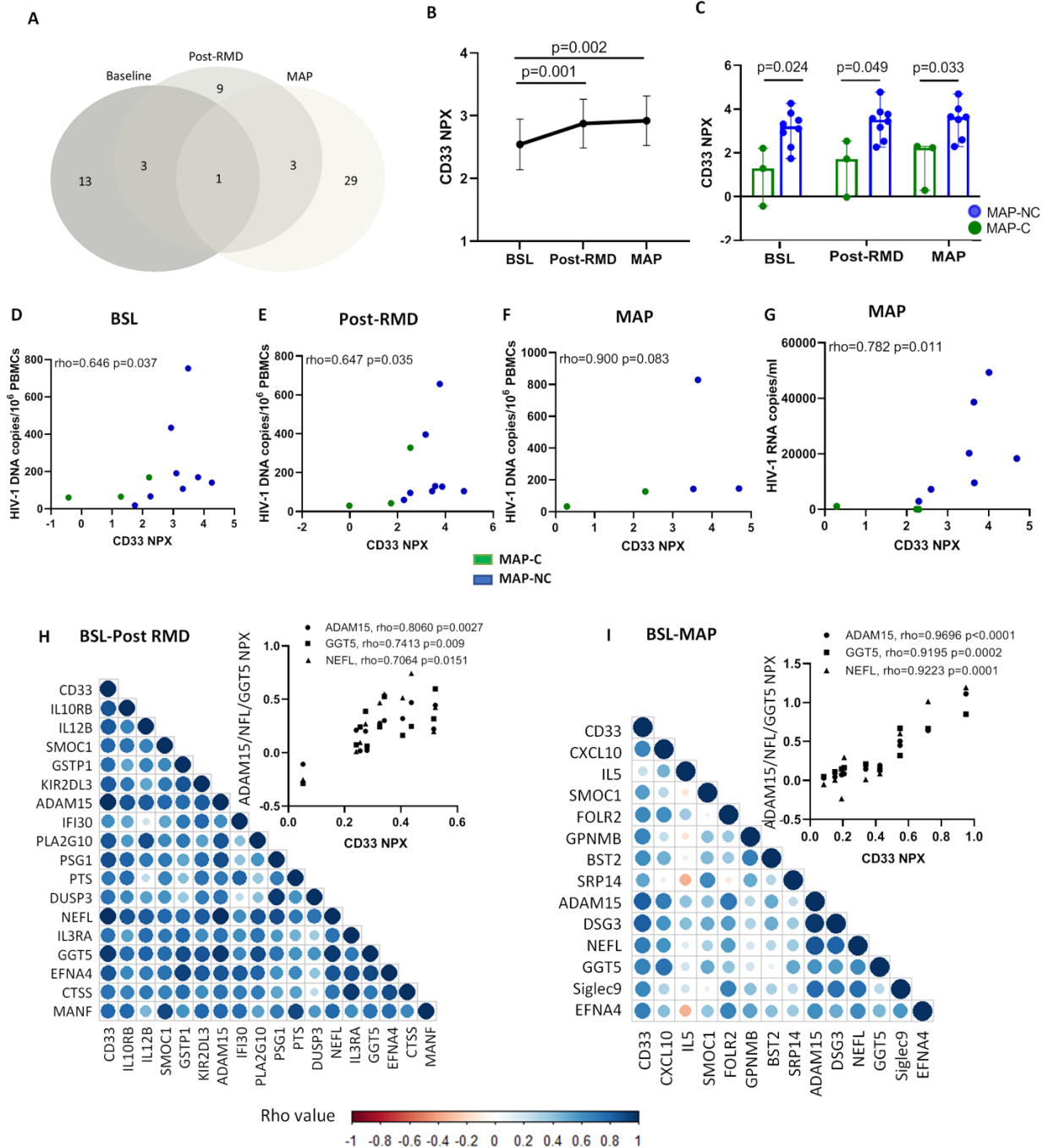
Figure 27. CD33 plasma protein levels differentiate MAP-C and MAP-NC across the clinical trial. A) Venn diagram showing differentially detected proteins between MAP-C and MAP-NC in samples from each timepoint of the clinical trial (BSL, post-RMD and MAP). B) Plot showing the relative plasma CD33 levels (NPX, y-axis) during the intervention (x-axis). P-values <0.05 were consider significant (Mann-Whitney *U* test). C) Longitudinal representation of the relative CD33 plasma levels in MAP-C (green

symbols) and MAP-NC (blue symbols) individuals over the duration of the clinical trial. Clinical trial timepoints are shown on the x-axis, and relative plasma levels of CD33 shown on the y-axis. Values are shown as median and standard deviation. Longitudinal changes over time were assessed using the Wilcoxon test. D-F) Correlation analysis between relative CD33 protein levels (NPX, x-axis) vs HIV proviral DNA levels (HIV DNA copies/10^6 PBMCs, y-axis) are shown on the y-axis in each timepoint of the study including (D) baseline, (E) post-RMD and (F) MAP phase. G) Correlation analysis showing the association between relative CD33 protein levels (NPX, x-axis) vs plasma viral load (HIV RNA copies/ml, x-axis) in MAP phase. Green dots indicate MAP-C and blue dots indicate MAP-NC. H-I) Correlogram plots of the significant proteins detected between BSL vs post-RMD (H) and BSL vs MAP phase (I) that correlate with CD33 relative plasma levels. Dots indicate the level of correlation (blue: positive correlation and red: negative correlation). Inserted graphs indicate the strongest associations observed between CD33 and three proteins (NFL, GGT5 and ADAM15) in the neurology panel. The Spearman's rank test was used for correlation analyses. Statistical significance was set at p<0.05.

4.3.4. CD33/SIGLEC3 validation in chronic untreated HIV-1 infected cohort

To validate the relationship between CD33 plasma levels and virus control, we tested samples from an unrelated cohort of chronically untreated HIV-1 infected individuals with different levels of virus control by determining plasma protein and gene expression levels of CD33. This untreated HIV-1 infection cohort included HIV-1 individuals with high plasma viral loads ("HIV-high", n= 47, pVL >50,000 HIV-1 RNA copies/ml) or low plasma viral loads ("HIV-low", n= 49, pVL <10,000 HIV-1 RNA copies/ml) (Methods section Table 6). Significantly higher CD33 plasma protein levels were detected in HIV-high compared with HIV-low individuals (Figure 28A, p=0.0016, Mann-Whitney test). Similarly, CD33 gene expression in PBMCs, from the same cohort, showed higher *CD33* expression levels in HIV-high individuals compared with HIV-low (Figure 28B, p<0.0001, Mann-Whitney test). CD33 proteomic and gene expression levels at PBMCs were also related (Figure 28C, rho=0.319 p=0.051, Spearman rank test), indicating again that PBMCs could be one of the major sources of soluble CD33 protein levels in the plasma. As observed in the MAP phase of the BCN02 study, CD33 plasma levels and gene expression levels also correlated positively with plasma viral loads (Figure 28D-E and H, CD33 protein levels vs pVL rho=0.2771 p=0.0063, and *CD33* gene expression levels vs pVL rho=0.457 p=0.004, Spearman rank test) and also

correlated with HIV-1 proviral DNA copy numbers (Figure 28F-G and H, CD33 protein levels vs proviral rho=0.2933 p=0.0297, and *CD33* gene expression levels vs proviral).
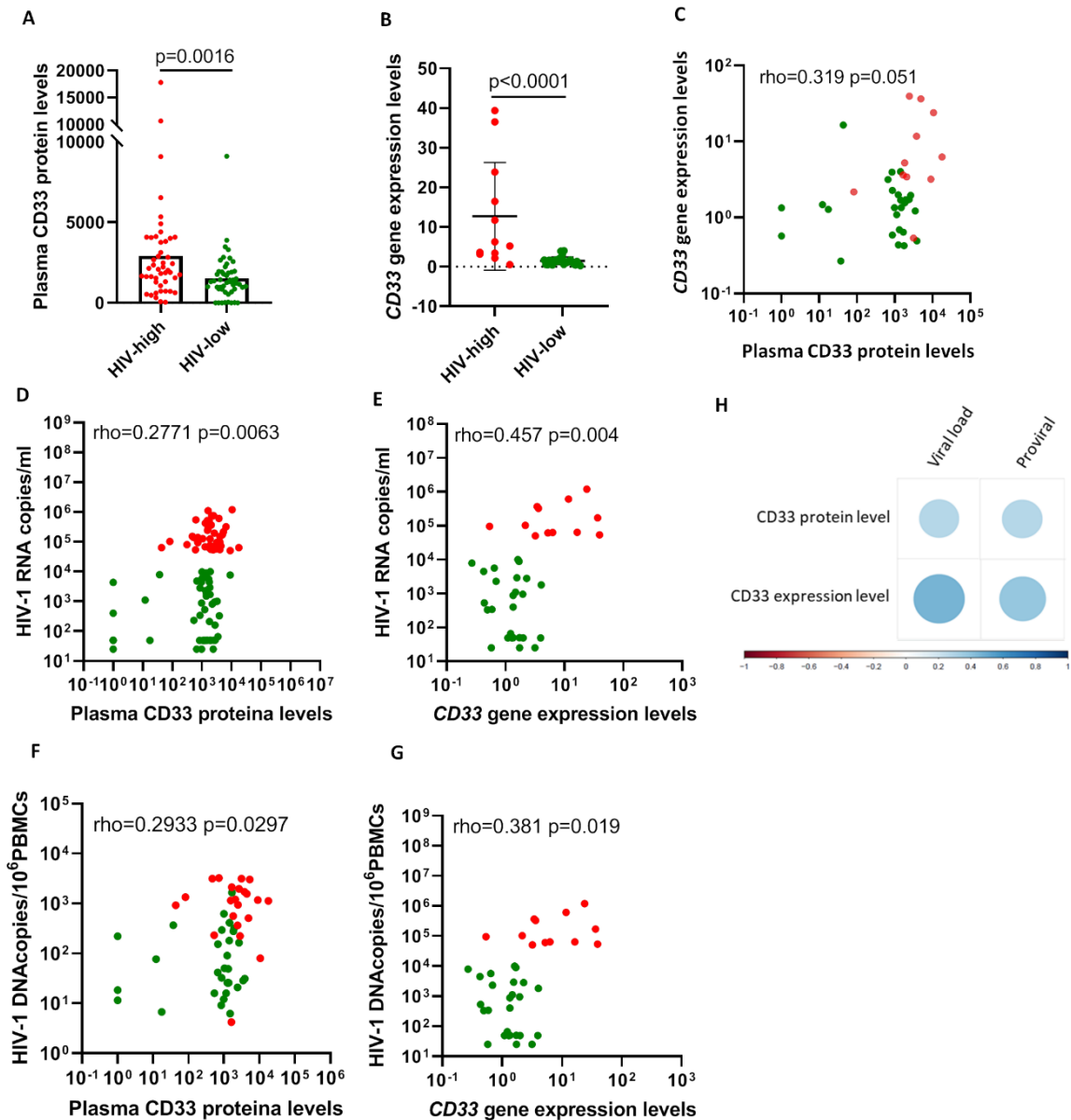
Figure 28. CD33 levels in natural untreated HIV-1 infection. Proteomic array using plasma samples from chronically untreated HIV-1 individuals with different degrees of HIV-1 control (n=96), categorized as HIV-high and HIV-low according to their viral load. A) Scatter plot showing the plasma CD33 protein levels (y-axis) in either groups (x-axis); HIV-low (n=49, green dots) and HIV-high (n= 47, red dots). B) *CD33* gene expression (y-axis, relative *CD33* gene expression corrected for CD4 counts) measured in PBMCs in HIV-high (n=12, red dots) and HIV-low (n=25 green dots) (x-axis) individuals. C) Correlation analysis between *CD33* gene expression (corrected for CD4 counts, y-axis) and CD33 protein levels in plasma considering all individuals. D-E) Correlation analysis between (D) CD33 plasma protein levels and (E) *CD33* gene expression levels (x-axis) and viral load levels (HIV-1 RNA copies/ml, y-axis). HIV-high, n=47, red dots and HIV-low, n=49, green dots. (F-G) Correlation analysis between (F) CD33 plasma protein levels and (G) *CD33* gene expression levels (x-axis) and HIV-1 proviral DNA levels in total PBMCs (HIV-1 DNA copies/10^6 PBMCs, y-axis) considering all the individuals (HIV-high, n=47, red dots and HIV-low, n=49, green dots. (H) Correlogram plot between CD33 levels in plasma and PBMCs expression and

viral parameters. CD33 differences between groups were analyzed using the Mann-Whitney test. The Spearman's rank test was used for correlation analyses. Statistical significance was set at p<0.05.

4.3.5. *In vitro* CD33 targeting reduces HIV-1 replication and virus reactivation

To investigate furher the potential involvement of CD33 in HIV-1 replication and viral reservoir, we tested whether targeting CD33 *in vitro* on PHA-activated T-cells and monocyte-derived macrophages (MDMs) would impact viral replication. Indeed, adding an anti-CD33 mAb to HIV-1$_{NL4-3}$ infected PHA-activated T-cell cells reduced virus production in a dose-dependent manner (Figure 29A) without affecting the cell viability (Annex section Figure S4A). In parallel, the amount of total HIV-1 DNA was also decreased in the presence of an anti-CD33 mAb (Figure 29B, p=ns). The same was observed when HIV-1$_{BaL}$ infected MDMs were cultured in presence of anti-CD33 antibody, with HIV-1 replication being reduced in a dose-dependent manner (Figure 29C) (Annex section Table S4B). The reduction in proviral copy numbers in monocytes reached statistical significance as well (Figure 29D). Together, these data suggest that targeting CD33 can reduce HIV-1 replication and/or infection, indicating that CD33 is required at some point of the HIV-1 viral life cycle for effective viral propagation.
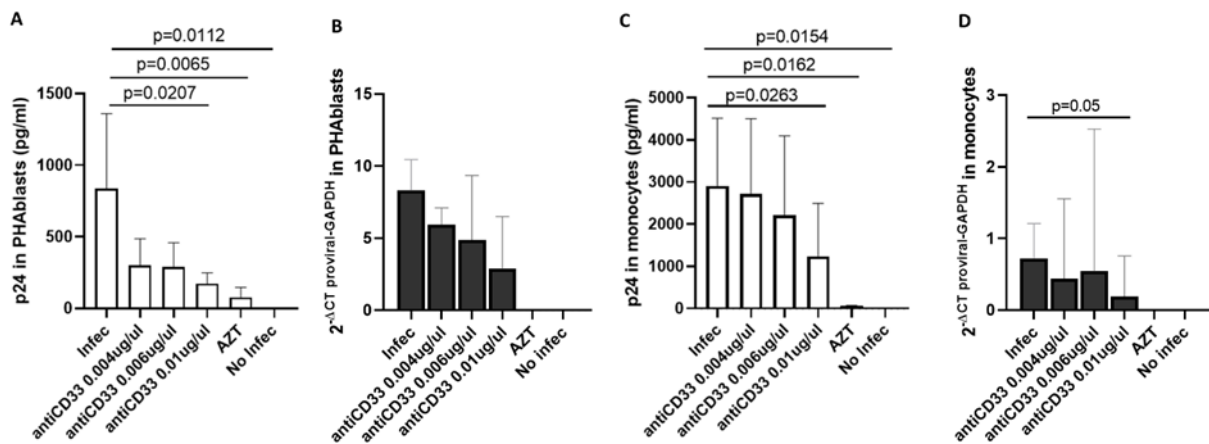
Figure 29. Targeting CD33 reduces HIV-1 replication and provirus levels. A and C) Inhibition of HIV-1 replication in the presence of anti-CD33 mAb, tested in (A) PHA-activated T-cells (six independent experiments in duplicates) infected with the HIV-1$_{NL4-3}$ strain; (C) HIV-1 infected monocyte-derived macrophages (five independent experiments in duplicates) infected with the HIV-1$_{BaL}$ strain. Experimental conditions are shown on the x-axis and quantification of absolute p24 supernatant (pg/ml) is shown on the y-axis. B and D) Total HIV-1 DNA quantification in cells from the same PHA-activated T-cell and MDMs experiments as in A and C. Experimental conditions are shown on the x-axis and quantification of total HIV-1 DNA is shown on the y-axis. For HIV-1 infected T-cells and MDMs, ANOVA test was used to analyze differences between conditions. For all comparisons, $p < 0.05$ was considered statistically significant. The plots show the median and standard deviation of all experiments for each condition.

DISCUSSION

5. DISCUSSION

HIV-1 has caused millions of deaths since its discovery in 1981. The implementation and progressive development of combination antiretroviral therapy (cART) was the first big success to convert this disease into a chronic infection instead of a terminal disease as it suppresses plasma viremia to undetectable levels. It does thereby reduce the morbidity, mortality and the risk of viral transmission while, at least partly, also restoring immune function (187)(188). However, cART is not the cure of the HIV-1 infection because the treatment is not able to eliminate the viral reservoir comprised of latently infected cells (189). Thus, in almost all individuals in whom cART is interrupted, plasma viral loads rebound within 2-8 weeks as the latently infected cells can gives raise to full blow viral replication again.

So far, several strategies have been explored to achieve an effective HIV-1 cure, from gene therapy and stem cell transplantation to "kick and kill" or "block and lock" strategies or HIV-1 specific immune enhancement trough vaccinations. Strategies focused on gene therapy and stem cell transplantation are complex and risky strategies as these therapies imply the modification of the host genome or require a suitable stem cell donor or autologous cells. The strategies focused on the reactivation or the silencing of the reservoir ("kick and kill" or "block and lock" strategies) may be suitable for a wider target population, but none of the compounds tested to date, has been able to significantly impact the reservoir *in vivo*. In fact, a recent study has demonstrated that current LRAs and LPAs lack selectivity and are not able to reactivate more than 5% of all the latently infected cells that form the viral reservoir (190)(191). Finally, HIV-1 specific immune enhancement strategies have been tested and shown to generate improved immune responses but not strong enough to serve as an effective cure strategy on its own. Conducting potential combination trials, which combine some of these strategies, is further complicated by the absence of well-defined biomarkers of disease progression and viral control.

To this end, we aimed to identify soluble biomarkers in individuals with natural control of HIV-1 infection and in post-treatment interruption samples to predict outcome after cART stop and to identify potentially novel therapeutic targets for future HIV-1 cure

strategies. At the same time, we also related these biomarkers to inflammatory markers and neurological status in HIV-1 infected individuals as the brain may serve as an important, but hard to target site of the latent viral reservoir and since HIV-1 associated neurological diseases remain an important clinical issue, despite increasing cART availability.

A main goal of HIV-1 cure strategies is to achieve a functional cure of HIV-1 infection, similarly what occurs in elite controllers (EC) or long-term non-progressors (LTNP). These HIV-1 infected individuals represent a small proportion of people living with HIV-1, approximately between 5 and 10% who are able to control the viral replication in the absence of combined antiretroviral therapy (cART) (192)(193). A proportion of such HIV-1 controllers has been shown to present specific genetic markers that benefit or help to control the HIV-1 infection. Others individuals control HIV-1 infection without such beneficial host genetics and represent thus an interesting population to define mechanisms of HIV-1 control that may be more broadly applicable to the general population. In particular, understanding the mechanisms that allow to these individuals to have low HIV-1 RNA levels (172)(165), especially in the absence of beneficial genetic factors, may help in the identification of key factors involved in control of HIV-1 and to develop refined HIV-1 cure strategies.

Identification of plasma biomarkers in natural control of HIV-1 infection in the absence of cART

In Chapter I, we applied sensitive proteomics analyses to CSF and plasma samples using three different focused panels (neurology, neuro-exploratory and inflammatory) to identify immunological and neurological factors in plasma and CSF that are associated with HIV-1 control. We found that CSF and plasma proteomes differed between HIV-1 infected individuals and HIV-1 seronegatives, at both compartments, CSF and plasma. Among the HIV-1 infected participants, individuals who can control HIV-1 infection without cART, showed an intermedium profile between HIV-high and HIV-1 seronegative individuals. Comparing the abundance of differentially present

proteins in CSF and plasma, the differences in plasma were less numerous between HIV-1 infected individuals and HIV-1 seronegatives than in CSF. One possible explanation could be that plasma reflects protein signatures from multiple body compartments, introducing wider variability and reflecting signals from compartments or organs beyond the peripheral blood. Moreover, the proteins included in the selected panels in the Proximity Extension Assay were focused on neurology and inflammatory processes, favoring the detection of proteins involves in central nervous system processes (194). Interestingly, as most of the significantly altered CSF proteins connected with processes involve the CD8A protein, our data indicate a possible effect on or even infiltration of CD8 T-cell response into the central nervous system. Thus, the presence of HIV-1 and its active replication in the CNS may cause an intense inflammatory reaction with potential influx of CD8 lymphocytes (195). Moreover, as HIV-1 infection causes a reduction of the CD4 T-cell subset, the balance between CD4 T-cells and CD8 T-cells at peripheral blood but also in the brain are imbalanced (196). Such CD4 and CD8 T-cells imbalance itself can generate an activation of microglial cells, through chemokine and cytokine secretion, which at the same time can change the integrity of the blood brain barrier (BBB), providing more chemo-attractants for T-cells to cross the BBB (197). Thus, as changes in BBB permeability have been noted in HIV-1 infection, it is plausible that CD8 T-cell infiltration into the CNS could be detected through some proteomic imprints at CSF (198).

The comparative proteomics analysis in plasma and CSF identified 5 differentially modulated molecules in both compartments: SIGLEC1, CRTAM, GZMA, IFI30 and ANXA10, of which the levels of three (SIGLEC1, CRTAM and GZMA) were positively correlated between both anatomical compartments. Focusing on these candidates, CRTAM is a cell surface marker for activated CD8 T-cells and NKT cells in the peripheral blood, with low levels of expression under physiological conditions but significantly increased in pathological states including viral infections (199)(200). In our analyses, CRTAM was indeed detectable at higher levels in individuals with high viral loads compared with HIV-low individuals or HIV-1 seronegative individuals. In addition, this marker is common in activated CD8 T-cells as well as NKT cells, which are both cell subtypes that share cytolytic properties such as the secretion of granzyme A (GZMA).

Accordingly, we also observed that individuals with poor virus control had higher levels of GZMA in both compartments, compared to HIV-low and HIV-1 seronegative individuals, potentially reflecting an increased number of activated CRTAM+ CD8-T cells and NKT cells driven by the increased viral replication. In line with this, we observed that CRTAM and GZMA in both compartments correlated with viral load levels in plasma and in the CSF fluid. Furthermore, correlation analysis showed that CRTAM and GZMA had both a negative association with the CD4/CD8 ratio in PBMCs. One possible explanation behind this inverse relation is that CD4 T-cells are decreased in the peripheral blood of individuals with higher HIV-1 viremia and that HIV-1 infection promotes the activation of CD8 T-cells expressing cytotoxic molecules and additional markers, such as CRTAM and GZMA.

Aside from immune and virological markers, the CD4/CD8 ratio has also been linked to the presence of neurocognitive disorders, suggesting that persistence T-cell dysfunction contributes to neurocognitive decline (201). Supporting this notion, our results show the levels of CRTAM and GMZA to positively correlate in both compartments with the levels of neopterin, a marker of immune activation in the brain during the processes of neuroinflammation (202).

In parallel, we also observed that SIGLEC1 was highly expressed in HIV-high individuals compared with HIV-low or HIV-1 seronegative individuals. Moreover, we observed a positive correlation between levels of SIGLEC1 and viral load in plasma and CSF. SIGLEC1 is a sialic acid binding Ig like lectin 1 and surface adhesion molecule mainly expressed in myeloid cells and is thought to enhance virus infectivity and dissemination through a mechanisms known as HIV-1 trans-infection (203). Interestingly, SIGLEC1 is also highly expressed in microglial cells in the brain upon CNS injury or blood-brain barrier breakdown (204). Specifically, when the blood brain barrier is injured and permeable, some plasma soluble factors infiltrate into the CNS causing elevated expression of SIGLEC1 in microglia cells, facilitating viral dissemination (205)(204). Curiously, a study that analyzed the phenotypes and transcriptional changes in blood monocytes from HIV-1 infected (with and without HAND) and uninfected individuals, showed that SIGLEC1 surface expression was increased in HAND compared to uninfected individuals (206). In line with this, we

observed levels of SIGLEC1 to correlate positively with plasma and CSF levels of neopterin, an immune activation marker reflecting neuroinflammation processes in the brain (202). Thus, is tentative to speculate that HIV-high individuals that cannot control the virus replication in the peripheral blood and central nervous system, will present high neopterin levels and may suffer from possible neuroinflammation due to enhanced virus replication, including in the CNS. This neuroinflammation can provoke a permeabilization of BBB causing an infiltration of plasma and immune cells into the brain increasing the levels of SIGLEC1 and further drive neurological disease (205).

Finally, the plasma levels of SIGLEC1, CRTAM and GZMA decreased after one year on cART treatment as seen in our validation cohort of longitudinally followed individuals. Similar results were obtained in a study that compared proteomes of HIV-1 infected individuals on long-term successfully cART, with those in treatment-naïve individuals with high viremia and in HIV-1 seronegative individuals. Confirming our findings, SIGLEC1, GZMA and CRTAM were among the proteins that were upregulated in HIV-1 infected individuals with high viremia compared to cART controlled infection and seronegative individuals (207). Overall, these results identify CSF and plasma levels of SIGLEC1, CRTAM and GZMA as markers of uncontrolled HIV-1 infection and show their plasma levels to reflect a CD4/CD8 T-cell misbalance and neuroinflammation. Interestingly, cART treatment restored these aberrations to levels seen in HIV-1 seronegative individuals.

Plasma HDAC class II factor (Sirtuin-2) as biomarker and potential therapeutic target for HIV-1 infection and neurological dysfunction

One of the most frequent comorbidities associated with HIV-1 infection are HIV-associated neurocognitive disorders (148), which can present with different clinical severity. Since the introduction of cART, the severity of such neurological complications of HIV infection has been drastically reduced (208). However, neurological disorders are frequently reported in PWH, possibly due to treatment toxicity, inflammation and viral replication in the brain (209). Factors not directly

related to HIV-1 infection, such as comorbidities, co-infections and lifestyle related factors, do probably also contribute to cognitive symptom as well immune activation and other biomarker variations commonly found in PWH on suppressive cART (210)(211)(212). Of note, some forms of HAND may share similar clinical manifestations and underlying mechanisms as those observed in other neurological diseases such as Alzheimer's disease and premature aging (213). However, limited access to CNS tissue complicates the identification of the precise mechanisms involved in the pathogenesis of HAND, hampering early diagnosis of the disease. There is thus an urgent need to identify plasma biomarkers that that are associated with the level of HIV-1 viral control and are indicative of neurological dysfunction and which could identify novel therapeutic targets in HIV-1 infection.

In Chapter II, we identify SIRT2 (NAD-dependent deacetylase) as the most differentially detected plasma protein between HIV-1 infected individuals with high and low plasma viral loads. SIRT2 is one of the seven sirtuin family members, which are class III histone deacetylases with a wide range of functions and involvement in multiple processes in the cell (214). Compared to other family members, less research has been carried out for SIRT2. Still, several target proteins involved in numerous immune and neurological pathways have been identified in recent years, suggesting the involvement of SIRT2 in physiologic and pathologic processes. In the context of neurological and inflammatory disorders, a dual effect of SIRT2 in the brain environment has been described, showing that SIRT2 can accelerate the development of neurological pathologies but also protect the brain from deterioration (215)(216). The former aspect has also been described in Alzheimer's and Parkinson's diseases, where SIRT2 is thought to contribute to the pathogenic mechanism underlying deacetylation of the α-tubulin molecule and for which specific SIRT2-targeting therapies are under development (217)(218)(219)(220).

In our study in chronic HIV-1 infection, we identified a strong association between plasma levels of SIRT2 with other prominent biomarkers of neurological disorders, such as BDNF, MAPT, and SNCA (221)(181). These associations are in line with *SIRT2* gene expression in brain tissue (218) and, from our analyses, seen at especially elevated levels in untreated HIV-1 infected individuals with HAD. Moreover, we also found *SIRT2* expression levels in CNS to be associated with MAPT and NFL, further

supporting the identified associations between the plasma levels of these markers and HIV-1 related diseases.

Past studies have found *SIRT2* to be highly expressed in the temporal cortex of individuals with AD (218). Our results in PWH who underwent longitudinal neuropsychological and neuroimaging assessments, also indicate that decreased brain volume near the orbitofrontal cortex was associated with elevated plasma levels of SIRT2. Evidently, more and larger studies determining the *SIRT2* expression patterns in these specific regions of the brain of HIV-1 infected individuals will be needed to link these observations with neurological outcomes during HIV-1 infection. Still, our data are consistent with findings in a mouse model of frontotemporal dementia, where specific inhibition of SIRT2 by AK-1 in the hippocampus revealed a neuroprotective effect and prevented neuronal loss in this area (181). Indeed, SIRT2 inhibitors have been shown to improve microtubule dynamics and help increase binding of MAPT and SNCA to α-tubulin (217). As such, AK-1 and other SIRT2 inhibitors are being tested *in vitro* and *in vivo* models of Parkinson and Alzheimer disease (212)(215)(182).

In addition, the role of SIRT2 has recently begun to be explored in a wider set of infectious diseases (216). Specifically, SIRT2 has been found to accelerate viral replication of Hepatitis B virus (HBV), and the use of sirtuin inhibitors has been proposed as a potential new therapeutic intervention (222)(223). In *Listeria monocytogenes* infection, SIRT2 translocates to the nucleus and deacetylates H3K18, which associates with a subset of host genes that are crucial during the bacterial life cycle (224). Furthermore, *Helicobacter pylori* infection upregulates *SIRT2* expression in gastric epithelial cells, and specific inhibition is being considered as a therapeutic strategy (225). Similarly, in chronic *Staphylococcal aureus* infection in mice, the survival rate was increased with SIRT2 deficiency (226), and in a SIRT2$^{-/-}$ murine model, bacterial infections were reduced (224). More recently, in the context of HIV-1 infection, the potential roles of SIRT2 in different HIV-1 associated comorbidities (insulin resistance and cardiovascular diseases), neurocognitive disorders (227) and virus life cycle (228) have emerged. In particular, SIRT1, SIRT2 and SIRT3 can deacetylate and regulate HIV-1 Tat activity; and for SIRT1 is has been shown that its interaction with Tat activates the HIV-1 promoter (229). In line with these

observations, the present study shows that control of HIV-1 infection in the absence of cART is associated with lower SIRT2 levels and that plasma protein and gene expression levels correlate positively with plasma viral loads and HIV-1 proviral levels. Our results also show that *in vitro* inhibition of SIRT2 activity by AK-1 in HIV-1 infected PHA-blasts and in MDMs reduced HIV-1 replication, suggesting that HIV-1 (as other pathogens) may have evolved to hijack Sirtuins to enhance their replication (230).

It is widely accepted that early initiation of treatment is crucial for reducing the size of the HIV-1 reservoir in different anatomical compartments, including the CNS (231)(180). Particularly, frontal white matter seems to be the main site of HIV-1 reservoir compared to other cerebral regions (232), with microglia cells and macrophages being major compartments harboring HIV-1 proviral DNA. Interestingly, a number of studies have addressed the biological actions of SIRT2 on microglia cells and macrophages, all outside of HIV-1 infection context. In a murine model for neurological inflammation, SIRT2 was shown to drive brain injury and activation of microglia upon stimulation with lipopolysaccharides (233)(234). The results we obtained after *in vitro* infection of glial cells directly support this model and suggest that SIRT2 may play an important role in brain injury and the HIV-1 viral cycle, including maintaining the HIV-1 reservoir in the brain .

Plasma proteomics analysis in the BCN02 clinical trial, based on a "kick and kill" strategy for HIV-1 cure

Current guidelines recommend that HIV-1 infected individuals be treated with cART immediately after diagnosis. As cART doesn't clean and eliminate the viral reservoir, other strategies such as "kick and kill", "block and lock", gene therapy and stem cell transplantation have been explored in a wide set of clinical trials. However, the HIV cure field still lacks a robust and functional (plasma) biomarker to assess the efficacy of these interventions and validate any HIV-1 therapeutic or cure strategy during a monitored antiretroviral phase (MAP).

The BCN02 clinical trial was a proof of concept study of a "kick and kill" HIV-1 cure strategy employing the latency reversing agent romidepsin (RMD) and MVA.HIVconsv

vaccination to boost antiviral cellular immunity (156)(118). The results of BCN02 demonstrated that this strategy caused different effects on the organism at immunological (118), microbiome (235), epigenetic (159) and neurological level (236) and allowed 1/3 of the participants to remain off cART for the duration of a 32 weeks long treatment interruption. Here, we explored the impact of the administration of RMD on the peripheral blood proteome and the identification of soluble biomarkers that could predict the outcome of such an intervention. Our longitudinal comparative proteome analysis revealed that the administration of RMD increased the abundance of several plasma proteins involved in the inflammatory immune response and in neurological processes, and that most of these changes were carried into the cART interruption phase of the study.

As a histone deacetylation inhibitor, RMD causes opening of the chromatin and enhances gene expression, of both, the integrated virus as well as host genes (159). The latter can translate into higher secretion of proteins into peripheral blood plasma, and may at least partly reflect changes in different organs, including the CNS. In addition, "kick and kill" interventions could also generate some cell death, as our earlier data showed the induction of apoptotic proteins including CASP-8 or TNF. This was observed especially during the MAP phase of the BCN02 trial, suggesting that part of the soluble plasma proteome may stem from cell death caused by the cummulative effect of boosted cytolytic immune mechanisms, RMD toxicity and reactivated viral replication (118). As RMD can have beneficial effects in some neurological disease states (237) and since one of the anatomical compartments where the latent HIV-1 reservoir is established, is the CNS (238), the participants in the BCN02 trial underwent various cognitive evaluations (236). No harmful effects on cognitive status, functional outcomes or brain imaging parameters were observed after RMD. Also, additional neurological assessments after the completion of the MAP were performed to demonstrate CNS safety. Howerver, and although RMD was apparently well-tolerated, we observed the plasma levels of two neuroprotective proteins (MANF and GDNF) to be increased by RMD infusions (239)(240)(241)(242). Subsequently, plasma levels of two neurological damage markers (NFL and GPNMB) were increased during the MAP phase (243)(244), suggestive of some effects on the CNS. It is tempting to speculate

that RMD administration indeed exerted a protective effect on the CNS, while some CNS damage may be induced by stopping cART and allowing the virus to rebound.

Aside from longitudinally evaluating the effects of cART stop and RMD administration on the plasma proteomes, we also tested whether these plasma signatures could inform on the efficacy of the intervention and virus control during the 32 weeks MAP. Our recent studies have identified gut microbiome composition (in particular the *Bacteroidales/Clostridiales* ratio) as a novel marker of HIV-1 reservoir size and post-intervention virus control (235). Interestingly, the individuals with high *Bacteroidales/Clostridiales* ratio also showed gene expression signatures related to immune activation, in line with the plasma proteomics findings. Furthermore, parallel epigenetic studies in samples from the BCN02 clinical trial identified specific methylation profiles that were related to viral load, proviral levels as well as the HIV-1 specific T-cell responses. These analyses also showed that specific epigenetic imprints at study baseline could predict virus control during MAP (159). This was mirrored by our proteomics analysis, where baseline plasma proteomes were already different between future MAP-C and MAP-NC individuals and for which in some cases (i.e. immnutity activation and cell signaling) epigenetic imprints also differentiated MAP-C from MAP-NC. Further ongoing studies now aim to integrate the different -omics data sets to validate whether epigenetic predisposition, microbiota composition and plasma proteomics are interrelated and can predict post-intervention HIV-1 control.

Some of the emerging markers may also confirm recent reports that have linked increased expression of host restriction factors (including APOBEC3G and SLFN11 or immunological features such as PD-1, Tim-3 and Lag-3) prior to ART initiation with durable control of virus post cART treatment interruption (245)(142). Indeed, our data show that prior to the intervention, plasma proteomes were different between MAP-C and MAP-NC, with proteins related to adaptive and innate immunity being elevated in MAP-NC. This observation appears somewhat counterintuitive, but may be explained by these individuals showing strong viral replication in the context of a more activated immune system. In line with this, at RMD timepoint, MAP-C showed increased levels of proteins involved in the negative regulation of inflammatory interleukins such as IL-5 and IL-13 and of interferon-gamma-mediated signaling pathways. This might be due to

the effect of RMD itself or due to the activation of virus-specific T-cell which could lead to an inibition or regulation of the Th2 cytokine profile in an attempt to control the burst of immune activation (246).

Interestingly, CD33 (SIGLEC3) protein was the unique plasma marker whose levels were increased upon RMD administration and maintained elevated when cART was stopped. In addition, CD33 plasma levels allowed for the discrimination of MAP-C from MAP-NC individuals, already at the baseline timepoint. Intriguingly, CD33 also known as SIGLEC3, can be expressed in myeloid lineage and to a lesser extent on activated T-cells and natural killer cells but can also modulate immune responses partly due to its ability to inhibit monocytes (247). The binding with its ligands; C1q and sialylated glycoproteins (the latter highly expressed in brain microglia), leads to the recruitment of inhibitory proteins via its immunoreceptor tyrosine-based inhibition motif domains. This induces signaling cascades that inhibit cell activation and functions associated with cytokine release or virus phagocytosis (248). Previous reports have shown that homeostatic basal levels of CD33 are low but are strongly increased under pathogenic conditions, including viral infections (248). As CD33 is an interferon inducible factor (249), higher viral burden could induce its production. In more extreme situations, the shedding of CD33/SIGLEC3 protein into the plasma as has been described for SIGLEC7 in uncontrolled HIV-1 infection. Specifically, a higher plasma levels of SIGLEC7 were observed in PWH compared to HIV-1 seronegative individuals and these plasma levels correlated positively with HIV-1 viral loads (249). This is in line with our findings of higher CD33 protein plasma levels in MAP-NC compared to MAP-C, even though the comparison of total PBMCs transcriptomics in this small set of BCN02 participants did not reach in all cases statistical significance. Interestingly, gene expression analysis of *CD33* showed an increase during the intervention, mirroring the plasma CD33 protein leves that followed the same pattern. However, it was not until the MAP timepoint that we observed a difference of CD33 gene expression levels between MAP-C and MAP-NC individuals.

In addition to its effects in viral infections, CD33 has also been implicated in neuroinflammation, where its activation reduces phagocytic activity of microglia cells, causing an accumulation of pathogenic Aβ plaques and contribute to an elevated risk

for Alzheimer's disease (248)(205)(250). In our present study, we indeed observed very strong associations between CD33 and the gamma-glutamyltransferase 5 (GGT5), ADAM metallopeptidase domain 15 (ADAM15) and neurofilament light protein (NFL). Specifically, NFL has been reported to be a biomarker of neurological injury and for Alzheimer's disease (251)(252). Intriguingly, in the epigenetic studies of the BCN02 trial, differentially methylated positions (DMPs) in the CD33 gene were identified between MAP-C and MAP-NC. One of these DMPs regions, also includes a Single Nucleotide Polymorphism (SNP) associated with AD risk (253)(254). Thus, it will be interesting to assess to what degree CD33 also influences the disease progression in HIV-1 infected individuals who suffer from HIV-1 associated neurocognitive disorders (HAND).

To validate the plasma and gene expression levels of CD33 seen in BCN02 participants, especially during the MAP phase, a cohort of chronically untreated HIV-1 infected individuals with a wide range of viral load set points was analyzed. These results showed that HIV-1 individuals with poor virus control (HIV-high) had elevated plasma levels of CD33, which were also positively correlated with both, viral loads and proviral HIV-1 DNA copy numbers. This is in line with a report by Rempel et al, showing that several members of the Siglec family can facilitate infection and viral replication (3SIGLEC3 or CD33, -5, -7 and -9) (255). It has also been suggested that the direct interaction between sialylactose-containing gangliosides in the HIV-1 viral membrane and the cellular lectin SIGLEC1 is critical for HIV-1 capture and storage by mature dendritic cells and for trans-infection between infected dendritic cells and T-cells (256). In addition, the HIV-1 Gp120 surface protein has been shown to serve as viral ligand for SIGLEC3 (250), which is thought to facilitate infection of macrophages and T-cells (249)(257). The results from the BCN02 study and data from untreated chronically HIV-1 infected individuals also could indicate that individuals with high viral loads present high cytotoxic immune activation and thus more cell death, which in turn may cause the observed increase in soluble CD33 in plasma. Based on our observation that CD33 can predict post-treatment control in BCN02 and the described physical associations between CD33/SIGLEC3 and HIV-1 particles, we explored the possibility to inhibit HIV-1 replication by targeting CD33 in *in vitro* cultures using an anti-CD33 mAb. Indeed, viral

replication was strongly suppressed in T-cells and MDMs in a dose-dependent manner and showed a trend to reduced levels of integrated viral DNA as well.

Of note, and aside from a direct role in the HIV-1 life cycle, therapeutic antibodies against CD33 have been approved to treat acute myeloid leukemia, targeting the V-set domain or sialic acid-binding domain of the CD33 molecule (258). Also, in the context of Hepatitis B virus (HBV) infection, the use of anti-CD33 was able to reverse hHBV-mediated immunosuppression *in vitro* (259). Finally, a recent study in Alzheimer´s Disease has ranked lintuzumab (SGN-33) as one of the top repurposed drug candidates for treating AD (260). Given these evidences, it is tempting to propose that anti-CD33 mAb could be employed in HIV-1 infection, with a potential dual beneficial effect, by reducing HIV-1 replication and, on the other hand, improving HIV-associated neurodegeneration. Overall, our analyses document that the "kick and kill" strategy in BCN02 left specific marks on inflammatory and neurological plasma proteomes. Based on these data and MAP outcome, we identified soluble CD33 as a novel marker that was consistently elevated in individuals with poor virus control (both, in BCN02 and in natural infection). The fact that the CD33 plasma levels were elevated already in pre-intervention samples suggest that CD33 protein levels could be employed in future trials for more targeted patient selection and to design combination strategies that incorporate targeting of CD33 in HIV-1 cure approaches.

CONCLUDING DISCUSSION

Overall, proteomics analyses have allowed us to generate highly informative insights into HIV-1 related pathological events by testing different types of human samples including plasma and cerebrospinal fluid from different human cohorts and clinical trials. The information gained by these analyses will help to identify proteins that can serve as biomarkers associated with viral control, either in a situation of natural control or post-treatment control in the therapeutic setting and has the potential to guide further refinement of such cure strategies. Proteomics analyses in these samples also revealed potential links between HIV-1 infection and HIV-1 related

comorbidities, in particular neurological dysfunction. These insights support the potentially critical role of a CNS viral reservoir, with direct implications for the HIV cure agenda. Moreover, the gained information and future analyses with broader proteomics analyses in larger cohorts and placebo controlled clinical trials, has the potential to identify possible therapeutic immune targets. Together with the identification of targetable molecules involved in the viral live cycle, these results may allow for multipronged approaches towards effective HIV-1 cure.

CONCLUSIONS

6. CONCLUSIONS

CHAPTER I. Identification of plasma biomarkers in natural control of HIV-1 infection in the absence of cART.

I. Neurological and inflammatory soluble factors at CSF and plasma compartments clearly differed between HIV-1 infected individuals who spontaneously control or not HIV-1 replication and when compared to seronegative individuals.

II. SIGLEC1, CRTAM and GZMA levels in CSF and plasma compartments discriminate seronegative from HIV-1 infected individuals, and their levels are positively associated with viral load and negatively with CD4/CD8 ratio, in both compartments.

III. Neopterin, a marker of neuroinflammation and immune activation, correlated positively with SIGLEC1, CRTAM and GZMA levels in CSF and plasma.

IV. Longitudinally evaluated individuals showed that after one year on cART, plasma levels of SIGLEC1, CRTAM and GZMA decreased significantly compared to early infection time points, reaching levels similar to those detected in seronegative individuals.

CHAPTER II. Plasma HDAC class II factor (Sirtuin-2) as biomarker and potential therapeutic target of HIV-1 infection and neurological dysfunction.

V. SIRT2 plasma levels and PBMCs gene expression were higher in HIV-1 infected individuals with high viral loads compared to HIV-1 infected individuals with low viral loads and were positively associated with the size of the proviral reservoir in PBMC.

VI. SIRT2 plasma levels were positively associated with biomarkers of neurological dysfunction (TAU, BDNF, SNCA) in chronically untreated HIV-1 infected individuals.

VII. Individuals who started cART early or later after infection continue to show different SIRT2 plasma levels after one year on cART treatment, and these levels correlated negatively with medial orbitofrontal volumetry.

VIII. Inhibition of SIRT2 with the small molecule inhibitor AK-1, reduced viral replication in peripheral blood cells and in primary glial cells and reduced virus reactivation in latently HIV-1 infected J-LAT A2 cells.

CHAPTER III. Plasma proteomics analysis in the BCN02 clinical trial, based on a "kick and kill" strategy for HIV-1 cure.

IX. Plasma proteomics profiles were modified during the "kick and kill" intervention in the BCN02 clinical trial, especially after romidepsin infusions and during MAP.

X. CD33 emerged as a marker of uncontrolled viral infection, and in the BCN02 clinical trial, predicted time to restart of cART during a monitored antiretroviral pause.

XI. Addition of an antibody against CD33 reduced viral replication in vitro, indicating that CD33 is required for effective HIV-1 replication in peripheral blood cells.

REFERENCES

7. REFERENCES

1.   Gottlieb MS. Pneumocystis pneumonia--Los Angeles. 1981. Am J Public Health. 2006;96(6).

2.   Marx JL. New disease baffles medical community. Science (80-) [Internet]. 1982 [cited 2023 Feb 28];217(4560):618–21. Available from: https://www.science.org/doi/10.1126/science.7089584

3.   Chermann JC, Barré-Sinoussi F, Dauguet C, Brun-Vezinet F, Rouzioux C, Rozenbaum W, et al. Isolation of a New Retrovirus in a Patient at Risk for Acquired Immunodeficiency Syndrome. Antibiot Chemother [Internet]. 1984 [cited 2023 Feb 28];32:48–53. Available from: https://www.karger.com/Article/FullText/409704

4.   Gallo RC, Sarin PS, Gelmann EP, Robert-Guroff M, Richardson E, Kalyanaraman VS, et al. Isolation of Human T-Cell Leukemia Virus in Acquired Immune Deficiency Syndrome (AIDS). Science (80-) [Internet]. 1983 [cited 2023 Feb 28];220(4599):865–7. Available from: https://www.science.org/doi/10.1126/science.6601823

5.   Daniel MD, Letvin NL, King NW, Kannagi M, Sehgal PK, Hunt RD, et al. Isolation of T-Cell Tropic HTLV-III-Like Retrovirus from Macaques. Science (80-) [Internet]. 1985 [cited 2023 Feb 28];228(4704):1201–4. Available from: https://www.science.org/doi/10.1126/science.3159089

6.   Case K. Nomenclature: Human immunodeficiency virus. Ann Intern Med. 1986;105(1):133.

7.   Gao F, Balles E, Robertson DL, Chen Y, Rodenburg CM, Michael SF, et al. Origin of HIV-1 in the chimpanzee Pan troglodytes troglodytes. Nat 1999 3976718 [Internet]. 1999 Feb 4 [cited 2023 Feb 28];397(6718):436–41. Available from: https://www.nature.com/articles/17130

8.   Sharp PM, Bailes E, Gao F, Beer BE, Hirsch VM, Hahn BH. Origins and evolution of AIDS viruses: estimating the time-scale. Biochem Soc Trans [Internet]. 2000 Feb 1 [cited 2023 Feb 28];28(2):275–82. Available from: /biochemsoctrans/article/28/2/275/63043/Origins-and-evolution-of-AIDS-viruses-estimating

9.   Fact sheet - Latest global and regional statistics on the status of the AIDS epidemic. | UNAIDS [Internet]. [cited 2023 Feb 28]. Available from: https://www.unaids.org/en/resources/documents/2022/UNAIDS_FactSheet

10.   DerSarkissian M, Bhak RH, Oglesby A, Priest J, Gao E, Macheca M, et al. Retrospective analysis of comorbidities and treatment burden among patients with HIV infection in a US Medicaid population. Curr Med Res Opin [Internet]. 2020 May 3 [cited 2023 Feb 28];36(5):781–8. Available from: https://www.tandfonline.com/doi/abs/10.1080/03007995.2020.1716706

11.   Gallant J, Hsue PY, Shreay S, Meyer N. Comorbidities Among US Patients With Prevalent HIV Infection—A Trend Analysis. J Infect Dis [Internet]. 2017 Dec 19 [cited 2023 Feb 28];216(12):1525–33. Available from: https://academic.oup.com/jid/article/216/12/1525/4743770

12.   Ali M. Ninth Report of the International Committee on Taxonomy of Viruses [Internet].

[cited 2023 Mar 1]. Available from: https://www.academia.edu/8097730/Ninth_Report_of_the_International_Committee_on_Taxonomy_of_Viruses

13. Lu K, Heng X, Summers MF. Structural Determinants and Mechanism of HIV-1 Genome Packaging. 2011 [cited 2023 Mar 1]; Available from: http://www.hiv.lanl.gov/

14. Arthur LO, Bess JW, Sowder RC, Benveniste RE, Mann DL, Chermann JC, et al. Cellular Proteins Bound to Immunodeficiency Viruses: Implications for Pathogenesis and Vaccines. Science (80-) [Internet]. 1992 Dec 18 [cited 2023 Mar 1];258(5090):1935–8. Available from: https://www.science.org/doi/10.1126/science.1470916

15. Turner BG, Summers MF. Structural biology of HIV. J Mol Biol. 1999 Jan 8;285(1):1–32.

16. Rossi E, Meuser ME, Cunanan CJ, Cocklin S. Structure, Function, and Interactions of the HIV-1 Capsid Protein. Life [Internet]. 2021 Feb 1 [cited 2023 Mar 1];11(2):1–25. Available from: /pmc/articles/PMC7910843/

17. Ratner L, Haseltine W, Patarca R, Livak KJ, Starcich B, Josephs SF, et al. Complete nucleotide sequence of the AIDS virus, HTLV-III. Nat 1985 3136000 [Internet]. 1985 [cited 2023 Mar 1];313(6000):277–84. Available from: https://www.nature.com/articles/313277a0

18. van Heuvel Y, Schatz S, Rosengarten JF, Stitz J. Infectious RNA: Human Immunodeficiency Virus (HIV) Biology, Therapeutic Intervention, and the Quest for a Vaccine. Toxins 2022, Vol 14, Page 138 [Internet]. 2022 Feb 14 [cited 2023 Mar 1];14(2):138. Available from: https://www.mdpi.com/2072-6651/14/2/138/htm

19. Wain-Hobson S, Sonigo P, Danos O, Cole S, Alizon M. Nucleotide sequence of the AIDS virus, LAV. Cell [Internet]. 1985 Jan 1 [cited 2023 Mar 1];40(1):9–17. Available from: http://www.cell.com/article/0092867485903034/fulltext

20. Sattentau QJ, Moore JP. The role of CD4 in HIV binding and entry. Philos Trans R Soc London Ser B Biol Sci [Internet]. 1993 Oct 29 [cited 2023 Mar 1];342(1299):59–66. Available from: https://royalsocietypublishing.org/doi/10.1098/rstb.1993.0136

21. Yandrapally S, Mohareer K, Arekuti G, Vadankula GR, Banerjee S. HIV co-receptor-tropism: cellular and molecular events behind the enigmatic co-receptor switching. https://doi.org/101080/1040841X20211902941 [Internet]. 2021 [cited 2023 Mar 1];47(4):499–516. Available from: https://www.tandfonline.com/doi/abs/10.1080/1040841X.2021.1902941

22. Melikyan GB. Common principles and intermediates of viral protein-mediated fusion: The HIV-1 paradigm. Retrovirology [Internet]. 2008 Dec 10 [cited 2023 Mar 1];5(1):1–13. Available from: https://retrovirology.biomedcentral.com/articles/10.1186/1742-4690-5-111

23. Clapham PR, McKnight Á. Cell surface receptors, virus entry and tropism of primate lentiviruses. J Gen Virol [Internet]. 2002 Aug 1 [cited 2023 Mar 1];83(8):1809–29. Available from: https://www.microbiologyresearch.org/content/journal/jgv/10.1099/0022-1317-83-8-1809

24. Hu WS, Hughes SH. HIV-1 Reverse Transcription. Cold Spring Harb Perspect Med [Internet]. 2012 [cited 2023 Mar 1];2(10). Available from: /pmc/articles/PMC3475395/

25. Smyth RP, Davenport MP, Mak J. The origin of genetic diversity in HIV-1. Virus Res. 2012

Nov 1;169(2):415–29.

26. Engelman A, Mizuuchi K, Craigie R. HIV-1 DNA integration: Mechanism of viral DNA cleavage and DNA strand transfer. Cell [Internet]. 1991 Dec 20 [cited 2023 Mar 1];67(6):1211–21. Available from: http://www.cell.com/article/009286749190297C/fulltext

27. Laspia MF, Rice AP, Mathews MB. HIV-1 Tat protein increases transcriptional initiation and stabilizes elongation. Cell [Internet]. 1989 Oct 20 [cited 2023 Mar 1];59(2):283–92. Available from: http://www.cell.com/article/0092867489902900/fulltext

28. Nekhai S, Jeang KT. Transcriptional and post-transcriptional regulation of HIV-1 gene expression: role of cellular factors for Tat and Rev. http://dx.doi.org/102217/1746091314417 [Internet]. 2006 Dec 5 [cited 2023 Mar 1];1:417–26. Available from: https://www.futuremedicine.com/doi/10.2217/17460913.1.4.417

29. Bukrinskaya AG. HIV-1 assembly and maturation. Arch Virol [Internet]. 2004 Jun 5 [cited 2023 Mar 1];149(6):1067–82. Available from: https://link.springer.com/article/10.1007/s00705-003-0281-8

30. Shaw GM, Hunter E. HIV Transmission. Cold Spring Harb Perspect Med [Internet]. 2012 Nov 1 [cited 2023 Mar 1];2(11):a006965. Available from: http://perspectivesinmedicine.cshlp.org/content/2/11/a006965.full

31. Moir S, Chun TW, Fauci AS. Pathogenic Mechanisms of HIV Disease*. https://doi.org/101146/annurev-pathol-011110-130254 [Internet]. 2011 Jan 24 [cited 2023 Mar 1];6:223–48. Available from: https://www.annualreviews.org/doi/abs/10.1146/annurev-pathol-011110-130254

32. van den Berg LM, Geijtenbeek TBH. Antiviral Immune Responses by Human Langerhans Cells and Dendritic Cells in HIV-1 Infection. 2012 [cited 2023 Mar 1];45–70. Available from: https://link.springer.com/chapter/10.1007/978-1-4614-4433-6_2

33. Fenwick C, Joo V, Jacquier P, Noto A, Banga R, Perreau M, et al. T-cell exhaustion in HIV infection. Immunol Rev [Internet]. 2019 Nov 1 [cited 2023 Mar 1];292(1):149–63. Available from: https://onlinelibrary.wiley.com/doi/full/10.1111/imr.12823

34. Khaitan A, Unutmaz D. Revisiting Immune Exhaustion During HIV Infection. Curr HIV/AIDS Rep [Internet]. 2011 Mar [cited 2023 Mar 1];8(1):4. Available from: /pmc/articles/PMC3144861/

35. Borrow P. Innate immunity in acute HIV-1 infection.

36. Cohen MS, Gay CL, Busch MP, Hecht FM. The Detection of Acute HIV Infection. J Infect Dis [Internet]. 2010 Oct 1 [cited 2023 Mar 1];202(Supplement_2):S270–7. Available from: https://academic.oup.com/jid/article/202/Supplement_2/S270/852813

37. Mei Y, Wang L, Holte SE. A comparison of methods for determining HIV viral set point. Stat Med [Internet]. 2008 Jan 15 [cited 2023 Mar 1];27(1):121–39. Available from: https://onlinelibrary.wiley.com/doi/full/10.1002/sim.3038

38. Follansbee SE. Pathogenesis and clinical manifestations of AIDS. J Am Podiatr Med Assoc [Internet]. 1988 [cited 2023 Mar 1];78(3):120–6. Available from: https://pubmed.ncbi.nlm.nih.gov/3075663/

39. Guaraldi G, Orlando G, Zona S, Menozzi M, Carli F, Garlassi E, et al. Premature Age-

Related Comorbidities Among HIV-Infected Persons Compared With the General Population. Clin Infect Dis [Internet]. 2011 Dec 1 [cited 2023 Mar 1];53(11):1120–6. Available from: https://academic.oup.com/cid/article/53/11/1120/304955

40. Pourcher V, Gourmelen J, Bureau I, Bouee S. Comorbidities in people living with HIV: An epidemiologic and economic analysis using a claims database in France. PLoS One [Internet]. 2020 Dec 1 [cited 2023 Mar 1];15(12):e0243529. Available from: https://journals.plos.org/plosone/article?id=10.1371/journal.pone.0243529

41. Spudich S, Gonzalez-Scarano F. HIV-1-related central nervous system disease: current issues in pathogenesis, diagnosis, and treatment. Cold Spring Harb Perspect Med [Internet]. 2012 Jun 1 [cited 2023 Mar 1];2(6):a007120–a007120. Available from: https://pubmed.ncbi.nlm.nih.gov/22675662/

42. András IE, Pu H, Deli MA, Nath A, Hennig B, Toborek M. HIV-1 Tat protein alters tight junction protein expression and distribution in cultured brain endothelial cells. J Neurosci Res [Internet]. 2003 Oct 15 [cited 2023 Mar 1];74(2):255–65. Available from: https://onlinelibrary.wiley.com/doi/full/10.1002/jnr.10762

43. Schnell G, Price RW, Swanstrom R, Spudich S. Compartmentalization and Clonal Amplification of HIV-1 Variants in the Cerebrospinal Fluid during Primary Infection. J Virol [Internet]. 2010 Mar [cited 2023 Mar 1];84(5):2395. Available from: /pmc/articles/PMC2820937/

44. Hashimoto D, Chow A, Noizat C, Teo P, Beasley MB, Leboeuf M, et al. Tissue resident macrophages self-maintain locally throughout adult life with minimal contribution from circulating monocytes. Immunity [Internet]. 2013 Apr 4 [cited 2023 Mar 1];38(4):792–804. Available from: /pmc/articles/PMC3853406/

45. Bethel-Brown C, Yao H, Hu G, Buch S. Platelet-derived growth factor (PDGF)-BB-mediated induction of monocyte chemoattractant protein 1 in human astrocytes: Implications for HIV-associated neuroinflammation. J Neuroinflammation [Internet]. 2012 Dec 1 [cited 2023 Mar 1];9(1):1–14. Available from: https://jneuroinflammation.biomedcentral.com/articles/10.1186/1742-2094-9-262

46. Zayyad Z, Spudich S. Neuropathogenesis of HIV: From Initial Neuroinvasion to HIV Associated Neurocognitive Disorder (HAND).

47. Siangphoe U, Archer KJ, Nguyen C, Lee KR. Associations of antiretroviral therapy and comorbidities with neurocognitive outcomes in HIV-1-infected patients. AIDS [Internet]. 2020 May 1 [cited 2023 Mar 1];34(6):893–902. Available from: https://journals.lww.com/aidsonline/Fulltext/2020/05010/Associations_of_antiretroviral_therapy_and.10.aspx

48. Saylor D, Dickens AM, Sacktor N, Haughey N, Slusher B, Pletnikov M, et al. HIV-associated neurocognitive disorder — pathogenesis and prospects for treatment. Nat Rev Neurol 2016 124 [Internet]. 2016 Mar 11 [cited 2023 Mar 1];12(4):234–48. Available from: https://www.nature.com/articles/nrneurol.2016.27

49. Borjabad A, Volsky DJ. Common Transcriptional Signatures in Brain Tissue from Patients with HIV-Associated Neurocognitive Disorders, Alzheimer's Disease, and Multiple Sclerosis. J Neuroimmune Pharmacol 2012 74 [Internet]. 2012 Oct 12 [cited 2023 Mar 1];7(4):914–26. Available from: https://link.springer.com/article/10.1007/s11481-012-9409-5

50. Mirsattari SM, Power C, Nath A. Parkinsonism with HIV infection. Mov Disord [Internet].

1998 Jul 1 [cited 2023 Mar 1];13(4):684–9. Available from: https://onlinelibrary.wiley.com/doi/full/10.1002/mds.870130413

51. Engelhardt B. Molecular mechanisms involved in T cell migration across the blood-brain barrier. J Neural Transm [Internet]. 2006 Apr [cited 2023 Mar 1];113(4):477–85. Available from: https://link.springer.com/article/10.1007/s00702-005-0409-y

52. Carty M, Guy C, Bowie AG. Detection of Viral Infections by Innate Immunity. Biochem Pharmacol. 2021 Jan 1;183:114316.

53. Yin X, Langer S, Zhang Z, Herbert KM, Yoh S, König R, et al. Sensor Sensibility—HIV-1 and the Innate Immune Response. Cells 2020, Vol 9, Page 254 [Internet]. 2020 Jan 20 [cited 2023 Mar 1];9(1):254. Available from: https://www.mdpi.com/2073-4409/9/1/254/htm

54. Jia X, Zhao Q, Xiong Y. HIV suppression by host restriction factors and viral immune evasion. Curr Opin Struct Biol. 2015 Apr 1;31:106–14.

55. Gulzar N, Copeland K. CD8+ T-Cells: Function and Response to HIV Infection. Curr HIV Res. 2005 Mar 25;2(1):23–37.

56. Piguet V, Trono D. Living in oblivion: HIV immune evasion. Semin Immunol. 2001 Feb 1;13(1):51–7.

57. Moir S, Fauci AS. B-cell responses to HIV infection. Immunol Rev [Internet]. 2017 Jan 1 [cited 2023 Mar 1];275(1):33–48. Available from: https://onlinelibrary.wiley.com/doi/full/10.1111/imr.12502

58. Schommers P, Gruell H, Abernathy ME, Tran MK, Dingens AS, Gristick HB, et al. Restriction of HIV-1 Escape by a Highly Broad and Potent Neutralizing Antibody. Cell [Internet]. 2020 Feb 6 [cited 2023 Mar 1];180(3):471-489.e22. Available from: http://www.cell.com/article/S009286742030057X/fulltext

59. Brodin J, Zanini F, Thebo L, Lanz C, Bratt G, Neher RA, et al. Establishment and stability of the latent HIV-1 DNA reservoir. Elife. 2016 Nov 15;5(November2016).

60. Strain MC, Little SJ, Daar ES, Havlir D V., Günthard HF, Lam RY, et al. Effect of treatment, during primary infection, on establishment and clearance of cellular reservoirs of HIV-1. J Infect Dis [Internet]. 2005 May 1 [cited 2023 Mar 1];191(9):1410–8. Available from: https://pubmed.ncbi.nlm.nih.gov/15809898/

61. Ananworanich J, Chomont N, Eller LA, Kroon E, Tovanabutra S, Bose M, et al. HIV DNA Set Point is Rapidly Established in Acute HIV Infection and Dramatically Reduced by Early ART. EBioMedicine [Internet]. 2016 Sep 1 [cited 2023 Mar 1];11:68–72. Available from: http://www.thelancet.com/article/S2352396416303309/fulltext

62. Chun TW, Engel D, Berrey MM, Shea T, Corey L, Fauci AS. Early establishment of a pool of latently infected, resting CD4+ T cells during primary HIV-1 infection. Proc Natl Acad Sci U S A [Internet]. 1998 Jul 21 [cited 2023 Mar 1];95(15):8869–73. Available from: https://www.pnas.org/doi/abs/10.1073/pnas.95.15.8869

63. Henrich TJ, Hatano H, Bacon O, Hogan LE, Rutishauser R, Hill A, et al. HIV-1 persistence following extremely early initiation of antiretroviral therapy (ART) during acute HIV-1 infection: An observational study. PLoS Med [Internet]. 2017 Nov 1 [cited 2023 Mar 1];14(11). Available from: /pmc/articles/PMC5675377/

64. García M, Buzón MJ, Benito JM, Rallón N. Peering into the HIV reservoir. Rev Med Virol [Internet]. 2018 Jul 1 [cited 2023 Mar 1];28(4):e1981. Available from:

https://onlinelibrary.wiley.com/doi/full/10.1002/rmv.1981

65. Shen A, Siliciano JD, Pierson TC, Buck CB, Siliciano RF. Establishment of Latent HIV-1 Infection of Resting CD4+ T Lymphocytes Does Not Require Inactivation of Vpr. Virology. 2000 Dec 5;278(1):227–33.

66. Unutmaz D, KewalRamani VN, Marmon S, Littman DR. Cytokine Signals Are Sufficient for HIV-1 Infection of Resting Human T Lymphocytes. J Exp Med [Internet]. 1999 Jun 7 [cited 2023 Mar 1];189(11):1735–46. Available from: http://www.jem.org

67. Sahu GK, Lee K, Ji J, Braciale V, Baron S, Cloyd MW. A novel in vitro system to generate and study latently HIV-infected long-lived normal CD4+ T-lymphocytes. Virology. 2006 Nov 25;355(2):127–37.

68. Yang HC, Xing S, Shan L, O'Connell K, Dinoso J, Shen A, et al. Small-molecule screening using a human primary cell model of HIV latency identifies compounds that reverse latency without cellular activation. J Clin Invest [Internet]. 2009 Nov 11 [cited 2023 Mar 1];119(11):3473. Available from: /pmc/articles/PMC2769176/

69. Tyagi M, Pearson RJ, Karn J. Establishment of HIV Latency in Primary CD4 + Cells Is due to Epigenetic Transcriptional Silencing and P-TEFb Restriction . J Virol [Internet]. 2010 Jul [cited 2023 Mar 1];84(13):6425–37. Available from: https://journals.asm.org/doi/10.1128/JVI.01519-09

70. Tabler CO, Lucera MB, Haqqani AA, McDonald DJ, Migueles SA, Connors M, et al. CD4 + Memory Stem Cells Are Infected by HIV-1 in a Manner Regulated in Part by SAMHD1 Expression . J Virol [Internet]. 2014 May [cited 2023 Mar 1];88(9):4976–86. Available from: https://journals.asm.org/doi/10.1128/JVI.00324-14

71. Lugli E, Dominguez MH, Gattinoni L, Chattopadhyay PK, Bolton DL, Song K, et al. Superior T memory stem cell persistence supports long-lived T cell memory. J Clin Invest [Internet]. 2013 Feb 2 [cited 2023 Mar 1];123(2):594. Available from: /pmc/articles/PMC3561805/

72. Gattinoni L, Lugli E, Ji Y, Pos Z, Paulos CM, Quigley MF, et al. A human memory T cell subset with stem cell–like properties. Nat Med 2011 1710 [Internet]. 2011 Sep 18 [cited 2023 Mar 1];17(10):1290–7. Available from: https://www.nature.com/articles/nm.2446

73. Chiodi F, Institutet K, Teigler J, Velu V, Zaunders J, Phetsouphanh C, et al. hiV-1 and siV Predominantly Use ccr5 expressed on a Precursor Population to establish infection in T Follicular helper cells. 2017 [cited 2023 Mar 1];8:21. Available from: www.frontiersin.org

74. Perreau M, Savoye AL, De Crignis E, Jean-Marc Corpataux, Cubas R, Haddad EK, et al. Follicular helper T cells serve as the major CD4 T cell compartment for HIV-1 infection, replication, and production. J Exp Med [Internet]. 2013 Jan 1 [cited 2023 Mar 1];210(1):143. Available from: /pmc/articles/PMC3549706/

75. Clark IC, Mudvari P, Thaploo S, Smith S, Abu-Laban M, Hamouda M, et al. HIV silencing and cell survival signatures in infected T cell reservoirs. Nat 2023 6147947 [Internet]. 2023 Jan 4 [cited 2023 Mar 1];614(7947):318–25. Available from: https://www.nature.com/articles/s41586-022-05556-6

76. Wilson EB, Brooks DG. The role of IL-10 in regulating immunity to persistent viral infections.

77. Coiras M, Bermejo M, Descours B, Mateos E, García-Pérez J, López-Huertas M-R, et al.

IL-7 Induces SAMHD1 Phosphorylation in CD4+ T Lymphocytes, Improving Early Steps of HIV-1 Life Cycle HHS Public Access. Cell Rep [Internet]. 2016 [cited 2023 Mar 1];14(9):2100–7. Available from: http://dx.doi.org/10.1016/j.celrep.2016.02.022.

78. Wykes MN, Lewin SR. Immune checkpoint blockade in infectious diseases. Nat Rev Immunol 2017 182 [Internet]. 2017 Oct 9 [cited 2023 Mar 1];18(2):91–104. Available from: https://www.nature.com/articles/nri.2017.112

79. Fromentin R, Bakeman W, Lawani MB, Khoury G, Hartogensis W, DaFonseca S, et al. CD4+ T Cells Expressing PD-1, TIGIT and LAG-3 Contribute to HIV Persistence during ART. PLOS Pathog [Internet]. 2016 Jul 1 [cited 2023 Mar 1];12(7):e1005761. Available from:
https://journals.plos.org/plospathogens/article?id=10.1371/journal.ppat.1005761

80. Bruel T, Schwartz O. Markers of the HIV-1 reservoir: Facts and controversies. Curr Opin HIV AIDS [Internet]. 2018 Sep 1 [cited 2023 Mar 1];13(5):383–8. Available from: https://journals.lww.com/co-hivandaids/Fulltext/2018/09000/Markers_of_the_HIV_1_reservoir__facts_and.3.aspx

81. Hogan LE, Vasquez J, Hobbs KS, Hanhauser E, Aguilar-Rodriguez B, Hussien R, et al. Increased HIV-1 transcriptional activity and infectious burden in peripheral blood and gut-associated CD4+ T cells expressing CD30. PLOS Pathog [Internet]. 2018 Feb 1 [cited 2023 Mar 1];14(2):e1006856. Available from: https://journals.plos.org/plospathogens/article?id=10.1371/journal.ppat.1006856

82. Descours B, Petitjean G, López-Zaragoza JL, Bruel T, Raffel R, Psomas C, et al. CD32a is a marker of a CD4 T-cell HIV reservoir harbouring replication-competent proviruses. Nat 2017 5437646 [Internet]. 2017 Mar 15 [cited 2023 Mar 1];543(7646):564–7. Available from: https://www.nature.com/articles/nature21710

83. Iglesias-Ussel M, Vandergeeten C, Marchionni L, Chomont N, Romerio F. High Levels of CD2 Expression Identify HIV-1 Latently Infected Resting Memory CD4 + T Cells in Virally Suppressed Subjects . J Virol [Internet]. 2013 Aug 15 [cited 2023 Mar 1];87(16):9148–58. Available from: https://journals.asm.org/doi/10.1128/JVI.01297-13

84. Khoury G, Anderson JL, Fromentin R, Hartogensis W, Smith MZ, Bacchetti P, et al. Persistence of integrated HIV DNA in CXCR3+CCR6+ memory CD4+ T-cells in HIV-infected individuals on antiretroviral therapy.

85. Swingler S, Mann AM, Zhou J, Swingler C, Stevenson M. Apoptotic Killing of HIV-1–Infected Macrophages Is Subverted by the Viral Envelope Glycoprotein. PLOS Pathog [Internet]. 2007 Sep [cited 2023 Mar 1];3(9):e134. Available from: https://journals.plos.org/plospathogens/article?id=10.1371/journal.ppat.0030134

86. Gavegnano C, Schinazi RF. Antiretroviral therapy in macrophages: implication for HIV eradication.

87. Dupont M, Sattentau QJ. Macrophage Cell-Cell Interactions Promoting HIV-1 Infection. Viruses [Internet]. 2020 May 1 [cited 2023 Mar 1];12(5). Available from: https://pubmed.ncbi.nlm.nih.gov/32354203/

88. Mzingwane ML, Tiemessen CT. Mechanisms of HIV persistence in HIV reservoirs. Rev Med Virol [Internet]. 2017 Mar 1 [cited 2023 Mar 1];27(2):e1924. Available from: https://onlinelibrary.wiley.com/doi/full/10.1002/rmv.1924

89. Wallet C, De Rovere M, Van Assche J, Daouad F, De Wit S, Gautier V, et al. Microglial

Cells: The Main HIV-1 Reservoir in the Brain. Front Cell Infect Microbiol. 2019;9(October):1–18.

90. Okulicz JF, Marconi VC, Landrum ML, Wegner S, Weintrob A, Ganesan A, et al. Clinical Outcomes of Elite Controllers, Viremic Controllers, and Long-Term Nonprogressors in the US Department of Defense HIV Natural History Study. J Infect Dis [Internet]. 2009 Dec 1 [cited 2023 Mar 1];200(11):1714–23. Available from: https://academic.oup.com/jid/article/200/11/1714/832898

91. Okulicz JF, Lambotte O. Epidemiology and clinical characteristics of elite controllers. Curr Opin HIV AIDS [Internet]. 2011 May [cited 2023 Mar 1];6(3):163–8. Available from: https://journals.lww.com/co-hivandaids/Fulltext/2011/05000/Epidemiology_and_clinical_characteristics_of_elite.5.aspx

92. Blankson JN. Effector mechanisms in HIV-1 infected Elite Controllers: Highly Active Immune Responses?

93. Dalmau J, Puertas MC, Azuara M, Mariño A, Frahm N, Mothe B, et al. Contribution of immunological and virological factors to extremely severe primary HIV-1 infection. Clin Infect Dis [Internet]. 2009 Jan 1 [cited 2023 Mar 1];48(2):229. Available from: /pmc/articles/PMC2806184/

94. Gonzalo-Gil E, Ikediobi U, Sutton RE. Focus: Infectious Diseases: Mechanisms of Virologic Control and Clinical Characteristics of HIV+ Elite/Viremic Controllers. Yale J Biol Med [Internet]. 2017 Jun 1 [cited 2023 Mar 1];90(2):245. Available from: /pmc/articles/PMC5482301/

95. Laskey SB, Siliciano RF. A mechanistic theory to explain the efficacy of antiretroviral therapy. Nat Rev Microbiol 2014 1211 [Internet]. 2014 Sep 29 [cited 2023 Mar 1];12(11):772–80. Available from: https://www.nature.com/articles/nrmicro3351

96. Khan MA, Gupta KK, Singh SK. A Review on Pharmacokinetics Properties of Antiretroviral Drugs to Treat HIV-1 Infections. Curr Comput Aided Drug Des. 2020 Oct 7;17(7):850–64.

97. Shiau S, Kuhn L. Antiretroviral treatment in HIV-infected infants and young children: novel issues raised by the Mississippi baby. Expert Rev Anti Infect Ther [Internet]. 2014 Mar [cited 2023 Mar 1];12(3):307. Available from: /pmc/articles/PMC5389381/

98. Leite TF, Delatorre E, Côrtes FH, Ferreira ACG, Cardoso SW, Grinsztejn B, et al. Reduction of HIV-1 reservoir size and diversity after 1 year of cART among Brazilian individuals starting treatment during early stages of acute infection. Front Microbiol [Internet]. 2019 [cited 2023 Mar 1];10(FEB). Available from: /pmc/articles/PMC6378917/

99. Poluri A, Van Maanen M, Sutton RE. Genetic therapy for HIV/AIDS. http://dx.doi.org/101517/1471259836951 [Internet]. 2005 Sep [cited 2023 Mar 1];3(6):951–63. Available from: https://www.tandfonline.com/doi/abs/10.1517/14712598.3.6.951

100. Qin XF, An DS, Chen ISY, Baltimore D. Inhibiting HIV-1 infection in human T cells by lentiviral-mediated delivery of small interfering RNA against CCR5. Proc Natl Acad Sci U S A [Internet]. 2003 Jan 7 [cited 2023 Mar 1];100(1):183–8. Available from: https://www.pnas.org/doi/abs/10.1073/pnas.232688199

101. Veres G, Escaich S, Baker J, Barske C, Kalfoglou C, Ilves H, et al. Intracellular expression of RNA transcripts complementary to the human immunodeficiency virus type 1 gag gene inhibits viral replication in human CD4+ lymphocytes. J Virol [Internet]. 1996 Dec [cited 2023 Mar 1];70(12):8792–800. Available from: https://journals.asm.org/doi/10.1128/jvi.70.12.8792-8800.1996

102. Rossi C, Balboni PG, Betti M, Marconi PC, Bozzini R, Grossi MP, et al. Inhibition of HIV-1 replication by a Tat transdominant negative mutant in human peripheral blood lymphocytes from healthy donors and HIV-1-infected patients. Gene Ther 1997 411 [Internet]. 1997 [cited 2023 Mar 1];4(11):1261–9. Available from: https://www.nature.com/articles/3300522

103. Li Y, Starr SE, Lisziewicz J, Ho WZ. Inhibition of HIV-1 replication in chronically infected cell lines and peripheral blood mononuclear cells by retrovirus-mediated antitat gene transfer. Gene Ther 2000 74 [Internet]. 2000 Feb 17 [cited 2023 Mar 1];7(4):321–8. Available from: https://www.nature.com/articles/3301088

104. Harrison GS, Long CJ, Curiel TJ, Maxwell F, Maxwell IH. Inhibition of Human Immunodeficiency Virus-1 Production Resulting from Transduction with a Retrovirus Containing an HIV-Regulated Diphtheria Toxin A Chain Gene. https://home.liebertpub.com/hum [Internet]. 2008 Jun 13 [cited 2023 Mar 1];3(5):461–9. Available from: https://www.liebertpub.com/doi/10.1089/hum.1992.3.5-461

105. Rondon IJ, Marasco WA. INTRACELLULAR ANTIBODIES (INTRABODIES) FOR GENE THERAPY OF INFECTIOUS DISEASES. https://doi.org/101146/annurev.micro511257 [Internet]. 2003 Nov 28 [cited 2023 Mar 1];51:257–83. Available from: https://www.annualreviews.org/doi/abs/10.1146/annurev.micro.51.1.257

106. Yang ANG, Bai X, Huang XF, Yao C, Chen SY. Phenotypic knockout of HIV type 1 chemokine coreceptor CCR-5 by intrakines as potential therapeutic approach for HIV-1 infection. Proc Natl Acad Sci U S A [Internet]. 1997 Oct 10 [cited 2023 Mar 1];94(21):11567. Available from: /pmc/articles/PMC23540/

107. Sutton RE, Wu HTM, Rigg R, Böhnlein E, Brown PO. Human Immunodeficiency Virus Type 1 Vectors Efficiently Transduce Human Hematopoietic Stem Cells. J Virol [Internet]. 1998 Jul [cited 2023 Mar 1];72(7):5781–8. Available from: https://journals.asm.org/doi/10.1128/JVI.72.7.5781-5788.1998

108. Gansbacher B. Report of a second serious adverse event in a clinical trial of gene therapy for X-linked severe combined immune deficiency (X-SCID). J Gene Med [Internet]. 2003 Mar 1 [cited 2023 Mar 1];5(3):261–2. Available from: https://onlinelibrary.wiley.com/doi/full/10.1002/jgm.390

109. Gupta RK, Abdul-Jawad S, McCoy LE, Mok HP, Peppa D, Salgado M, et al. HIV-1 remission following CCR5Δ32/Δ32 haematopoietic stem-cell transplantation. Nat 2019 5687751 [Internet]. 2019 Mar 5 [cited 2023 Mar 1];568(7751):244–8. Available from: https://www.nature.com/articles/s41586-019-1027-4

110. Ding J, Liu Y, Lai Y. Knowledge From London and Berlin: Finding Threads to a Functional HIV Cure. Front Immunol. 2021 May 27;12:1852.

111. Grau-Expósito J, Luque-Ballesteros L, Navarro J, Curran A, Burgos J, Ribera E, et al. Latency reversal agents affect differently the latent reservoir present in distinct CD4+ T subpopulations. PLoS Pathog [Internet]. 2019 Aug 19 [cited 2023 Mar 1];15(8). Available from: https://pubmed.ncbi.nlm.nih.gov/31425551/

112. Kim Y, Anderson JL, Lewin SR. Getting the "kill" into "shock and kill": strategies to eliminate latent HIV. Cell Host Microbe [Internet]. 2018 Jan 1 [cited 2023 Mar 1];23(1):14. Available from: /pmc/articles/PMC5990418/

113. Søgaard OS, Graversen ME, Leth S, Olesen R, Brinkmann CR, Nissen SK, et al. The Depsipeptide Romidepsin Reverses HIV-1 Latency In Vivo. PLOS Pathog [Internet]. 2015 [cited 2023 Mar 1];11(9):e1005142. Available from: https://journals.plos.org/plospathogens/article?id=10.1371/journal.ppat.1005142

114. Li JH, Ma J, Kang W, Wang CF, Bai F, Zhao K, et al. The histone deacetylase inhibitor chidamide induces intermittent viraemia in HIV-infected patients on suppressive antiretroviral therapy. HIV Med [Internet]. 2020 Dec 1 [cited 2023 Mar 1];21(11):747–57. Available from: https://onlinelibrary.wiley.com/doi/full/10.1111/hiv.13027

115. Leth S, Schleimann MH, Nissen SK, Højen JF, Olesen R, Graversen ME, et al. Combined effect of Vacc-4x, recombinant human granulocyte macrophage colony-stimulating factor vaccination, and romidepsin on the HIV-1 reservoir (REDUC): a single-arm, phase 1B/2A trial. Lancet HIV [Internet]. 2016 Oct 1 [cited 2023 Mar 1];3(10):e463–72. Available from: http://www.thelancet.com/article/S2352301816300558/fulltext

116. Fidler S, Stöhr W, Pace M, Dorrell L, Lever A, Pett S, et al. Antiretroviral therapy alone versus antiretroviral therapy with a kick and kill approach, on measures of the HIV reservoir in participants with recent HIV infection (the RIVER trial): a phase 2, randomised trial. Lancet [Internet]. 2020 Mar 14 [cited 2023 Mar 1];395(10227):888–98. Available from: http://www.thelancet.com/article/S0140673619329903/fulltext

117. Moltó J, Rosás-Umbert M, Miranda C, Manzardo C, Puertas MC, Ruiz-Riol M, et al. Pharmacokinetic/pharmacodynamic analysis of romidepsin used as an HIV latency reversing agent. J Antimicrob Chemother [Internet]. 2021 Mar 12 [cited 2023 Mar 1];76(4):1032–40. Available from: https://academic.oup.com/jac/article/76/4/1032/6046149

118. Rosás-Umbert M, Ruiz-Riol M, Fernández MA, Marszalek M, Coll P, Manzardo C, et al. In vivo Effects of Romidepsin on T-Cell Activation, Apoptosis and Function in the BCN02 HIV-1 Kick&Kill Clinical Trial. Front Immunol. 2020;11(March):1–11.

119. Deeks SG. Shock and kill. Nat 2012 4877408 [Internet]. 2012 Jul 25 [cited 2023 Mar 1];487(7408):439–40. Available from: https://www.nature.com/articles/487439a

120. Zimmermann CA, Hoffmann A, Raabe F, Spengler D. Role of Mecp2 in Experience-Dependent Epigenetic Programming. Genes (Basel) [Internet]. 2015 Mar 6 [cited 2023 Mar 1];6(1):60. Available from: /pmc/articles/PMC4377834/

121. Ahlenstiel CL, Symonds G, Kent SJ, Kelleher AD. Block and Lock HIV Cure Strategies to Control the Latent Reservoir. Front Cell Infect Microbiol [Internet]. 2020 Aug 14 [cited 2023 Mar 1];10:424. Available from: /pmc/articles/PMC7457024/

122. Suzuki K, Shijuuku T, Fukamachi T, Zaunders J, Guillemin G, Cooper D, et al. Prolonged transcriptional silencing and CpG methylation induced by siRNAs targeted to the HIV-1 promoter region. J RNAi Gene Silencing [Internet]. 2005 Oct 11 [cited 2023 Mar 1];1(2):66. Available from: /pmc/articles/PMC2737205/

123. Moranguinho I, Valente ST. Block-And-Lock: New Horizons for a Cure for HIV-1. Viruses 2020, Vol 12, Page 1443 [Internet]. 2020 Dec 15 [cited 2023 Mar 1];12(12):1443. Available from: https://www.mdpi.com/1999-4915/12/12/1443/htm

124. León A, Gallart T. Therapeutic vaccines against HIV infection. 2012 [cited 2023 Mar 1]; Available from: http://dx.doi.org/10.4161/hv.19555

125. Ross AL, Bråve A, Scarlatti G, Manrique A, Buonaguro L. Progress towards development of an HIV vaccine: report of the AIDS Vaccine 2009 Conference. Lancet Infect Dis [Internet]. 2010 May 1 [cited 2023 Mar 1];10(5):305–16. Available from: http://www.thelancet.com/article/S1473309910700694/fulltext

126. T-cell responses induced in normal volunteers immunized with... : AIDS [Internet]. [cited 2023 Mar 1]. Available from: https://journals.lww.com/aidsonline/Fulltext/2002/11080/T_cell_responses_induced_in_normal_volunteers.5.aspx

127. Bailón L, Llano A, Cedeño S, Escribà T, Rosás-Umbert M, Parera M, et al. Safety, immunogenicity and effect on viral rebound of HTI vaccines in early treated HIV-1 infection: a randomized, placebo-controlled phase 1 trial. Nat Med 2022 2812 [Internet]. 2022 Oct 27 [cited 2023 Mar 1];28(12):2611–21. Available from: https://www.nature.com/articles/s41591-022-02060-2

128. Barin F, Braibant M. HIV-1 antibodies in prevention of transmission. Curr Opin HIV AIDS [Internet]. 2019 Jul 1 [cited 2023 Mar 1];14(4):273–8. Available from: https://journals.lww.com/co-hivandaids/Fulltext/2019/07000/HIV_1_antibodies_in_prevention_of_transmission.7.aspx

129. Julg B, Barouch D. Broadly neutralizing antibodies for HIV-1 prevention and therapy. Semin Immunol. 2021 Jan 1;51:101475.

130. Barouch DH, Whitney JB, Moldt B, Klein F, Oliveira TY, Liu J, et al. Therapeutic efficacy of potent neutralizing HIV-1-specific monoclonal antibodies in SHIV-infected rhesus monkeys. Nat 2013 5037475 [Internet]. 2013 Oct 30 [cited 2023 Mar 1];503(7475):224–8. Available from: https://www.nature.com/articles/nature12744

131. Hessell AJ, Jaworski JP, Epson E, Matsuda K, Pandey S, Kahl C, et al. Early short-term treatment with neutralizing human monoclonal antibodies halts SHIV infection in newborn macaques. Nat Med [Internet]. 2016 Apr 1 [cited 2023 Mar 1];22(4):362. Available from: /pmc/articles/PMC4983100/

132. Mendoza P, Gruell H, Nogueira L, Pai JA, Butler AL, Millard K, et al. Combination therapy with anti-HIV-1 antibodies maintains viral suppression. Nat 2018 5617724 [Internet]. 2018 Sep 26 [cited 2023 Mar 1];561(7724):479–84. Available from: https://www.nature.com/articles/s41586-018-0531-2

133. Kuhlmann AS, Peterson CW, Kiem HP. Chimeric antigen receptor T-cell approaches to HIV cure. Curr Opin HIV AIDS [Internet]. 2018 Sep 1 [cited 2023 Mar 1];13(5):446–53. Available from: https://journals.lww.com/co-hivandaids/Fulltext/2018/09000/Chimeric_antigen_receptor_T_cell_approaches_to_HIV.12.aspx

134. Mao Y, Zhao C, Zheng P, Zhang X, Xu J. Current status and future development of anti-HIV chimeric antigen receptor T-cell therapy. https://doi.org/102217/imt-2020-0199 [Internet]. 2020 Nov 23 [cited 2023 Mar 1];13(2):177–84. Available from: https://www.futuremedicine.com/doi/10.2217/imt-2020-0199

135. Mitsuyasu RT, Anton PA, Deeks SG, Scadden DT, Connick E, Downs MT, et al. Prolonged survival and tissue trafficking following adoptive transfer of CD4ζ gene-modified

autologous CD4+ and CD8+ T cells in human immunodeficiency virus–infected subjects. Blood. 2000 Aug 1;96(3):785–93.

136. Liu B, Zhang W, Xia B, Jing S, Du Y, Zou F, et al. Broadly neutralizing antibody–derived CAR T cells reduce viral reservoir in individuals infected with HIV-1. J Clin Invest [Internet]. 2021 Oct 10 [cited 2023 Mar 1];131(19). Available from: /pmc/articles/PMC8483761/

137. Qi J, Ding C, Jiang X, Gao Y. Advances in Developing CAR T-Cell Therapy for HIV Cure. Front Immunol [Internet]. 2020 Mar 10 [cited 2023 Mar 1];11:361. Available from: /pmc/articles/PMC7076163/

138. Côrtes FH, de Paula HHS, Bello G, Ribeiro-Alves M, de Azevedo SSD, Caetano DG, et al. Plasmatic levels of IL-18, IP-10, and activated CD8+ T cells are potential biomarkers to identify HIV-1 elite controllers with a true functional cure profile. Front Immunol [Internet]. 2018 Jul 11 [cited 2023 Mar 1];9(JUL):11. Available from: /pmc/articles/PMC6050358/

139. Phetsouphanh C, Aldridge D, Marchi E, Munier CML, Meyerowitz J, Murray L, et al. Maintenance of functional CD57+ cytolytic CD4+ T cells in HIV+ elite controllers. Front Immunol. 2019 Aug 8;10(AUG):1844.

140. [Elite controllers and the mechanisms behind spontaneous control of HIV] - PubMed [Internet]. [cited 2023 Mar 1]. Available from: https://pubmed.ncbi.nlm.nih.gov/24167935/

141. Abdel-Mohsen M, André R, Raposo S, Deng X, Li M, Liegler T, et al. Expression profile of host restriction factors in HIV-1 elite controllers. Retrovirology [Internet]. 2013 [cited 2023 Mar 1];10:1. Available from: http://www.retrovirology.com/content/10/1/106

142. Hurst J, Hoffmann M, Pace M, Williams JP, Thornhill J, Hamlyn E, et al. Immunological biomarkers predict HIV-1 viral rebound after treatment interruption. Nat Commun [Internet]. 2015;6:1–9. Available from: http://dx.doi.org/10.1038/ncomms9495

143. Aslam B, Basit M, Nisar MA, Khurshid M, Rasool MH. Proteomics: Technologies and Their Applications. J Chromatogr Sci [Internet]. 2017 Feb 1 [cited 2023 Mar 1];55(2):182–96. Available from: https://academic.oup.com/chromsci/article/55/2/182/2333796

144. Lindoso RS, Sandim V, Collino F, Carvalho AB, Dias J, da Costa MR, et al. Proteomics of cell–cell interactions in health and disease. Proteomics [Internet]. 2016 Jan 1 [cited 2023 Mar 1];16(2):328–44. Available from: https://onlinelibrary.wiley.com/doi/full/10.1002/pmic.201500341

145. Ruiz-Riol M, Berdnik D, Llano A, Mothe B, Gálvez C, Pérez-Álvarez S, et al. Identification of Interleukin-27 (IL-27)/IL-27 Receptor Subunit Alpha as a Critical Immune Axis for In Vivo HIV Control. J Virol [Internet]. 2017 Aug 8 [cited 2023 Mar 1];91(16):441–58. Available from: /pmc/articles/PMC5533920/

146. Oriol-Tordera B, Olvera A, Duran-Castells C, Llano A, Mothe B, Massanella M, et al. TL1A-DR3 Plasma Levels Are Predictive of HIV-1 Disease Control, and DR3 Costimulation Boosts HIV-1-Specific T Cell Responses. J Immunol [Internet]. 2020 Dec 15 [cited 2023 Mar 1];205(12):3348–57. Available from: https://pubmed.ncbi.nlm.nih.gov/33177161/

147. Robertson KR, Smurzynski M, Parsons TD, Wu K, Bosch RJ, Wu J, et al. The prevalence and incidence of neurocognitive impairment in the HAART era. AIDS [Internet]. 2007

Sep [cited 2023 Mar 1];21(14):1915–21. Available from: https://journals.lww.com/aidsonline/Fulltext/2007/09120/The_prevalence_and_incide nce_of_neurocognitive.11.aspx

148. Antinori A, Arendt G, Becker JT, Brew BJ, Byrd DA, Cherner M, et al. Updated research nosology for HIV-associated neurocognitive disorders. Neurology [Internet]. 2007 Oct 10 [cited 2023 Mar 1];69(18):1789. Available from: /pmc/articles/PMC4472366/

149. Norgren N, Rosengren L, Stigbrand T. Elevated neurofilament levels in neurological diseases. Brain Res. 2003 Oct 10;987(1):25–31.

150. Gisslén M, Price RW, Andreasson U, Norgren N, Nilsson S, Hagberg L, et al. Plasma Concentration of the Neurofilament Light Protein (NFL) is a Biomarker of CNS Injury in HIV Infection: A Cross-Sectional Study. EBioMedicine [Internet]. 2016 Jan 1 [cited 2023 Mar 1];3:135–40. Available from: http://www.thelancet.com/article/S235239641530219X/fulltext

151. Anderson AM, Easley KA, Kasher N, Franklin D, Heaton RK, Zetterberg H, et al. Neurofilament light chain in blood is negatively associated with neuropsychological performance in HIV-infected adults and declines with initiation of antiretroviral therapy. J Neurovirol [Internet]. 2018 Dec 1 [cited 2023 Mar 1];24(6):695–701. Available from: https://link.springer.com/article/10.1007/s13365-018-0664-y

152. Hategan A, Masliah E, Nath A. HIV and Alzheimer's Disease: Complex interactions of HIV-Tat with amyloid β peptide and Tau protein.

153. Zayyad Z, Spudich S. Neuropathogenesis of HIV: From Initial Neuroinvasion to HIV Associated Neurocognitive Disorder (HAND). Curr HIV/AIDS Rep [Internet]. 2015 Mar 22 [cited 2023 Mar 1];12(1):16. Available from: /pmc/articles/PMC4741099/

154. Hagberg L, Cinque P, Gisslen M, Brew BJ, Spudich S, Bestetti A, et al. Open Access REVIEW Cerebrospinal fluid neopterin: an informative biomarker of central nervous system immune activation in HIV-1 infection. AIDS Res Ther [Internet]. 2010 [cited 2023 Mar 1];7:15. Available from: http://www.aidsrestherapy.com/content/7/1/15

155. Prats A, Martínez-zalacaín I, Mothe B, Negredo E, Garolera M, Domènech-puigcerver S, et al. Central Nervous System (CNS) Effects of Therapy Initiation with Integrase Inhibitors. :439.

156. Mothe B, Rosás-Umbert M, Coll P, Manzardo C, Puertas MC, Morón-López S, et al. HIVconsv Vaccines and Romidepsin in Early-Treated HIV-1-Infected Individuals: Safety, Immunogenicity and Effect on the Viral Reservoir (Study BCN02). Front Immunol. 2020;11(May):1–15.

157. Ray S, Britschgi M, Herbert C, Takeda-Uchimura Y, Boxer A, Blennow K, et al. Classification and prediction of clinical Alzheimer's diagnosis based on plasma signaling proteins. Nat Med. 2007;13(11):1359–62.

158. Borjabad A, Morgello S, Chao W, Kim SY, Brooks AI, Murray J, et al. Significant effects of antiretroviral therapy on global gene expression in brain tissues of patients with hiv-1-associated neurocognitive disorders. PLoS Pathog. 2011;7(9).

159. Oriol-Tordera B, Esteve-Codina A, Berdasco M, Rosás-Umbert M, Gonçalves E, Duran-Castells C, et al. Epigenetic landscape in the kick-and-kill therapeutic vaccine BCN02 clinical trial is associated with antiretroviral treatment interruption (ATI) outcome. eBioMedicine. 2022;78:1–19.

160. Martínez-Bonet M, Puertas MC, Fortuny C, Ouchi D, Mellado MJ, Rojo P, et al. Establishment and Replenishment of the Viral Reservoir in Perinatally HIV-1-infected Children Initiating Very Early Antiretroviral Therapy. Clin Infect Dis. 2015;61(7):1169–78.

161. Gallastegui E, Millan-Zambrano G, Terme J-M, Chavez S, Jordan A. Chromatin Reassembly Factors Are Involved in Transcriptional Interference Promoting HIV Latency. J Virol. 2011;85(7):3187–202.

162. Jordan A, Bisgrove D, Verdin E. J Lat 10-6-HIV-repsoducibly establishes a latent infection after acute infection of T cells in vitro-cdg188. 2003;22(8).

163. Groves KC, Bibby DF, Clark DA. Europe PMC Funders Group Disease Progression in HIV-1 – Infected Viremic Controllers. 2013;61(4):407–16.

164. Dahl V, Peterson J, Spudich S, Lee E, Shacklett BL, Price RW, et al. Single-Copy Assay Quantification of HIV-1 RNA in Paired Cerebrospinal Fluid and Plasma Samples from Elite Controllers. AIDS [Internet]. 2013;27(7):1145–9. Available from: http://journals.lww.com/aidsonline/Abstract/2013/04240/

165. Gebara NY, El Kamari V, Rizk N. HIV-1 elite controllers: An immunovirological review and clinical perspectives. J Virus Erad. 2019;2019(5.3):e10–3.

166. Woldemeskel BA, Kwaa AK, Blankson JN. Viral reservoirs in elite controllers of HIV-1 infection: Implications for HIV cure strategies. EBioMedicine [Internet]. 2020;62:103118. Available from: https://doi.org/10.1016/j.ebiom.2020.103118

167. Garay E, Patiño-López G, Islas S, Alarcón L, Canche-Pool E, Valle-Rios R, et al. CRTAM: A molecule involved in epithelial cell adhesion. J Cell Biochem. 2010;111(1):111–22.

168. Zhang D, Shankar P, Xu Z, Harnisch B, Chen G, Lange C, et al. Most antiviral CD8 T cells during chronic viral infection do not express high levels of perforin and are not directly cytotoxic. Blood. 2003;101(1):226–35.

169. Andersson J, Behbahani H, Lieberman J, Connick E, Landay A, Patterson B, et al. Perforin is not co-expressed with granzyme A within cytotoxic granules in CD8 T lymphocytes present in lymphoid tissue during chronic HIV infection. Aids. 1999;13(11):1295–303.

170. Herzog S, Fragkou PC, Arneth BM, Mkhlof S, Skevaki C. Myeloid CD169/Siglec1: An immunoregulatory biomarker in viral disease. Front Med. 2022;9(September):1–9.

171. Williams ME, Stein DJ, Joska JA, Naudé PJW. Cerebrospinal fluid immune markers and HIV-associated neurocognitive impairments: A systematic review. J Neuroimmunol [Internet]. 2021 Sep 15 [cited 2022 Aug 22];358. Available from: http://www.jni-journal.com/article/S0165572821001764/fulltext

172. Dahl V, Peterson J, Spudich S, Lee E, Shacklett BL, Price RW, et al. Single-copy assay quantification of HIV-1 RNA in paired cerebrospinal fluid and plasma samples from elite controllers. Aids. 2013;27(7):1145–9.

173. de Oliveira RM, Vicente Miranda H, Francelle L, Pinho R, Szegö ÉM, Martinho R, et al. The mechanism of sirtuin 2–mediated exacerbation of alpha-synuclein toxicity in models of Parkinson disease. PLoS Biol. 2017;15(3):1–27.

174. Islas-Hernandez A, Aguilar-Talamantes HS, Bertado-Cortes B, De Jesus Mejia-Delcastillo G, Carrera-Pineda R, Cuevas-Garcia CF, et al. BDNF and Tau as biomarkers of severity in multiple sclerosis. Biomark Med. 2018;12(7):717–26.

175. Harting K, Knöll B. SIRT2-mediated protein deacetylation: An emerging key regulator in brain physiology and pathology. Eur J Cell Biol. 2010;89(2–3):262–9.

176. Yilmaz A, Blennow K, Hagberg L, Nilsson S, Price RW, Schouten J, et al. Neurofilament light chain protein as a marker of neuronal injury: review of its use in HIV-1 infection and reference values for HIV-negative controls. Expert Rev Mol Diagn [Internet]. 2017;17(8):761–70. Available from: https://doi.org/10.1080/14737159.2017.1341313

177. Oliveira MF, Chaillon A, Nakazawa M, Vargas M, Letendre SL, Strain MC, et al. Early Antiretroviral Therapy Is Associated with Lower HIV DNA Molecular Diversity and Lower Inflammation in Cerebrospinal Fluid but Does Not Prevent the Establishment of Compartmentalized HIV DNA Populations. PLoS Pathog. 2017;13(1).

178. Burbelo PD, Price RW, Hagberg L, Hatano H, Spudich S, Deeks SG, et al. Anti-Human Immunodeficiency Virus Antibodies in the Cerebrospinal Fluid: Evidence of Early Treatment Impact on Central Nervous System Reservoir? J Infect Dis. 2018;217(7):1024–32.

179. Hellmuth J, Slike BM, Sacdalan C, Best J, Kroon E, Phanuphak N, et al. Very Early Initiation of Antiretroviral Therapy During Acute HIV Infection Is Associated With Normalized Levels of Immune Activation Markers in Cerebrospinal Fluid but Not in Plasma. J Infect Dis. 2019;220(12):1885–91.

180. Gisslén M, Hunt PW. Antiretroviral Treatment of Acute HIV Infection Normalizes Levels of Cerebrospinal Fluid Markers of Central Nervous System (CNS) Inflammation: A Consequence of a Reduced CNS Reservoir? J Infect Dis. 2019;220(12):1867–9.

181. Spires-Jones TL, Fox LM, Rozkalne A, Pitstick R, Carlson GA, Kazantsev AG. Inhibition of sirtuin 2 with sulfobenzoic acid derivative AK1 is non-toxic and potentially neuroprotective in a mouse model of frontotemporal dementia. Front Pharmacol. 2012;3 MAR(March):1–7.

182. Outeiro TF, Kontopoulos E, Altmann SM, Kufareva I, Strathearn KE, Amore AM, et al. Sirtuin 2 inhibitors rescue α-synuclein-mediated toxicity in models of Parkinson's disease. Science (80-). 2007;317(5837):516–9.

183. Balzarini J, Van Herrewege Y, Vanham G. Metabolic activation of nucleoside and nucleotide reverse transcriptase inhibitors in dendritic and Langerhans cells. Aids. 2002;16(16):2159–63.

184. Castellano P, Prevedel L, Eugenin EA. HIV-infected macrophages and microglia that survive acute infection become viral reservoirs by a mechanism involving Bim. Sci Rep [Internet]. 2017;7(1):1–16. Available from: http://dx.doi.org/10.1038/s41598-017-12758-w

185. Aamodt WW, Waligorska T, Shen J, Tropea TF, Siderowf A, Weintraub D, et al. Neurofilament Light Chain as a Biomarker for Cognitive Decline in Parkinson Disease. Mov Disord. 2021;36(12):2945–50.

186. Ning L, Wang B. Neurofilament light chain in blood as a diagnostic and predictive biomarker for multiple sclerosis: A systematic review and meta-analysis. Sipilä JOT, editor. PLoS One [Internet]. 2022 Sep 14 [cited 2022 Sep 26];17(9):e0274565. Available from: https://dx.plos.org/10.1371/journal.pone.0274565

187. Perelson AS, Essunger P, Cao Y, Vesanen M, Hurley A, Saksela K, et al. Decay characteristics of HIV-1-infected compartments during combination therapy. Vol. 387,

Nature. 1997. p. 188–91.

188. Broder S. The development of antiretroviral therapy and its impact on the HIV-1/AIDS pandemic. Antiviral Res. 2010;85(1):1–18.

189. Chun TW, Finzi D, Margolick J, Chadwick K, Schwartz D, Siliciano RF. In vivo fate of HIV-1-infected T cells: Quantitative analysis of the transition to stable latency. Nat Med. 1995;1(12):1284–90.

190. Battivelli E, Dahabieh MS, Abdel-Mohsen M, Peter Svensson J, da Silva IT, Cohn LB, et al. Chromatin Functional States Correlate with HIV Latency Reversal in Infected Primary CD4^{+} T cells. bioRxiv. 2018;1–22.

191. Rasmussen TA, Tolstrup M, Brinkmann CR, Olesen R, Erikstrup C, Solomon A, et al. Panobinostat, a histone deacetylase inhibitor, for latent virus reactivation in HIV-infected patients on suppressive antiretroviral therapy: A phase 1/2, single group, clinical trial. Lancet HIV. 2014;1(1):e13–21.

192. Cockerham LR, Hatano H. Elite control of HIV: Is this the right model for a functional cure? Trends Microbiol [Internet]. 2015;23(2):71–5. Available from: http://dx.doi.org/10.1016/j.tim.2014.11.003

193. Berger CT, Alter G. Natural killer cells in spontaneous control of HIV infection. Curr Opin HIV AIDS. 2011;6(3):208–13.

194. Tobieson L, Zetterberg H, Blennow K, Marklund N. Extracellular fluid, cerebrospinal fluid and plasma biomarkers of axonal and neuronal injury following intracerebral hemorrhage. Sci Rep [Internet]. 2021;11(1):1–10. Available from: https://doi.org/10.1038/s41598-021-96364-x

195. Moulignier A, Lescure FX, Savatovsky J, Campa P. CD8 transverse myelitis in a patient with HIV-1 infection. BMJ Case Rep. 2014;2013–5.

196. Lucas SB, Wong KT, Nightingale S, Miller RF. HIV-Associated CD8 Encephalitis: A UK Case Series and Review of Histopathologically Confirmed Cases. Front Neurol. 2021;12(April):1–20.

197. Koper OM, Kaminska J, Sawicki K, Kemona H. CXCL9, CXCL10, CXCL11, and their receptor (CXCR3) in neuroinflammation and neurodegeneration. Adv Clin Exp Med. 2018;27(6):849–56.

198. Kadry H, Noorani B, Cucullo L. A blood–brain barrier overview on structure, function, impairment, and biomarkers of integrity. Fluids Barriers CNS [Internet]. 2020;17(1):1–24. Available from: https://doi.org/10.1186/s12987-020-00230-3

199. Patiño-Lopez G, Hevezi P, Lee J, Willhite D, Verge GM, Lechner SM, et al. Human class-I restricted T cell associated molecule is highly expressed in the cerebellum and is a marker for activated NKT and CD8+ T lymphocytes. J Neuroimmunol. 2006;171(1–2):145–55.

200. Takeuchi A, El M, Gadelhaq S, Miyauchi K, Ishihara C, Onishi R, et al. CRT AM determines the CD4 + cytotoxic T lymphocyte lineage. 2016;123–38.

201. Passos DF, Bremm JM, da Silveira LL, Jantsch MH, da Silva JLG, Disconzi E, et al. CD4/CD8 ratio, comorbidities, and aging in treated HIV infected individuals on viral suppression. J Med Virol. 2020;92(12):3254–64.

202. Jespersen S, Pedersen KK, Anesten B, Zetterberg H, Fuchs D, Gisslén M, et al. Soluble

CD14 in cerebrospinal fluid is associated with markers of inflammation and axonal damage in untreated HIV-infected patients: A retrospective cross-sectional study. BMC Infect Dis [Internet]. 2016;16(1):1–8. Available from: http://dx.doi.org/10.1186/s12879-016-1510-6

203.   Lerkvaleekul B, Veldkamp SR, Van Der Wal MM, Schatorj EJH, Kamphuis SSM, Van Den Berg JM, et al. Siglec-1 expression on monocytes is associated with the interferon signature in juvenile dermatomyositis and can predict treatment response. Rheumatol (United Kingdom). 2022;61(5):2144–55.

204.   Perry VH, Crocker PR, Gordon S. The blood-brain barrier regulates the expression of a macrophage sialic acid-binding receptor on microglia. J Cell Sci. 1992;101(1):201–7.

205.   Siddiqui SS, Matar R, Merheb M, Hodeify R, Vazhappilly CG, Marton J, et al. Siglecs in brain function and neurological disorders. Cells. 2019;8(10).

206.   Sharma V, Bryant C, Montero M, Creegan M, Slike B, Krebs SJ, et al. Monocyte and CD4+ T-cell antiviral and innate responses associated with HIV-1 inflammation and cognitive impairment. AIDS. 2020;34(9):1289–301.

207.   Sperk M, Zhang W, Nowak P, Neogi U. Plasma soluble factor following two decades prolonged suppressive antiretroviral therapy in HIV-1-positive males. Med (United States). 2018;97(5):1–7.

208.   McArthur JC, Steiner J, Sacktor N, Nath A. Human immunodeficiency virus-associated neurocognitive disorders mind the gap. Ann Neurol. 2010;67(6):699–714.

209.   Rosenthal J, Tyor W. Aging, comorbidities, and the importance of finding biomarkers for HIV-associated neurocognitive disorders. J Neurovirol. 2019;25(5):673–85.

210.   Mothe B, Ibarrondo J, Llano A, Brander C. Virological, immune and host genetics markers in the control of HIV infection. Dis Markers. 2009;27(3–4):106–20.

211.   Booiman T, Wit FW, Maurer I, De Francesco D, Sabin CA, Harskamp AM, et al. High cellular monocyte activation in people living with human immunodeficiency virus on combination antiretroviral therapy and lifestyle-matched controls is associated with greater inflammation in cerebrospinal fluid. Open Forum Infect Dis. 2017;4(3):1–11.

212.   Robertson J, Edén A, Nyström K, Hagberg L, Yilmaz A, Gostner JM, et al. Increased immune activation and signs of neuronal injury in HIV-negative people on preexposure prophylaxis. AIDS [Internet]. 2021 Nov 1 [cited 2022 Oct 20];35(13):2129–36. Available from: https://pubmed.ncbi.nlm.nih.gov/34115648/

213.   Canet G, Dias C, Gabelle A, Simonin Y, Gosselet F, Marchi N, et al. HIV neuroinfection and Alzheimer's disease: Similarities and potential links? Front Cell Neurosci. 2018;12(September):1–13.

214.   Vassilopoulos A, Fritz KS, Petersen DR, Gius D. The human sirtuin family: Evolutionary divergences and functions. Hum Genomics. 2011;5(5):485–96.

215.   Chen X, Lu W, Wu D. Sirtuin 2 (SIRT2): Confusing Roles in the Pathophysiology of Neurological Disorders. Front Neurosci. 2021;15(May):1–11.

216.   Wang Y, Yang J, Hong T, Chen X, Cui L. SIRT2: Controversy and multiple roles in disease and physiology. Ageing Res Rev [Internet]. 2019;55(April):100961. Available from: https://doi.org/10.1016/j.arr.2019.100961

217.   Esteves AR, Palma AM, Gomes R, Santos D, Silva DF, Cardoso SM. Acetylation as a major

determinant to microtubule-dependent autophagy: Relevance to Alzheimer's and Parkinson disease pathology. Biochim Biophys Acta - Mol Basis Dis [Internet]. 2019;1865(8):2008–23. Available from: https://doi.org/10.1016/j.bbadis.2018.11.014

218. Silva DF, Esteves AR, Oliveira CR, Cardoso SM. Mitochondrial Metabolism Power SIRT2-Dependent Deficient Traffic Causing Alzheimer's-Disease Related Pathology. Mol Neurobiol [Internet]. 2017;54(6):4021–40. Available from: http://dx.doi.org/10.1007/s12035-016-9951-x

219. Fernando KKM, Wijayasinghe YS. Sirtuins as Potential Therapeutic Targets for Mitigating Neuroinflammation Associated With Alzheimer's Disease. Front Cell Neurosci. 2021;15(September):1–15.

220. Liu Y, Zhang Y, Zhu K, Chi S, Wang C, Xie A. Emerging Role of Sirtuin 2 in Parkinson's Disease. Front Aging Neurosci. 2020;11(January):1–11.

221. Donmez G, Outeiro TF. SIRT1 and SIRT2: Emerging targets in neurodegeneration. EMBO Mol Med. 2013;5(3):344–52.

222. Yu HB, Jiang H, Cheng ST, Hu ZW, Ren JH, Chen J. AGK2, A SIRT2 inhibitor, inhibits hepatitis B virus replication in vitro and in vivo. Int J Med Sci. 2018;15(12):1356–64.

223. Kong F, Li Q, Zhang F, Li X, You H, Pan X, et al. Sirtuins as Potential Therapeutic Targets for Hepatitis B Virus Infection. Front Med. 2021;8(October):2–8.

224. Eskandarian HA, Impens F, Nahori MA, Soubigou G, Coppée JY, Cossart P, et al. A role for SIRT2-dependent histone H3K18 deacetylation in bacterial infection. Science (80-). 2013;341(6145).

225. Zandi S, Hedayati MA, Mohammadi E, Sheikhesmaeili F. Helicobacter pylori infection increases sirt2 gene expression in gastric epithelial cells of gastritis patients. Microb Pathog [Internet]. 2018;116(May 2017):120–3. Available from: https://doi.org/10.1016/j.micpath.2017.12.078

226. Ciarlo E, Heinonen T, Théroude C, Herderschee J, Mombelli M, Lugrin J, et al. Sirtuin 2 deficiency increases bacterial phagocytosis by macrophages and protects from chronic staphylococcal infection. Front Immunol. 2017;8(AUG):1–15.

227. Figarola-Centurión I, Escoto-Delgadillo M, González-Enríquez GV, Gutiérrez-Sevilla JE, Vázquez-Valls E, Torres-Mendoza BM. Sirtuins Modulation: A Promising Strategy for HIV-Associated Neurocognitive Impairments. Int J Mol Sci. 2022;23(2).

228. Jurkowska K, Szymańska B, Knysz B, Kuźniarski A, Piwowar A. Sirtuins as interesting players in the course of hiv infection and comorbidities. Cells. 2021;10(10):1–35.

229. Pagans S, Pedal A, North BJ, Kaehlcke K, Marshall BL, Dorr A, et al. SIRT1 regulates HIV transcription via Tat deacetylation. PLoS Biol. 2005;3(2):0210–20.

230. Hiatt J, Hultquist JF, McGregor MJ, Bouhaddou M, Leenay RT, Simons LM, et al. A functional map of HIV-host interactions in primary human T cells. Nat Commun. 2022;13(1):1–15.

231. Scutari R, Alteri C, Perno CF, Svicher V, Aquaro S. The role of HIV infection in neurologic injury. Brain Sci. 2017;7(4):10–8.

232. Ko A, Kang G, Hattler JB, Galadima HI, Zhang J, Li Q, et al. Macrophages but not Astrocytes Harbor HIV DNA in the Brains of HIV-1-Infected Aviremic Individuals on Suppressive Antiretroviral Therapy. J Neuroimmune Pharmacol. 2019;14(1):110–9.

233. Wang B, Zhang Y, Cao W, Wei X, Chen J, Ying W. SIRT2 Plays Significant Roles in Lipopolysaccharides-Induced Neuroinflammation and Brain Injury in Mice. Neurochem Res [Internet]. 2016;41(9):2490–500. Available from: http://dx.doi.org/10.1007/s11064-016-1981-2

234. Lee AS, Jung YJ, Kim D, Nguyen-Thanh T, Kang KP, Lee S, et al. SIRT2 ameliorates lipopolysaccharide-induced inflammation in macrophages. Biochem Biophys Res Commun [Internet]. 2014;450(4):1363–9. Available from: http://dx.doi.org/10.1016/j.bbrc.2014.06.135

235. Borgognone A, Noguera-Julian M, Oriol B, Noël-Romas L, Ruiz-Riol M, Guillén Y, et al. Gut Microbiome Signatures Linked to HIV-1 Reservoir Size and Viremia Control. bioRxiv [Internet]. 2021;2021.10.03.462590. Available from: http://biorxiv.org/content/early/2021/10/04/2021.10.03.462590.abstract

236. Munoz-Moreno JA, Carrillo-Molina S, Martinez-Zalacain I, Miranda C, Manzardo C, Coll P, et al. Preserved central nervous system functioning after use of romidepsin as a latency-reversing agent in an HIV cure strategy. AIDS [Internet]. 2022 Mar 1 [cited 2022 Aug 19];36(3):363–72. Available from: https://journals.lww.com/aidsonline/Fulltext/2022/03010/Preserved_central_nervous_system_functioning_after.5.aspx

237. Zeng H, Xu L, Zou Y, Wang S. Romidepsin and metformin nanomaterials delivery on streptozocin for the treatment of Alzheimer's disease in animal model. Biomed Pharmacother [Internet]. 2021;141(July):111864. Available from: https://doi.org/10.1016/j.biopha.2021.111864

238. Ash MK, Al-Harthi L, Schneider JR. HIV in the brain: Identifying viral reservoirs and addressing the challenges of an HIV cure. Vaccines. 2021;9(8).

239. Tseng KY, Danilova T, Domanskyi A, Saarma M, Lindahl M, Airavaara M. MANF is essential for neurite extension and neuronal migration in the developing cortex. eNeuro. 2017;4(5).

240. Eesmaa A, Yu LY, Göös H, Nõges K, Kovaleva V, Hellman M, et al. The cytoprotective protein MANF promotes neuronal survival independently from its role as a GRP78 cofactor. J Biol Chem [Internet]. 2021;296(22):100295. Available from: https://doi.org/10.1016/j.jbc.2021.100295

241. Björklund A, Rosenblad C, Winkler C, Kirik D. Studies on neuroprotective and regenerative effects of GDNF in a partial lesion model of Parkinson's disease. Neurobiol Dis. 1997;4(3–4):186–200.

242. Cintrón-Colón AF, Almeida-Alves G, Boynton AM, Spitsbergen JM. GDNF synthesis, signaling, and retrograde transport in motor neurons. Cell Tissue Res. 2020;382(1):47–56.

243. Kodidela S, Gerth K, Haque S, Gong Y, Ismael S, Singh A, et al. Extracellular Vesicles: A Possible Link between HIV and Alzheimer's Disease-Like Pathology in HIV Subjects? Cells. 2019;8(9).

244. Diaz-Ortiz ME, Seo Y, Posavi M, Cordon MC, Clark E, Jain N, et al. GPNMB confers risk for Parkinson's disease through interaction with α-synuclein. Science [Internet]. 2022 Aug 19 [cited 2022 Oct 18];377(6608). Available from: https://pubmed.ncbi.nlm.nih.gov/35981040/

245. De Scheerder MA, Van Hecke C, Zetterberg H, Fuchs D, De Langhe N, Rutsaert S, et al. Evaluating predictive markers for viral rebound and safety assessment in blood and lumbar fluid during HIV-1 treatment interruption. J Antimicrob Chemother. 2020;75(5):1311–20.

246. Gomes STM, Gomes ÉR, dos Santos MB, Lima SS, Queiroz MAF, Machado LFA, et al. Immunological and virological characterization of HIV-1 viremia controllers in the North Region of Brazil. BMC Infect Dis. 2017;17(1):1–13.

247. Gonzalez-Gil A, Schnaar RL. Siglec ligands. Cells. 2021;10(5):1–21.

248. Zhao L. CD33 in Alzheimer's disease - Biology, pathogenesis, and therapeutics: A mini-review. Gerontology. 2019;65(4):323–31.

249. Varchetta S, Lusso P, Hudspeth K, Mikulak J, Mele D, Paolucci S, et al. Sialic acid-binding Ig-like lectin-7 interacts with HIV-1 gp120 and facilitates infection of CD4pos T cells and macrophages. Retrovirology. 2013;10(1):1–13.

250. Chang YC, Nizet V. Siglecs at the Host–Pathogen Interface [Internet]. Vol. 1204, Advances in Experimental Medicine and Biology. Springer Singapore; 2020. 197–214 p. Available from: http://dx.doi.org/10.1007/978-981-15-1580-4_8

251. Brickman AM, Manly JJ, Honig LS, Sanchez D, Reyes-Dumeyer D, Lantigua RA, et al. Plasma p-tau181, p-tau217, and other blood-based Alzheimer's disease biomarkers in a multi-ethnic, community study. Alzheimer's Dement. 2021;17(8):1353–64.

252. Illán-Gala I, Lleo A, Karydas A, Staffaroni AM, Zetterberg H, Sivasankaran R, et al. Plasma Tau and Neurofilament Light in Frontotemporal Lobar Degeneration and Alzheimer Disease. Neurology. 2021;96(5):e671–83.

253. Lee MN, Ye C, Villani A, Raj T, Li W, Eisenhaure TM, et al. CD33 Alzheimer's disease locus: Altered monocyte function and amyloid biology. Nat Neurosci. 2013;343(6175):1–19.

254. Malik M, Chiles J, Xi HS, Medway C, Simpson J, Potluri S, et al. Genetics of CD33 in Alzheimer's disease and acute myeloid leukemia. Hum Mol Genet. 2015;24(12):3557–70.

255. Rempel H, Calosing C, Sun B, Pulliam L. Sialoadhesin expressed on IFN-induced monocytes binds HIV-1 and enhances infectivity. PLoS One. 2008;3(4).

256. Izquierdo-Useros N, Lorizate M, McLaren PJ, Telenti A, Kräusslich HG, Martinez-Picado J. HIV-1 Capture and Transmission by Dendritic Cells: The Role of Viral Glycolipids and the Cellular Receptor Siglec-1. PLoS Pathog. 2014;10(7).

257. Zou Z, Chastain A, Moir S, Ford J, Trandem K, Martinelli E, et al. Siglecs facilitate HIV-1 infection of macrophages through adhesion with viral sialic acids. PLoS One. 2011;6(9).

258. Walter RB. Investigational CD33-targeted therapeutics for acute myeloid leukemia. Expert Opin Investig Drugs [Internet]. 2018;27(4):339–48. Available from: https://doi.org/10.1080/13543784.2018.1452911

259. Tsai TY, Huang MT, Sung PS, Peng CY, Tao MH, Yang HI, et al. SIGLEC-3 (CD33) serves as an immune checkpoint receptor for HBV infection. J Clin Invest. 2021;131(11):1–15.

260. Zhang M, Schmitt-Ulms G, Sato C, Xi Z, Zhang Y, Zhou Y, et al. Drug repositioning for Alzheimer's disease based on systematic "omics" data mining. PLoS One. 2016;11(12):1–15.

ANNEXES

CHAPTER II. Plasma HDAC class II factor (Sirtuin-2) as biomarker and potential therapeutic target for HIV-1 infection and neurological dysfunction

ID	HIV-high1	HIV-high2	HIV-high3	HIV-high4	HIV-high5	HIV-high6	HIV-high7	HIV-high8	HIV-high9	HIV-high10	HIV-high11	HIV-high12	HIV-high13	HIV-high14	HIV-high15	HIV-high16	HIV-high17	HIV-high18	HIV-high19	HIV-high20	HIV-low1	HIV-low2	HIV-low3	HIV-low4	HIV-low5	HIV-low6	HIV-low7	HIV-low8	HIV-low9	HIV-low10	HIV-low11	HIV-low12	HIV-low13	HIV-low14	HIV-low15	HIV-low16	HIV-low17	HIV-low18	HIV-low19	HIV-low20	[-log10 pvalue]	log2FC
Sirtuin 2 mAb	0,017	0,026	0,037	0,013	0,028	0,041	0,036	0,025	0,056	0,016	0,012	0,028	0,025	0,014	0,044	0,087	0,033	0,083	0,075	0,072	0,110	0,024	0,087	0,032	0,139	0,041	0,061	0,130	0,094	0,040	0,052	0,185	0,110	0,073	0,139	0,019	0,164	0,026	0,025	0,023	2,478	1,039
Factor Ba	0,039	0,040	0,114	0,106	0,135	0,059	0,059	0,085	0,082	0,082	0,115	0,090	0,059	0,063	0,086	0,046	0,098	0,037	0,136	0,064	0,019	0,072	0,052	0,040	0,026	0,059	0,054	0,073	0,033	0,050	0,025	0,049	0,048	0,092	0,094	0,034	0,057	0,091	0,064	0,080	2,111	-0,518
CCL23/CKBeta 8-1 mAb	0,022	0,033	0,034	0,018	0,015	0,056	0,053	0,034	0,031	0,049	0,075	0,055	0,032	0,012	0,049	0,076	0,048	0,046	0,058	0,048	0,076	0,034	0,041	0,229	0,142	0,070	0,070	0,057	0,096	0,062	0,056	0,047	0,042	0,067	0,206	0,038	0,057	0,060	0,051	0,046	2,065	0,871
TFF3 mAb	0,040	0,000	0,048	0,020	0,039	0,049	0,023	0,027	0,081	0,028	0,030	0,042	0,065	0,009	0,043	0,070	0,034	0,023	0,044	0,057	0,045	0,032	0,132	0,198	0,113	0,052	0,063	0,255	0,076	0,072	0,054	0,028	0,043	0,049	0,042	0,032	0,061	0,068	0,050	0,051	1,994	0,974
alpha-fetoprotein mAb	0,070	0,024	0,037	0,031	0,072	0,082	0,069	0,032	0,067	0,023	0,046	0,070	0,030	0,015	0,052	0,035	0,020	0,046	0,043	0,045	0,033	0,041	0,155	0,094	0,101	0,019	0,140	0,169	0,045	0,117	0,153	0,043	0,099	0,048	0,112	0,035	0,021	0,038	0,063	0,020	1,902	0,763
BMP-9 mAb	0,060	0,015	0,040	0,031	0,067	0,029	0,035	0,028	0,037	0,028	0,017	0,057	0,034	0,009	0,046	0,026	0,014	0,070	0,050	0,049	0,011	0,028	0,113	0,178	0,080	0,020	0,077	0,219	0,021	0,074	0,105	0,042	0,020	0,051	0,038	0,027	0,029				1,899	1,007
iC3b (neoantigen)	0,044	0,063	0,044	0,174	0,079	0,113	0,049	0,067	0,083	0,076	0,045	0,050	0,060	0,090	0,156	0,076	0,094	0,042	0,109	0,045	0,023	0,083	0,043	0,069	0,031	0,039	0,061	0,031	0,051	0,031	0,037	0,047	0,041	0,044	0,061	0,060	0,031	0,059	0,086	0,131	1,797	-0,563
C4d (neoantigen)	0,043	0,023	0,059	0,172	0,073	0,102	0,036	0,077	0,102	0,055	0,065	0,034	0,060	0,164	0,142	0,061	0,098	0,040	0,112	0,034	0,019	0,050	0,039	0,061	0,030	0,050	0,049	0,052	0,057	0,034	0,033	0,043	0,040	0,069	0,054	0,055	0,035	0,091	0,045	0,106	1,796	-0,619
Noggin mAb	0,091	0,017	0,124	0,085	0,080	0,080	0,051	0,046	0,176	0,119	0,072	0,096	0,056	0,022	0,108	0,041	0,065	0,053	0,049	0,125	0,055	0,089	0,022	0,044	0,013	0,045	0,104	0,032	0,055	0,039	0,039	0,074	0,082	0,043	0,024	0,028	0,031	0,090	0,027	0,085	1,783	-0,606
GPIb alpha mAb	0,024	0,025	0,035	0,019	0,036	0,032	0,021	0,020	0,041	0,019	0,014	0,058	0,028	0,009	0,069	0,045	0,038	0,040	0,013	0,055	0,036	0,056	0,056	0,033	0,154	0,031	0,029	0,116	0,022	0,131	0,313	0,030	0,024	0,062	0,024	0,021	0,104	0,033	0,097	0,028	1,667	1,154
S Protein (Vitronectin)	0,027	0,075	0,066	0,160	0,065	0,129	0,038	0,059	0,075	0,059	0,038	0,038	0,077	0,201	0,135	0,046	0,079	0,036	0,083	0,052	0,023	0,084	0,060	0,053	0,039	0,038	0,050	0,047	0,045	0,030	0,042	0,073	0,072	0,041	0,072	0,044	0,031	0,053	0,054	0,089	1,615	-0,592
Siglec-2/CD22 mAb	0,039	0,035	0,042	0,020	0,045	0,053	0,094	0,072	0,052	0,016	0,037	0,041	0,047	0,016	0,033	0,048	0,043	0,031	0,031	0,046	0,076	0,024	0,193	0,248	0,085	0,093	0,074	0,086	0,082	0,074	0,050	0,037	0,051	0,027	0,049	0,024	0,130	0,033	0,020	0,023	1,589	0,817
Factor I	0,039	0,048	0,069	0,193	0,065	0,106	0,060	0,063	0,076	0,086	0,100	0,070	0,058	0,090	0,122	0,064	0,079	0,042	0,070	0,050	0,025	0,054	0,069	0,063	0,038	0,045	0,067	0,063	0,054	0,053	0,051	0,053	0,056	0,062	0,076	0,062	0,045	0,079	0,055	0,102	1,482	-0,402
BAFF/BLyS/TNFSF13B mAb	0,070	0,016	0,034	0,023	0,050	0,045	0,093	0,062	0,029	0,021	0,043	0,046	0,032	0,017	0,028	0,028	0,064	0,039	0,035	0,032	0,018	0,040	0,084	0,298	0,052	0,016	0,104	0,118	0,048	0,112	0,097	0,037	0,081	0,050	0,033	0,017	0,065	0,064	0,040	0,069	1,481	0,842
Progranulin pAb (0.5 mg/ml)	0,071	0,039	0,050	0,032	0,067	0,043	0,055	0,069	0,043	0,029	0,079	0,062	0,117	0,014	0,055	0,062	0,056	0,087	0,056	0,067	0,028	0,036	0,079	0,072	0,045	0,050	0,067	0,158	0,068	0,115	0,133	0,083	0,069	0,088	0,077	0,035	0,060	0,093	0,107	0,084	1,479	0,425
Furin mAb	0,072	0,039	0,065	0,037	0,070	0,050	0,034	0,044	0,079	0,039	0,031	0,092	0,064	0,025	0,034	0,052	0,021	0,046	0,057	0,112	0,068	0,160	0,044	0,055	0,030	0,100	0,108	0,035	0,117	0,140	0,018	0,128	0,157	0,074	0,038	0,037	0,027	0,027	0,043		1,478	0,581
von Willebrand Factor A2 mAb	0,037	0,023	0,136	0,013	0,056	0,035	0,085	0,069	0,029	0,015	0,049	0,019	0,072	0,009	0,049	0,014	0,021	0,057	0,030	0,019	0,015	0,036	0,120	0,077	0,154	0,112	0,096	0,222	0,062	0,133	0,076	0,078	0,041	0,081	0,036	0,029	0,020	0,031	0,020	0,020	1,476	0,798
Jagged 1 mAb	0,019	0,012	0,055	0,030	0,071	0,033	0,029	0,038	0,052	0,062	0,058	0,034	0,053	0,014	0,039	0,091	0,056	0,046	0,032	0,059	0,024	0,030	0,179	0,183	0,046	0,093	0,064	0,221	0,098	0,064	0,097	0,029	0,052	0,032	0,045	0,037	0,026	0,078	0,036	0,014	1,316	0,713
C8	0,058	0,052	0,069	0,094	0,073	0,062	0,063	0,082	0,063	0,065	0,066	0,075	0,078	0,054	0,107	0,085	0,056	0,205	0,071	0,048	0,050	0,053	0,073	0,055	0,037	0,037	0,067	0,059	0,083	0,063	0,060	0,058	0,080	0,079	0,096	0,044	0,042	0,067	0,051	0,057	1,173	-0,333
CD18	0,036	0,052	0,088	0,201	0,075	0,101	0,055	0,107	0,041	0,061	0,081	0,048	0,050	0,082	0,063	0,072	0,071	0,049	0,065	0,100	0,035	0,080	0,031	0,064	0,047	0,050	0,093	0,025	0,045	0,022	0,039	0,046	0,104	0,036	0,047	0,059	0,061	0,058	0,034	0,142	1,124	-0,423
C1q	0,115	0,123	0,054	0,070	0,105	0,075	0,099	0,081	0,076	0,200	0,052	0,053	0,066	0,033	0,081	0,038	0,054	0,019	0,044	0,069	0,141	0,044	0,072	0,020	0,033	0,041	0,047	0,086	0,056	0,037	0,036	0,040	0,045	0,142	0,014	0,030	0,014	0,027	0,021		1,120	-0,529
Tau-12	0,014	0,125	0,008	0,020	0,027	0,046	0,021	0,031	0,016	0,012	0,068	0,017	0,032	0,011	0,030	0,099	0,042	0,025	0,018	0,019	0,239	0,054	0,202	0,015	0,121	0,080	0,042	0,024	0,070	0,089	0,182	0,013	0,025	0,014	0,019	0,027	0,053	0,004	0,004	0,013	1,089	0,922
SOST mAb	0,021	0,035	0,118	0,046	0,066	0,058	0,052	0,013	0,069	0,021	0,031	0,052	0,024	0,016	0,042	0,046	0,047	0,079	0,055	0,018	0,028	0,048	0,142	0,074	0,065	0,013	0,268	0,134	0,028	0,067	0,100	0,015	0,035	0,063	0,039	0,048	0,056	0,043	0,090	0,044	1,047	0,629
C4 Binding Protein	0,148	0,086	0,101	0,022	0,052	0,013	0,061	0,103	0,068	0,096	0,123	0,129	0,056	0,035	0,073	0,085	0,038	0,058	0,093	0,054	0,085	0,078	0,053	0,069	0,012	0,063	0,042	0,077	0,032	0,056	0,109	0,075	0,075	0,067	0,091	0,029	0,032	0,069	0,020	0,025	1,000	-0,367
alpha-synuclein mAb	0,029	0,020	0,042	0,014	0,036	0,033	0,079	0,030	0,024	0,016	0,033	0,155	0,034	0,008	0,034	0,026	0,023	0,141	0,034	0,055	0,056	0,018	0,069	0,180	0,073	0,043	0,033	0,108	0,031	0,089	0,121	0,036	0,018	0,124	0,019	0,043	0,041	0,048	0,207	0,013	0,999	0,662
Abeta 13-28	0,033	0,037	0,029	0,018	0,051	0,074	0,017	0,054	0,052	0,025	0,037	0,024	0,064	0,109	0,037	0,072	0,029	0,039	0,112	0,067	0,040	0,116	0,062	0,148	0,054	0,058	0,010	0,094	0,141	0,090	0,020	0,034	0,061	0,039	0,075	0,036	0,047	0,212			0,998	0,517
MIA mAb	0,065	0,043	0,027	0,019	0,040	0,057	0,109	0,038	0,044	0,020	0,052	0,038	0,066	0,010	0,039	0,042	0,183	0,032	0,038	0,060	0,079	0,038	0,068	0,165	0,098	0,097	0,171	0,054	0,084	0,085	0,069	0,035	0,047	0,034	0,064	0,037	0,120	0,038	0,027		0,984	0,496
Neurofilaments (SMI-31) mAb	0,078	0,045	0,099	0,123	0,108	0,089	0,089	0,109	0,098	0,062	0,108	0,065	0,123	0,036	0,043	0,051	0,072	0,028	0,034	0,041	0,076	0,091	0,059	0,098	0,047	0,055	0,092	0,077	0,081	0,086	0,043	0,082	0,053	0,074	0,036	0,026	0,019	0,063	0,020	0,022	0,970	-0,323
C3c	0,094	0,050	0,071	0,098	0,096	0,082	0,052	0,074	0,091	0,085	0,090	0,063	0,103	0,065	0,103	0,069	0,067	0,032	0,042	0,067	0,036	0,062	0,033	0,051	0,087	0,069	0,094	0,115	0,051	0,051	0,090	0,069	0,045	0,041	0,118	0,045	0,049				0,968	-0,246
C4c	0,068	0,042	0,047	0,067	0,026	0,074	0,035	0,046	0,082	0,100	0,088	0,036	0,129	0,066	0,133	0,135	0,068	0,082	0,112	0,028	0,040	0,054	0,037	0,069	0,023	0,020	0,060	0,039	0,076	0,059	0,062	0,060	0,083	0,102	0,110	0,067	0,039	0,088	0,062	0,048	0,949	-0,322
CD11b	0,034	0,035	0,092	0,082	0,095	0,098	0,049	0,073	0,082	0,055	0,058	0,052	0,055	0,076	0,127	0,067	0,093	0,060	0,075	0,115	0,035	0,087	0,052	0,056	0,039	0,048	0,063	0,075	0,076	0,058	0,058	0,061	0,073	0,061	0,070	0,058	0,056	0,071	0,055	0,130	0,940	-0,238
Pref-1/DLK-1/FA1 mAb	0,019	0,016	0,021	0,038	0,028	0,046	0,084	0,010	0,035	0,062	0,012	0,071	0,240	0,007	0,028	0,034	0,011	0,032	0,011	0,027	0,100	0,022	0,078	0,068	0,120	0,026	0,144	0,078	0,044	0,079	0,124	0,001	0,043	0,098	0,019	0,012	0,170	0,058	0,032	0,015	0,928	0,681
Beclin 1 (K-15)	0,078	0,060	0,094	0,056	0,118	0,063	0,086	0,099	0,068	0,063	0,095	0,071	0,110	0,022	0,083	0,083	0,056	0,058	0,082	0,064	0,035	0,069	0,060	0,091	0,041	0,054	0,073	0,042	0,080	0,062	0,057	0,054	0,071	0,075	0,074	0,038	0,042	0,147	0,068	0,037	0,918	-0,249
Progranulin mAb (Clone 1)	0,104	0,082	0,064	0,036	0,083	0,054	0,093	0,096	0,051	0,032	0,077	0,076	0,050	0,017	0,050	0,056	0,043	0,068	0,065	0,057	0,061	0,046	0,081	0,068	0,060	0,045	0,090	0,153	0,069	0,106	0,124	0,078	0,055	0,076	0,055	0,026	0,063	0,081	0,096	0,072	0,908	0,268
Abeta 1-5 (3D6)	0,050	0,047	0,056	0,031	0,116	0,085	0,073	0,045	0,058	0,064	0,046	0,057	0,066	0,080	0,058	0,076	0,035	0,103	0,042	0,087	0,037	0,067	0,089	0,113	0,058	0,055	0,115	0,050	0,081	0,076	0,104	0,100	0,088	0,059	0,102	0,031	0,066	0,099	0,070	0,050	0,906	0,245
FGF acidic mAb	0,047	0,040	0,046	0,038	0,067	0,049	0,056	0,059	0,078	0,037	0,054	0,042	0,052	0,048	0,061	0,104	0,054	0,060	0,066	0,128	0,066	0,049	0,084	0,084	0,185	0,107	0,099	0,067	0,096	0,084	0,104	0,100	0,066	0,046	0,053	0,022	0,072	0,046	0,030	0,028	0,905	0,329
CYR61 mAb	0,032	0,052	0,052	0,038	0,079	0,083	0,038	0,074	0,053	0,049	0,028	0,068	0,066	0,020	0,044	0,079	0,036	0,093	0,054	0,101	0,049	0,056	0,138	0,088	0,124	0,068	0,107	0,066	0,073	0,044	0,106	0,034	0,085	0,069	0,029	0,029	0,186	0,060	0,031	0,027	0,892	0,369
C6	0,053	0,028	0,070	0,085	0,095	0,074	0,086	0,075	0,095	0,084	0,105	0,061	0,077	0,054	0,106	0,074	0,073	0,034	0,123	0,052	0,019	0,058	0,034	0,071	0,030	0,044	0,065	0,058	0,068	0,101	0,049	0,071	0,066	0,072	0,103	0,051	0,053	0,121	0,062	0,076	0,865	-0,243
Factor P	0,043	0,037	0,097	0,061	0,108	0,056	0,090	0,076	0,070	0,080	0,111	0,079	0,116	0,027	0,084	0,085	0,062	0,061	0,102	0,052	0,022	0,050	0,066	0,079	0,032	0,062	0,064	0,073	0,072	0,071	0,058	0,071	0,067	0,067	0,078	0,044	0,037	0,142	0,067	0,049	0,852	-0,243
Beclin 1 mAb	0,005	0,348	0,006	0,004	0,008	0,004	0,006	0,007	0,005	0,005	0,007	0,005	0,008	0,001	0,006	0,006	0,004	0,306	0,007	0,005	0,002	0,005	0,004	0,006	0,003	0,004	0,005	0,005	0,004	0,004	0,004	0,005	0,005	0,003	0,005	0,005	0,005	0,010	0,005	0,003	0,841	-3,051
IL-32 alpha mAb	0,069	0,026	0,011	0,021	0,016	0,042	0,034	0,009	0,017	0,016	0,032	0,038	0,011	0,008	0,022	0,011	0,022	0,059	0,027	0,010	0,018	0,017	0,044	0,036	0,088	0,022	0,040	0,018	0,021	0,409	0,042	0,014	0,030	0,018	0,019	0,015	0,044	0,020	0,044	0,059	0,820	1,099
LD78beta pAb	0,001	0,086	0,060	0,030	0,001	0,130	0,001	0,001	0,001	0,001	0,001	0,008	0,001	0,000	0,012	0,001	0,016	0,001	0,001	0,107	0,001	0,001	0,040	0,021	0,123	0,001	0,001	0,001	0,001	0,045	0,001	0,093	0,350	0,158	0,001	0,001	0,000				0,786	1,422
SQSTM1/p62	0,053	0,035	0,067	0,243	0,001	0,108	0,001	0,092	0,000	0,162	0,026	0,082	0,014	0,019	0,090	0,110	0,035	0,034	0,044	0,093	0,068	0,030	0,079	0,003	0,033	0,076	0,053	0,000	0,026	0,000	0,096	0,000	0,023	0,030	0,025	0,068	0,062	0,001	0,118	0,074	0,785	-0,597
C5	0,112	0,026	0,060	0,096	0,077	0,072	0,064	0,055	0,065	0,065	0,122	0,070	0,103	0,036	0,090	0,071	0,059	0,057	0,103	0,087	0,037	0,058	0,059	0,057	0,027	0,042	0,055	0,062	0,070	0,054	0,063	0,063	0,048	0,064	0,092	0,045	0,034	0,155	0,100	0,072	0,758	-0,243
Sorl1/LR11	0,001	0,052	0,002	0,001	0,001	0,002	0,001	0,002	0,001	0,001	0,002	0,002	0,001	0,002	0,059	0,002	0,057	0,001	0,156	0,002	0,001	0,144	0,001	0,001	0,001	0,001	0,001	0,083	0,001	0,032	0,001	0,173	0,001	0,161	0,001	0,003	0,313	0,001			0,748	1,400
Vitamin D binding protein mAb	0,042	0,018	0,050	0,054	0,049	0,051	0,054	0,056	0,033	0,099	0,039	0,084	0,071	0,086	0,047	0,063	0,142	0,106	0,127	0,138	0,035	0,029	0,023	0,036	0,018	0,032	0,080	0,031	0,052	0,085	0,067	0,068	0,046	0,042	0,040	0,043	0,062	0,039	0,060		0,744	-0,369
SC5b-9	0,028	0,035	0,044	0,196	0,031	0,096	0,000	0,017	0,051	0,036	0,043	0,034	0,075	0,167	0,173	0,089	0,073	0,029	0,079	0,034	0,034	0,075	0,059	0,032	0,033	0,029	0,024	0,032	0,052	0,018	0,086	0,085	0,046	0,140	0,101	0,028	0,022	0,014	0,059		0,729	-0,483
Aspartate Aminotransferase pAb	0,000	0,000	0,000	0,000	0,016	0,012	0,156	0,000	0,034	0,000	0,000	0,000	0,011	0,000	0,000	0,006	0,000	0,014	0,000	0,192	0,000	0,000	0,000	0,000	0,035	0,011	0,124	0,006	0,295	0,000	0,000	0,069	0,050	0,002	0,007	0,158	0,080	0,097	0,036	0,013	0,722	1,161
Tau-C3	0,002	0,034	0,025	0,016	0,004	0,055	0,007	0,018	0,022	0,019	0,023	0,034	0,087	0,017	0,044	0,057	0,046	0,011	0,023	0,004	0,076	0,013	0,137	0,009	0,383	0,046	0,056	0,030	0,015	0,021	0,015	0,010	0,035	0,014	0,032	0,017	0,090	0,000	0,022	0,022	0,712	0,960
SorL1 pAb	0,001	0,092	0,007	0,000	0,001	0,130	0,001	0,001	0,001	0,001	0,001	0,035	0,001	0,000	0,003	0,004	0,000	0,002	0,041	0,000	0,161	0,020	0,000	0,054	0,000	0,019	0,001	0,001	0,000	0,032	0,001	0,031	0,297	0,260	0,001	0,000	0,022				0,712	1,464
GALP	0,032	0,015	0,179	0,120	0,068	0,064	0,050	0,035	0,239	0,116	0,019	0,012	0,003	0,003	0,015	0,035	0,039	0,093	0,020	0,083	0,028	0,025	0,030	0,023	0,037	0,036	0,040	0,120	0,000	0,000	0,027	0,064	0,048	0,006	0,174	0,047	0,000	0,033	0,062		0,704	-0,633
alpha-macroglobulin mAb	0,053	0,064	0,089	0,047	0,124	0,067	0,073	0,119	0,059	0,065	0,074	0,052	0,115	0,019	0,086	0,086	0,058	0,065	0,097	0,076	0,038	0,053	0,072	0,066	0,037	0,048	0,049	0,085	0,072	0,070	0,059	0,062	0,068	0,068	0,079	0,034	0,049	0,148	0,073	0,049	0,702	-0,218
Netrin1 pAb	0,039	0,030	0,087	0,063	0,064	0,093	0,047	0,042	0,058	0,052	0,063	0,128	0,061	0,122	0,120	0,093	0,061	0,051	0,092	0,101	0,050	0,082	0,041	0,046	0,037	0,053	0,056	0,020	0,047	0,053	0,048	0,066	0,055	0,134	0,058	0,065	0,047	0,056	0,063	0,148	0,693	-0,261
BDNF mAb (Clone 2)	0,038	0,079	0,074	0,039	0,075	0,079	0,047	0,046	0,070	0,060	0,078	0,058	0,055	0,023	0,015	0,090	0,058	0,062	0,045	0,071	0,054	0,047	0,105	0,124	0,054	0,040	0,121	0,124	0,065	0,073	0,111	0,090	0,075	0,076	0,095	0,051	0,029	0,048	0,084	0,047	0,682	0,222
PTHLH pAb	0,085	0,090	0,103	0,083	0,120	0,088	0,089	0,116	0,042	0,038	0,053	0,072	0,086	0,025	0,054	0,102	0,038	0,054	0,046	0,069	0,049	0,101	0,083	0,099	0,065	0,047	0,091	0,015	0,091	0,058	0,049	0,023	0,074	0,071	0,073	0,034	0,026	0,119	0,042	0,030	0,677	-0,247
C3d (neoantigen)	0,079	0,075	0,052	0,098	0,071	0,088	0,090	0,067	0,076	0,097	0,072	0,092	0,029	0,093	0,070	0,059	0,055	0,087	0,061	0,042	0,061	0,054	0,084	0,033	0,046	0,084	0,097	0,093	0,082	0,068	0,055	0,063	0,072	0,048	0,038	0,026	0,106	0,056	0,063	0,072	0,674	-0,162
GFAP mAb	0,122	0,000	0,195	0,060	0,087	0,083	0,078	0,061	0,065	0,072	0,065	0,011	0,051	0,013	0,182	0,021	0,070	0,044	0,024	0,069	0,049	0,027	0,021	0,079	0,055	0,054	0,080	0,047	0,070	0,039	0,019	0,097	0,132	0,077	0,066	0,022	0,030	0,030	0,010	0,057	0,673	-0,411
BMP-13 pAb	0,123	0,091	0,110	0,046	0,121	0,052	0,074	0,047	0,054	0,053	0,149	0,050	0,087	0,019	0,054	0,059	0,102	0,061	0,052	0,068	0,078	0,099	0,076	0,045	0,044	0,111	0,041	0,048	0,079	0,064	0,038	0,055	0,101	0,065	0,050	0,040	0,059	0,064	0,039	0,055	0,659	-0,234
Netrin 4 mAb	0,130	0,097	0,059	0,061	0,022	0,156	0,050	0,018	0,087	0,106	0,026	0,077	0,058	0,173	0,026	0,069	0,010	0,041	0,038	0,070	0,088	0,029	0,051	0,054	0,010	0,027	0,003	0,088	0,095	0,087	0,014	0,103	0,016	0,068	0,000	0,056					0,642	-0,389
Progranulin mAb (Clone 2)	0,048	0,054	0,078	0,024	0,067	0,053	0,055	0,078	0,086	0,052	0,052	0,049	0,094	0,018	0,115	0,045	0,229	0,058	0,118	0,032	0,021	0,072	0,051	0,057	0,046	0,023	0,080	0,078	0,037	0,037	0,051	0,156	0,050	0,062	0,054	0,025	0,061	0,046	0,026	0,071	0,640	-0,346
Factor Bb (neoantigen)	0,023	0,155	0,048	0,201	0,057	0,091	0,143	0,044	0,065	0,088	0,044	0,060	0,040	0,075	0,070	0,040	0,049	0,030	0,039	0,035	0,030	0,061	0,117	0,056	0,033	0,049	0,040	0,043	0,084	0,038	0,111	0,076	0,068	0,046	0,110	0,043	0,023	0,026	0,016	0,028	0,628	-0,348

Target																																									
Clusterin	0,145	0,049	0,090	0,034	0,087	0,070	0,044	0,066	0,087	0,074	0,082	0,085	0,044	0,038	0,055	0,073	0,085	0,060	0,102	0,111	0,062	0,059	0,084	0,067	0,018	0,066	0,070	0,094	0,035	0,057	0,069	0,069	0,055	0,054	0,069	0,047	0,040	0,073	0,082	0,122	0,624	-0,196
Progranulin pAb (Clone 2)	0,048	0,040	0,061	0,038	0,052	0,061	0,102	0,047	0,045	0,039	0,112	0,033	0,063	0,044	0,064	0,082	0,095	0,070	0,066	0,064	0,048	0,061	0,065	0,042	0,023	0,199	0,047	0,072	0,088	0,057	0,090	0,041	0,118	0,096	0,087	0,087	0,055	0,061	0,050	0,087	0,603	0,246
SCGF/CLEC11a mAb	0,051	0,028	0,048	0,015	0,047	0,046	0,050	0,040	0,080	0,032	0,040	0,036	0,097	0,112	0,073	0,051	0,047	0,062	0,069	0,030	0,086	0,109	0,027	0,020	0,056	0,046	0,045	0,040	0,185	0,062	0,210	0,066	0,092	0,037	0,031	0,065	0,031	0,019	0,121	0,590	0,349	
APP 444-592 mAb (Clone 2)	0,046	0,048	0,063	0,042	0,059	0,064	0,042	0,111	0,064	0,026	0,069	0,117	0,048	0,032	0,055	0,081	0,045	0,046	0,058	0,120	0,053	0,075	0,102	0,066	0,064	0,061	0,048	0,155	0,116	0,138	0,080	0,037	0,054	0,034	0,090	0,068	0,066	0,064	0,039	0,043	0,587	0,233
C7	0,050	0,066	0,104	0,071	0,132	0,074	0,088	0,051	0,062	0,065	0,066	0,068	0,092	0,036	0,086	0,083	0,057	0,067	0,058	0,046	0,038	0,064	0,062	0,091	0,044	0,053	0,069	0,101	0,074	0,064	0,083	0,055	0,079	0,081	0,103	0,032	0,037	0,098	0,050	0,038	0,586	-0,170
Transferrin mAb	0,093	0,063	0,077	0,050	0,070	0,085	0,044	0,120	0,058	0,102	0,083	0,089	0,125	0,035	0,108	0,070	0,067	0,038	0,070	0,030	0,057	0,085	0,080	0,086	0,020	0,056	0,059	0,052	0,083	0,084	0,086	0,058	0,090	0,072	0,065	0,037	0,030	0,102	0,064	0,043	0,582	-0,183
Pro-BDNF mAb	0,075	0,032	0,063	0,040	0,054	0,073	0,034	0,035	0,060	0,033	0,065	0,040	0,066	0,180	0,112	0,038	0,056	0,044	0,212	0,083	0,047	0,103	0,073	0,052	0,028	0,056	0,037	0,042	0,046	0,053	0,050	0,056	0,042	0,047	0,081	0,087	0,024	0,042	0,044	0,118	0,566	-0,308
Haptoglobin mAb	0,059	0,070	0,070	0,066	0,104	0,071	0,062	0,109	0,039	0,083	0,085	0,090	0,101	0,021	0,074	0,105	0,057	0,054	0,072	0,083	0,042	0,062	0,073	0,067	0,050	0,050	0,083	0,066	0,065	0,054	0,072	0,049	0,088	0,056	0,104	0,023	0,055	0,134	0,079	0,043	0,554	-0,168
Bcl-2 (N19)	0,074	0,000	0,086	0,055	0,119	0,061	0,077	0,093	0,069	0,070	0,101	0,072	0,109	0,020	0,087	0,089	0,059	0,063	0,099	0,069	0,037	0,066	0,057	0,091	0,042	0,055	0,075	0,066	0,075	0,063	0,063	0,056	0,068	0,074	0,080	0,041	0,045	0,131	0,075	0,037	0,554	-0,182
MCP (CD46)	0,040	0,035	0,046	0,108	0,066	0,077	0,036	0,040	0,032	0,052	0,035	0,068	0,103	0,143	0,085	0,081	0,112	0,076	0,113	0,079	0,025	0,059	0,059	0,042	0,021	0,029	0,065	0,031	0,040	0,081	0,058	0,060	0,152	0,073	0,063	0,036	0,068	0,049	0,036	0,147	0,548	-0,255
C5b neo-epitope	0,021	0,228	0,035	0,027	0,059	0,063	0,018	0,078	0,033	0,050	0,021	0,277	0,036	0,038	0,049	0,061	0,019	0,047	0,023	0,062	0,021	0,028	0,037	0,033	0,038	0,025	0,072	0,023	0,113	0,051	0,041	0,035	0,085	0,029	0,062	0,039	0,044	0,064	0,042	0,020	0,539	-0,468
mTOR 7C10	0,002	0,002	0,003	0,002	0,003	0,002	0,003	0,003	0,003	0,002	0,002	0,003	0,253	0,003	0,001	0,002	0,270	0,002	0,219	0,003	0,002	0,127	0,002	0,003	0,001	0,002	0,002	0,002	0,002	0,002	0,002	0,002	0,116	0,001	0,005	0,004	0,002	0,002	0,001	0,001	0,539	-1,325
Pan-neuronal marker (SMI311)	0,042	0,046	0,031	0,043	0,107	0,067	0,070	0,104	0,253	0,064	0,063	0,050	0,086	0,017	0,066	0,053	0,052	0,057	0,071	0,060	0,050	0,061	0,084	0,068	0,044	0,028	0,094	0,043	0,060	0,048	0,056	0,085	0,068	0,065	0,061	0,033	0,035	0,081	0,049	0,050	0,525	-0,273
TARDBP mAb (Clone 2)	0,002	0,002	0,002	0,001	0,003	0,002	0,002	0,003	0,002	0,334	0,003	0,182	0,003	0,001	0,002	0,002	0,001	0,018	0,002	0,157	0,001	0,001	0,002	0,002	0,002	0,001	0,016	0,002	0,002	0,002	0,002	0,002	0,002	0,002	0,001	0,001	0,004	0,215	0,001	0,521	-1,476	
Neuroligin 3 mAb	0,043	0,021	0,060	0,034	0,076	0,094	0,073	0,044	0,077	0,045	0,287	0,046	0,087	0,074	0,093	0,033	0,038	0,022	0,056	0,039	0,025	0,062	0,060	0,061	0,036	0,054	0,051	0,061	0,061	0,061	0,079	0,123	0,062	0,047	0,060	0,026	0,028	0,032	0,024	0,044	0,508	-0,341
human PHF-Tau monoclonal	0,004	0,052	0,033	0,000	0,001	0,071	0,001	0,001	0,001	0,045	0,001	0,145	0,001	0,356	0,001	0,027	0,001	0,082	0,001	0,001	0,068	0,001	0,000	0,061	0,000	0,000	0,001	0,001	0,001	0,001	0,001	0,001	0,099	0,001	0,029	0,001	0,186	0,000		0,495	-1,073	
Vps34	0,000	0,034	0,060	0,031	0,019	0,000	0,094	0,030	0,000	0,035	0,000	0,011	0,001	0,141	0,000	0,000	0,000	0,000	0,010	0,000	0,008	0,301	0,000	0,023	0,039	0,067	0,000	0,000	0,039	0,000	0,000	0,000	0,182	0,000	0,000	0,008	0,216	0,001	0,000	0,000	0,493	0,923
TARDBP mAb (Clone 1)	0,006	0,025	0,040	0,066	0,000	0,000	0,032	0,000	0,449	0,000	0,000	0,000	0,000	0,000	0,000	0,000	0,000	0,091	0,000	0,013	0,000	0,000	0,000	0,007	0,000	0,000	0,000	0,000	0,000	0,000	0,000	0,000	0,010	0,000	0,000	0,000	0,215	0,000	0,000	0,000	0,491	-2,238
QPCT (4E11) mAb	0,035	0,050	0,070	0,047	0,103	0,059	0,074	0,068	0,057	0,067	0,065	0,076	0,165	0,038	0,083	0,109	0,049	0,070	0,091	0,085	0,023	0,075	0,056	0,059	0,027	0,053	0,064	0,063	0,075	0,079	0,073	0,085	0,081	0,096	0,081	0,043	0,050	0,108	0,061	0,050	0,489	-0,169
BDNF mAb (Clone 1)	0,042	0,061	0,018	0,041	0,080	0,078	0,069	0,047	0,057	0,062	0,073	0,044	0,133	0,017	0,073	0,088	0,034	0,050	0,045	0,054	0,031	0,065	0,057	0,084	0,055	0,034	0,232	0,090	0,067	0,053	0,072	0,084	0,096	0,097	0,055	0,038	0,033	0,090	0,044	0,017	0,473	0,256
Hemopexin mAb	0,078	0,000	0,091	0,066	0,106	0,065	0,077	0,072	0,080	0,086	0,089	0,081	0,112	0,026	0,091	0,089	0,055	0,047	0,073	0,073	0,036	0,060	0,064	0,077	0,038	0,053	0,081	0,044	0,092	0,071	0,066	0,042	0,077	0,062	0,088	0,037	0,047	0,143	0,082	0,038	0,462	-0,164
APP pAb	0,153	0,021	0,080	0,050	0,080	0,082	0,008	0,000	0,000	0,150	0,000	0,057	0,014	0,000	0,088	0,060	0,050	0,090	0,096	0,074	0,186	0,021	0,000	0,039	0,026	0,000	0,098	0,000	0,016	0,000	0,012	0,000	0,057	0,024	0,005	0,022	0,039	0,012	0,036	0,230	0,457	-0,488
Beclin 1 (H-300)	0,064	0,021	0,058	0,033	0,035	0,087	0,064	0,016	0,052	0,072	0,063	0,027	0,040	0,040	0,075	0,040	0,041	0,039	0,030	0,108	0,250	0,083	0,021	0,035	0,010	0,172	0,051	0,009	0,150	0,012	0,037	0,023	0,057	0,066	0,043	0,047	0,040	0,019	0,058	0,040	0,454	0,354
TFF2 mAb	0,042	0,035	0,090	0,032	0,068	0,088	0,093	0,085	0,103	0,110	0,058	0,088	0,061	0,021	0,124	0,075	0,073	0,063	0,046	0,095	0,044	0,056	0,098	0,082	0,027	0,030	0,062	0,111	0,032	0,066	0,080	0,084	0,074	0,106	0,055	0,042	0,078	0,086	0,025	0,054	0,442	-0,166
TGF-B mAb	0,026	0,000	0,077	0,073	0,003	0,089	0,000	0,000	0,000	0,101	0,035	0,000	0,000	0,281	0,036	0,031	0,020	0,049	0,029	0,037	0,145	0,023	0,077	0,089	0,098	0,038	0,042	0,002	0,070	0,051	0,045	0,115	0,014	0,028	0,028	0,025	0,048	0,097	0,089	0,073	0,439	0,426
Beclin 1 pAb	0,067	0,041	0,092	0,021	0,125	0,100	0,073	0,054	0,079	0,055	0,156	0,031	0,055	0,024	0,070	0,046	0,125	0,088	0,059	0,075	0,050	0,073	0,062	0,056	0,041	0,113	0,041	0,057	0,072	0,062	0,060	0,069	0,112	0,083	0,055	0,063	0,039	0,057	0,025	0,081	0,423	-0,177
4-1BB ligand/TNFSF9 mAb	0,035	0,052	0,081	0,036	0,048	0,103	0,097	0,048	0,073	0,044	0,027	0,059	0,072	0,075	0,093	0,056	0,037	0,081	0,078	0,106	0,041	0,102	0,080	0,049	0,090	0,034	0,107	0,084	0,060	0,058	0,111	0,035	0,064	0,092	0,081	0,064	0,050	0,124	0,064	0,064	0,407	0,153
CR1 (CD35)	0,038	0,043	0,060	0,035	0,061	0,059	0,066	0,076	0,051	0,044	0,068	0,051	0,077	0,022	0,056	0,071	0,072	0,177	0,054	0,074	0,044	0,038	0,110	0,071	0,127	0,101	0,050	0,096	0,138	0,076	0,090	0,052	0,096	0,065	0,049	0,040	0,075	0,043	0,027	0,030	0,407	0,189
Ubiquitin	0,028	0,071	0,064	0,225	0,036	0,096	0,034	0,070	0,067	0,055	0,042	0,044	0,043	0,031	0,120	0,061	0,063	0,034	0,044	0,058	0,031	0,037	0,039	0,035	0,033	0,244	0,039	0,027	0,064	0,028	0,038	0,041	0,051	0,032	0,060	0,045	0,031	0,040	0,035	0,086	0,402	-0,310
Midkine pAb	0,058	0,072	0,031	0,018	0,051	0,068	0,146	0,053	0,044	0,021	0,054	0,019	0,039	0,021	0,111	0,040	0,057	0,139	0,052	0,083	0,050	0,013	0,061	0,065	0,033	0,118	0,040	0,103	0,126	0,090	0,033	0,040	0,096	0,091	0,142	0,080	0,023	0,097	0,050	0,021	0,397	0,226
Reelin (E-5) mAb	0,095	0,080	0,079	0,070	0,085	0,072	0,061	0,099	0,048	0,029	0,054	0,109	0,091	0,029	0,058	0,118	0,049	0,067	0,060	0,086	0,048	0,087	0,068	0,062	0,052	0,050	0,077	0,012	0,099	0,082	0,029	0,035	0,070	0,077	0,079	0,041	0,052	0,153	0,076	0,047	0,389	-0,152
NAP2 pAb	0,038	0,062	0,076	0,047	0,075	0,103	0,097	0,105	0,034	0,093	0,096	0,069	0,090	0,028	0,050	0,101	0,051	0,070	0,066	0,099	0,041	0,057	0,081	0,050	0,035	0,060	0,107	0,070	0,075	0,063	0,110	0,044	0,078	0,066	0,095	0,026	0,040	0,106	0,083	0,025	0,388	-0,142
Raptor	0,023	0,052	0,082	0,054	0,001	0,078	0,000	0,087	0,000	0,038	0,145	0,064	0,011	0,110	0,118	0,011	0,051	0,020	0,111	0,062	0,006	0,075	0,058	0,000	0,073	0,000	0,023	0,077	0,000	0,000	0,143	0,000	0,129					0,171	0,023	0,058	0,386	-0,353
Abeta 42	0,051	0,022	0,028	0,025	0,036	0,100	0,094	0,047	0,057	0,047	0,054	0,064	0,044	0,162	0,077	0,039	0,026	0,028	0,084	0,021	0,097	0,101	0,052	0,047	0,018	0,051	0,038	0,036	0,167	0,089	0,209	0,061	0,074	0,041	0,068	0,028	0,038	0,028	0,021	0,049	0,375	0,258
C1r	0,100	0,064	0,175	0,063	0,099	0,128	0,035	0,082	0,041	0,032	0,139	0,020	0,014	0,030	0,038	0,035	0,038	0,037	0,025	0,105	0,054	0,147	0,025	0,051	0,158	0,059	0,101	0,023	0,058	0,015	0,025	0,094	0,029	0,029	0,045	0,022	0,057	0,000	0,071	0,013	0,373	-0,275
FGF3 mAb	0,063	0,067	0,061	0,050	0,094	0,123	0,129	0,064	0,044	0,062	0,073	0,061	0,068	0,032	0,118	0,053	0,055	0,039	0,043	0,037	0,056	0,057	0,087	0,129	0,083	0,050	0,073	0,148	0,038	0,117	0,047	0,080	0,102	0,109	0,069	0,060	0,036	0,033	0,056	0,033	0,365	0,163
C3aR	0,065	0,001	0,119	0,078	0,104	0,068	0,038	0,051	0,066	0,044	0,057	0,060	0,063	0,078	0,095	0,057	0,113	0,073	0,075	0,109	0,040	0,137	0,068	0,059	0,054	0,044	0,045	0,075	0,027	0,045	0,061	0,080	0,043	0,045	0,062	0,051	0,049	0,070	0,055	0,158	0,348	-0,155
Beclin 2	0,063	0,069	0,043	0,035	0,083	0,058	0,115	0,060	0,047	0,046	0,083	0,033	0,058	0,037	0,053	0,052	0,074	0,151	0,059	0,052	0,045	0,053	0,111	0,058	0,044	0,159	0,087	0,058	0,096	0,067	0,103	0,040	0,102	0,040	0,054	0,042	0,110	0,059	0,036	0,048	0,327	0,152
MBL	0,052	0,031	0,040	0,095	0,142	0,074	0,076	0,101	0,071	0,071	0,107	0,056	0,075	0,036	0,091	0,054	0,033	0,050	0,087	0,071	0,041	0,043	0,048	0,039	0,048	0,092	0,096	0,061	0,071	0,065	0,056	0,075	0,079	0,080	0,044	0,036	0,041	0,091	0,053	0,326	-0,120	
Factor V pAb	0,083	0,061	0,073	0,050	0,084	0,065	0,075	0,083	0,055	0,073	0,068	0,069	0,105	0,029	0,089	0,093	0,079	0,077	0,067	0,091	0,058	0,051	0,070	0,069	0,048	0,084	0,086	0,061	0,067	0,064	0,068	0,066	0,084	0,087	0,095	0,040	0,067	0,112	0,087	0,063	0,326	-0,080
Nanog pAb	0,182	0,094	0,022	0,005	0,022	0,043	0,188	0,060	0,067	0,042	0,115	0,021	0,043	0,005	0,038	0,017	0,092	0,122	0,052	0,025	0,052	0,044	0,010	0,012	0,103	0,054	0,063	0,013	0,104	0,068	0,030	0,120	0,027	0,131	0,059	0,033	0,021	0,008	0,022	0,077	0,309	-0,257
C1Inhib	0,056	0,043	0,059	0,065	0,088	0,074	0,068	0,120	0,048	0,085	0,075	0,074	0,084	0,023	0,072	0,093	0,057	0,088	0,083	0,094	0,036	0,046	0,060	0,072	0,049	0,043	0,073	0,056	0,076	0,048	0,073	0,089	0,094	0,070	0,096	0,054	0,054	0,131	0,102	0,042	0,308	-0,107
Reelin (G-20) pAb	0,075	0,048	0,061	0,051	0,064	0,070	0,064	0,096	0,058	0,040	0,051	0,112	0,091	0,033	0,075	0,136	0,050	0,052	0,061	0,110	0,036	0,059	0,048	0,038	0,035	0,058	0,016	0,133	0,040	0,033	0,108	0,089	0,092	0,041	0,041	0,161	0,060	0,040			0,307	-0,154
Rab5	0,052	0,046	0,040	0,073	0,062	0,063	0,061	0,059	0,041	0,073	0,053	0,065	0,048	0,034	0,054	0,065	0,034	0,062	0,277	0,081	0,020	0,038	0,057	0,076	0,072	0,033	0,079	0,050	0,064	0,050	0,083	0,083	0,074	0,062	0,072	0,027	0,041	0,077	0,058	0,063	0,297	-0,188
Wnt3a pAb	0,009	0,103	0,036	0,017	0,042	0,046	0,021	0,060	0,040	0,026	0,088	0,044	0,115	0,012	0,132	0,032	0,060	0,048	0,037	0,122	0,029	0,033	0,033	0,025	0,012	0,037	0,029	0,052	0,038	0,044	0,079	0,074	0,042	0,111	0,073	0,189	0,081	0,198	0,048	0,050	0,289	0,226
Rictor	0,020	0,062	0,124	0,125	0,016	0,060	0,000	0,051	0,000	0,102	0,073	0,086	0,107	0,002	0,138	0,095	0,050	0,076	0,000	0,030	0,114	0,011	0,034	0,011	0,062	0,012	0,036	0,000	0,000	0,014	0,046	0,035	0,067	0,054	0,057	0,029	0,223	0,000	0,051	0,057	0,288	-0,258
Beclin 1 (NT)	0,078	0,000	0,055	0,022	0,066	0,076	0,049	0,052	0,074	0,074	0,143	0,054	0,088	0,039	0,063	0,046	0,205	0,039	0,063	0,057	0,025	0,032	0,053	0,045	0,032	0,089	0,020	0,034	0,065	0,069	0,054	0,057	0,143	0,096	0,041	0,048	0,061	0,098	0,034	0,101	0,266	-0,167
C1s	0,040	0,063	0,029	0,045	0,044	0,068	0,035	0,184	0,038	0,043	0,062	0,049	0,044	0,020	0,053	0,055	0,055	0,090	0,050	0,078	0,037	0,042	0,047	0,056	0,084	0,026	0,064	0,030	0,082	0,042	0,080	0,250	0,058	0,077	0,080	0,023	0,047	0,080	0,058	0,043	0,260	0,187
Neuropeptide Y pAb	0,093	0,098	0,096	0,032	0,156	0,035	0,127	0,069	0,027	0,040	0,173	0,027	0,045	0,039	0,032	0,034	0,068	0,044	0,061	0,057	0,041	0,050	0,079	0,069	0,046	0,166	0,066	0,064	0,062	0,078	0,043	0,051	0,032	0,038	0,033	0,058					0,253	-0,154
Factor H	0,061	0,045	0,074	0,038	0,104	0,064	0,081	0,086	0,056	0,079	0,093	0,086	0,098	0,025	0,095	0,096	0,054	0,059	0,084	0,061	0,035	0,057	0,058	0,087	0,037	0,059	0,071	0,086	0,082	0,073	0,077	0,065	0,083	0,070	0,079	0,035	0,042	0,141	0,081	0,034	0,246	-0,089
alpha 1 antitrypsin pAb	0,089	0,084	0,059	0,041	0,066	0,094	0,081	0,077	0,046	0,058	0,069	0,054	0,074	0,051	0,077	0,064	0,053	0,111	0,051	0,084	0,065	0,047	0,101	0,061	0,128	0,048	0,076	0,052	0,080	0,069	0,062	0,080	0,066	0,097	0,081	0,035	0,059	0,064	0,082	0,099	0,240	0,073
Abeta 17-24	0,016	0,034	0,046	0,049	0,037	0,069	0,041	0,031	0,074	0,057	0,022	0,064	0,025	0,041	0,052	0,036	0,056	0,064	0,032	0,107	0,042	0,033	0,043	0,042	0,040	0,018	0,067	0,122	0,047	0,058	0,111	0,119	0,034	0,065	0,035	0,050	0,050	0,031	0,037	0,033	0,231	-0,208
AGRP pAb	0,000	0,023	0,043	0,028	0,039	0,079	0,015	0,095	0,133	0,085	0,025	0,073	0,047	0,020	0,077	0,098	0,053	0,055	0,090	0,036	0,036	0,000	0,035	0,052	0,050	0,057	0,058	0,021	0,039	0,026	0,025	0,049	0,102	0,096	0,103	0,238	0,098	0,027	0,110	0,069	0,230	0,185
Beta-Defensin 3 pAb	0,127	0,091	0,052	0,019	0,064	0,061	0,205	0,053	0,030	0,047	0,086	0,031	0,063	0,009	0,044	0,019	0,058	0,110	0,045	0,078	0,036	0,025	0,040	0,040	0,086	0,081	0,031	0,016	0,053	0,086	0,033	0,094	0,043	0,167	0,086	0,031	0,051	0,007	0,030	0,113	0,225	-0,168
C2	0,085	0,060	0,064	0,047	0,090	0,066	0,082	0,102	0,054	0,054	0,093	0,060	0,100	0,024	0,071	0,071	0,070	0,073	0,079	0,098	0,051	0,046	0,052	0,053	0,065	0,065	0,044	0,083	0,059	0,085	0,063	0,056	0,076	0,067	0,136	0,085	0,036	0,060	0,108	0,087	0,223	-0,076
PHF Tau mAb (AT270)	0,004	0,000	0,048	0,020	0,000	0,032	0,000	0,018	0,000	0,401	0,033	0,080	0,000	0,043	0,022	0,017	0,004	0,000	0,032	0,000	0,017	0,155	0,021	0,005	0,006	0,003	0,052	0,000	0,010	0,034	0,083	0,019	0,011	0,022	0,023	0,025	0,001	0,000		0,051	0,211	-0,489
Fibrinogen	0,153	0,068	0,089	0,044	0,017	0,079	0,005	0,030	0,056	0,116	0,035	0,122	0,017	0,039	0,059	0,064	0,043	0,040	0,047	0,049	0,148	0,132	0,100	0,019	0,013	0,049	0,085	0,010	0,084	0,044	0,055	0,085	0,101	0,023	0,128	0,043	0,015	0,033	0,103	0,028	0,203	0,148
Ghrelin mAb	0,108	0,034	0,064	0,037	0,078	0,092	0,118	0,050	0,087	0,067	0,069	0,064	0,073	0,061	0,076	0,051	0,072	0,035	0,045	0,038	0,065	0,125	0,050	0,075	0,030	0,072	0,093	0,130	0,058	0,084	0,025	0,032	0,096	0,056	0,084	0,025	0,054	0,110	0,024	0,024	0,194	0,090
MASP2 pAb	0,079	0,232	0,014	0,049	0,074	0,039	0,147	0,041	0,030	0,043	0,092	0,046	0,039	0,039	0,054	0,081	0,055	0,076	0,059	0,038	0,065	0,105	0,091	0,050	0,032	0,053	0,087	0,042	0,074	0,049	0,054	0,012	0,076	0,056	0,058	0,054	0,058	0,087	0,043	0,073	0,186	-0,123
Defensin alpha 1 pAb	0,003	0,002	0,003	0,002	0,004	0,002	0,003	0,004	0,002	0,003	0,003	0,003	0,004	0,008	0,003	0,003	0,002	0,002	0,291	0,002	0,001	0,002	0,002	0,003	0,001	0,002	0,003	0,003	0,003	0,002	0,002	0,002	0,002	0,003	0,003	0,001	0,262	0,005	0,003	0,250	0,185	0,665
CD59 (MEM43 epitope)	0,049	0,094	0,056	0,050	0,105	0,094	0,073	0,064	0,096	0,056	0,064	0,061	0,078	0,018	0,077	0,066	0,071	0,042	0,048	0,082	0,025	0,039	0,058	0,074	0,033	0,049	0,070	0,132	0,079	0,106	0,062	0,067	0,077	0,064	0,088	0,135	0,067	0,101	0,040	0,051	0,184	0,077
Progranulin pAb (Clone 1)	0,087	0,236	0,201	0,081	0,060	0,032	0,000	0,081	0,000	0,000	0,000	0,000	0,001	0,003	0,000	0,034	0,000	0,000	0,057	0,000	0,187	0,084	0,151	0,022	0,029	0,000	0,118	0,102	0,000	0,000	0,000	0,000	0,000	0,000	0,000	0,000	0,000	0,001	0,000	0,000	0,183	-0,332

Protein																																									
LAP (TGF-B1)	0,009	0,179	0,021	0,005	0,000	0,073	0,000	0,009	0,016	0,000	0,000	0,025	0,000	0,002	0,011	0,039	0,015	0,101	0,032	0,105	0,044	0,012	0,016	0,000	0,013	0,020	0,038	0,013	0,000	0,000	0,000	0,000	0,059	0,000	0,097	0,345	0,123	0,000	0,020	0,025	0,183	0,364
WISP2 pAb	0,061	0,055	0,060	0,041	0,063	0,081	0,077	0,072	0,046	0,054	0,106	0,056	0,059	0,032	0,070	0,074	0,127	0,113	0,048	0,073	0,074	0,063	0,085	0,048	0,044	0,110	0,063	0,059	0,079	0,054	0,088	0,046	0,132	0,070	0,073	0,081	0,048	0,081	0,182	0,067
Osteopontin mAb	0,077	0,042	0,065	0,022	0,067	0,085	0,073	0,050	0,040	0,068	0,048	0,107	0,056	0,091	0,076	0,068	0,039	0,092	0,074	0,091	0,053	0,066	0,100	0,045	0,036	0,051	0,054	0,047	0,080	0,049	0,111	0,179	0,087	0,070	0,071	0,045	0,058	0,071	0,067	0,068	0,182	0,081
p-mTOR Ser2481	0,000	0,000	0,047	0,004	0,046	0,047	0,173	0,164	0,139	0,000	0,000	0,020	0,000	0,000	0,000	0,007	0,000	0,000	0,000	0,000	0,007	0,008	0,001	0,047	0,013	0,023	0,001	0,075	0,075	0,236	0,241	0,012	0,008	0,000	0,016	0,000	0,000	0,001	0,070	0,000	0,182	0,359
Neurexin II alpha pAb	0,057	0,191	0,060	0,101	0,287	0,017	0,040	0,001	0,000	0,000	0,025	0,031	0,003	0,046	0,024	0,003	0,009	0,017	0,052	0,005	0,047	0,059	0,074	0,140	0,001	0,101	0,065	0,100	0,000	0,000	0,000	0,052	0,006	0,002	0,020	0,109	0,023	0,000	0,004	0,000	0,179	-0,272
Neprilysin pAb	0,140	0,127	0,045	0,024	0,062	0,059	0,112	0,062	0,053	0,034	0,063	0,024	0,053	0,011	0,028	0,031	0,065	0,126	0,021	0,056	0,067	0,024	0,034	0,041	0,165	0,078	0,095	0,037	0,092	0,074	0,047	0,086	0,035	0,152	0,081	0,031	0,047	0,008	0,022	0,088	0,179	0,127
Prion protein Prp pAb	0,069	0,018	0,080	0,036	0,083	0,086	0,063	0,042	0,094	0,051	0,075	0,049	0,100	0,140	0,094	0,064	0,055	0,042	0,095	0,089	0,071	0,074	0,050	0,073	0,044	0,065	0,063	0,066	0,084	0,072	0,063	0,065	0,052	0,071	0,103	0,065	0,036	0,082	0,044	0,117	0,169	-0,066
Tenascin D pAb	0,092	0,069	0,061	0,045	0,132	0,053	0,165	0,088	0,041	0,042	0,049	0,039	0,068	0,012	0,038	0,066	0,055	0,077	0,055	0,059	0,058	0,046	0,094	0,054	0,089	0,066	0,092	0,108	0,063	0,061	0,118	0,059	0,056	0,053	0,044	0,020	0,096	0,104	0,040	0,065	0,167	0,086
Neurexin III alpha pAb	0,052	0,166	0,030	0,037	0,057	0,078	0,048	0,034	0,106	0,020	0,055	0,056	0,095	0,019	0,073	0,070	0,038	0,045	0,063	0,148	0,030	0,042	0,030	0,053	0,020	0,036	0,070	0,075	0,042	0,047	0,023	0,124	0,050	0,039	0,059	0,206	0,091	0,049	0,045	0,053	0,166	-0,124
CR2 (CD21)	0,035	0,048	0,068	0,169	0,036	0,120	0,026	0,082	0,023	0,045	0,033	0,050	0,020	0,166	0,057	0,069	0,038	0,048	0,055	0,043	0,021	0,027	0,097	0,041	0,045	0,022	0,047	0,000	0,126	0,044	0,065	0,000	0,072	0,018	0,040	0,043	0,056	0,013	0,058	0,110	0,160	-0,142
MIS/AMH Propeptide mAb	0,059	0,055	0,081	0,039	0,120	0,064	0,082	0,063	0,069	0,064	0,063	0,064	0,128	0,018	0,102	0,068	0,072	0,079	0,063	0,074	0,039	0,046	0,077	0,108	0,046	0,063	0,036	0,091	0,088	0,079	0,076	0,080	0,050	0,084	0,066	0,049	0,060	0,119	0,058	0,054	0,159	-0,061
beta-amyloid 33-40	0,069	0,053	0,053	0,046	0,107	0,064	0,065	0,078	0,053	0,077	0,097	0,072	0,099	0,030	0,072	0,101	0,053	0,070	0,097	0,078	0,037	0,063	0,066	0,075	0,037	0,052	0,093	0,070	0,083	0,061	0,083	0,071	0,077	0,071	0,091	0,043	0,045	0,138	0,076	0,044	0,158	-0,057
Progranulin pAb (Clone 3)	0,056	0,058	0,078	0,084	0,052	0,059	0,095	0,057	0,053	0,058	0,108	0,038	0,050	0,032	0,082	0,087	0,101	0,059	0,065	0,091	0,093	0,092	0,055	0,063	0,055	0,137	0,046	0,033	0,099	0,046	0,061	0,061	0,125	0,060	0,054	0,082	0,057	0,059	0,055	0,087	0,152	0,061
Neuroligin 4 mAb	0,084	0,013	0,064	0,013	0,010	0,038	0,000	0,007	0,092	0,082	0,038	0,067	0,026	0,024	0,051	0,012	0,240	0,064	0,045	0,090	0,028	0,070	0,001	0,024	0,011	0,066	0,088	0,011	0,081	0,048	0,026	0,256	0,050	0,017	0,019	0,030	0,009	0,000	0,005	0,091	0,146	-0,187
TGF-B1 mAb	0,052	0,011	0,033	0,026	0,056	0,083	0,021	0,023	0,073	0,028	0,041	0,022	0,145	0,257	0,067	0,028	0,015	0,035	0,046	0,005	0,043	0,104	0,078	0,037	0,027	0,077	0,091	0,035	0,033	0,165	0,070	0,050	0,045	0,098	0,036	0,022	0,028	0,024	0,023	0,094	0,145	0,144
LC3B	0,094	0,000	0,000	0,021	0,143	0,096	0,135	0,000	0,000	0,000	0,050	0,144	0,002	0,067	0,027	0,051	0,028	0,187	0,000	0,000	0,086	0,000	0,000	0,000	0,047	0,128	0,156	0,000	0,041	0,026	0,068	0,108	0,023	0,084	0,075	0,002	0,025	0,090	0,139	-0,172		
SPARC mAb	0,021	0,035	0,050	0,033	0,033	0,054	0,032	0,049	0,037	0,061	0,063	0,041	0,085	0,036	0,093	0,118	0,085	0,095	0,195	0,113	0,073	0,026	0,062	0,024	0,056	0,043	0,039	0,032	0,093	0,080	0,103	0,090	0,080	0,042	0,133	0,037	0,062	0,085	0,059	0,030	0,135	-0,088
LC3B	0,000	0,001	0,198	0,000	0,000	0,000	0,000	0,000	0,219	0,078	0,000	0,000	0,037	0,000	0,000	0,000	0,000	0,072	0,000	0,043	0,112	0,000	0,106	0,085	0,090	0,255	0,000	0,000	0,000	0,090	0,000	0,000	0,000	0,000	0,000	0,000	0,000	0,000	0,000	0,000	0,132	0,283
Wnt1 pAb	0,240	0,112	0,000	0,094	0,079	0,047	0,000	0,000	0,024	0,077	0,000	0,076	0,000	0,001	0,012	0,059	0,112	0,062	0,017	0,025	0,155	0,028	0,083	0,000	0,041	0,003	0,000	0,000	0,069	0,007	0,029	0,016	0,145	0,022	0,004	0,029	0,043	0,001	0,147	0,104	0,125	-0,168
HHV-8 viral MIP-II pAb	0,062	0,086	0,041	0,031	0,059	0,096	0,092	0,061	0,063	0,045	0,067	0,058	0,071	0,069	0,083	0,051	0,060	0,126	0,061	0,087	0,046	0,040	0,054	0,037	0,174	0,049	0,056	0,028	0,076	0,028	0,058	0,111	0,043	0,096	0,073	0,034	0,062	0,067	0,030	0,142	0,123	-0,068
A222	0,042	0,002	0,097	0,013	0,040	0,044	0,052	0,140	0,050	0,054	0,139	0,033	0,161	0,113	0,106	0,054	0,046	0,006	0,027	0,010	0,031	0,056	0,012	0,044	0,021	0,041	0,032	0,032	0,091	0,051	0,081	0,131	0,004	0,100	0,135	0,058	0,010	0,131	0,028	0,053	0,120	-0,107
Somatostatin pAb	0,136	0,123	0,054	0,064	0,060	0,066	0,069	0,032	0,057	0,052	0,041	0,107	0,031	0,020	0,035	0,094	0,096	0,063	0,060	0,107	0,087	0,167	0,037	0,056	0,028	0,043	0,061	0,064	0,103	0,031	0,033	0,033	0,092	0,068	0,062	0,034	0,050	0,094	0,053	0,092	0,117	-0,070
Progranulin pAb	0,055	0,046	0,025	0,024	0,081	0,060	0,025	0,044	0,015	0,033	0,058	0,026	0,038	0,010	0,029	0,055	0,341	0,053	0,044	0,035	0,031	0,061	0,138	0,066	0,056	0,037	0,076	0,052	0,052	0,044	0,053	0,086	0,039	0,042	0,040	0,022	0,035	0,025	0,034	0,011	0,113	-0,135
Pleiotrophin pAb	0,062	0,167	0,029	0,017	0,011	0,167	0,026	0,064	0,072	0,044	0,027	0,023	0,028	0,009	0,084	0,062	0,044	0,169	0,019	0,022	0,032	0,005	0,068	0,010	0,120	0,055	0,029	0,000	0,161	0,014	0,050	0,119	0,032	0,103	0,105	0,021	0,065	0,000	0,035	0,080	0,113	-0,121
alpha-synuclein pAb	0,112	0,072	0,036	0,027	0,076	0,058	0,107	0,096	0,051	0,038	0,091	0,045	0,068	0,014	0,046	0,050	0,056	0,133	0,059	0,064	0,027	0,039	0,057	0,039	0,129	0,061	0,054	0,030	0,116	0,078	0,048	0,112	0,063	0,140	0,079	0,035	0,054	0,053	0,040	0,103	0,113	0,065
Neuroligin 1 mAb	0,068	0,001	0,002	0,001	0,002	0,046	0,002	0,002	0,001	0,120	0,114	0,001	0,002	0,000	0,002	0,210	0,001	0,013	0,221	0,001	0,125	0,001	0,001	0,067	0,041	0,001	0,001	0,001	0,002	0,001	0,001	0,001	0,001	0,001	0,022	0,022	0,040	0,003	0,182	0,177	0,113	-0,230
Factor D	0,027	0,071	0,047	0,048	0,046	0,098	0,021	0,282	0,038	0,056	0,036	0,045	0,034	0,027	0,058	0,065	0,038	0,054	0,019	0,071	0,035	0,022	0,039	0,035	0,051	0,035	0,078	0,155	0,032	0,020	0,088	0,064	0,072	0,050	0,072	0,027	0,053	0,051	0,044	0,031	0,110	-0,110
Otoraplin pAb	0,147	0,103	0,034	0,017	0,063	0,051	0,172	0,061	0,051	0,034	0,111	0,009	0,101	0,015	0,054	0,014	0,079	0,072	0,029	0,044	0,040	0,026	0,026	0,033	0,080	0,077	0,032	0,029	0,084	0,098	0,051	0,090	0,030	0,173	0,098	0,035	0,030	0,063	0,012	0,080	0,108	-0,088
Nodal pAb	0,153	0,037	0,141	0,093	0,035	0,022	0,181	0,042	0,038	0,054	0,081	0,053	0,033	0,005	0,048	0,019	0,051	0,040	0,044	0,024	0,034	0,051	0,059	0,070	0,055	0,148	0,039	0,100	0,017	0,025	0,028	0,035	0,050	0,019	0,038	0,190	0,093	0,000	0,032	0,027	0,108	-0,105
Factor XIIIa mAb	0,010	0,055	0,028	0,021	0,011	0,026	0,003	0,009	0,019	0,011	0,207	0,188	0,068	0,016	0,026	0,067	0,018	0,027	0,045	0,193	0,078	0,025	0,019	0,000	0,047	0,001	0,008	0,081	0,031	0,017	0,091	0,157	0,050	0,071	0,045	0,003	0,053	0,137	0,108	-0,143		
Presenilin-1	0,215	0,106	0,083	0,223	0,033	0,033	0,000	0,000	0,022	0,044	0,024	0,075	0,000	0,000	0,000	0,000	0,000	0,000	0,000	0,248	0,070	0,087	0,076	0,055	0,013	0,047	0,000	0,009	0,050	0,023	0,024	0,044	0,000	0,000	0,000	0,000	0,000	0,000	0,108	-0,202		
p-mTOR Ser2448	0,002	0,002	0,016	0,287	0,003	0,002	0,003	0,003	0,002	0,002	0,003	0,002	0,003	0,001	0,002	0,002	0,002	0,002	0,003	0,002	0,001	0,002	0,002	0,003	0,356	0,002	0,002	0,002	0,002	0,002	0,002	0,002	0,002	0,002	0,001	0,001	0,004	0,080	0,001	0,107	0,457	
rC5a	0,068	0,000	0,095	0,059	0,122	0,047	0,099	0,081	0,067	0,065	0,116	0,076	0,082	0,025	0,063	0,074	0,057	0,066	0,063	0,091	0,046	0,055	0,050	0,072	0,055	0,080	0,066	0,074	0,072	0,072	0,078	0,051	0,087	0,070	0,082	0,056	0,045	0,118	0,092	0,056	0,105	-0,042
DLL1 pAb	0,060	0,047	0,061	0,034	0,072	0,049	0,111	0,028	0,072	0,038	0,090	0,035	0,074	0,023	0,083	0,044	0,143	0,055	0,107	0,057	0,062	0,064	0,062	0,049	0,036	0,204	0,041	0,053	0,071	0,063	0,063	0,043	0,077	0,101	0,061	0,057	0,040	0,079	0,029	0,087	0,102	0,063
CCL23/MPIF-1 mAb	0,037	0,000	0,063	0,011	0,015	0,098	0,004	0,025	0,047	0,057	0,068	0,048	0,010	0,295	0,064	0,007	0,035	0,068	0,090	0,025	0,000	0,075	0,027	0,014	0,053	0,056	0,017	0,084	0,047	0,073	0,064	0,047	0,035	0,095	0,041	0,067	0,025	0,021	0,160	0,092	-0,108	
TGF-B1 pAb (0.5 mg/ml)	0,047	0,057	0,049	0,031	0,072	0,070	0,116	0,050	0,064	0,047	0,077	0,038	0,056	0,041	0,058	0,068	0,140	0,077	0,057	0,077	0,054	0,050	0,056	0,048	0,040	0,218	0,069	0,056	0,099	0,049	0,076	0,040	0,099	0,055	0,058	0,061	0,049	0,041	0,037	0,085	0,091	0,056
apoE, gHE3-18	0,227	0,166	0,178	0,109	0,066	0,000	0,000	0,000	0,000	0,000	0,015	0,000	0,000	0,001	0,000	0,000	0,000	0,000	0,000	0,000	0,175	0,147	0,132	0,119	0,066	0,000	0,000	0,000	0,000	0,000	0,000	0,021	0,000	0,000	0,000	0,001	0,000	0,000	0,000	0,000	0,091	-0,203
Phospho alpha synuclein pAb	0,002	0,002	0,003	0,002	0,003	0,002	0,003	0,003	0,002	0,189	0,003	0,148	0,003	0,001	0,002	0,002	0,002	0,063	0,003	0,002	0,001	0,002	0,036	0,003	0,097	0,002	0,002	0,002	0,002	0,002	0,002	0,002	0,002	0,002	0,379	0,001	0,089	0,311				
MASP1 pAb	0,060	0,101	0,058	0,041	0,084	0,041	0,136	0,060	0,021	0,049	0,083	0,067	0,082	0,060	0,023	0,116	0,060	0,080	0,097	0,062	0,078	0,072	0,050	0,066	0,039	0,030	0,065	0,028	0,075	0,065	0,104	0,014	0,090	0,091	0,096	0,040	0,068	0,123	0,061	0,088	0,079	-0,040
Osteopontin pAb	0,002	0,132	0,002	0,001	0,003	0,002	0,002	0,003	0,002	0,002	0,003	0,308	0,003	0,001	0,002	0,002	0,002	0,102	0,003	0,002	0,133	0,002	0,002	0,002	0,001	0,001	0,002	0,002	0,002	0,002	0,002	0,002	0,002	0,002	0,053	0,001	0,001	0,004	0,270	0,001	0,078	-0,251
Atg5	0,051	0,026	0,042	0,043	0,034	0,124	0,040	0,052	0,093	0,070	0,055	0,039	0,165	0,017	0,054	0,050	0,051	0,055	0,041	0,100	0,031	0,038	0,022	0,028	0,016	0,035	0,034	0,074	0,076	0,071	0,090	0,059	0,034	0,068	0,266	0,054	0,070	0,030	0,076	-0,073		
SHBG mAb	0,069	0,044	0,098	0,046	0,087	0,050	0,117	0,111	0,080	0,075	0,089	0,071	0,074	0,029	0,083	0,065	0,050	0,064	0,066	0,029	0,042	0,057	0,072	0,095	0,032	0,052	0,095	0,079	0,072	0,051	0,095	0,068	0,074	0,062	0,087	0,035	0,035	0,148	0,072	0,041	0,090	-0,035
N3pE-3	0,083	0,105	0,094	0,030	0,095	0,037	0,074	0,044	0,035	0,040	0,119	0,034	0,057	0,029	0,045	0,055	0,173	0,093	0,053	0,052	0,109	0,061	0,070	0,031	0,034	0,124	0,056	0,066	0,073	0,041	0,081	0,029	0,115	0,082	0,053	0,058	0,075	0,067	0,034	0,047	0,073	-0,044
C9	0,071	0,033	0,067	0,046	0,075	0,067	0,116	0,066	0,078	0,062	0,065	0,047	0,091	0,025	0,066	0,089	0,097	0,044	0,117	0,078	0,044	0,033	0,034	0,043	0,032	0,068	0,048	0,084	0,112	0,092	0,084	0,044	0,104	0,072	0,108	0,057	0,071	0,102	0,080	0,056	0,071	-0,032
Adiponectin pAb	0,031	0,066	0,147	0,094	0,001	0,103	0,017	0,078	0,001	0,096	0,001	0,081	0,001	0,007	0,001	0,001	0,001	0,000	0,162	0,067	0,080	0,239	0,099	0,001	0,045	0,099	0,014	0,001	0,001	0,001	0,083	0,000	0,019	0,001	0,151	0,036	0,012	0,001	0,001	0,018	0,052	-0,083
M-CSF	0,004	0,000	0,053	0,002	0,000	0,069	0,000	0,015	0,050	0,019	0,026	0,038	0,158	0,170	0,130	0,169	0,051	0,009	0,113	0,015	0,068	0,029	0,017	0,000	0,010	0,016	0,021	0,061	0,035	0,038	0,045	0,108	0,080	0,124	0,110	0,045	0,150	0,029	0,044	0,017	0,052	-0,062
Abeta 13-28 (22D12)	0,060	0,046	0,045	0,044	0,101	0,115	0,077	0,052	0,066	0,053	0,071	0,047	0,081	0,130	0,087	0,076	0,044	0,053	0,088	0,061	0,044	0,105	0,074	0,143	0,035	0,051	0,063	0,059	0,051	0,056	0,078	0,089	0,052	0,062	0,075	0,045	0,099	0,057	0,084	0,053	0,050	-0,023
TARDBP pAb	0,058	0,001	0,002	0,001	0,002	0,051	0,002	0,002	0,001	0,002	0,002	0,001	0,002	0,000	0,002	0,293	0,001	0,150	0,002	0,001	0,069	0,001	0,001	0,002	0,001	0,001	0,001	0,001	0,002	0,001	0,001	0,001	0,001	0,001	0,001	0,001	0,001	0,267	0,003	0,160	0,048	-0,153
Pan-specific TGF-B neutralizing	0,066	0,050	0,036	0,033	0,068	0,064	0,127	0,052	0,056	0,051	0,081	0,043	0,057	0,031	0,063	0,053	0,146	0,033	0,072	0,059	0,037	0,055	0,050	0,048	0,028	0,073	0,048	0,079	0,039	0,064	0,047	0,050	0,034	0,035	0,045	0,045	-0,038					
CD59	0,053	0,000	0,074	0,060	0,098	0,073	0,078	0,079	0,064	0,077	0,069	0,076	0,082	0,041	0,076	0,097	0,067	0,057	0,089	0,092	0,043	0,075	0,061	0,102	0,048	0,054	0,078	0,069	0,086	0,104	0,079	0,061	0,092	0,081	0,077	0,043	0,049	0,104	0,053	0,063	0,044	0,017
Ferritin mAb	0,039	0,083	0,071	0,060	0,081	0,107	0,159	0,077	0,068	0,042	0,043	0,044	0,042	0,100	0,061	0,085	0,044	0,049	0,038	0,068	0,062	0,067	0,102	0,066	0,125	0,066	0,116	0,038	0,124	0,040	0,057	0,026	0,050	0,040	0,088	0,032	0,047	0,082	0,042	0,065	0,043	-0,024
Neuroligin 2 pAb	0,088	0,082	0,109	0,000	0,015	0,082	0,007	0,017	0,151	0,013	0,022	0,050	0,017	0,005	0,013	0,008	0,002	0,017	0,062	0,087	0,027	0,137	0,000	0,071	0,000	0,042	0,027	0,031	0,000	0,000	0,000	0,000	0,031	0,000	0,028	0,034	0,069	0,000	0,021	0,040	0,037	-0,071
CD15 mAb	0,044	0,032	0,075	0,047	0,067	0,098	0,038	0,044	0,042	0,068	0,088	0,068	0,199	0,018	0,081	0,057	0,057	0,044	0,054	0,063	0,045	0,074	0,032	0,042	0,046	0,033	0,120	0,036	0,060	0,029	0,075	0,129	0,121	0,046	0,068	0,029	0,035	0,153	0,041	0,054	0,026	-0,020
Chordin pAb	0,066	0,056	0,028	0,106	0,048	0,078	0,079	0,036	0,075	0,056	0,052	0,034	0,068	0,025	0,119	0,032	0,059	0,021	0,052	0,034	0,142	0,152	0,031	0,053	0,020	0,272	0,042	0,026	0,045	0,023	0,048	0,043	0,043	0,050	0,042	0,044	0,010	0,011	0,025	0,025	0,026	0,028
BMP-10 propeptide pAb	0,161	0,000	0,052	0,024	0,059	0,074	0,083	0,086	0,070	0,069	0,072	0,026	0,120	0,009	0,041	0,035	0,074	0,111	0,033	0,051	0,067	0,030	0,046	0,038	0,087	0,028	0,078	0,040	0,042	0,092	0,088	0,022	0,069	0,068	0,019	0,153	0,057	0,026	0,056	0,064	0,024	0,019
DAF (CD55)	0,079	0,009	0,122	0,032	0,020	0,073	0,019	0,025	0,067	0,018	0,112	0,027	0,067	0,075	0,115	0,065	0,132	0,098	0,064	0,069	0,098	0,150	0,044	0,067	0,033	0,031	0,049	0,017	0,042	0,075	0,020	0,050	0,057	0,042	0,071	0,097	0,105	0,042	0,071	0,129	0,021	-0,016
beta 2 microglobulin mAb	0,039	0,000	0,056	0,073	0,085	0,085	0,059	0,065	0,075	0,080	0,083	0,061	0,100	0,055	0,103	0,086	0,074	0,054	0,073	0,081	0,030	0,059	0,036	0,042	0,050	0,079	0,051	0,074	0,068	0,081	0,083	0,083	0,099	0,098	0,065	0,048	0,144	0,073	0,069	0,017	0,008	
WISP3 pAb	0,034	0,123	0,058	0,062	0,063	0,108	0,043	0,060	0,055	0,055	0,042	0,075	0,058	0,041	0,069	0,110	0,052	0,065	0,044	0,152	0,044	0,027	0,070	0,059	0,038	0,050	0,079	0,050	0,096	0,058	0,063	0,088	0,093	0,042	0,086	0,114	0,102	0,044	0,017	-0,009		
Proteoglycan 1 mAb	0,115	0,001	0,144	0,209	0,142	0,044	0,027	0,069	0,027	0,053	0,020	0,024	0,023	0,008	0,000	0,000	0,000	0,000	0,000	0,130	0,207	0,132	0,116	0,062	0,024	0,060	0,035	0,052	0,015	0,000	0,050	0,022	0,016	0,000	0,000	0,000	0,000	0,010	0,017			
FABP (10-E1) mAb	0,040	0,033	0,090	0,040	0,056	0,091	0,046	0,051	0,109	0,049	0,063	0,061	0,048	0,131	0,106	0,087	0,074	0,053	0,083	0,091	0,061	0,063	0,062	0,071	0,057	0,078	0,067	0,047	0,106	0,056	0,067	0,083	0,057	0,071	0,101	0,067	0,073	0,056	0,053	0,109	0,009	0,004
BMP8b mAb	0,134	0,028	0,080	0,025	0,036	0,096	0,030	0,055	0,064	0,055	0,032	0,090	0,038	0,054	0,065	0,042	0,050	0,033	0,053	0,208	0,076	0,096	0,104	0,061	0,030	0,079	0,059	0,110	0,045	0,027	0,059	0,113	0,120	0,051	0,047	0,034	0,057	0,022	0,020	0,064	0,009	0,007
Myostatin mAb	0,039	0,037	0,077	0,072	0,000	0,111	0,000	0,024	0,106	0,047	0,036	0,078	0,008	0,182	0,129	0,070	0,033	0,060	0,041	0,046	0,119	0,159	0,089	0,022	0,051	0,019	0,024	0,070	0,016	0,031	0,096	0,071	0,074	0,044	0,052	0,046	0,023	0,000	0,118	0,081	0,008	0,007

Table S1. Cell-to-cell communicome array (185 proteins)

Patients	ELISA SIRT2 (ng/ml)	Global brain image assessment (cm^3)	Medial orbitofrontal cortex brain image assessment (a.u.)	Evaluation of CNS functioning (NPZ12)
Early-cART1_t0	1.875	818.930	0.447	-0.125
Early-cART2_t0	0.796	630.188	0.329	0.842
Early-cART3_t0	1.231	631.082	0.304	0.592
Early-cART4_t0	1.592	760.060	0.382	0.075
Early-cART5_t0	0.490	673.883	0.370	0.967
Early-cART6_t0	0.837	739.790	0.350	-0.200
Early-cART7_t0	0.969	793.197	0.460	0.367
Early-cART8_t0	2.996	697.289	0.401	0.000
Early-cART9_t0	0.912	703.614	0.382	0.575
Early-cART1_t48	1.814	833.048	0.424	-0.533
Early-cART2_t48	0.639	638.473	0.302	0.733
Early-cART3_t48	1.078	634.807	0.333	0.892
Early-cART4_t48	2.026	749.111	0.355	-0.233
Early-cART5_t48	0.319	657.125	0.368	1.158
Early-cART6_t48	0.119	751.895	0.334	-0.075
Early-cART7_t48	0.548	778.229	0.389	0.575
Early-cART8_t48	0.036	705.423	0.396	0.475
Early-cART9_t48	0.946	711.199	0.351	0.642
Later-cART1_t0	0.959	850.686	0.496	0.917
Later-cART2_t0	0.868	753.710	0.366	0.733
Later-cART3_t0	0.547	773.725	0.437	0.708
Later-cART4_t0	2.040	716.441	0.350	0.442
Later-cART5_t0	1.803	670.009	0.243	0.692
Later-cART6_t0	1.909	710.208	0.355	0.158
Later-cART7_t0	1.275	N.D	N.D	N.D
Later-cART8_t0	0.979	N.D	N.D	0.600
Later-cART9_t0	2.286	711.307	0.322	-0.117
Later-cART10_t0	2.272	N.D	N.D	0.217
Later-cART1_t48	1.111	830.125	0.430	1.408
Later-cART2_t48	1.635	762.894	0.322	0.917
Later-cART3_t48	1.187	N.D	N.D	0.617
Later-cART4_t48	1.844	713.595	0.332	1.300
Later-cART5_t48	1.836	664.881	0.234	0.833
Later-cART6_t48	2.692	708.699	0.289	-0.125
Later-cART7_t48	0.870	N.D	N.D	N.D
Later-cART8_t48	0.736	N.D	N.D	0.992
Later-cART9_t48	2.703	N.D	N.D	N.D
Later-cART10_t48	2.751	774.740	0.376	0.433

Table S2. Longitudinal neurological evaluation and SIRT2 plasma levels in ARBRE study. ND: not determined, SIRT2: ng/ml, global brain image assessment: cm^3, medial orbitofrontal cortex brain image assessment: arbitrary units, evaluation of CNS functioning: NPZ12 score.

CHAPTER 3. Proteomics analysis in the BCN02 clinical trial, based on a "kick and kill" strategy for HIV-1 cure.
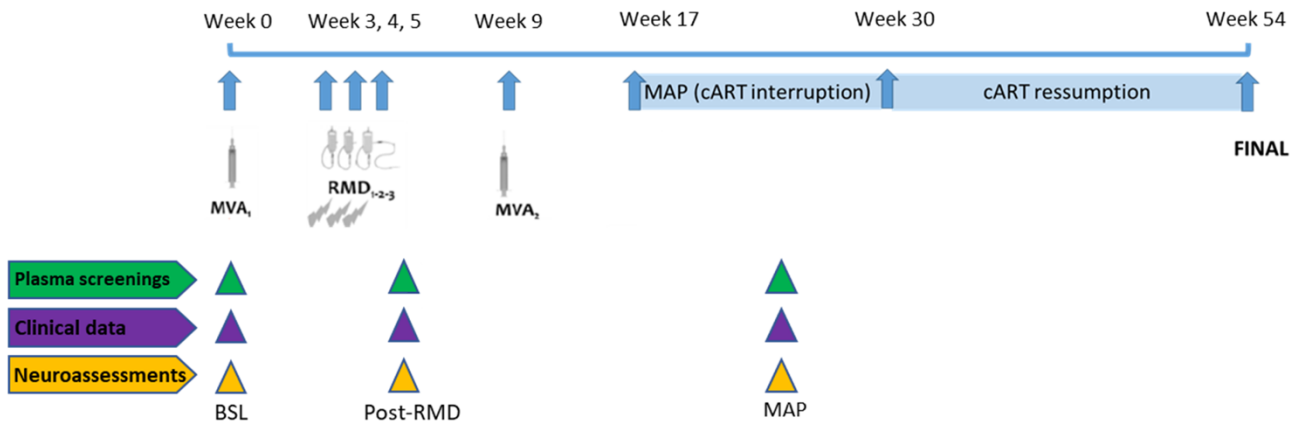

Figure S1. BCN02 clinical trial scheme. Schematic representation of the BCN02 clinical trial with sampling timepoints: baseline (BSL timepoint), three RMD infusions at week 3, 4, 5 and 6 (week 6 is post-RMD timepoint used in this study) followed by cART interruption at week 17 until viral rebound or week 30 cART resumption (MAP timepoint). Week 54 end of the BCN02 clinical trial. Analyzed timepoints labeled in arrows: baseline (BSL), post-RMD infusions (post-RMD) and monitored antiretroviral pause phase (MAP), when plasma proteomics and neurological assessments were conducted.

A

BSL vs Post-RMD					
Protein	Median BSL	Median post-RMD	p-value	Higher/lower levels after RMD	Plasma proteome profiling
MCP3	2.354	1.958	0.001	↓	II
CXCL5	12.207	13.596	0.001	↑	I
CD33	2.930	3.171	0.001	↑	II
IL3RA	1.162	1.483	0.001	↑	II
Siglec9	4.627	4.908	0.001	↑	I
CCL25	6.144	6.900	0.002	↑	I
GPNMB	0.707	0.905	0.002	↑	II
SCGB1A1	1.212	2.964	0.002	↑	II
FCAR	1.401	1.863	0.002	↑	II
IL15	1.189	1.457	0.003	↑	I
ISLR2	1.198	1.416	0.003	↑	I
CTF1	0.347	0.748	0.005	↑	II
CLSTN1	0.524	0.896	0.005	↑	II
ADAM15	8.202	8.307	0.005	↑	II
PAEP	-1.081	-0.476	0.005	↑	II
EFNA4	2.010	2.562	0.005	↑	II
FcRL2	4.415	4.689	0.005	↑	I
BST2	4.349	4.566	0.007	↑	I
SRP14	2.272	3.225	0.007	↑	II
CRIP2	2.338	2.555	0.007	↑	I
CARHSP1	0.924	1.642	0.007	↑	II
KIR2DL3	2.049	2.455	0.010	↑	II
NEFL	2.342	2.466	0.010	↑	II
CD8A	10.380	10.749	0.014	↑	I
BetaNGF	2.445	2.386	0.014	↑	I
ANXA10	1.400	1.762	0.014	↑	I
IL5	4.233	1.456	0.019	↓	II
PLA2G10	3.651	4.488	0.019	↑	II
GGT5	1.610	1.836	0.019	↑	II
MANF	9.047	9.373	0.019	↑	II
TNR	4.349	4.420	0.019	↑	I
TSLP	0.562	0.752	0.024	↑	II
TNF	1.114	0.613	0.024	↓	II
CCL23	5.484	5.714	0.024	↓	I
CEACAM3	1.061	0.676	0.024	↓	II
DSG3	6.634	6.917	0.024	↑	I
IFI30	0.291	0.481	0.024	↑	II
DPEP2	2.029	2.223	0.024	↑	I
MAD1L1	1.223	1.891	0.024	↑	II
VSTM1	0.515	0.892	0.024	↑	I
IL20RA	0.863	0.891	0.032	↑	I
CXCL10	10.693	10.127	0.032	↓	I
TDGF1	0.642	0.007	0.032	↓	II
SMOC1	3.824	4.066	0.032	↑	II
FOLR2	4.535	4.628	0.042	↑	II
RPS6KB1	2.835	3.526	0.042	↑	II
AKT1S1	4.878	5.952	0.042	↑	II
GDNF	0.890	1.133	0.042	↓	I
CD38	4.941	4.988	0.042	↑	I

B

BSL-MAP					
Protein	Median BSL	Median MAP	p-value	Higher/lower levels during MAP	Plasma Proteome Profiling
MCP_3	2.421115	1.707205	0.002	↓	II
TNF	1.137815	0.37583	0.002	↓	II
LIF	0.87738	0.30415	0.002	↓	III
IL5	4.240235	1.128655	0.002	↓	II
EIF4B	7.222625	8.22865	0.002	↑	III
TDGF1	0.632605	0.00725	0.002	↓	II
RPS6KB1	2.86346	4.069835	0.002	↑	II
CD33	2.67816	3.058815	0.002	↑	II
ADAM15	8.222375	8.45106	0.002	↑	II
CEACAM3	1.08565	0.6545	0.002	↓	II
NAA10	3.793345	4.956015	0.002	↑	III
TBCB	8.38766	9.52571	0.002	↑	III
AKT1S1	4.930195	6.493555	0.002	↑	II
PFDN2	1.428535	1.91753	0.002	↑	III
CARHSP1	0.95532	2.136905	0.002	↑	II
RNF31	0.614335	0.98962	0.002	↑	III
IL3RA	1.14481	1.45911	0.002	↑	II
AOC1	0.667235	0.07897	0.002	↓	III
KIF1BP	4.925605	5.886345	0.002	↑	III
PMVK	7.439515	8.16266	0.002	↑	III
WWP2	5.971085	7.00089	0.002	↑	III
GGT5	1.601365	1.87467	0.002	↑	II
EFNA4	2.122625	2.870925	0.002	↑	II
LAT	6.887385	8.26106	0.002	↑	III
MANF	9.046575	9.47429	0.002	↑	II
GDNF	2.75992	2.38671	0.004	↓	III
IL_20	0.588045	0.29721	0.004	↓	III
GPNMB	0.76975	1.063855	0.004	↑	II
SRP14	2.27743	3.40022	0.004	↑	II
SCGB1A1	1.1834	3.151395	0.004	↓	III
CLSTN1	0.53356	1.008885	0.004	↑	II
NXPH1	1.245405	1.1069	0.004	↓	III
PAEP	-1.094875	-0.510025	0.004	↑	II
FKBP5	6.224075	7.043905	0.004	↑	III
CD63	5.461305	6.34012	0.004	↑	III
FGF_23	3.35201	3.94895	0.006	↑	III
CTF1	0.352745	0.893885	0.006	↑	II
FCAR	1.47457	1.913005	0.006	↑	II
NPM1	1.05406	1.613915	0.006	↑	III
4E_BP1	9.248445	10.31638	0.010	↑	III
CRADD	6.35642	7.29832	0.010	↑	III
PTPN1	6.33223	6.846335	0.010	↑	III
PSME1	3.45447	3.936215	0.010	↑	III
HMOX2	4.7685	5.142385	0.010	↑	III
EREG	0.895545	1.937305	0.014	↑	III
NDRG1	1.669565	2.15035	0.014	↑	III
KIRREL2	2.022695	2.338235	0.014	↑	III
AARSD1	2.18663	2.70844	0.014	↑	III
CASP_8	3.045465	3.956475	0.020	↑	III
SMOC1	3.87284	4.22917	0.020	↑	II
ATP6V1F	0.739735	1.232105	0.020	↑	III
GSTP1	0.04143	0.1093	0.020	↑	III
SIGLEC1	5.211245	5.35303	0.020	↑	III
IL_10RB	5.678385	6.11103	0.027	↑	III
FHIT	0.95002	1.513355	0.027	↑	III
LEPR	5.16893	5.59483	0.027	↑	III
IFI30	0.366415	0.754555	0.027	↑	II
PSG1	1.56295	1.8791	0.027	↑	III
CTSS	6.14212	6.33652	0.027	↑	III
TSLP	0.58906	0.75193	0.037	↑	II
IL_22_RA1	2.81364	2.385745	0.037	↓	III
IL_12B	6.455325	6.732755	0.037	↑	III
IL13	0.935125	0.97651	0.037	↑	III
FKBP7	0.549805	0.912665	0.037	↑	III
IMPA1	1.51246	1.97267	0.037	↑	III
MAD1L1	1.25823	1.85883	0.037	↑	II
PTS	1.96038	1.75097	0.037	↓	III
EZR	5.07442	5.325785	0.037	↑	III
gal_8	8.52177	9.041675	0.037	↑	III
FOLR2	4.347155	4.851225	0.049	↑	II
KIR2DL3	2.23887	2.634915	0.049	↑	III
GBP2	0.154155	-0.01545	0.049	↓	III
PLA2G10	3.84918	4.503355	0.049	↑	II
DUSP3	0.85441	0.95025	0.049	↑	III
NEFL	2.451385	2.7142	0.049	↑	II
NEP	2.978135	2.604925	0.049	↓	III

Table S3. Plasma protein levels during the BCN02 clinical trial. A) Significantly different plasma protein levels between baseline vs. post-romidepsin infusions. B) Significantly different plasma protein levels between baseline vs MAP. P-value (paired Wilcoxon test), from plasma proteome profiles represented in Figure 25B, red arrows indicate up-regulated, green arrows indicate down-regulated plasma levels and the different profiles: *Profile I:* Significant protein profiles only detected when comparing BSL vs post-RMD infusions; *Profile II*: Significant protein profiles shared when comparing BSL vs post-RMD and BSL vs MAP timepoints; and *Profile III:* Significant protein profiles only detected when comparing BSL vs MAP phase.
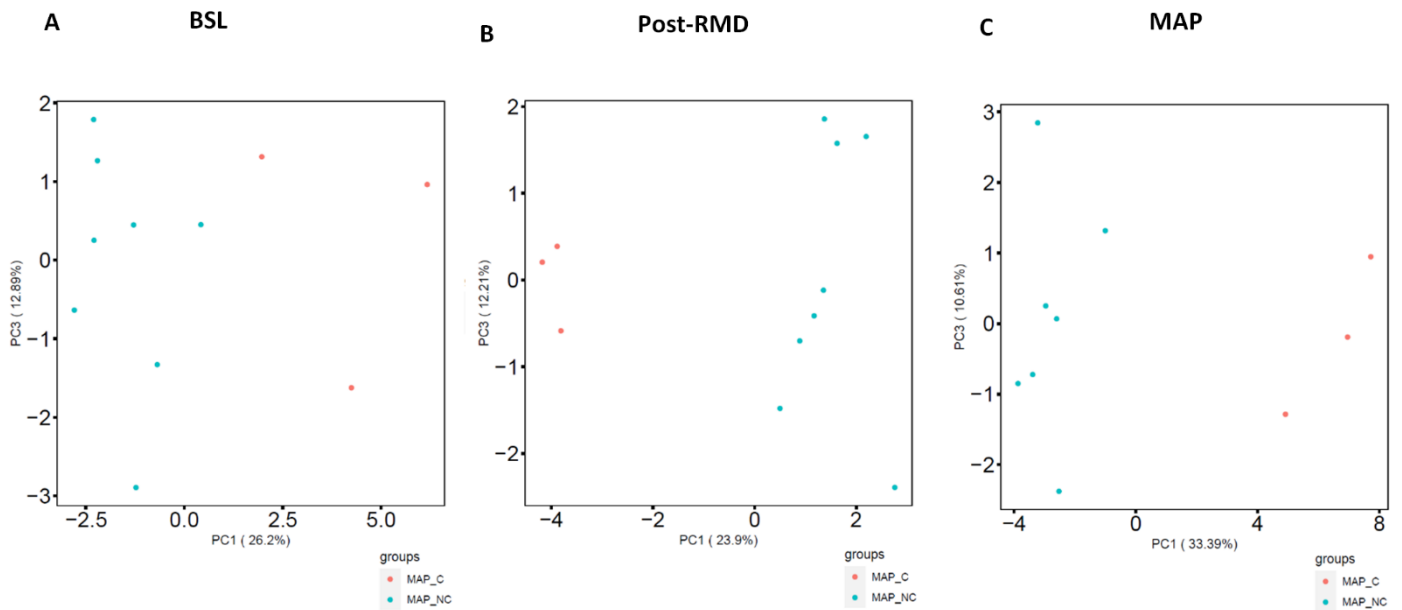
Figure S2. Principal component analysis (PCA) of plasma proteomes in BCN02 trial. A-C) PCA plots of differentially detected proteins between MAP-C and MAP-NC at A) baseline, B) post-RMD infusions and C) MAP phase. Orange dots indicate MAP-NC and green dots MAP-C participants.
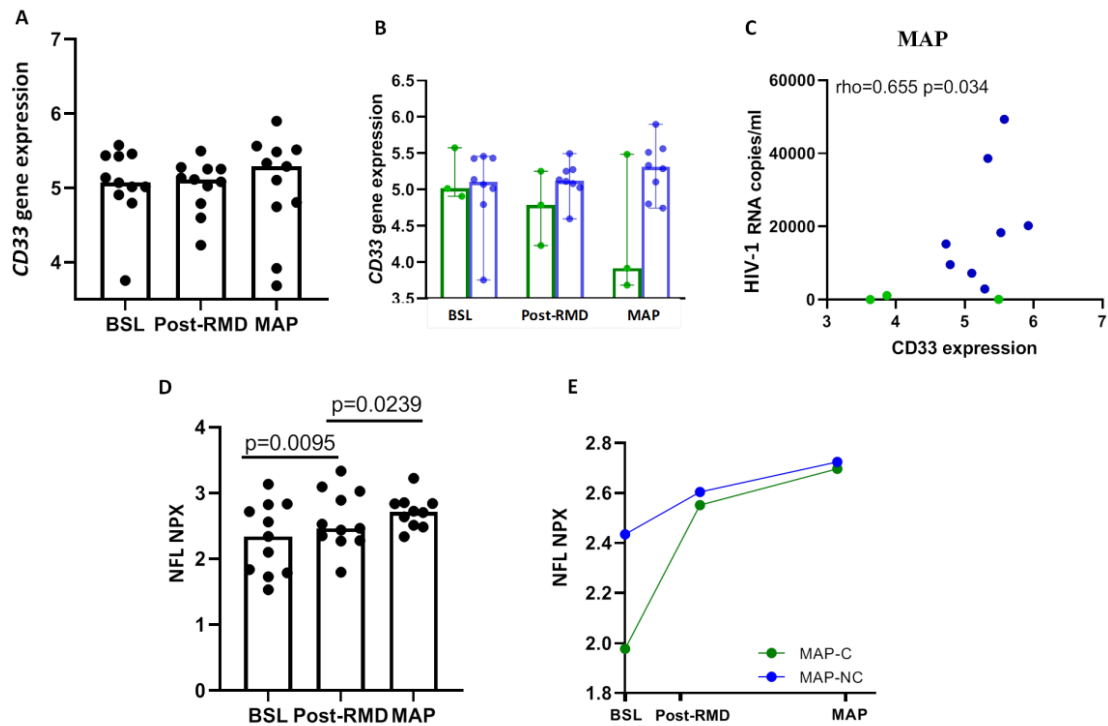
Figure S3. *CD33* **gene expression is consistently modulated across the BCN02 clinical trial**. A) *CD33* gene expression levels at baseline (BSL), post-RMD infusions (post-RMD) and at MAP phase (MAP). The upper limit of the bar is the median value of CD33 plasma levels. B) Longitudinal representation of *CD33* gene expression levels in MAP-C (green symbols) and MAP-NC (blue symbols) individuals over the duration of the clinical trial. Clinical trial timepoints are shown on the x-axis, and gene expression levels of *CD33* shown on the y-axis. Values are shown as median and standard deviation. C) Correlation between *CD33* gene expression levels and plasma viral load in the MAP phase. MAP-C individuals in green line and MAP-NC individuals in blue lines, respectively. D) Relative NFL plasma levels (NPX) at baseline (BSL), post-RMD infusions (post-RMD) and at MAP phase (MAP). The upper limit of the bar is the median value of relative NFL plasma levels. E) Plot representing relative NFL plasma levels in MAP-C (green line) and MAP-NC (blue line) individuals over the duration of the clinical trial. Weeks off treatment are shown on the x-axis, and relative NFL plasma levels shown on the y-axis. Values are shown as medians and standard deviation. Changes over time were assessed using the paired *t* test and the correlation analysis was based on the Spearman's rank test. Statistical significance was set at $p < 0.05$.
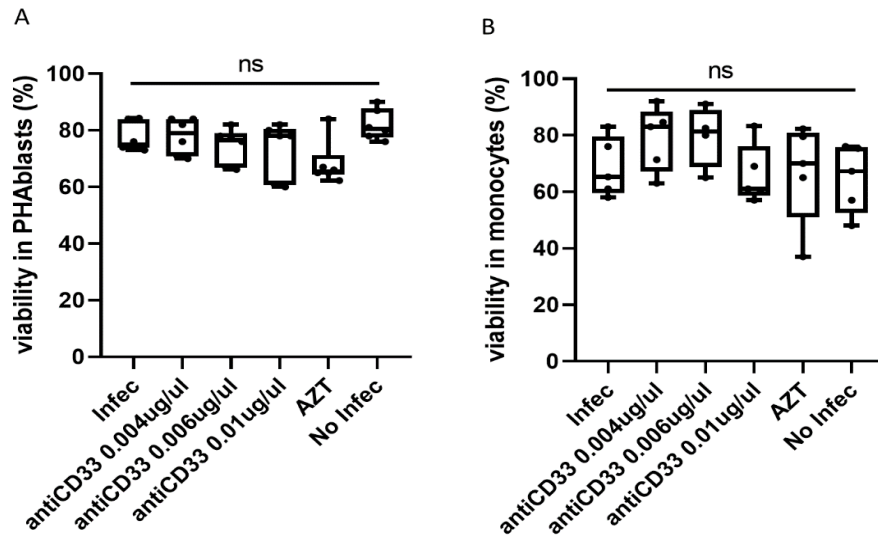
Figure S4. Evaluation *in vitro* cell viability in the presence of anti-CD33 mAb. Cell viability in the presence of increasing concentration of the anti-CD33 mAb, tested in A) HIV HIV-1$_{NL4-3}$ infected PHA-activated T-cells (six independent experiments) and in B) monocyte-derived macrophages infected with HIV-1$_{BAL}$ strain (five independent experiments). Experimental conditions are shown on the x-axis; quantification of viability (% live cells) is shown on the y-axis.

PUBLICATIONS

9. PUBLICATIONS

Oriol-Tordera B, Berdasco M, Llano A, Mothe B, Gálvez C, Martinez-Picado J, Carrillo J, Blanco J, **Duran-Castells C**, Ganoza C, Sanchez J, Clotet B, Calle ML, Sánchez-Pla A, Esteller M, Brander C, Ruiz-Riol M. Methylation regulation of Antiviral host factors, Interferon Stimulated Genes (ISGs) and T-cell responses associated with natural HIV control. PLoS Pathog. 2020 Aug.

Oriol-Tordera B, Olvera A, **Duran-Castells C**, Llano A, Mothe B, Massanella M, Dalmau J, Ganoza C, Sanchez J, Calle ML, Clotet B, Martinez-Picado J, Negredo E, Blanco J, Hartigan-O'Connor D, Brander C, Ruiz-Riol M. TL1A-DR3 Plasma Levels Are Predictive of HIV-1 Disease Control, and DR3 Costimulation Boosts HIV-1-Specific T Cell Responses. J Immunol. 2020 Dec.

Oriol-Tordera B, Esteve-Codina A, Berdasco M, Rosás-Umbert M, Gonçalves E, **Duran-Castells C**, Català-Moll F, Llano A, Cedeño S, Puertas MC, Tolstrup M, Søgaard OS, Clotet B, Martínez-Picado J, Hanke T, Combadiere B, Paredes R, Hartigan-O'Connor D, Esteller M, Meulbroek M, Calle ML, Sanchez-Pla A, Moltó J, Mothe B, Brander C, Ruiz-Riol M. Epigenetic landscape in the kick-and-kill therapeutic vaccine BCN02 clinical trial is associated with antiretroviral treatment interruption (ATI) outcome. EBioMedicine. 2022 Apr.

Borgognone A, Noguera-Julian M, Oriol-Tordera B, Noël-Romas L, Ruiz-Riol M, Guillén Y, Parera M, Casadellà M, **Duran-Castells C**, Puertas MC, Català-Moll F, De Leon M, Knodel S, Birse K, Manzardo C, Miró JM, Clotet B, Martinez-Picado J, Moltó J, Mothe B, Burgener A, Brander C, Paredes R; BCN02 Study Group. Gut microbiome signatures linked to HIV-1 reservoir size and viremia control. Microbiome. 2022 Apr.

Romero-Martín, Luis; **Duran-Castells, Clara**; Olivella, Mireia; Rosás-Umbert, Míriam; Ruiz-Riol, Marta; Sanchez, Jorge; Hartigan-O´Connor, Dennis; Mothe, Beatriz; Olvera,

Àlex; Brander, Christian. Disruption of the HLA-E/NKG2X axis is associated with uncontrolled HIV infections. Front. immunol. 2022 Nov.

Duran-Castells C, Llano A, Kawana-Tachikawa A, Prats A, Martinez-Zalacain I, Kobayashi-Ishihara M, Oriol-Tordera B, Penya R, Gálvez C, Silva-Arrieta S, Clotet B, Riveira-Muñoz E, Ballana E, Prado JG, Martinez-Picado J, Sanchez J, Mothe B, Hartigan-O'Connor D, Wyss-Coray T, Meyerhans A, Gisslen M, Price RW, Soriano-Mas C, Muñoz-Moreno JA, Brander C, Ruiz-Riol M. Sirtuin-2, NAD-dependent deacetylase, is a new potential therapeutic target for HIV-1 infection and HIV-related neurological dysfunction. J Virol. 2023 Jan.

Mie Kobayashi-Ishihara, Katarína Frazão Smutná, Florencia E. Alonso, Jordi Argilaguet, Anna Esteve-Codina, Kerstin Geiger, Meritxell Genescà, Judith Grau-Expósito, **Clara Duran-Castells**, Selina Rogenmoser, René Böttcher, Jennifer Jungfleisch, Baldomero Oliva, Javier P. Martinez, Manqing Li, Michael David, Makoto Yamagishi, Marta Ruiz-Riol, Christian Brander, Yasuko Tsunetsugu-Yokota, Maria J. Buzon, Juana Díez and Andreas Meyerhans. Schlafen 12 restricts HIV latency reversal by a codon-usage dependent post-transcriptional block in CD4+ T cells. Commun Biol (Under Review).

Duran-Castells C, Prats A, Oriol-Tordera B, Llano A, Galvez C, Martinez-Picado J, Ballana E, Garcia E, Clotet B, Muñoz-Moreno J.A, Hanke T, Moltó J, Mothe B, Brander C, Ruiz-Riol M. Plasma proteomic profiling identifies CD33 as a marker of HIV control in BCN02 clinical trial and natural infection. EBioMedicine (Under Review).

Duran-Castells C, Oriol-Tordera B, Prats A, Muñoz-Moreno J, Clotet B, Gisslen M, Price RW, Brander C, Ruiz-Riol M. Proteomic CSF candidates, GZMA, CRTAM and SIGLEC1 reflected at plasma in chronic untreated HIV-infected individuals. Viruses (in preparation).

ACKNOWLEDGEMENTS

10. ACKNOWLEDGEMENTS

I per últim però no menys important s'acaba una etapa de gairebé cinc anys on he d'agrair el suport, la confiança i l'ajuda de molta gent amb la qui m'he creuat durant aquest camí.

Primer de tot al Christian i a la Marta per donar-me la gran oportunitat de fer el doctorat amb ells, on he pogut créixer tant laboralment, científicament com personalment. A la Marta per ensenyar-me que de tots els resultats i experiments se'n treu quelcom i serveixen tot i que no siguin els esperats, a relativitzar les coses i descobrir i interpretar la meva cara de "pocker face". A tot el grup TIV per ser un equip magnífic, sobretot a la Tuixent per compartir rutes i restaurants on anar i juntament a la Sam per estar sempre disposades a ajudar en qualsevol cosa. A la Sandra, per felicitar-me de tots els assoliments per petits que em semblessin. Al Lluís per recordar-me que ja quedava poc. A la Cris per animar-me en tot moment. A l'Alex per distreure'm de tant en tant i fer un petit "break" mental. A l'Igor per posar tot el possible de la seva part perquè tot rutlli i a la Marta N que tot i compartir pocs mesos juntes i ser el meu "pinche" tot ens ha sortit com esperàvem i també ha sigut gràcies a tu. I als membres del grup que ja han marxat, el Luís per compartir mil experiències i consells que mai oblidaré i sempre me'ls enduré com a un gran record i a la Bruna per compartir els primers anys de doctorat i ensenyar-me tot el que calia saber per després anar sola.

A tots els predocs (Carlos, Miguel, Ana, Anna, Angel i Lucia) que vam entrar junts i hem compartit un mateixa etapa ja que gràcies això s'ha fet més fàcil perquè sempre hi havia algú amb els mateixos dubtes, pors o problemes. I els ja postdocs (Luis, Edurne, Raquel, Oscar, Ify i Dani) amb qui també he compartit bona part d'aquest camí i ens han ajudat a poder avançar. Sense oblidar les escapades, scape rooms, sopars, calçotades, barbacoes, congresos, festes... perquè tot i coneixe'ns en l'àmbit laboral també hem sapigut desconnectar i passar-nos-ho bé. I especialment a l'Oscar que ha fet el disseny de la portada de la tesi.

A la Penelope, l'Arnau i la Cristina per fer que els temes administratius i burocràtics siguin més fàcils, ràpids i inclús divertits.

I a cada un de tots de la família IrsiCaixa per compartir protocols, màquines, reactius i aportar el vostre granet de sorra i fer que aquest pas per Can Ruti hagi sigut per recordar.

I no m'oblido del grup "Aneto challenge" o aquest any dit "Pica challenge" per gaudir, sentir i estimar la muntanya d'aquesta manera tant especial. Especialment a la Marta Massanella, Cristina, Ester, Roger, Anna Ponts, Albert, Aroa, Jordi, Pep, Maria José, Jose i Carla. Com diu en Roger tot acaba al Puigmal, per allà sempre m'hi trobareu.

I per últim agrair al meu entorn més proper, fora d'IrsiCaixa, que ha patit indirecta i directament el doctorat. Sobretot el pare, la mare i la Maria per tenir una paciència infinita i voler entendre el que faig que per ells no és fàcil. A l'Arnau per recordar-me que tot anirà bé i que puc amb tot i tenir la mateixa paciència o més que la meva família. A les amigues de sempre, les nenes de l'escola (Anna, Caro, Carlota, Inés, Cande, Monica, Blanca, Judith, Claudia, Maria), que crec que mai han arribat a entendre que he fet i que faig però sempre m'han escoltat i animat. I a les amigues de la uni com l'Ana i la Lena amb qui també hem compartit camí de doctorat i amb la Bruna, Ivet i Blanca que sempre ens han recorda't com de boges estàvem escollint aquest camí però ens han recolzat en tot moment.

Moltes gràcies a tots!